121

TEXAS INSTRUMENTS
INCORPORATED
SCIENCE SERVICES DIVISION
100 EXCHANGE PARK NORTH
P. O. BOX 35084 • DALLAS, TEXAS

ARPA Order No. 292, Amendment 7
ARPA Project Code No. 8100

NOISE STUDY

By
George D. Hair, James H. Funk
and Research Staff

Special Report No. X
15 November 1964

Project Manager
R. R. Guidroz

Telephone

Dallas, Texas
Area Code 214
Fleetwood 7-5411
Extension 447

Contractor: Texas Instruments Incorporated
Date of Contract: 15 May 1961
Contract Expiration Date: 15 November 1964

Contract No. AF 19(604)-8517

TABLE OF CONTENTS

Section	Title	Page
I	SUMMARY AND CONCLUSIONS	I-1
II	POWER DENSITY SPECTRA	II-1
	A. PROCEDURE	II-1
	B. METHOD	II-2
III	EVALUATION OF POWER DENSITY SPECTRA	III-1
IV	VISUAL NOISE MEASUREMENTS	IV-1
V	RECOMMENDATIONS	IV-6

APPENDICES

A	ABSOLUTE POWER DENSITY SPECTRA
B	NOISE MAPS

REFERENCES

LIST OF ILLUSTRATIONS

Figure	Title	Page
II-1	Flow Diagram for Obtaining Absolute Power Density Spectra by Polarity Method	II-3
II-2	Data Example for Obtaining Absolute Power Density Spectra by Polarity Method	II-4
II-3	Sampling Rate for Power Density Spectra Data (a) 1960; (b) 1963	II-5
II-4	Frequency Response of the USC&GS World-Wide Standard Short Period Seismograph System	II-8
III-1	Comparison of Spectra Slopes at Frequency of 1.0 CPS or Greater	III-2
III-2	Power Density (Frequency = 0.33 cps) vs Distance of Station From Large Body of Water	III-3
III-3	Power Density (Frequency = 1.25 cps) vs Distance of Station From Large Body of Water	III-4
IV-1	Frequency Response of the USC&GS World-Wide Standard Seismograph Systems	IV-2
IV-2	Frequency Response of the Canadian Network Seismograph Systems (Vertical Components)	IV-3

LIST OF ILLUSTRATIONS (CONT'D)

Figure	Title	Page
A-1a	Absolute Power Density Spectra Obtained From 1963 Data	A-3
A-1b	Absolute Power Density Spectra Obtained From 1963 Data	A-5
A-1c	Absolute Power Density Spectra Obtained From 1963 Data	A-7
A-1d	Absolute Power Density Spectra Obtained From 1963 Data	A-9
A-1e	Absolute Power Density Spectra Obtained From 1963 Data	A-11
A-1f	Absolute Power Density Spectra Obtained From 1963 Data	A-13
B-1	World Map of 0.5-2.0 Second Microseismic Activity, January, 1963	B-2
-2	World Map of 3.0-8.0 Second Microseismic Activity, January, 1963	B-3
B-3	World Map of 0.5-2.0 Second Microseismic Activity, February, 1963	B-4
B-4	World Map of 3.0-8.0 Second Microseismic Activity, February, 1963	B-5
B-5	World Map of 0.5-2.0 Second Microseismic Activity, March, 1963	B-6
B-6	World Map of 3.0-8.0 Second Microseismic Activity March, 1963	B-7
B-7	World Map of 0.5-2.0 Second Microseismic Activity, April, 1963	B-8
B-8	World Map of 3.0-8.0 Second Microseismic Activity, April, 1963	B-9
B-9	World Map of 0.5-2.0 Second Microseismic Activity, May, 1963	B-10
B-10	World Map of 3.0-8.0 Second Microseismic Activity, May, 1963	B-11
B-11	World Map of 0.5-2.0 Second Microseismic Activity, June, 1963	B-12
B-12	World Map of 3.0-8.0 Second Microseismic Activity, June, 1963	B-13
B-13	World Map of 0.5-2.0 Second Microseismic Activity, October, 1963	B-14
B-14	World Map of 3.0-8.0 Second Microseismic Activity, October, 1963	B-15
B-15	World Map of 0.5-2.0 Second Microseismic Activity, November, 1963	B-16
B-16	World Map of 3.0-8.0 Second Microseismic Activity, November, 1963	B-17
B-17	World Map of 0.5-2.0 Second Microseismic Activity, December, 1963	B-18
B-18	World Map of 3.0-8.0 Second Microseismic Activity, December, 1963	B-19

SECTION I

SUMMARY AND CONCLUSIONS

Worldwide seismic noise levels and characteristics for 1963 are discussed in this report. Data for evaluation includes absolute power density spectra and contour maps of average worldwide microseismic activity.

Relative power density spectra were computed from 1963 data from Worldwide Standard Stations. Slopes of the least-mean-square line through the power density points were computed and a pattern of slope changes appeared at a frequency of 1.0 cps. A uniform worldwide pattern of slopes was observed between 1 cps and 2 cps. This suggests two separate sources generating microseisms above and below 1 cps, respectively, and that the spectra above 1 cps are independent of storms, fronts, etc.

The spectra for frequencies less than 1.0 cps show greater seasonal variations. These were concluded to be mostly meteorological in origin.

Monthly contour maps of average noise show that noise is seasonally variable and that it is attenuated at continental structures.

SECTION II

POWER DENSITY SPECTRA

A. PROCEDURE

Power density spectra were computed using short-period instruments from selected Worldwide Standard Stations. The data were obtained from the Coast and Geodetic Survey on 70 mm film clips. These were chosen over the 35 mm film clips because of the larger image size and better reproduction quality.

To assure that the same method of determining input data was used throughout the program, one person made all data reductions. The selected noise sample was projected approximately ten times the original gram size on a large wall-mounted grid.

The availability of film largely determined the samples chosen. Effort was concentrated on the first six months of 1963 when it became apparent that film for the latter months of the year would not be available.

The noise samples were objectively chosen to be representative of the recording period. An attempt was made to eliminate extremely high cultural noise if it was present only during part of the recording period.

As far as was practical, the horizontal instruments were sampled at the same time that the corresponding vertical sample was chosen. Any exceptions were caused by poor optics in the original gram, missing grams or reduced quality of reproduction.

Several samples were taken from the same station at different times of the same day to show the repeatibility of the method. Refer to the following spectra in Appendix A:

Station	Code	Component	Date
Nurmijarvi, Finland	NUR	N, E	15 January
Quetta, W. Pakistan	QUE	Z	24 January

Four samples were taken on different days in the same month to show variations at a station during the month. Refer to the following:

Station	Code	Component	Date
Valentia, Ireland	VAL	Z	15 Jan., 18 Jan.
Kevo, Finland	KEV	Z	5 March, 13 March

Station	Code	Component	Date
Valentia, Ireland	VAL	Z	2 April, 3 April
Anpu, Taiwan	ANP	Z	14 April, 28 April

Twenty spectra were computed from one station to show seasonal variations. Valentia, Ireland (VAL) was chosen as the station because of film availability and the quality of recordings.

A total number of 151 absolute power density spectra were computed from data recorded during nine months in 1963.

B. METHOD

The method used in the determination of absolute power density spectra was the technique developed by Texas Instruments for use with film data. The previously used polarity technique[1] was improved by the following:

- Film traces were differentiated before infinite clipping to pre-emphasize the high frequency energy, and
- Compensation was made for station response.

The flow diagram (Figure II-1) and the data example (Figure II-2) illustrate the individual operations involved in the method and their proper sequence.

The polarity technique applies only to time series having a Gaussian distribution of amplitudes. The sampling rate on the 1960 short-period data was four times per second or a sampling interval of 0.25 seconds. For the 1963 study, it was found that in most cases 300 seconds of noise gave good results with a sampling rate of eight times per second or a sampling interval of 0.125 seconds. Figure II-3 compares the sampling rate and results using data from (a) 1960 and (b) 1963.

1. Film Measurements

The noise samples were projected from film strips and a time sample of 300 seconds was traced. The tracings were sampled at intervals of 0.125 seconds, yielding 2400 digital samples each. A sample was recorded as +1 if the amplitude at that point was greater than that at the preceding sample point and -1 if less. This corresponds to differentiating the trace, then clipping at the +1 and -1 levels. The +1's were then punched

[1] Semiannual Technical Report No. III, Contract AF 19(604)-8517, 31 October 1962.

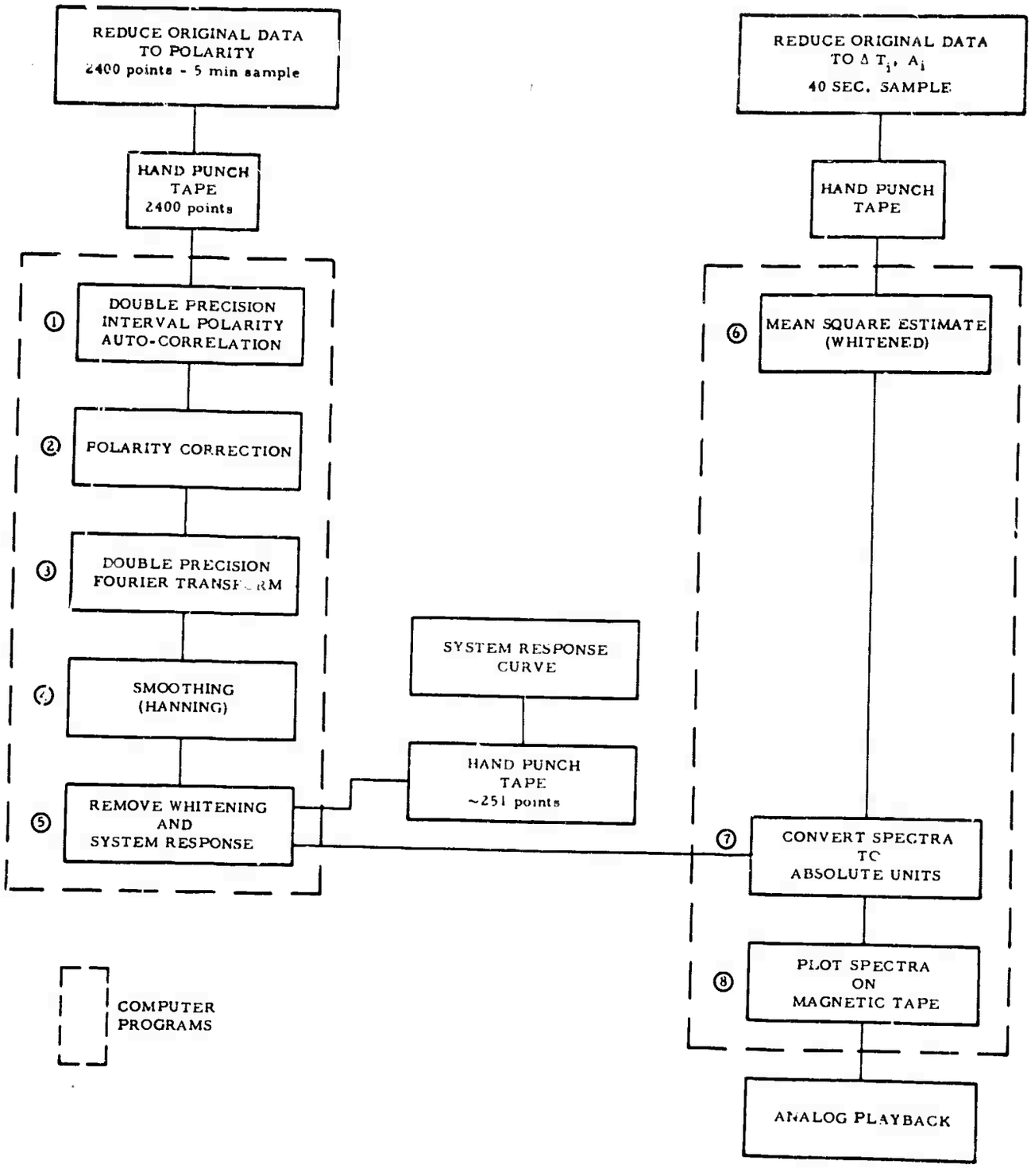

Figure II-1. Flow Diagram for Obtaining Absolute Power Density Spectra by Polarity Method

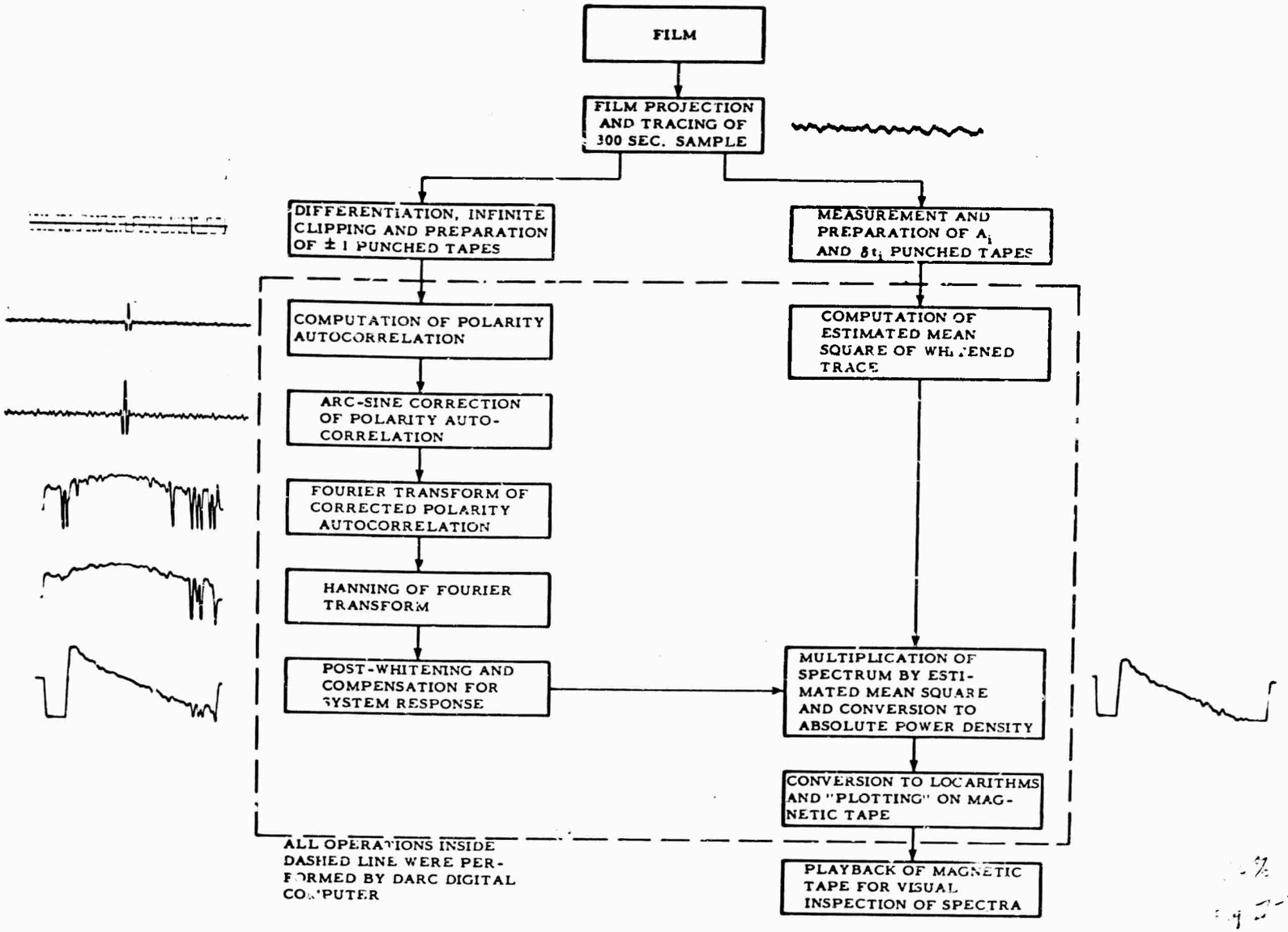

Figure II-2. Data Example for Obtaining Absolute Power Density Spectra by Polarity Method

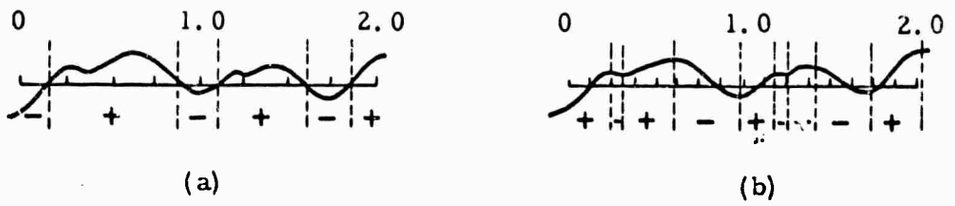

(a) (b)

Figure II-3. Sampling Rate for Power Density Spectra Data (a) 1960; (b) 1963

on paper tape suitable for input to the DARC computer for computation of relative power density spectra.

Another set of measurements was made on a selected 40-second section of each tracing for the purpose of estimating the mean square of the differentiated trace. See paragraph 6 for a discussion of the mean-square estimate. These measurements consisted of measuring the amplitude of the trace (relative to any base line parallel to the axis of the film) at each relative maxima and minima, and measuring the time intervals between successive relative maxima and minima. For example, if the total number of maxima and minima in the 40-second sample was N, then N amplitude and N-1 time-interval measurements were made. These measurements were also punched on paper tape suitable for computer input.

2. Pre-Whitening by Differentiation

Past experience with the noise recorded by the Worldwide Stations has shown that the power spectra (before allowance for system response) generally fall off rather rapidly with increasing frequency. Since the polarity technique gives highest fidelity when the spectra are roughly "white," the performance of any operation tending to whiten the noise before infinite clipping would improve the spectral estimates. One such operation is differentiation, which corresponds to a 6 db/octave multiplication of the power spectrum. With digitized data, differentiation may be approximated by subtracting the previous sample from a given sample. Symbolically, the operation is

$$\Delta t\, g'(t) = g(t) - g(t - \Delta t)$$

This operation is equivalent to convolution with a two-point (+1, -1) operator whose power response is $2(1 - \cos 2\pi f \Delta t)$.

3. Computation and Correction of Polarity Autocorrelations

The polarity autocorrelations were computed as

$$\phi(k\Delta t) = \sum_{n=1}^{2400-k} h(n\Delta t)\, h(n\Delta t + k\Delta t) \text{ for } k = 0,\ 1,\ 2,\ \ldots\ldots,\ 250$$

where $h(n\Delta t)$ is either +1 or -1, and $\Delta t = 0.125$ second.

The autocorrelations were then "arc-sine corrected" to obtain estimates of the autocorrelations that would have been obtained if the data had been fully quantized. This correction is

$$\phi'(k\Delta t) = \sin\left[\frac{\pi}{2}\,\frac{\phi(k\Delta t)}{\phi(0)}\right] \text{ for } k = 0,\ 1,\ 2,\ \ldots\ldots,\ 250.$$

The theory of polarity autocorrelations and the arc-sine correction has been fully presented in a previous report[2] and thus will not be repeated here.

4. Computation of Relative Power Density Spectra

The corrected polarity autocorrelations were Fourier transformed as follows:

$$\Phi(j\Delta f) = \sum_{k\,-\,250}^{250} \phi'(k\Delta t) \cos\left[2\pi(j\Delta f)\,(k\Delta t)\right] \Delta t$$

$j = 0,\ 1,\ 2,\ \ldots\ldots,\ 125$, where $\Delta f = \dfrac{1}{500\Delta t}$.

These Fourier transforms were then Hanned by convolving with a three-point (1/4, 1/2, 1/4) operator to obtain the smoothed power density spectra. These spectra are relative spectra only, since the $\phi'(k\Delta t)$ are normalized autocorrelation functions.

5. Post-Whitening and Compensation for System Response

These two operations were performed simultaneously for reasons of computer efficiency and precision. Since the power response of the whitening operation is $2(1 - \cos 2\pi f\Delta t)$, post-whitening to remove this effect consists of dividing the spectrum by $2(1 - \cos 2\pi f\Delta t)$. Compensation for system response consists of dividing the spectra by $H^2(f)$ where $H(f)$ is the amplitude response of the system. Amplitude response was obtained

---

[2] Ibid

from U. S. Department of Commerce bulletin "Instrumentation of the World-Wide Seismograph System," Figure II-4. This system response includes all effects of the recording apparatus (seismometers, galvanometers, etc.) and relates absolute ground motion to film trace deflection.

6. Mean Square Estimation

To obtain absolute power density spectra from the relative power density spectra obtained with normalized autocorrelations, it is necessary to multiply each by the mean square of the corresponding time function. Using polarity data, we have no way of computing the mean square; however, we may obtain a good estimate of the mean square of each whitened trace. We approximate the unwhitened film trace between successive relative maxima and minima by half cycles of cosine functions of appropriate amplitudes and frequencies. This approximation is illustrated by the $g_i(t)$ in the diagram below:

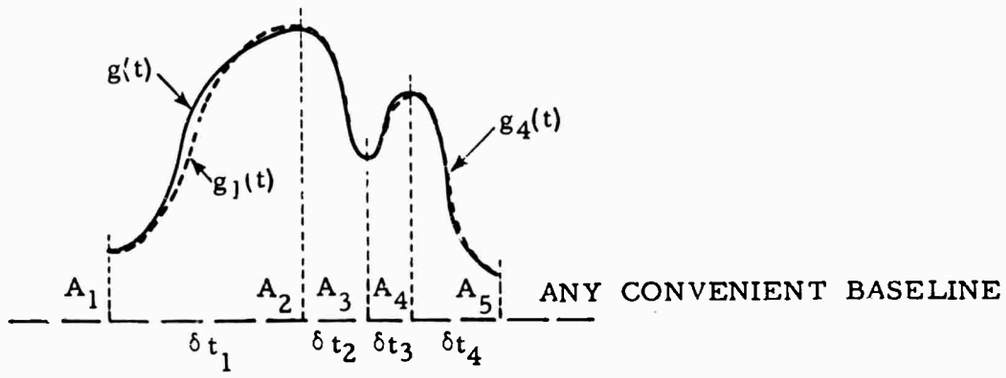

Then $g_i(t) = \frac{A_i + A_{i+1}}{2} + \frac{A_i - A_{i+1}}{2} \cos\left(\pi \frac{t}{\delta t_i}\right)$ for the interval δt_i.

Differentiating $g_i(t)$ we obtain

$$g'_i(t) = \frac{A_{i+1} - A_i}{2} \frac{\pi}{\delta t_i} \sin\left(\pi \frac{t}{\delta t_i}\right) \text{ for the interval } \delta t_i.$$

Then the mean square of $g'(t)$ may be estimated as

$$\text{E.M.S.} = \frac{1}{\sum_i \delta t_i} \sum_i \int_{t=0}^{\delta t_i} \left| g'_i(t) \right|^2 dt$$

$$\text{E.M.S.} = \frac{1}{\sum_i \delta t_i} \sum_i \frac{(A_{i+1} - A_i)^2 \pi^2}{4 \delta t_i^2} \int_{t=0}^{\delta t_i} \sin^2\left(\pi \frac{t}{\delta t_i}\right) dt$$

$$\text{E.M.S.} = \frac{1}{\sum_i \delta t_i} \sum_i \frac{\pi^2 (A_{i+1} - A_i)^2}{8 \delta t_i}$$

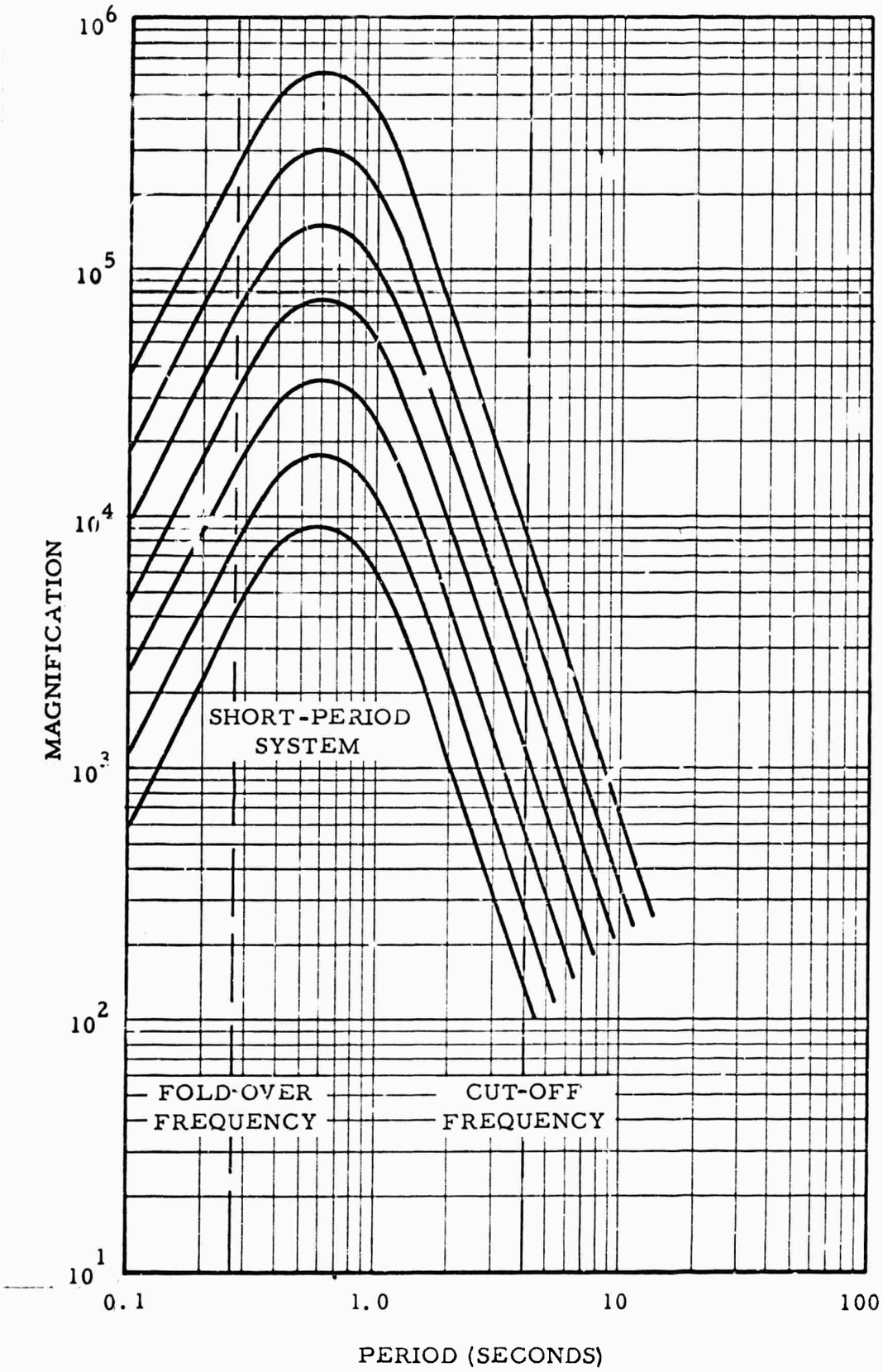

Figure II-4. Frequency Response of the USC&GS World-Wide Standard Short Period Seismograph System

The A_i and δt_i measurements were made directly from the film as described in paragraph 1. These measurements were input to DARC, and estimated mean squares for each whitened noise sample were computed using the formula just derived.

7. Conversion of Relative Spectra to Absolute Spectra

Absolute power density spectra were obtained by multiplication of the relative power density spectra, previously corrected for whitening and system response, by their respective mean-square estimates, and by a constant. This constant contains such scaling factors as:

- Magnification factor involved in projecting film and measuring A_i's
- Variations in gain from that gain at which the system response was calibrated, and
- Computer scale factors introduced in data processing.

8. Presentation of Spectra

The logarithm of each point of each absolute power density spectrum was written on magnetic tape by the DARC computer in a special configuration. This configuration was such as to provide a plot of the logarithm of the power density function versus linear frequency by playback of the magnetic tape through a digital-to-analog converter and oscillograph.

SECTION III

EVALUATION OF POWER DENSITY SPECTRA

The power density spectra, computed on a worldwide basis and converted to absolute values, lends itself to a study of the noise of the world.

The spectra plots are located in Appendix A. In each case, the slope of the plots were determined by the least mean square method. It is interesting to note the change in slope on the plots in the range of 1.0 cps. This slope change is interpreted to suggest that two source mechanisms are causing the noise above and below 1.0 cps. The same change in slope was observed by Vinnik and Pruchkina (1964).

Several comparisons were made between the slopes obtained from the spectra plots. The first is the number of stations whose spectral slope (frequency 1.0 cps or greater) falls within each slope increment of 10 db/octave (Figure III-1). It was noted that 84.1 percent of the slopes' values fall within the range of 10-40 db/octave and that of these 48.8 percent fall within the range of 20-30 db/octave. This worldwide uniformity in noise betweer the periods of 0.5 sec to 1.0 sec suggests a constant universal noise.

Several theories have been advanced thus far as to the reason for the presence of microseisms throughout the world. Iyer (1962) suggests that the earth itself is filled with noise. Other causes from cultural noise to sea storms have been investigated. The problem lends itself for further study.

The power density spectra plots yield an increase in slope between 0.25 cps to 1.0 cps. This spectral range corresponds with the theory that microseisms in the 2-6 sec period range receive their energy from pressure fronts.

A comparison was made between the slopes of the spectra plots and the station distance from large bodies of water. Station geologic structures were also taken into consideration (refer to Figures III-2 and III-3). As can be seen from Figure III-2, the noise present in the 3 sec period range levels off at a distance of around 300 miles from the shore. The high frequency spectra (Figure III-3) drops off much more rapidly although it apparently levels off at about 300 miles also. There is no apparent relationship of these noise spectra with the geologic environment near the recording stations.

The results from the seasonal study at Valentia, Ireland show that the seasonal change in the spectra around 1.0 cps and above is less than that below 1.0 cps.

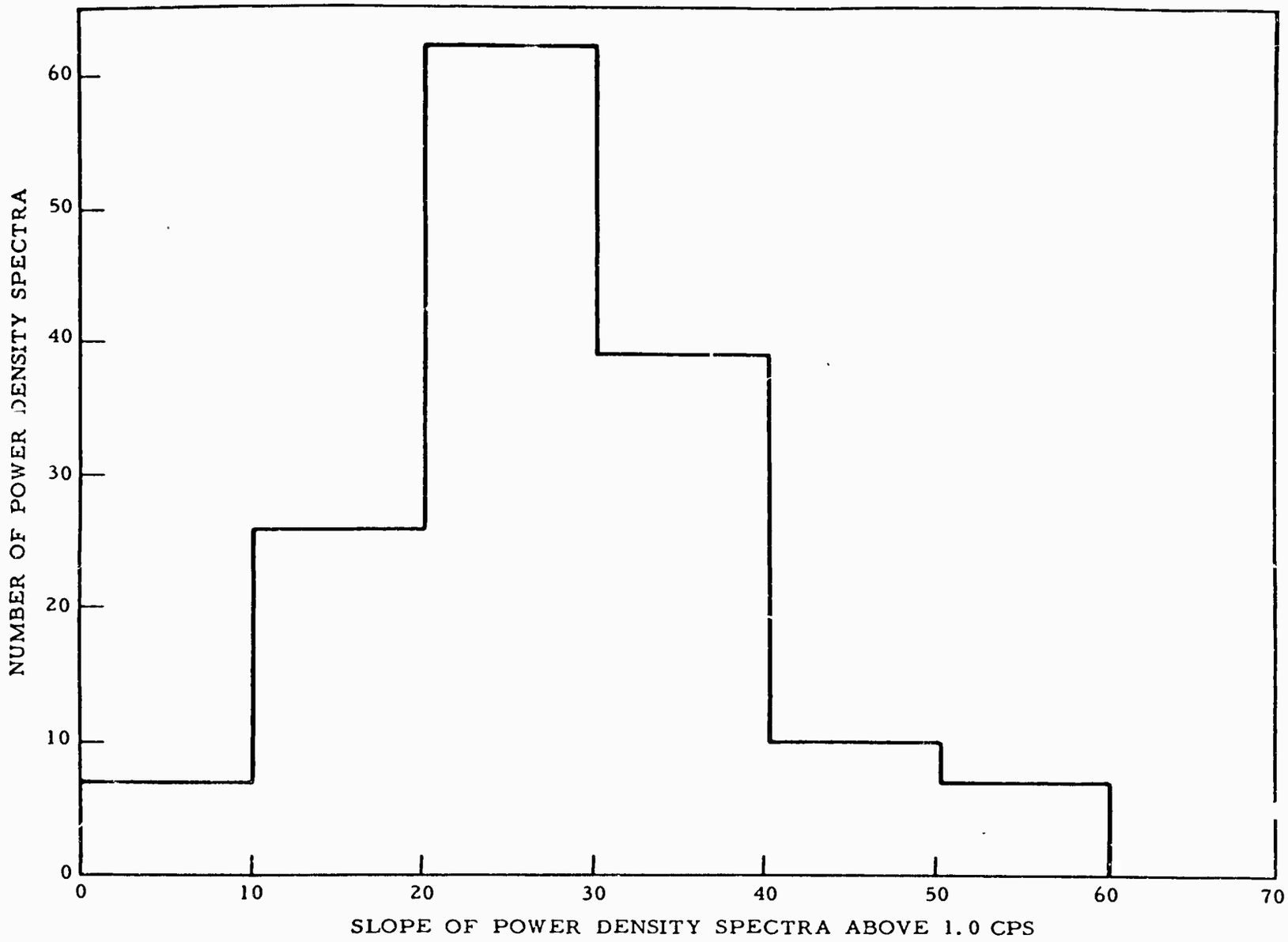

Figure III-1. Comparison of Spectra Slopes at Frequency of 1.0 CPS or Greater

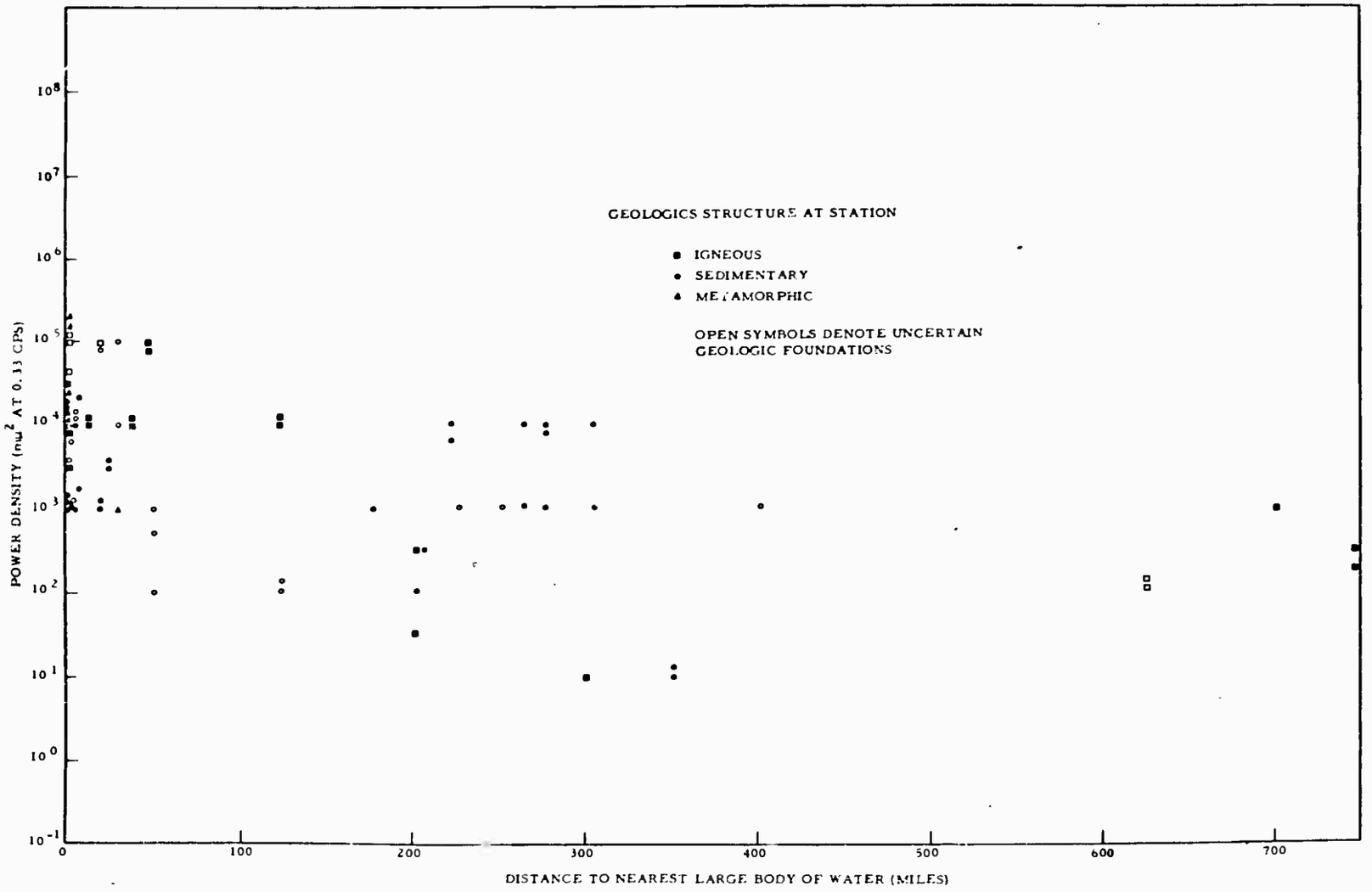

Figure III-2. Power Density (Frequency = 0.33 cps) vs Distance of Station From Large Body of Water

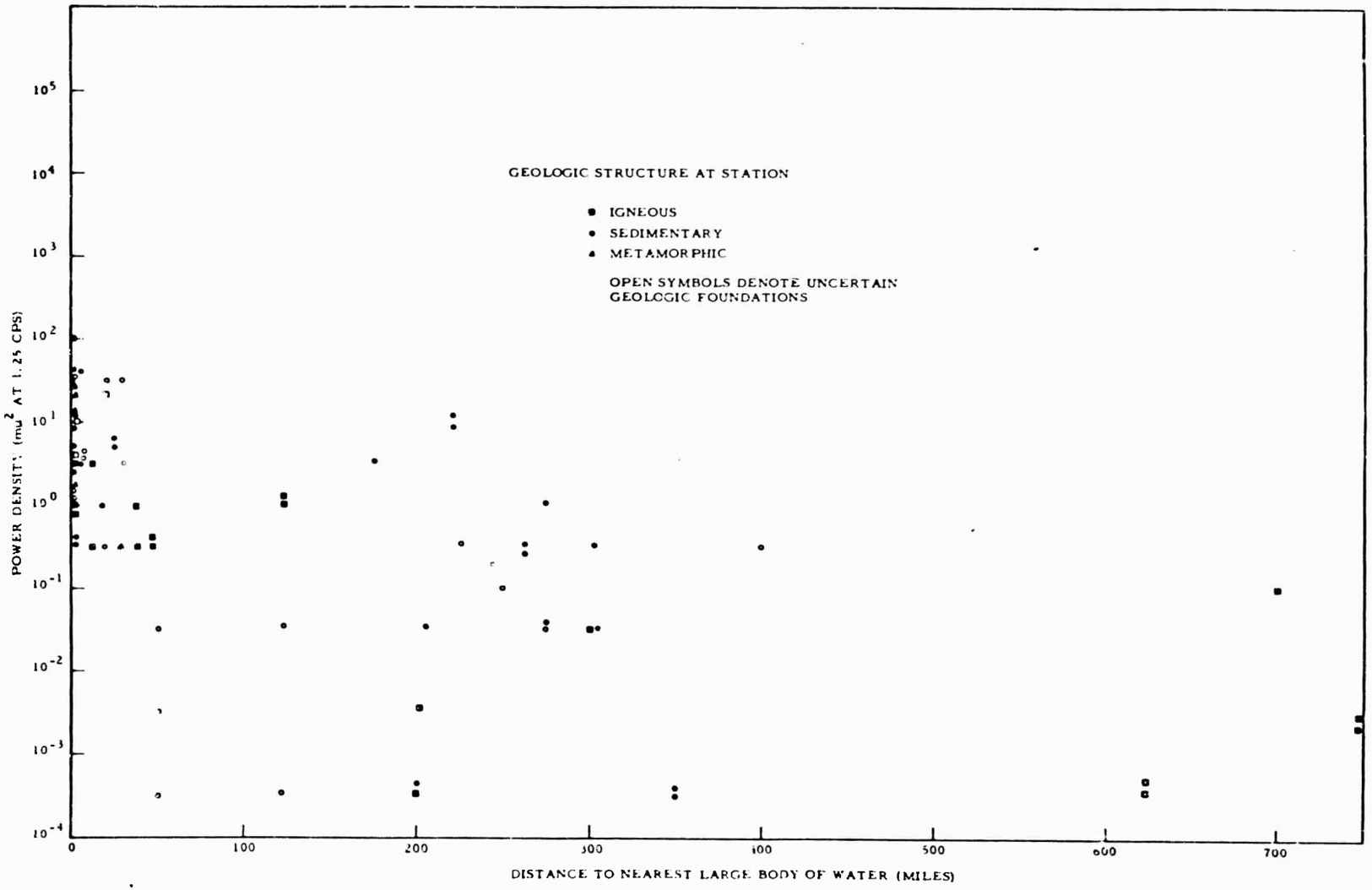

Figure III-3. Power Density (Frequency = 1.25 cps) vs Distance of Station From Large Body of Water

SECTION IV

VISUAL NOISE MEASUREMENTS

In addition to the noise power density spectra study, measurements and companions of average microseismic levels on a worldwide basis were made. Visual noise measurements were made at selected stations in order that noise levels could be compared. To improve station distribution, 35 mm records from the Canadian Network were obtained and used along with Worldwide Standard Station records.

Measurements of period and amplitude of the average maximum short-period and long-period noise on the respective instruments were made at each station. A comparison was made between one measurement each day, one measurement every other day, one measurement every third day and one measurement every fifth day at several stations. It was decided that ten measurements each month could be made and not significantly affect the average maximum measurements.

The measurements were taken at the same time at each station, within limits. Anomalous data, e.g., long-period noise on short-period instruments, were eliminated by limiting the measurements to noise in the 0.5 to 2.0 sec period range as the short-period instruments and the 3.0 to 8.0 sec period range on the long-period instruments.

The measurements were converted to ground motion using the approximate response curves (Figure IV-1 - USC&GS Standard Stations; Figure IV-2 - Canadian Network Stations) and averaged for each month.

Contour maps of the average maximum noise for each month were constructed. These maps are contained in Appendix B. Only nine months of the year were included as data for July, August and September were not available when data reduction was terminated.

To assure consistency in measuring techniques, the measurements were made by one person, and one analyst was responsible for data reduction and the preparing of the maps.

Several large areas of the world have sparse data available for this study. An attempt has been made to subjectively qualify the maps. Solid lines indicate adequate control points and dashed lines indicate a lack of control points.

As can be seen from the maps, the noise level increases during the winter months and, as was expected, the noise level was attenuated at continental structures.

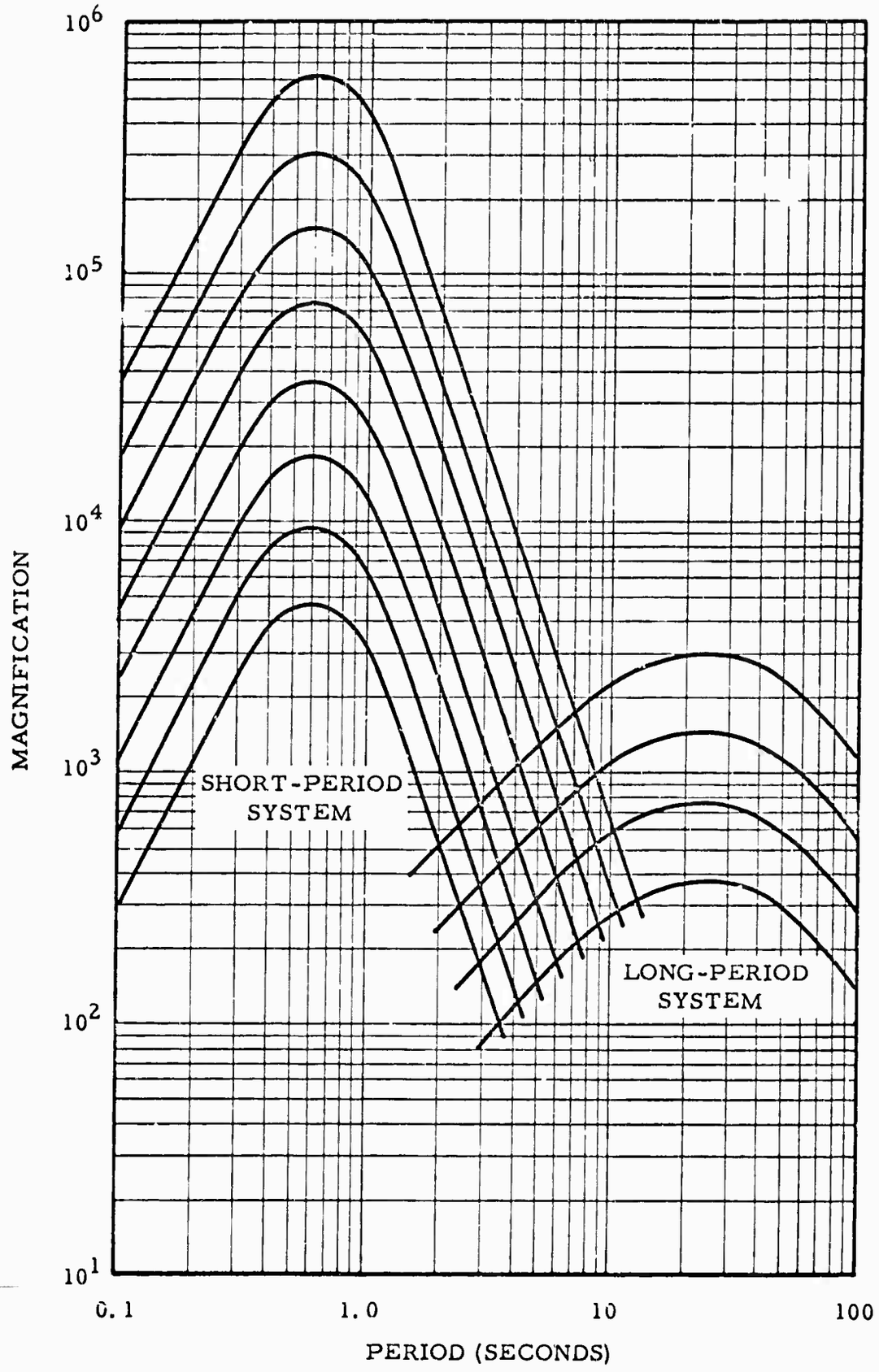

Figure IV-1. Frequency Response of the USC&GS World-Wide Standard Seismograph Systems

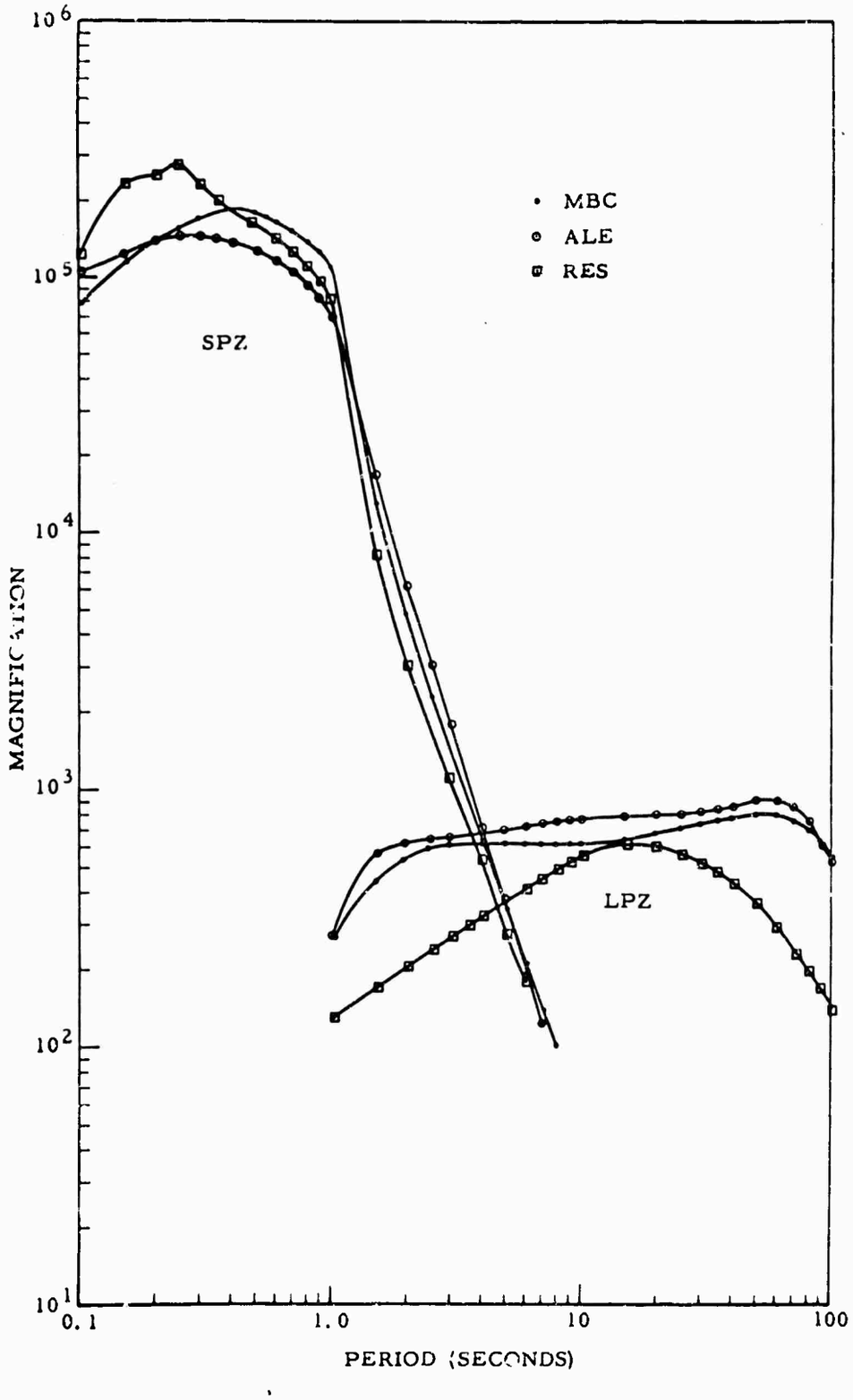

Figure IV-2. Frequency Response of the Canadian Network Seismograph Systems (Vertical Components)

Microseisms studies are needed in conjunction with seismicity studies to obtain a better understanding of the noise that can be expected at various stations around the world. This noise can be used to calculate the theoretical limits of perceptibility for each station.

Microseisms studies should also add to the knowledge of seasonal variations at the stations studied. This information could aid in determining what stations, if any, should change their gains to cope with these variations.

The 1963 microseisms study yielded the following results as to the gain and noise at the stations studied.

List of Stations with Cultural Noise Limiting the Gain

Addis Ababa, Ethiopia
Ann Arbor, Michigan
Athens, Greece
Baguio, Philippines
Bogota, Colombia
Helwan, Egypt
Hong Kong
La Paz, Bolivia
Lubbock, Texas
Malaga, Spain
Minneapolis, Minnesota
Quito, Ecuador
Rabaul, New Britain
Stuttgart, West Germany

List of Stations with Noise in the 4-8 Second Range on SP Instruments

Albuquerque, New Mexico
Blacksburg, Virginia
Bulawayo, Southern Rhodesia
Chiengmai, Thailand
Golden, Colorado
Kipapa, Hawaii
Kongsberg, Norway
State College, Pennsylvania
South Pole, Antarctica
Tasmanian University, Tasmania
Tucson, Arizona

List of Stations Where Gains Could Be Raised

Chiengmai, Thailand (LP only)
Hong Kong
Nairobi, Kenya (only if better photographic technique employed)
New Delhi, India

Any further work in this area should include more stations as they become available and, if no World Standard Stations are available for areas such as Eastern South America and Western Africa, reliably calibrated non-Standard station data should be used.

The overall quality of the film reproductions used in this study varied widely from excellent to, in a few cases, unuseable. The reasons

t at some records were unuseable could, in some cases, be attributed to p reproductions while others were due to poor original grams. In addition, m stations had excessive trace width which made accurate measurements of low noise levels difficult.

The most common problem of the World Standard Network records, as a whole, is excessive drift on the long-period horizontal instruments, possibly caused by inadequately insulated vaults.

SECTION V

RECOMMENDATIONS

1. Noise background studies are greatly improved if a technique of obtaining power density spectra is used.

2. Continued worldwide effort should include gathering of meteorological information to aid in the interpretation of spectra.

3. Any additional effort to investigate worldwide microseisms should have as a prime objective the association of spectra and observations with existing theories of microseisms origin.

4. Additional theoretical and practical work should be associated to explain constant microseismic background apparently not associated with storms, fronts, etc.

APPENDIX A

ABSOLUTE POWER DENSITY SPECTRA

APPENDIX A

ABSOLUTE POWER DENSITY SPECTRA

This appendix contains absolute power density spectra obtained from the 1963 data. The station abbreviations are listed with the location of each station in Table A-1. The spectra are presented in Figures A-1a through A-1f. The list of stations used and the dates of the records are presented in Tables A-2a through A-2f for the associated spectral illustrations.

TABLE A-1

STATION ABBREVIATIONS

STATION	LOCATION	STATION	LOCATION
AAE	Addis Ababa, Ethiopia	KIP	Kipapa, Hawaii
ADE	Adelaide, S. Australia	KON	Kongsberg, Norway
AFI	Afiamalu, W. Samoa	LON	Longmire, Washington
ALQ	Albuquerque, New Mexico	MAL	Malaga, Spain
ANP	Anpu, Taiwan	MAN	Manila, Philippines
ATU	Athens, Greece	MDS	Madison, Wisconsin
BAG	Baguio, Philippines	MUN	Mundaring, W. Australia
BKS	Berkeley, California	NAI	Nairobi, Kenya
BLA	Blacksburg, Virginia	NUR	Nurmijarvi, Finland
BUL	Bulawayo, S. Rhodesia	PLM	Palomar, California
CCG	Camp Century, Greenland	PMG	Port Moresby, New Guinea
CHG	Chiengmai, Thailand	PRE	Pretoria, S. Africa
CMC	Copper Mine, Canada	PTO	Porto, Portugal
COP	Copenhagen, Denmark	QUE	Quetta, W. Pakistan
COR	Corvallis, Oregon	SCP	State College, Pennsylvania
GDH	Godhavn, Greenland	SEO	Seoul, S. Korea
GOL	Golden, Colorado	SHL	Shillong, India
GSC	Goldstone, California	SPA	South Pole, Antarctica
GUA	Guam, Mariana Islands	TOL	Toledo, Spain
HUR	Honiara, Solomon Islands	VAL	Valentia, Ireland
IST	Istanbul, Turkey	WES	Weston, Massachusetts
KEV	Kevo, Finland	WIN	Windhoek, S. Africa

TABLE A-2a

ABSOLUTE POWER DENSITY SPECTRA LOCATED IN FIGURE A-1a

STATION	DATE	COMPONENT	GAIN(K)
AAE	16 January	SPZ	25
ADE	15 January	SPZ	25
ADE	15 January	SPN	25
ADE	15 January	SPE	25
ADE	16 April	SPZ	25
AFI	16 January	SPZ	12.5
ALQ	7 January	SPZ	200
ALQ	19 April	SPZ	400
ALQ	19 April	SPN	400
ALQ	19 April	SPE	400
ANP	14 April	SPZ	6.25
ANP	28 April	SPZ	6.25
ANP	28 April	SPN	6.25
ANP	28 April	SPE	6.25
ATU	16 January	SPZ	12.5
ATU	19 April	SPZ	12.5
ATU	19 April	SPN	12.5
ATU	19 April	SPE	12.5
BAG	21 January	SPZ	25
BAG	21 January	SPN	25
BAG	21 January	SPE	25
BAG	19 April	SPZ	25
BAG	19 April	SPN	25
BAG	19 April	SPE	25
BKS	10 January	SPZ	25

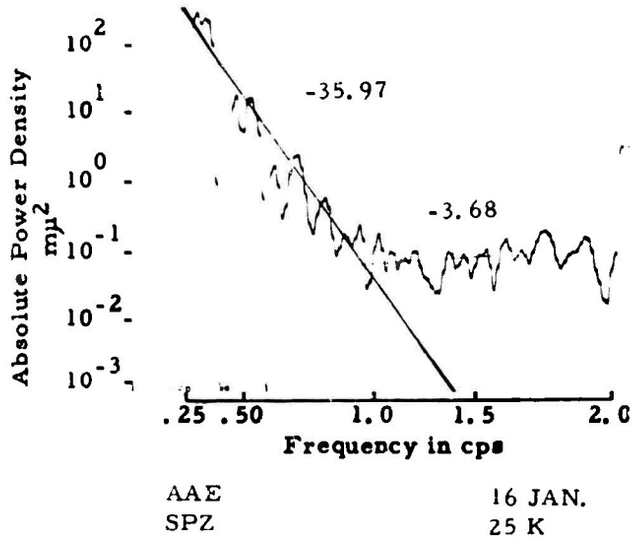

AAE
SPZ
16 JAN.
25 K

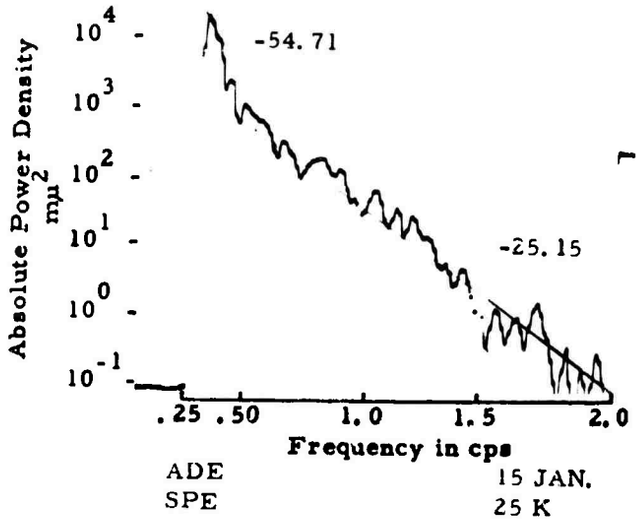

ADE
SPE
15 JAN.
25 K

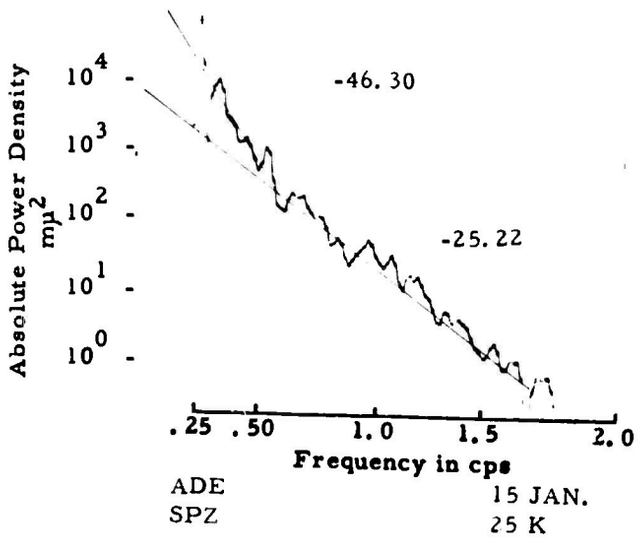

ADE
SPZ
15 JAN.
25 K

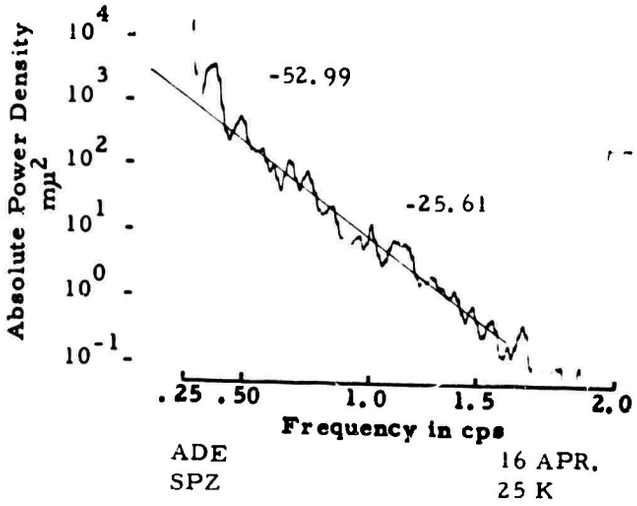

ADE
SPZ
16 APR.
25 K

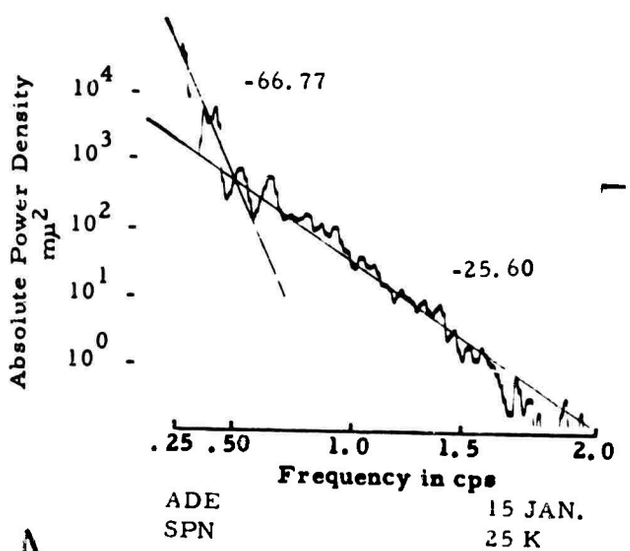

ADE
SPN
15 JAN.
25 K

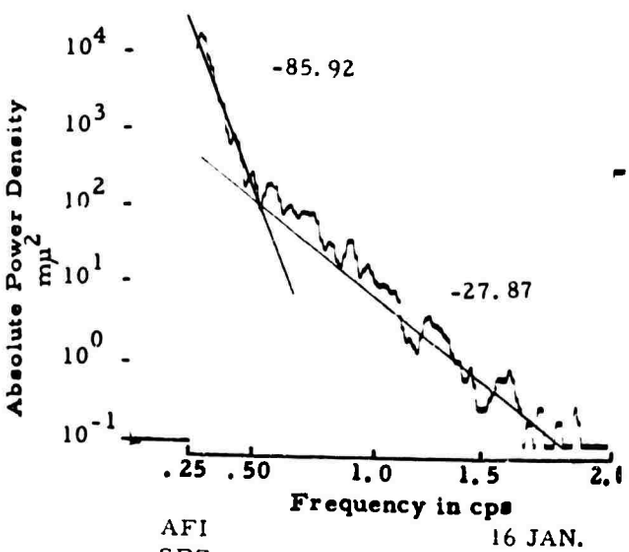

AFI
SPZ
16 JAN.
12.5 K

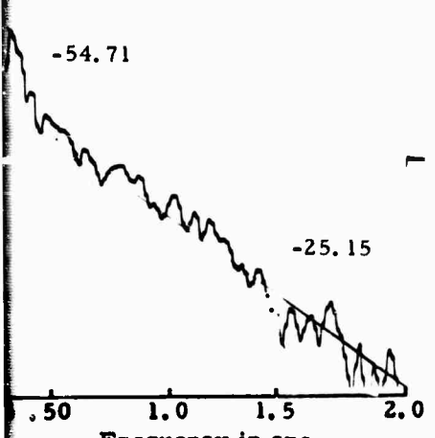

DE 15 JAN.
E 25 K

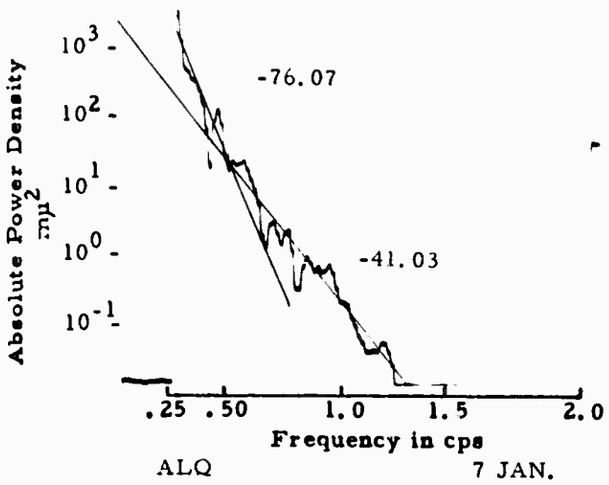

ALQ 7 JAN.
SPZ 200 K

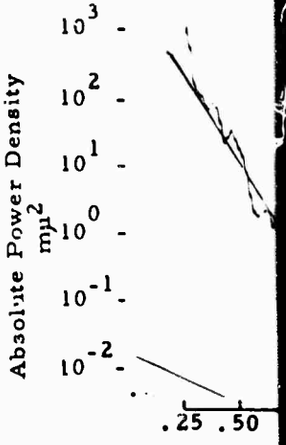

ALQ
SPE

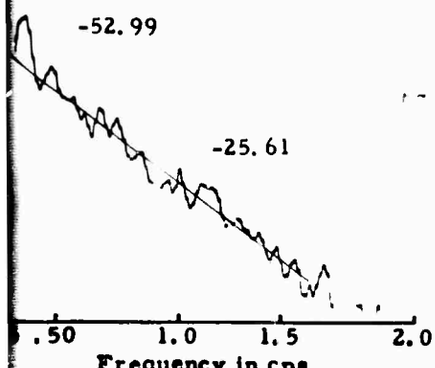

DE 16 APR.
Z 25 K

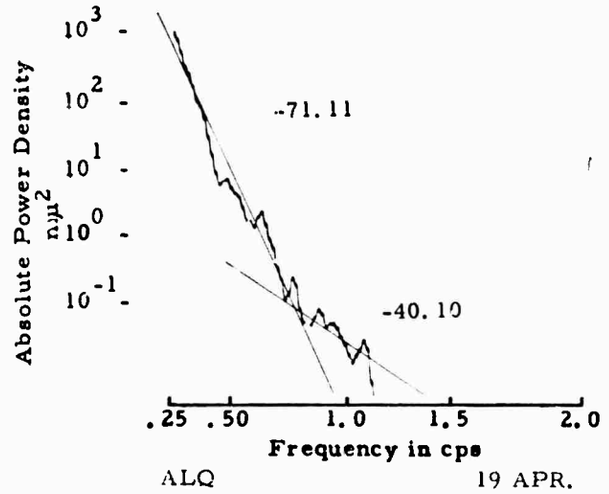

ALQ 19 APR.
SPZ 400 K

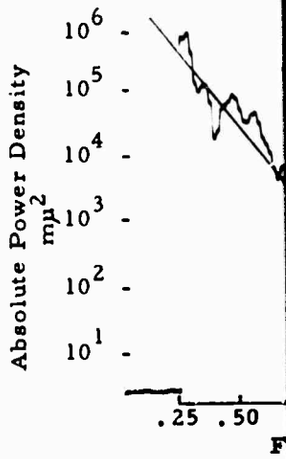

ANP
SPZ

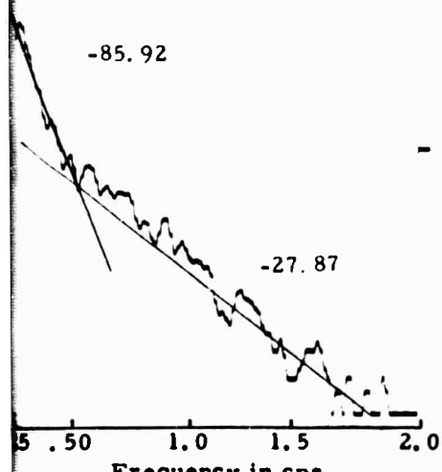

I 16 JAN.
Z 12.5 K

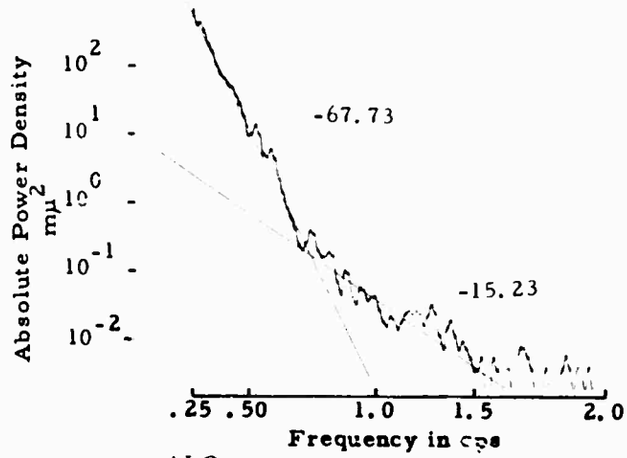

ALQ 19 APR.
SPN 400 K

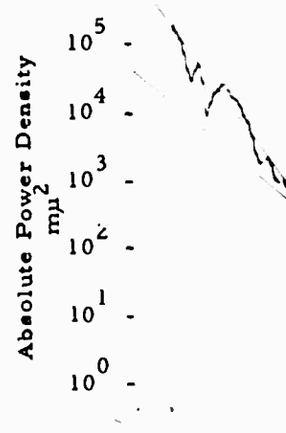

ANP
SPZ

B

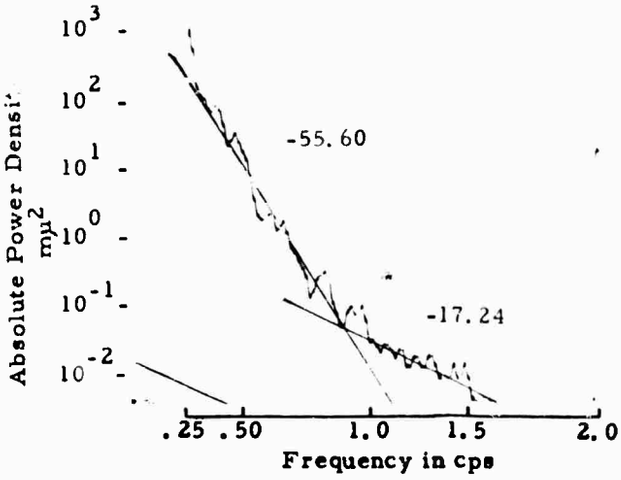

ALQ 19 APR.
SPE 400 K

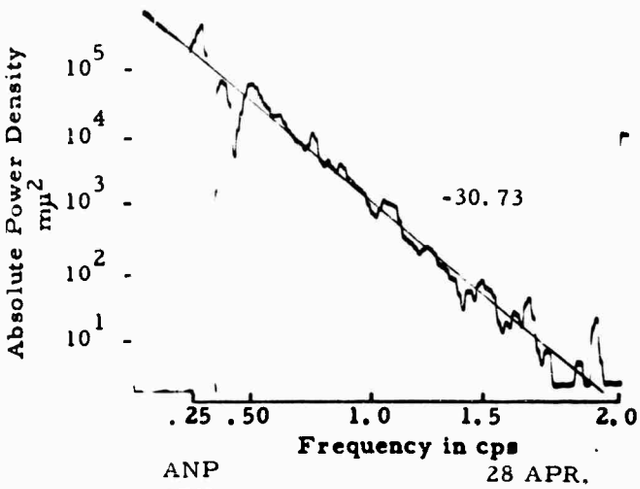

ANP 28 APR.
SPN 6.25 K

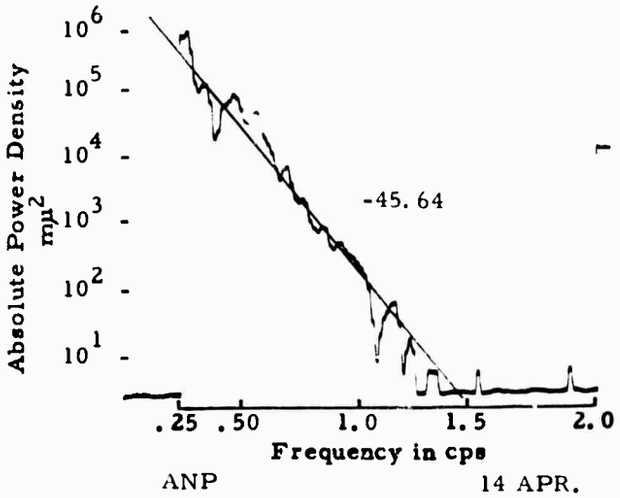

ANP 14 APR.
SPZ 6.25 K

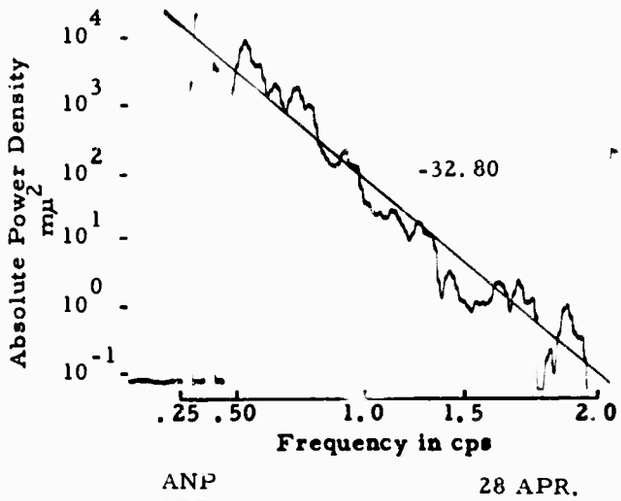

ANP 28 APR.
SPE 6.25 K

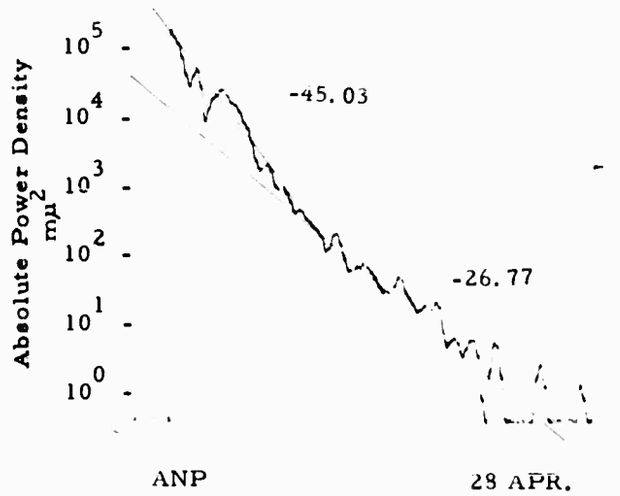

ANP 28 APR.
SPZ 6.25 K

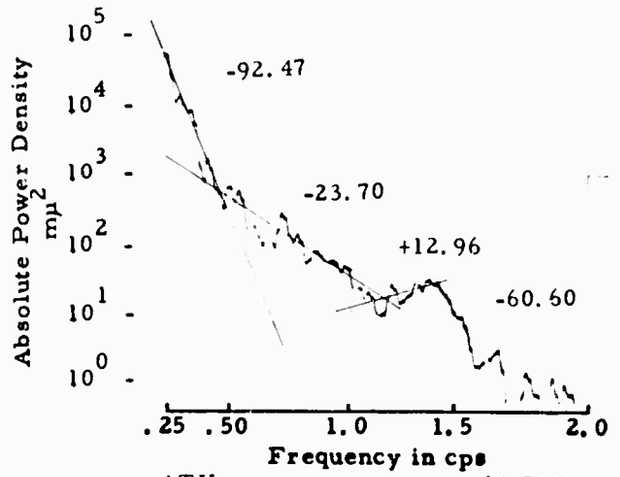

ATU 16 JAN.
SPZ 12.5 K

C

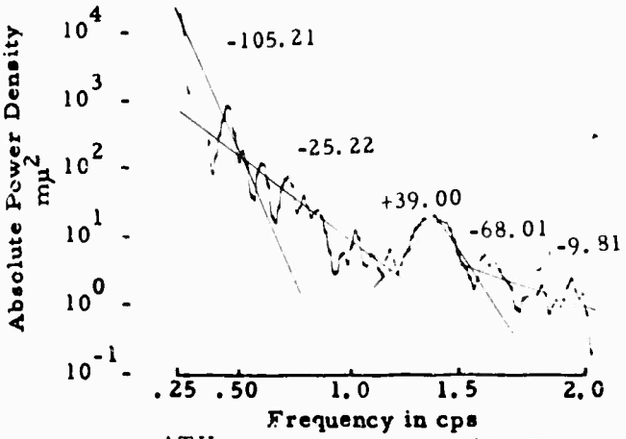

ATU 19 APR.
SPZ 12.5 K

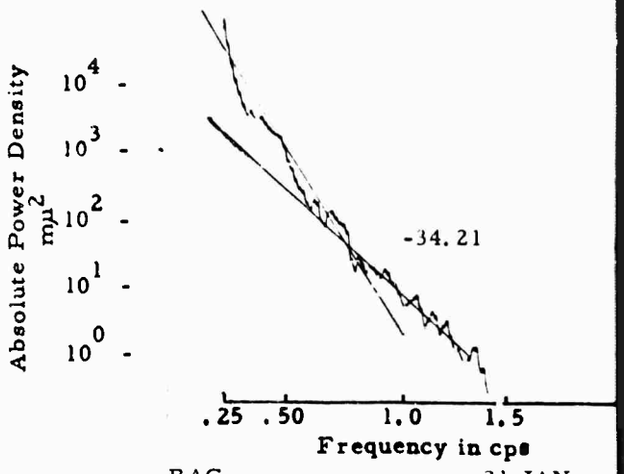

BAG 21 JAN.
SPZ 25 K

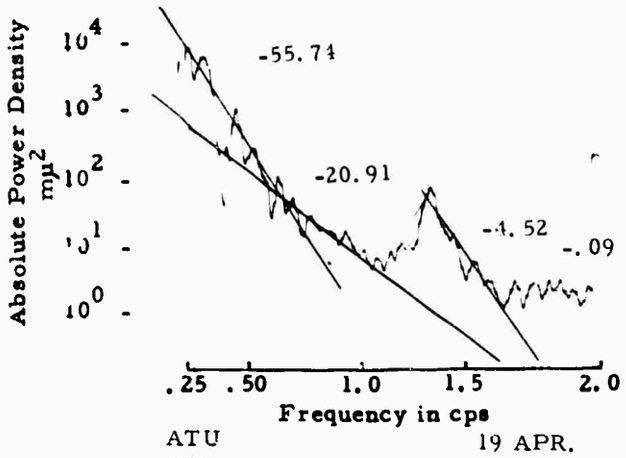

ATU 19 APR.
SPN 12.5 K

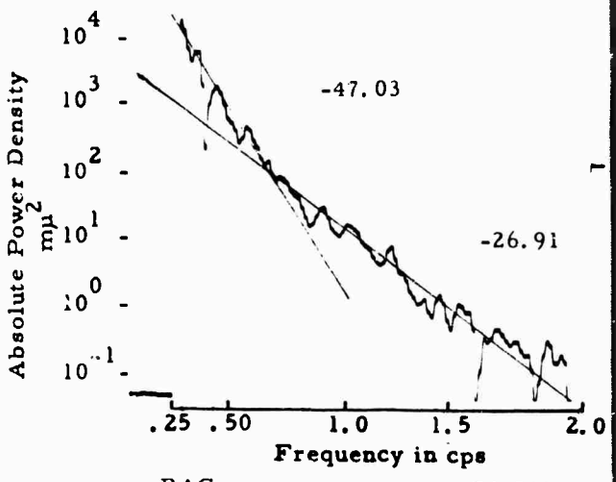

BAG 21 JAN.
SPN 25 K

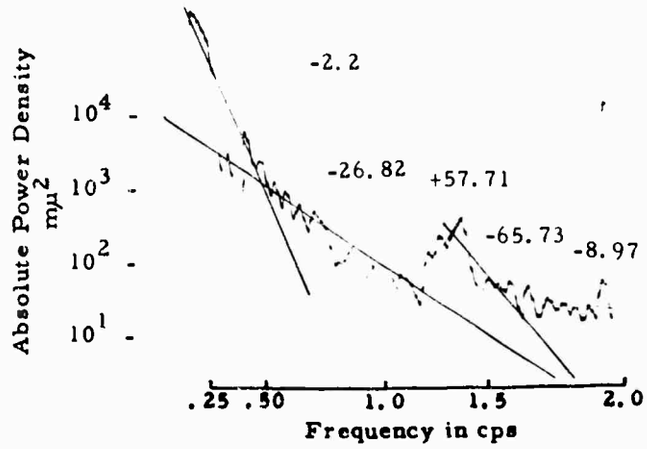

ATU 19 APR.
SPE 12.5 K

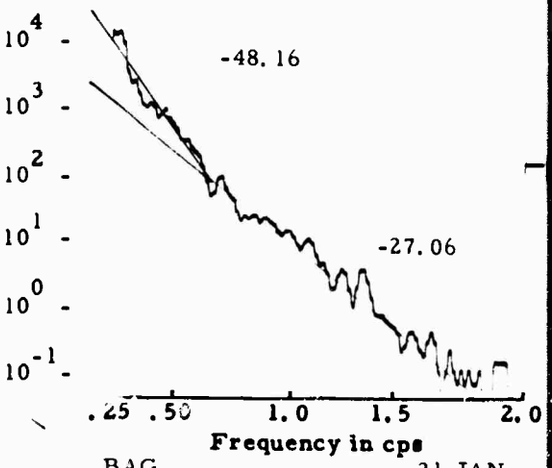

BAG 21 JAN.
SPE 25 K

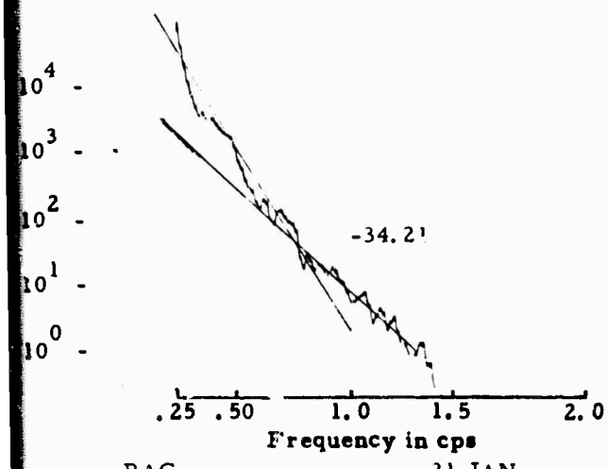

BAG 21 JAN.
SPZ 25 K

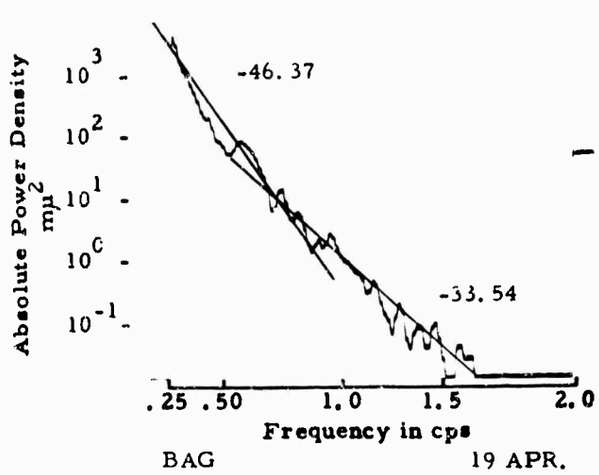

BAG 19 APR.
SPZ 25 K

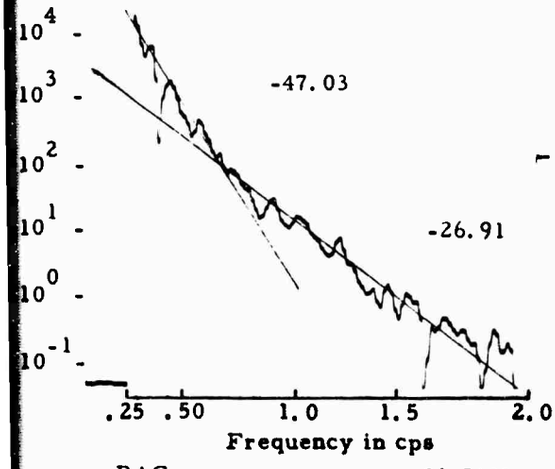

BAG 21 JAN.
SPN 25 K

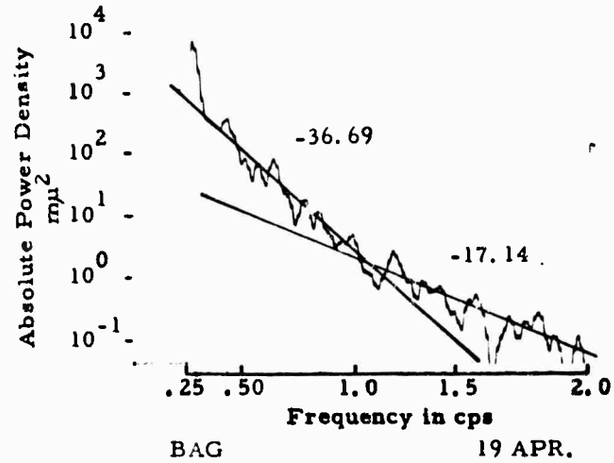

BAG 19 APR.
SPN 25 K

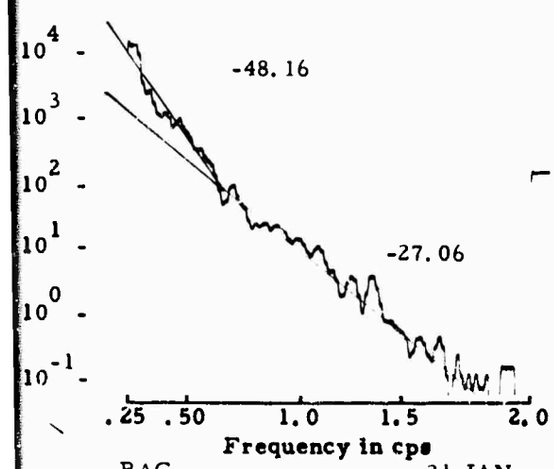

BAG 21 JAN.
SPE 25 K

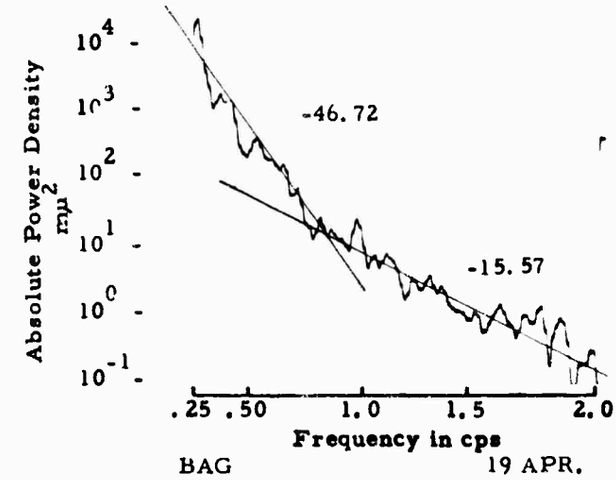

BAG 19 APR.
SPE 25 K

Figure A-1a. Absolute Power Density Spectra Obta

E

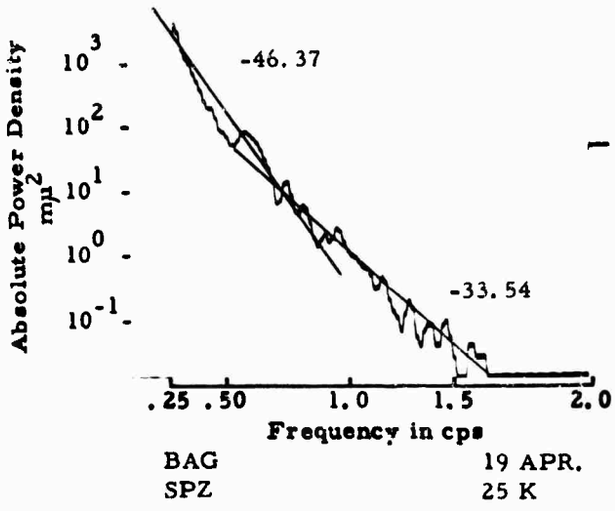

BAG 19 APR.
SPZ 25 K

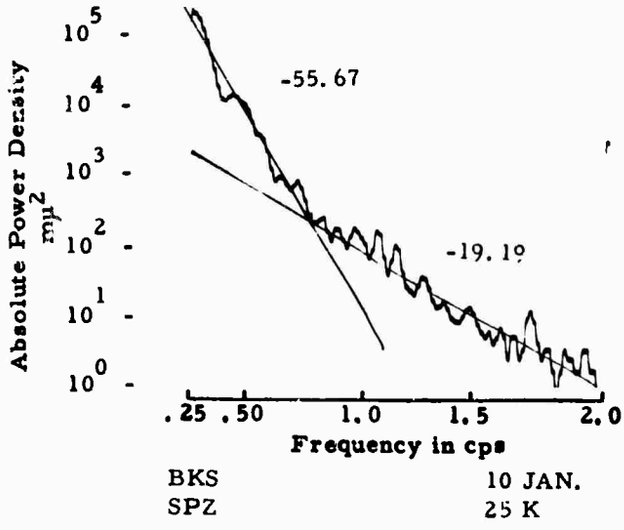

BKS 10 JAN.
SPZ 25 K

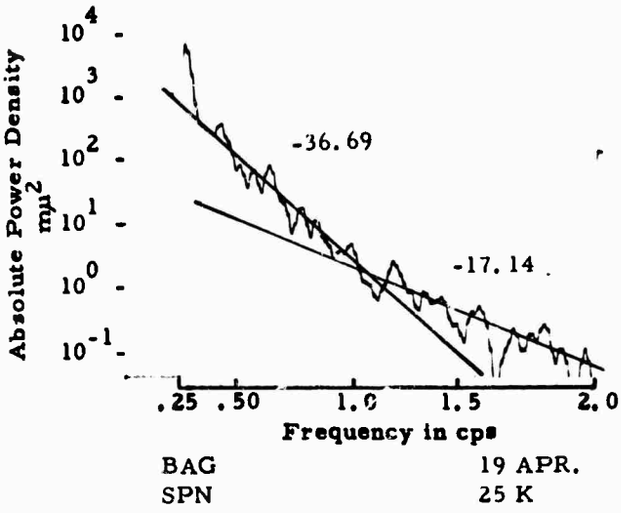

BAG 19 APR.
SPN 25 K

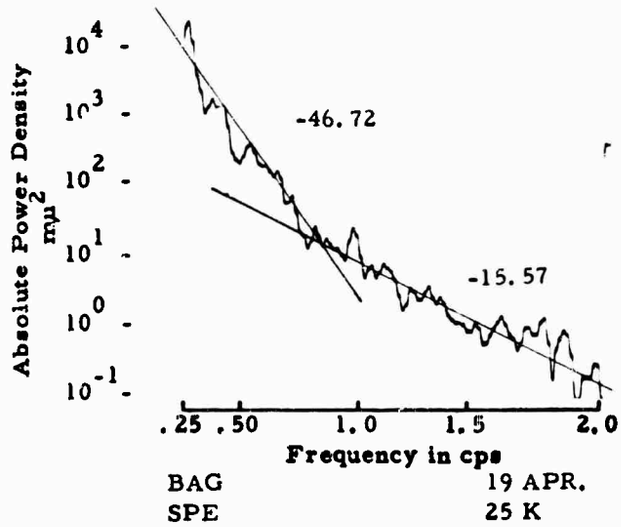

BAG 19 APR.
SPE 25 K

Figure A-1a. Absolute Power Density Spectra Obtained From 1963 Data

TABLE A-2b

ABSOLUTE POWER DENSITY SPECTRA LOCATED IN FIGURE A-1b

STATION	DATE	COMPONENT	GAIN(K)
BKS	19 April	SPZ	25
BKS	19 April	SPN	25
BKS	19 April	SPE	25
BLA	14 January	SPZ	50
BLA	10 April	SPZ	25
BUL	15 April	SPZ	100
CCG	7 April	SPZ	100
CHG	18 March	SPZ	400
CHG	7 June	SPZ	400
CHG	7 June	SPN	400
CHG	7 June	SPE	400
CMC	1 May	SPZ	200
CMC	1 May	SPN	200
CMC	1 May	SPE	200
COP	15 January	SPZ	12.5
COP	19 April	SPZ	12.5
COR	5 January	SPZ	25
COR	1 April	SPZ	25
GDH	16 January	SPZ	12.5
GOL	16 January	SPZ	400
GOL	5 April	SPZ	400
GSC	3 April	SPZ	200
GUA	26 May	SPZ	6.25
GUA	26 May	SPN	6.25
GUA	26 May	SPE	6.25
HNR	16 January	SPZ	12.5
HNR	16 January	SPN	12.5

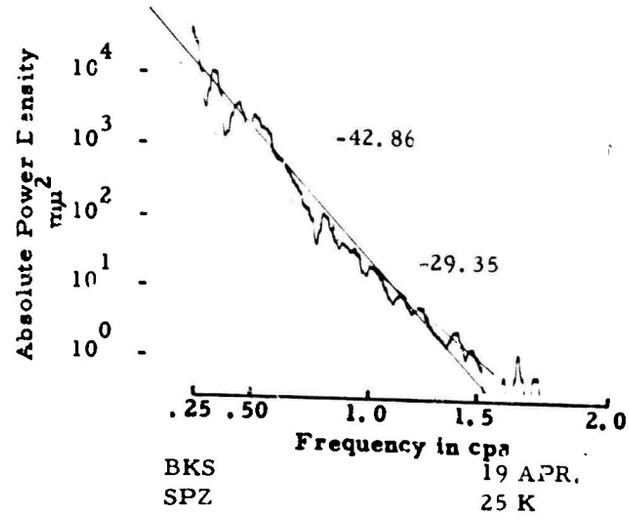

BKS 19 APR.
SPZ 25 K

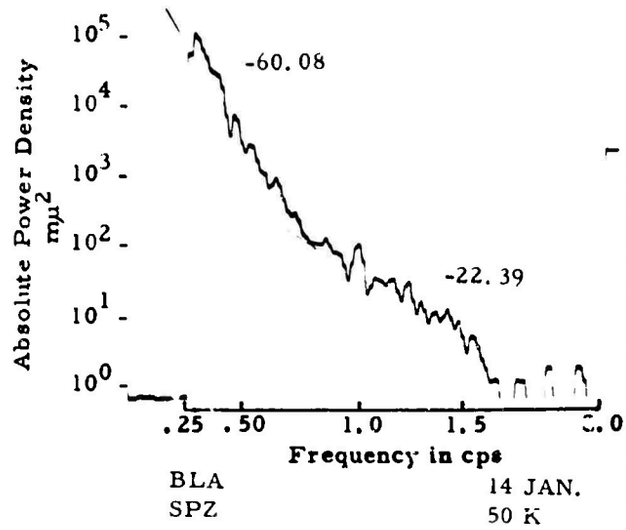

BLA 14 JAN.
SPZ 50 K

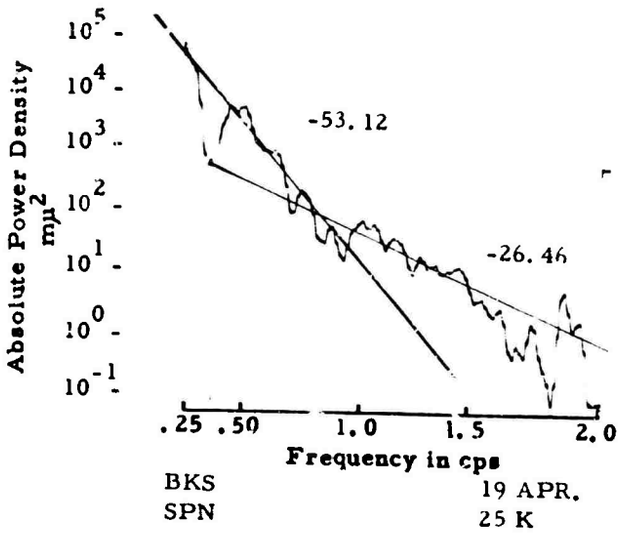

BKS 19 APR.
SPN 25 K

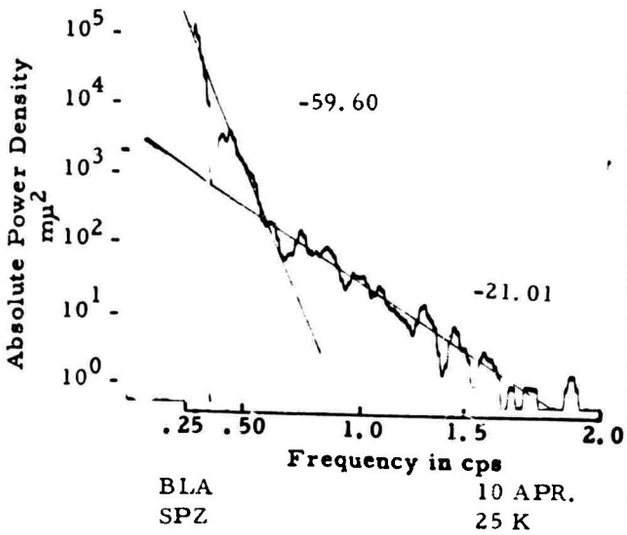

BLA 10 APR.
SPZ 25 K

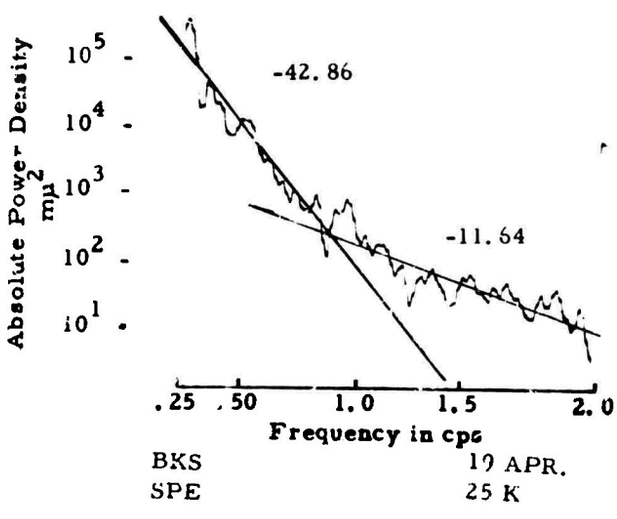

BKS 19 APR.
SPE 25 K

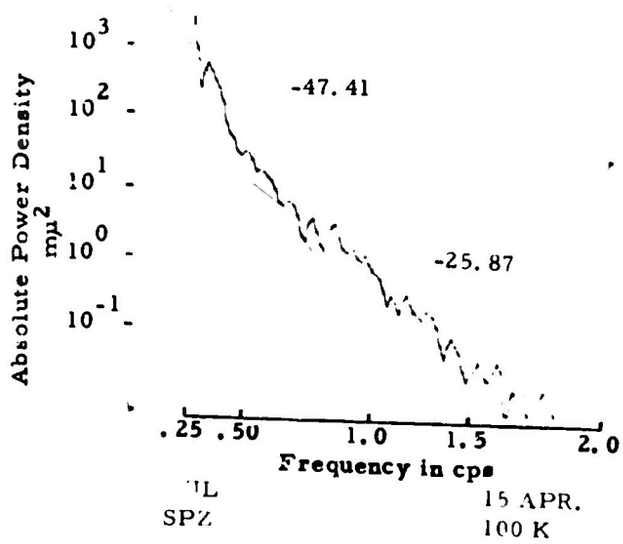

[illegible]L 15 APR.
SPZ 100 K

-22.39

1.5 2.0

cps

14 JAN.

50 K

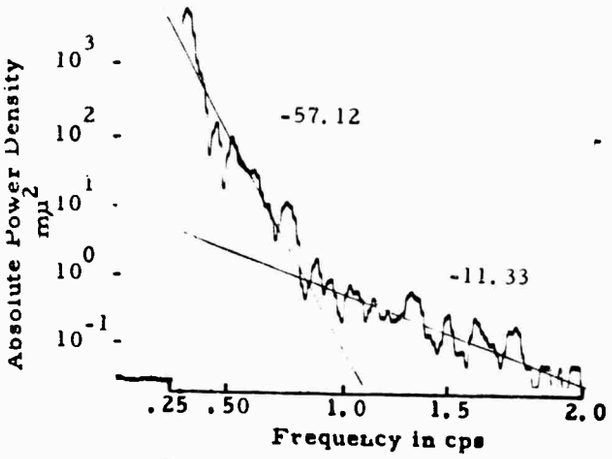

CCG

SPZ

7 APR.

100 K

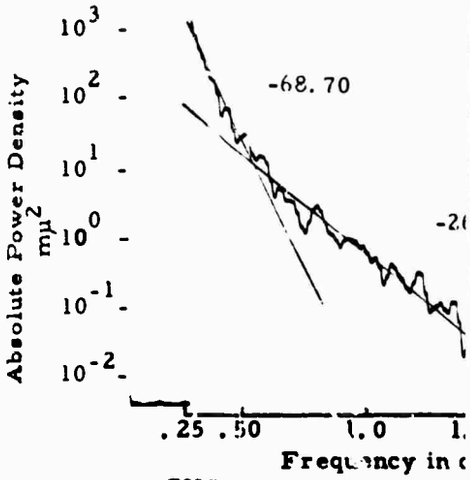

CHG

SPN

-21.01

1.5 2.0

cps

10 APR.

25 K

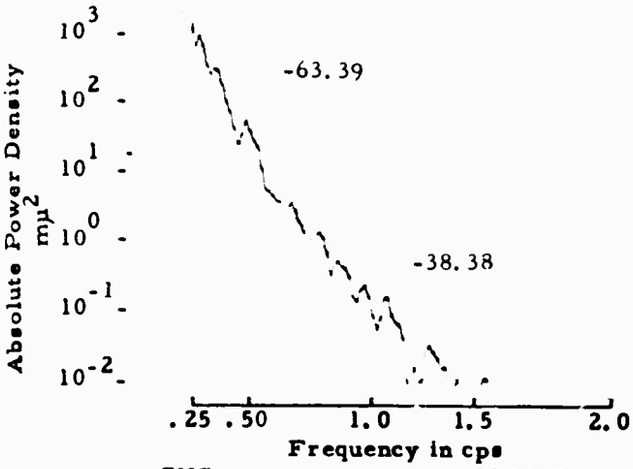

CHG

SPZ

18 MAR.

400 K

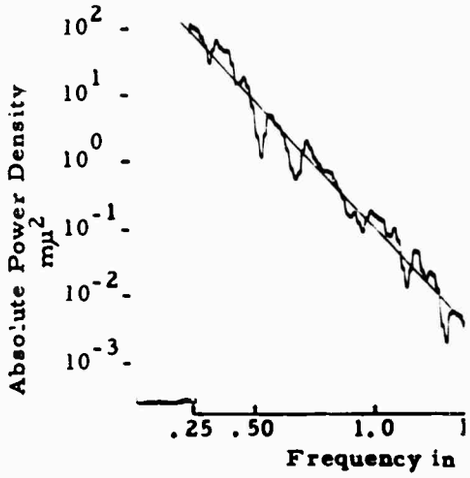

CHG

SPE

25.87

1.5 2.0

cps

15 APR.

100 K

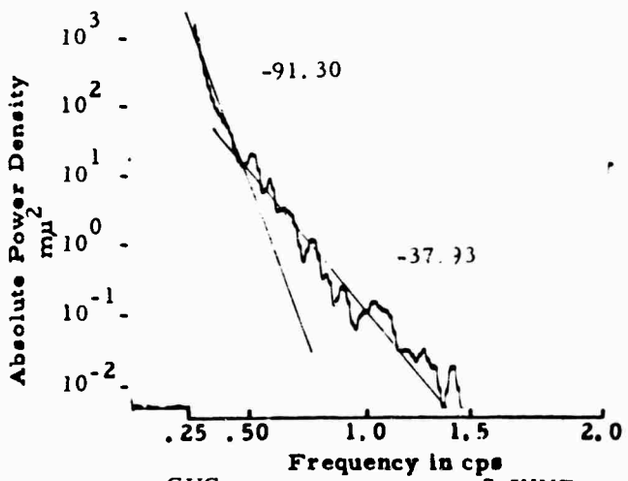

CHG

SPZ

7 JUNE

400 K

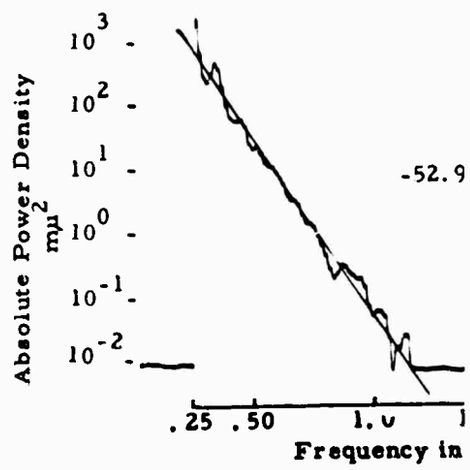

CMC

SPZ

B

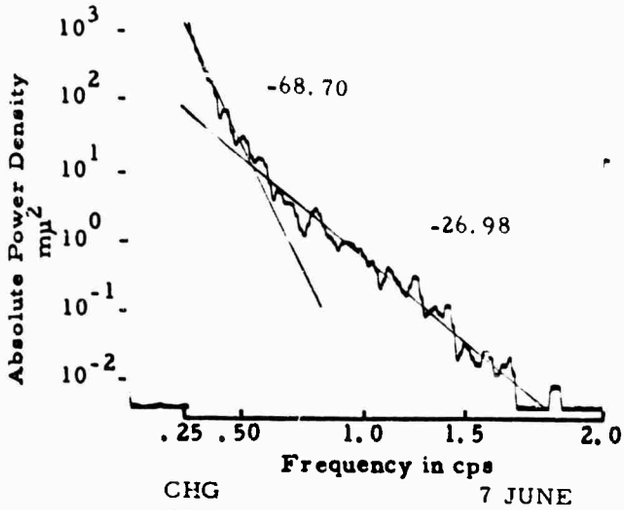

CHG 7 JUNE
SPN 400 K

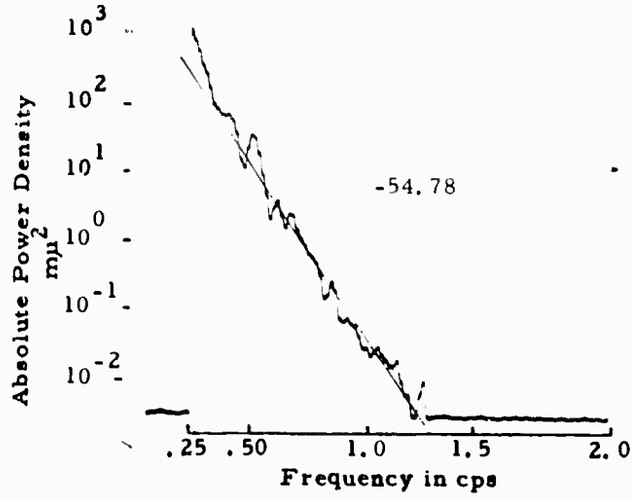

CMC 1 MAY
SPN 200 K

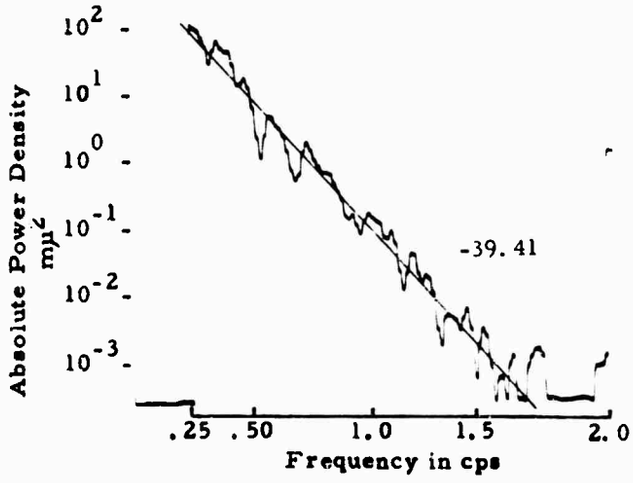

CHG 7 JUNE
SPE 400 K

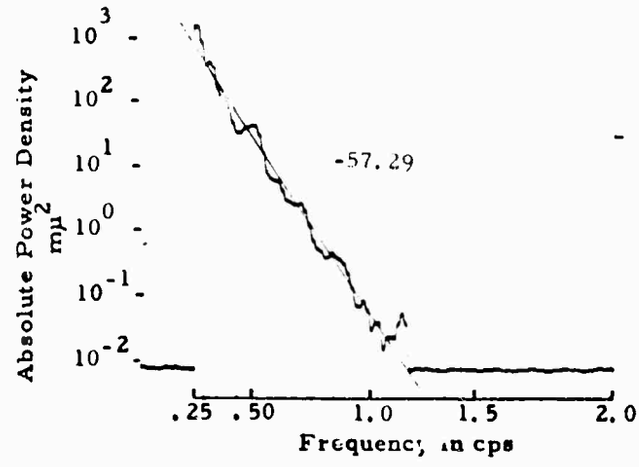

CMC 1 MAY
SPE 200 K

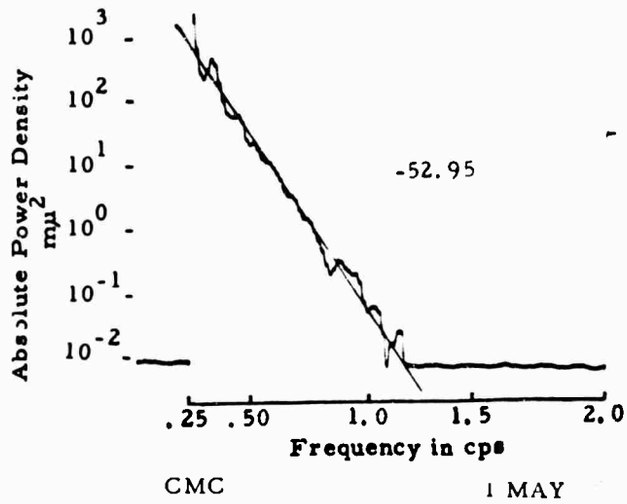

CMC 1 MAY
SPZ 200 K

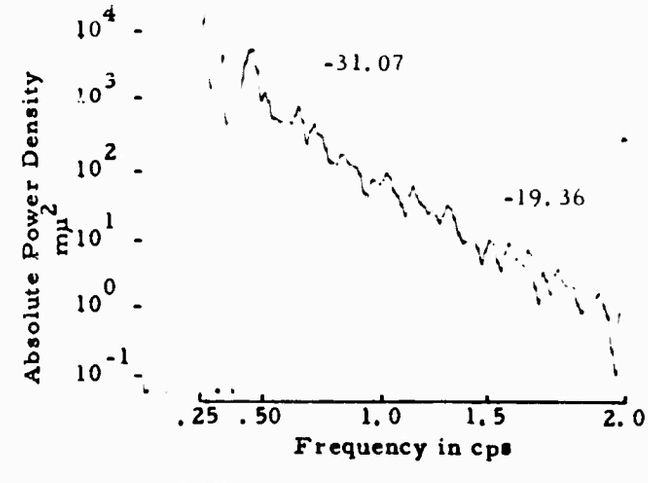

COP 15 JAN.
SPZ 12.5 K

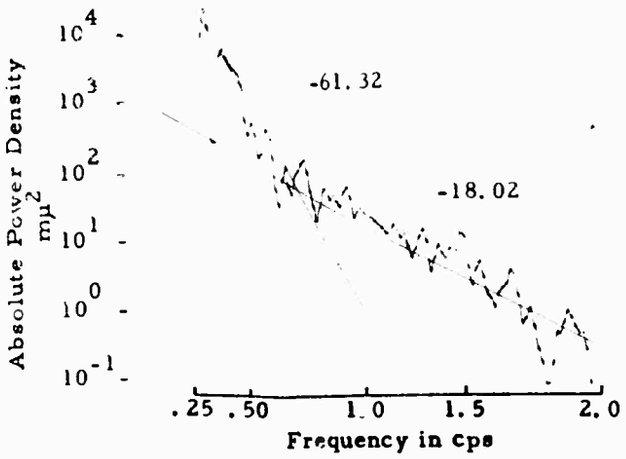

COP 19 APR.
SPZ 12.5 K

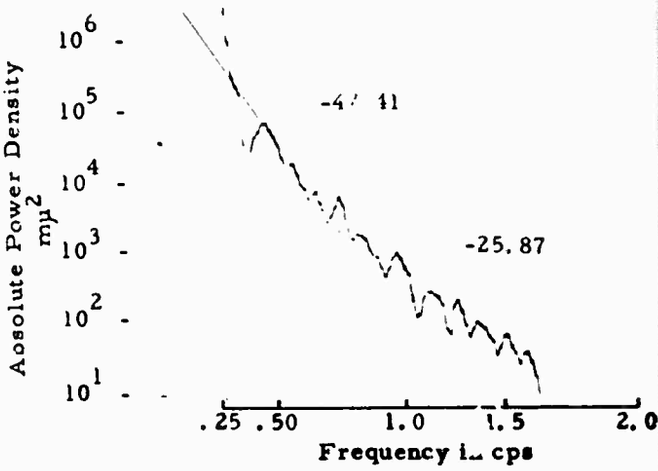

GDH 16 JAN.
SPZ 12.5 K

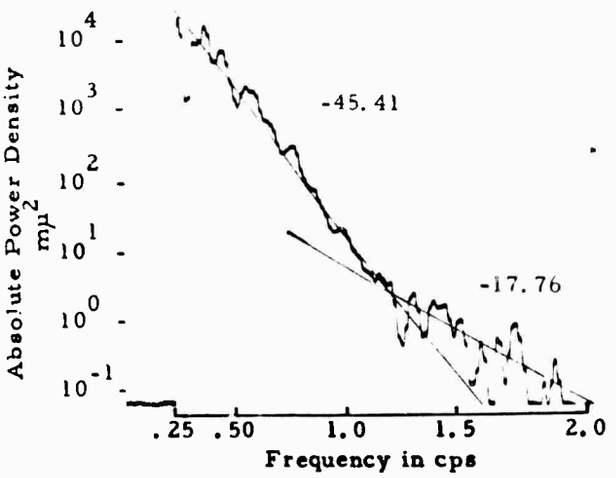

COR 5 JAN.
SPZ 25 K

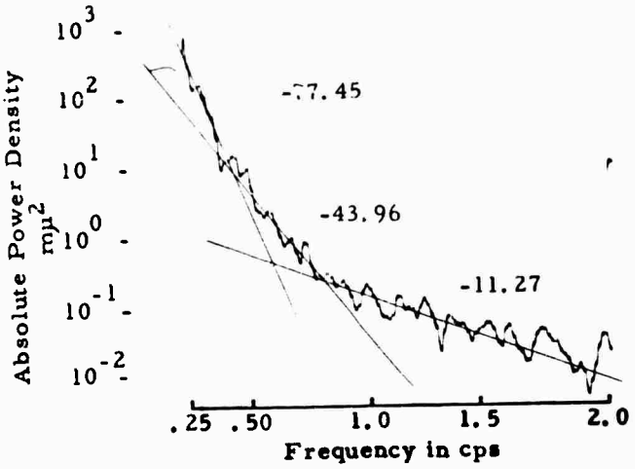

GOL 16 JAN.
SPZ 400 K

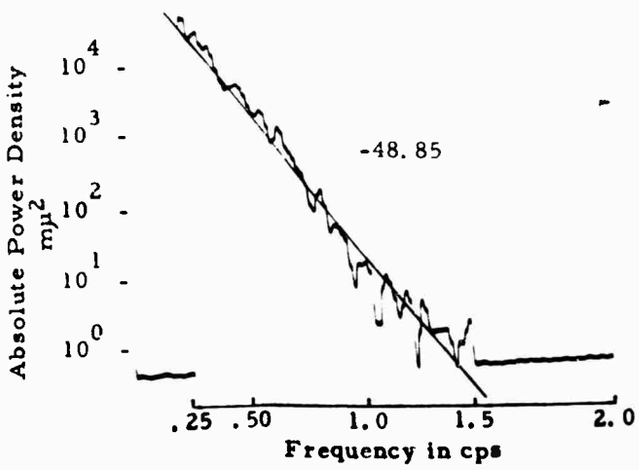

COR 1 APR.
SPZ 25 K

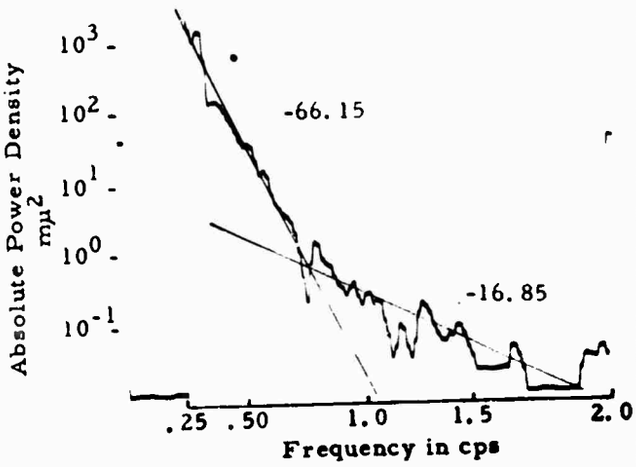

GOL 5 APR.
SPZ 400 K

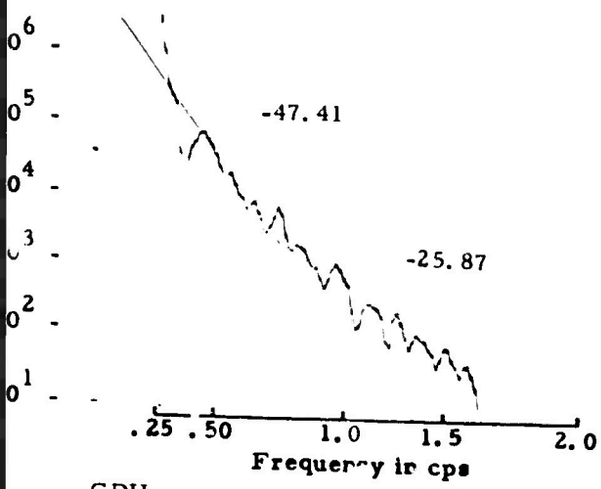

GDH
SPZ
16 JAN.
12.5 K

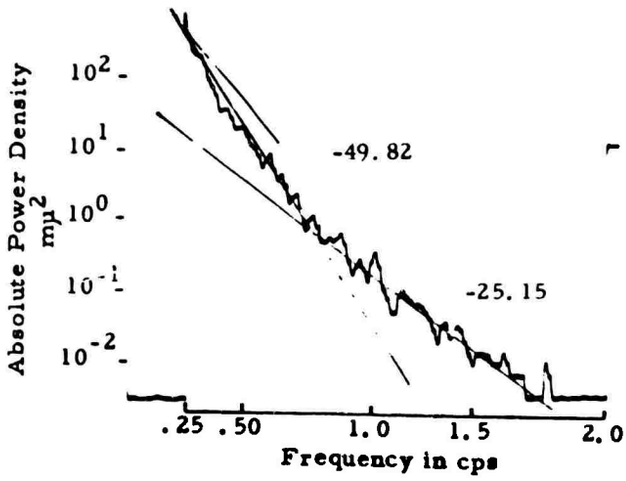

GSC
SPZ
3 APR.
200 K

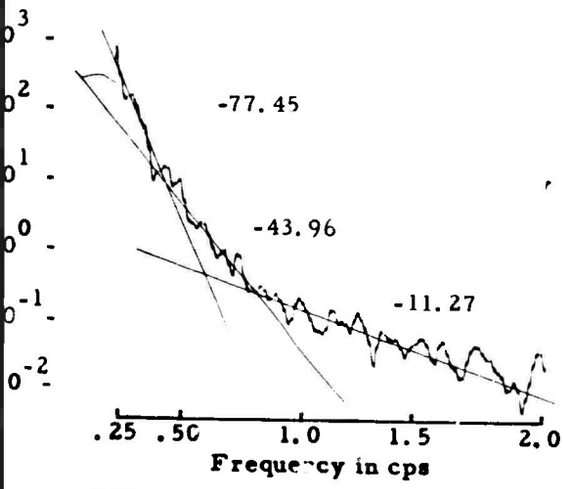

GOL
SPZ
16 JAN.
400 K

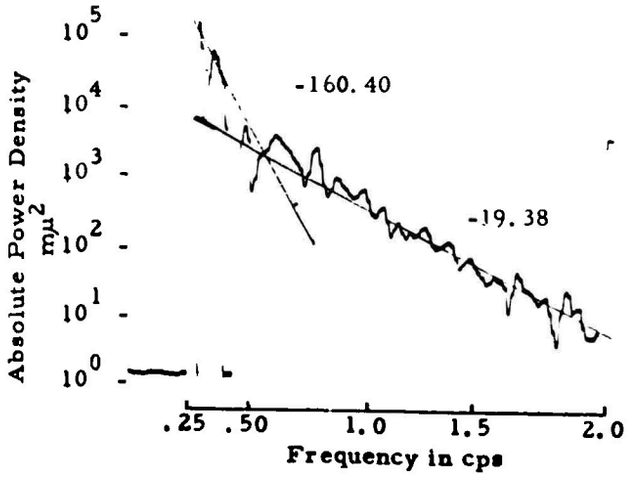

GUA
SFZ
26 MAY
6.25 K

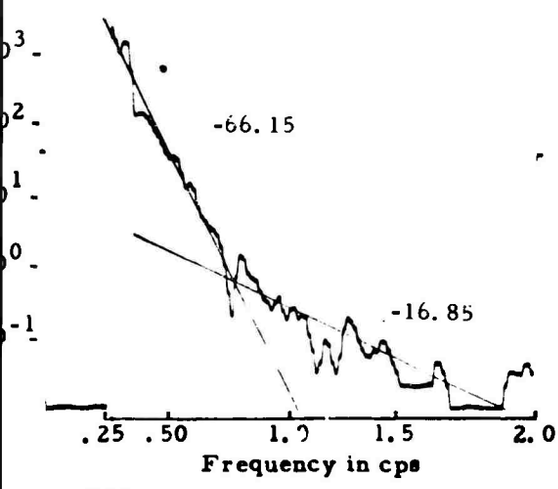

GOL
SPZ
5 APR.
400 K

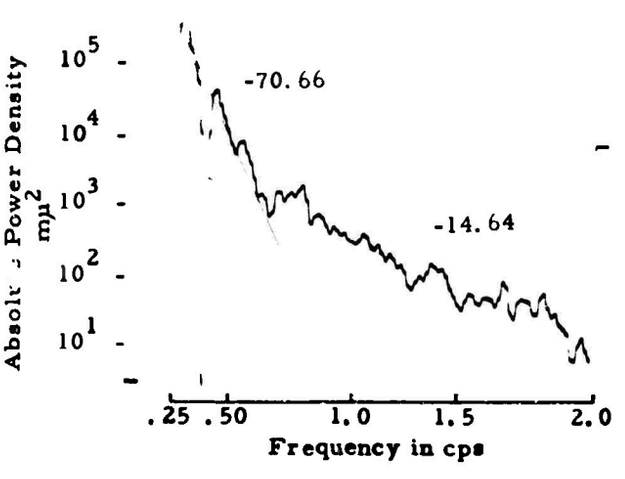

GUA
SPN
26 MAY
6.25 K

Figure A-1b. Absolute Power Density Spect

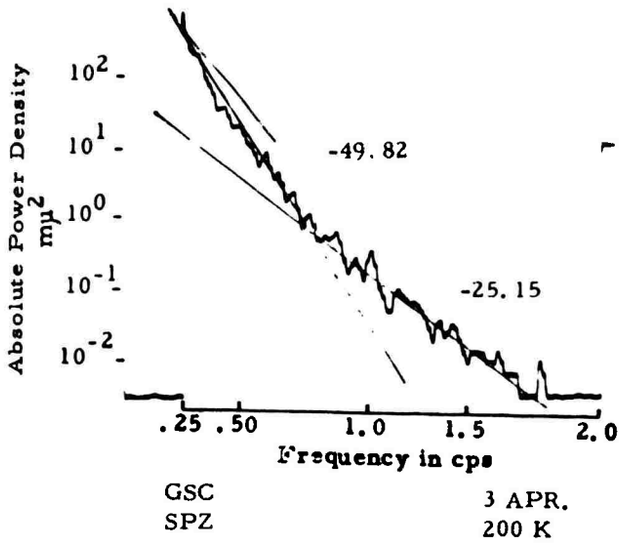

GSC 3 APR.
SPZ 200 K

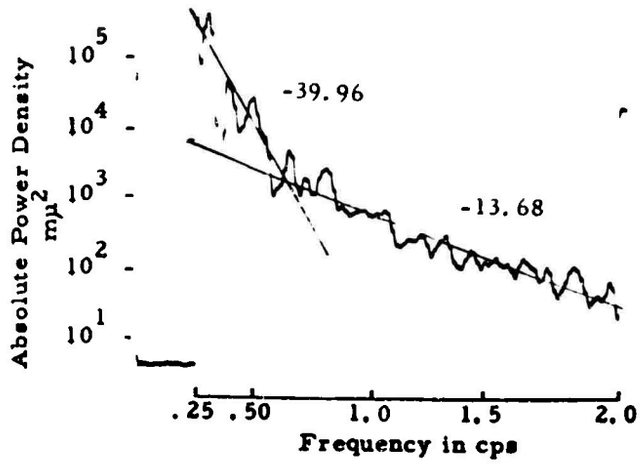

GUA 26 MAY
SPE 6.25 K

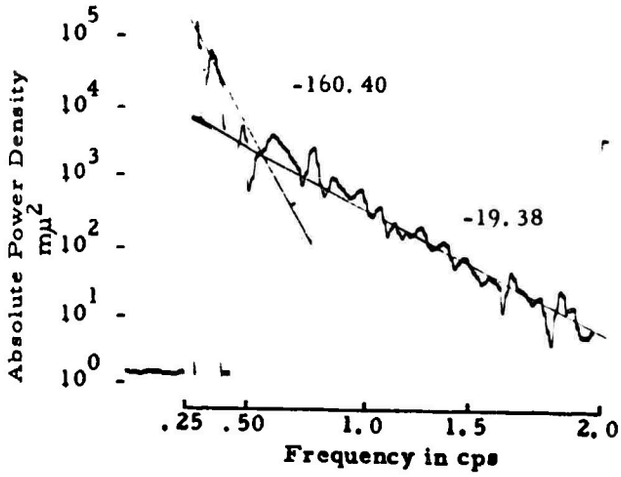

GUA 26 MAY
SPZ 6.25 K

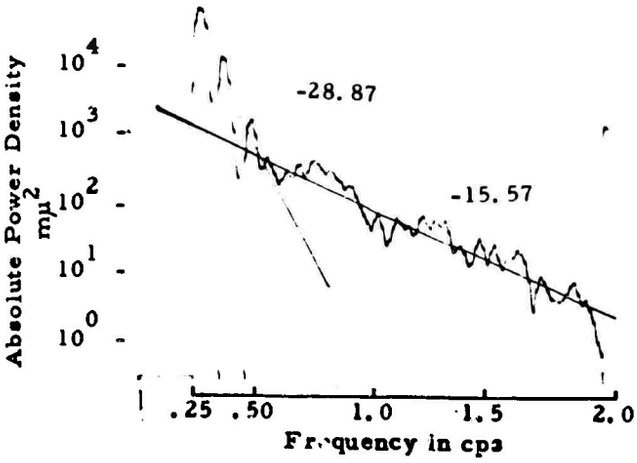

HNR 16 JAN.
SPZ 12.5 K

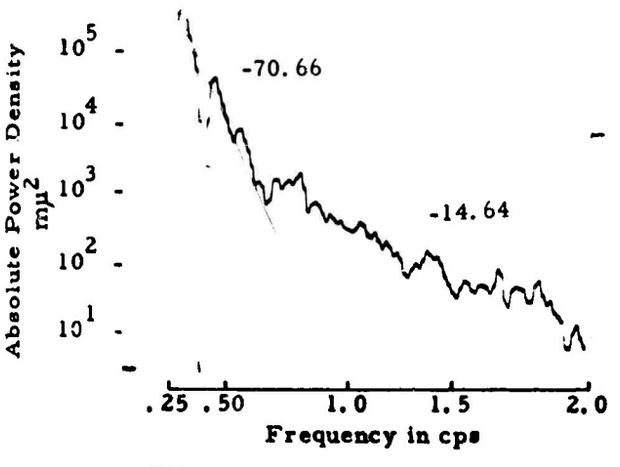

GUA 26 MAY
SPN 6.25 K

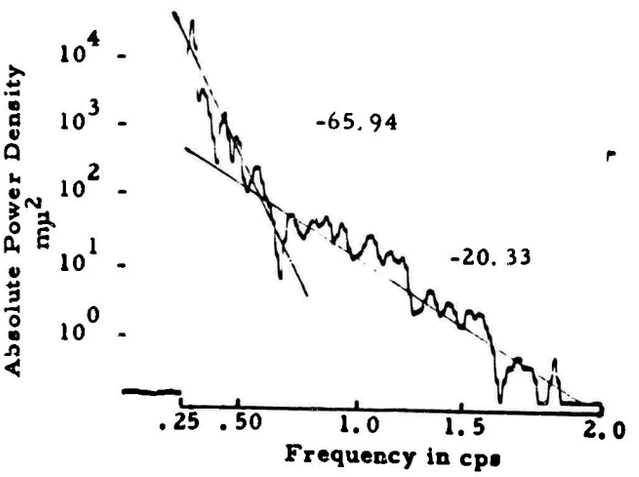

HNR 16 JAN.
SPN 12.5 K

Figure A-1b. Absolute Power Density Spectra Obtained From 1963 Data

TABLE A-2c

ABSOLUTE POWER DENSITY SPECTRA LOCATED IN FIGURE A-1c

STATION	DATE	COMPONENT	GAIN(K)
HNR	4 March	SPZ	12.5
IST	2 January	SPZ	25
IST	19 January	SPZ	25
IST	20 April	SPZ	25
IST	20 April	SPN	25
IST	20 April	SPE	25
KEV	12 January	SPZ	25
KEV	5 March	SPZ	25
KEV	13 March	SPZ	25
KIP	16 January	SPZ	12.5
KIP	15 April	SPZ	12.5
KIP	15 April	SPN	12.5
KIP	15 April	SPE	12.5
KON	7 April	SPZ	50
KON	7 April	SPN	50
KON	7 April	SPE	50
LON	7 January	SPZ	100
LON	5 April	SPZ	100
MAL	7 April	SPZ	50
MAN	15 January	SPZ	12.5
MAN	15 January	SPN	12.5
MAN	15 January	SPE	12.5
MAN	20 April	SPZ	12.5
MAN	20 April	SPN	12.5
MAN	20 April	SPE	12.5

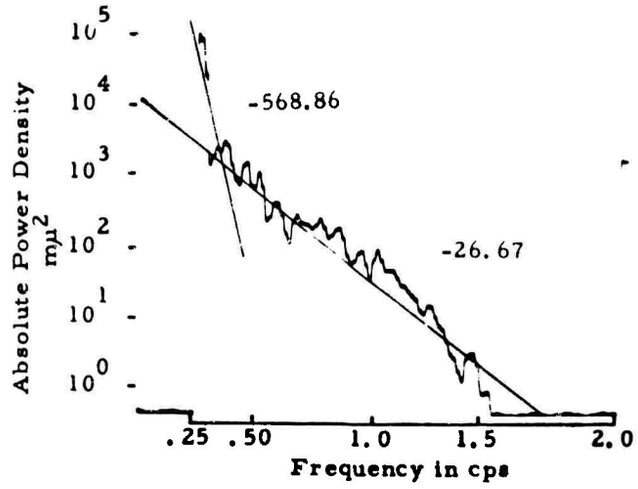

HNR 4 MAR.
SPZ 12.5 K

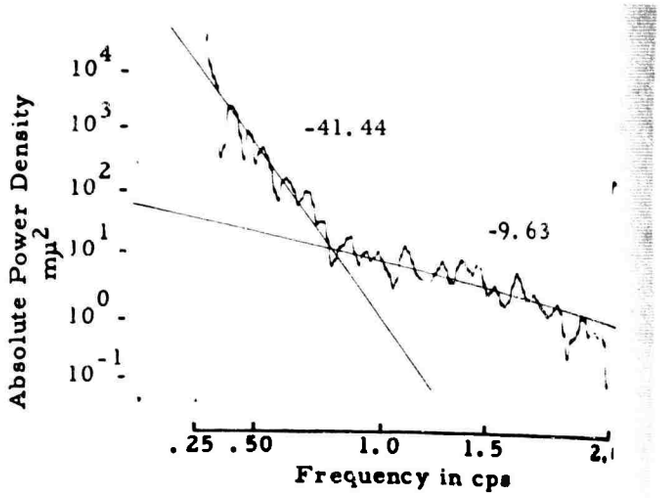

IST 20 APR.
SPZ 25 K

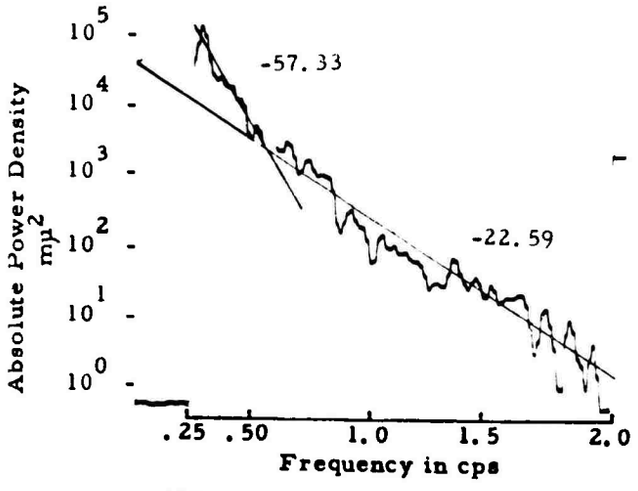

IST 2 JAN.
SPZ 25 K

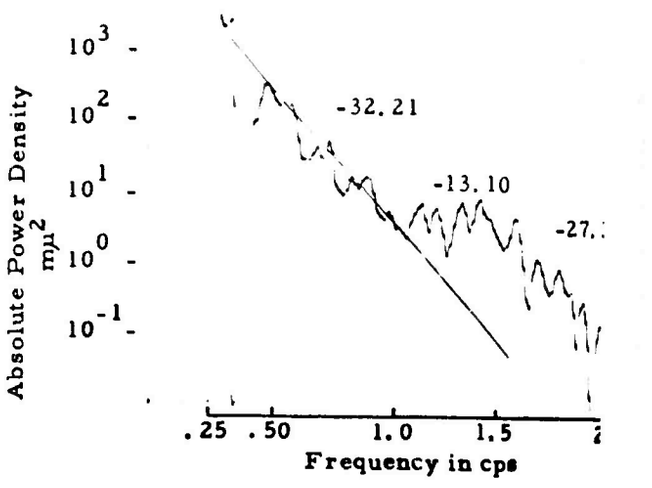

IST 20 APR.
SPN 25 K

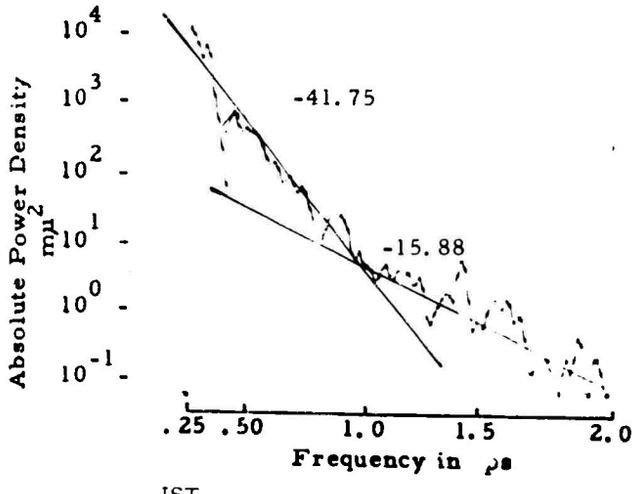

IST 19 JAN.
SPZ 25 K

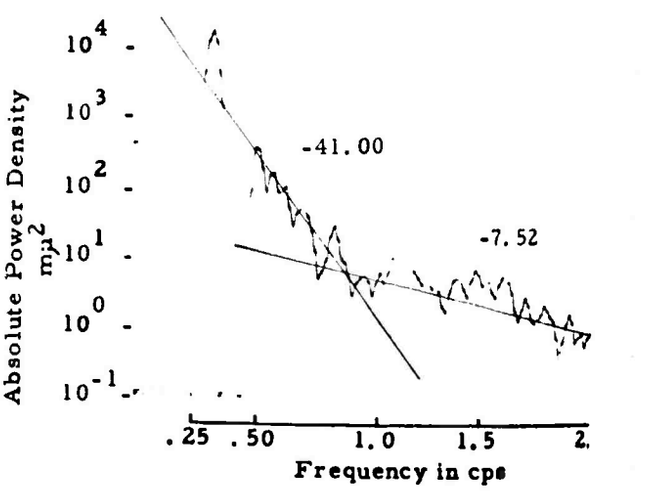

IST 20 APR.
SPE 25 K

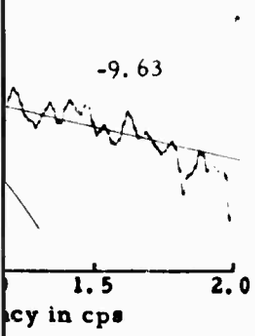

20 APR.
25 K

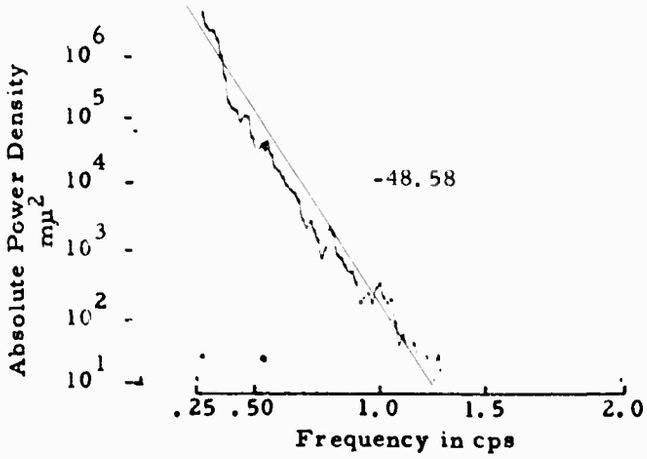

KEV
SPZ

12 JAN.
25 K

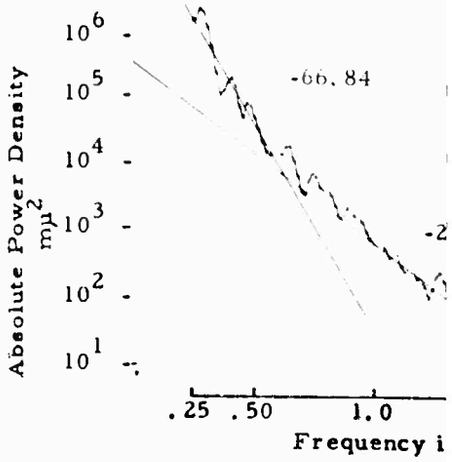

KIP
SPZ

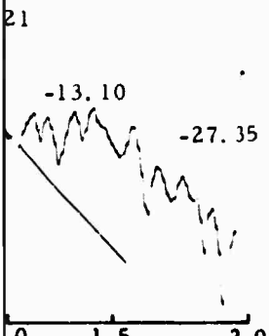

20 APR.
25 K

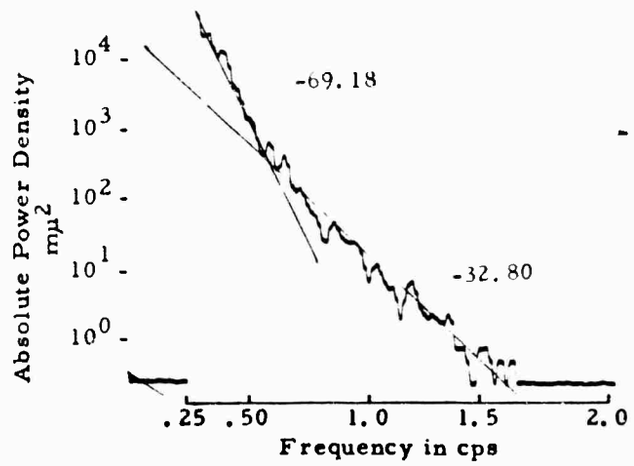

KEV
SPZ

5 MAR.
25 K

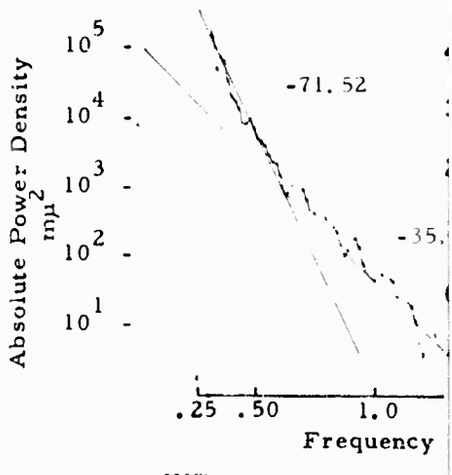

KIP
SPZ

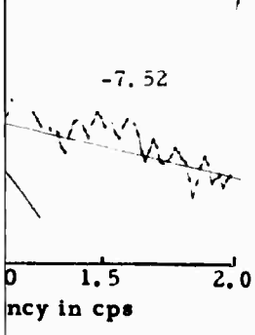

20 APR.
25 K

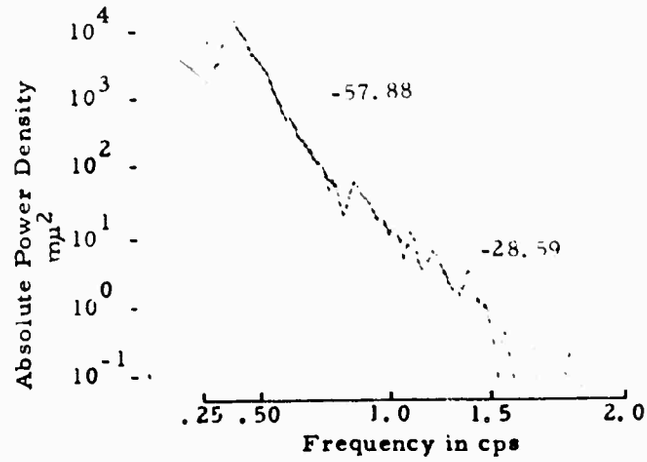

KEV
SPZ

13 MAR.
25 K

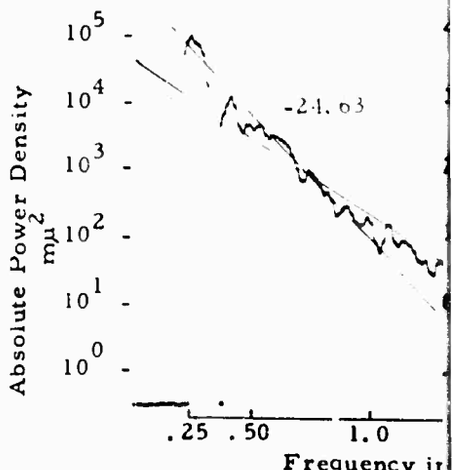

KIP
SPN

B

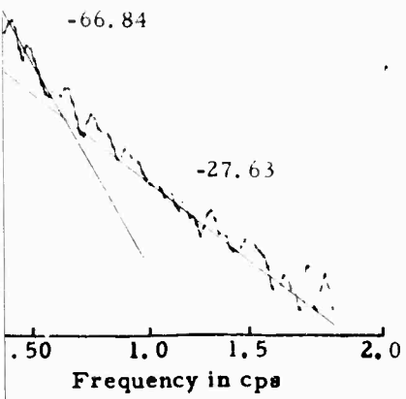

16 JAN.
12.5 K

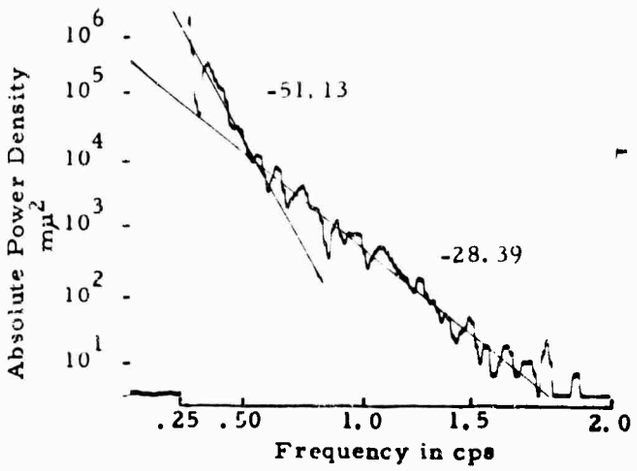

KIP
SPE

15 APR.
12.5 K

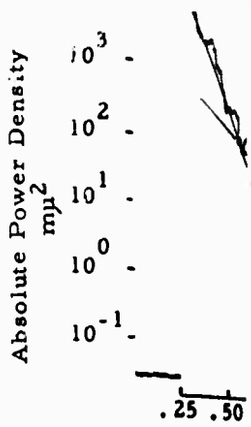

KON
SPE

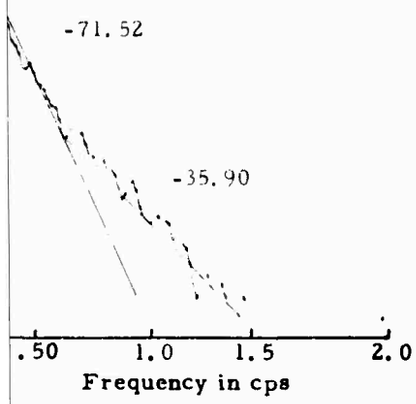

15 APR.
12.5 K

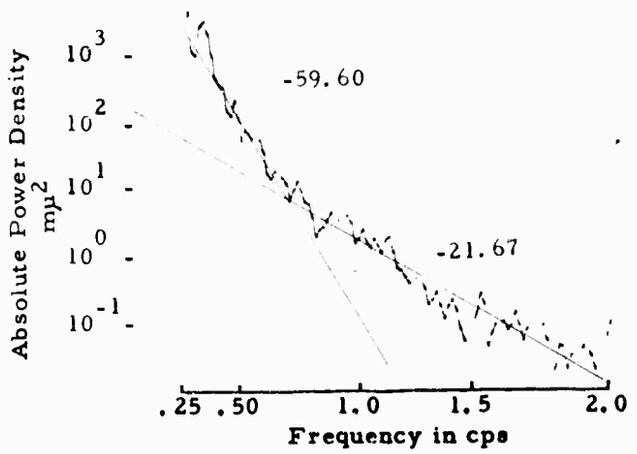

KON
SPZ

7 APR.
50 K

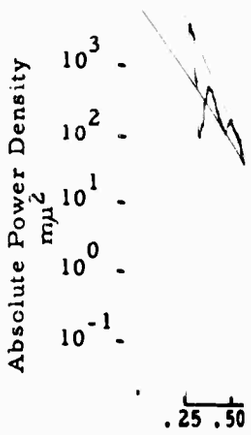

LON
SPZ

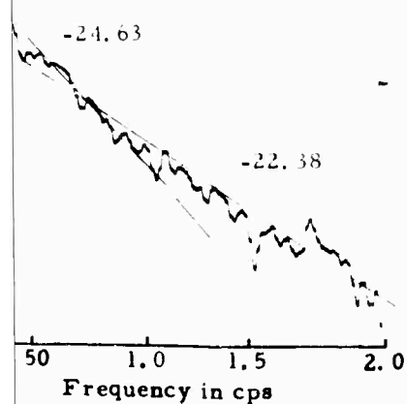

15 APR.
12.5 K

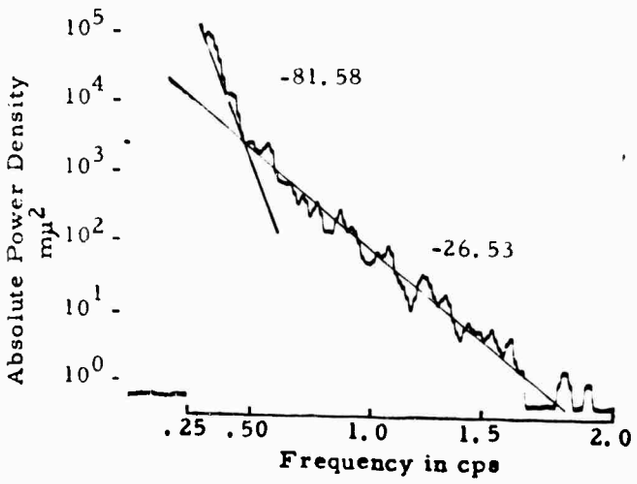

KON
SPN

7 APR.
50 K

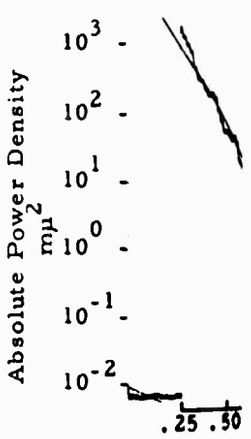

LON
SPZ

C

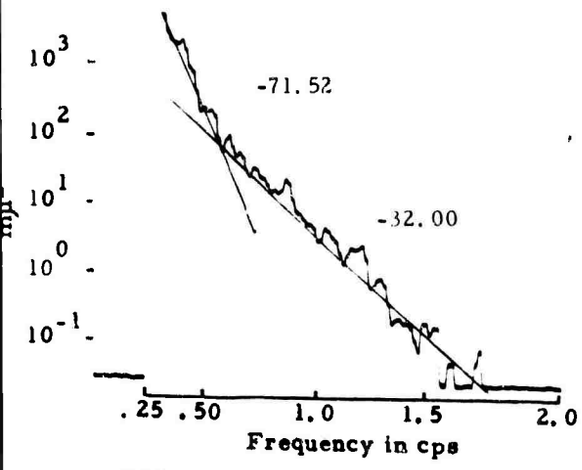

KON
SPE

7 APR.
50 K

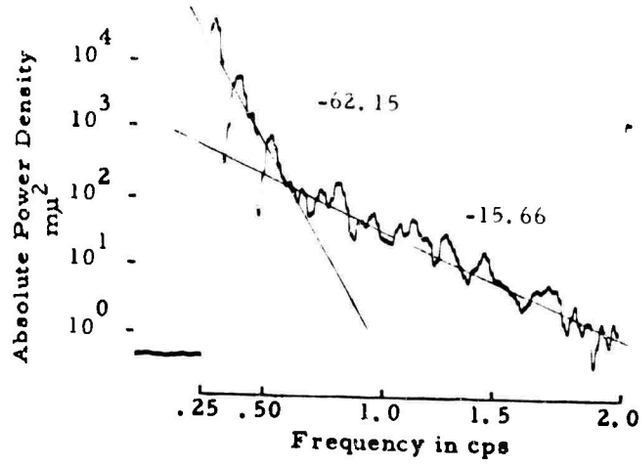

MAL
SPZ

7 APR.
50 K

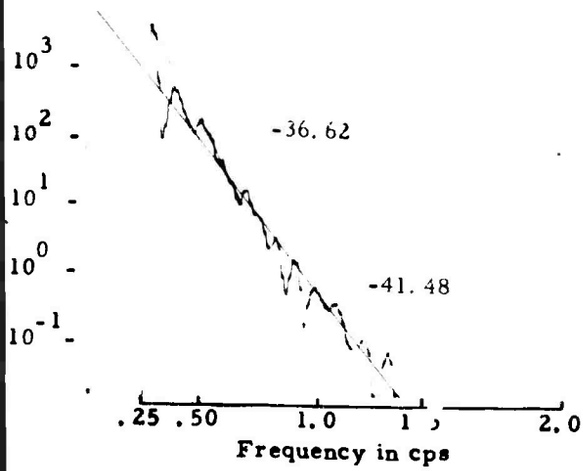

LON
SPZ

7 JAN.
100 K

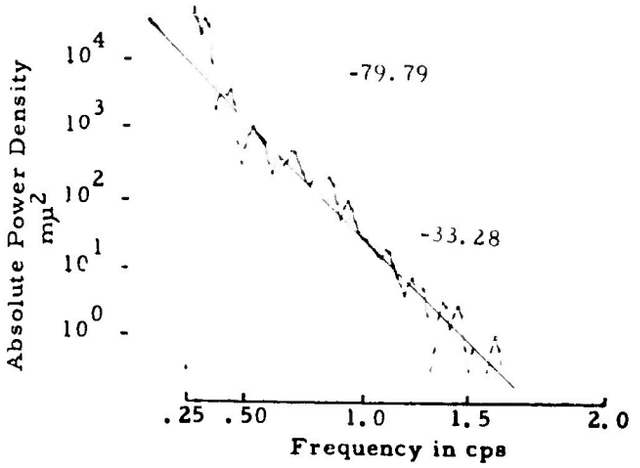

MAN
SPZ

15 JAN.
12.5 K

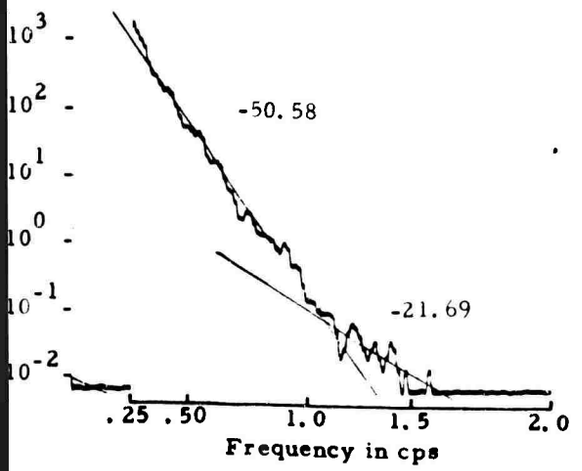

LON
SPZ

5 APR.
100 K

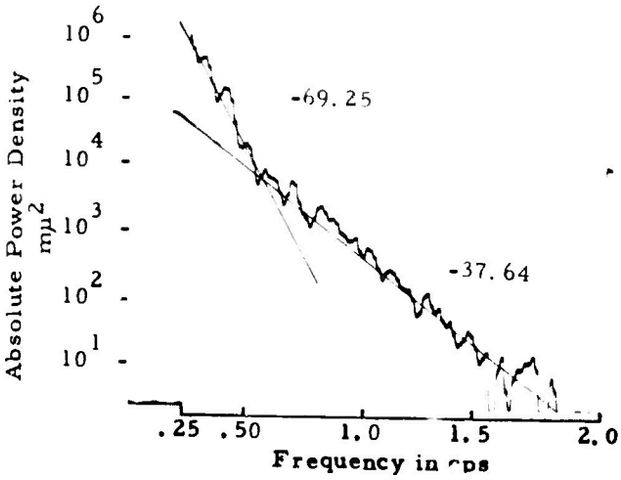

MAN
SPN

15 JAN.
12.5 K

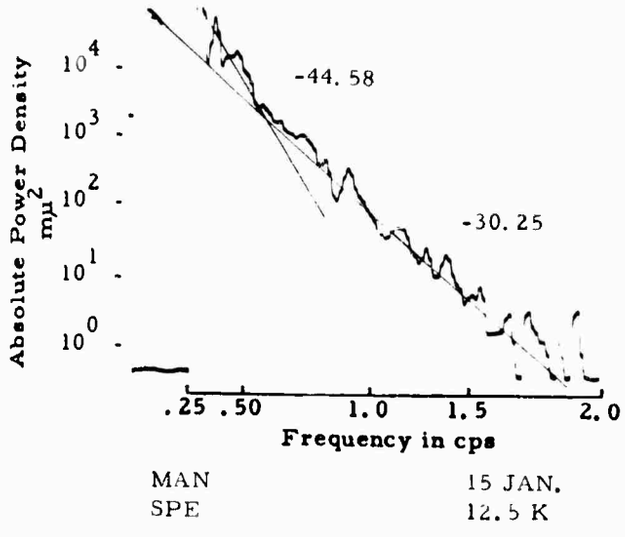

MAN 15 JAN.
SPE 12.5 K

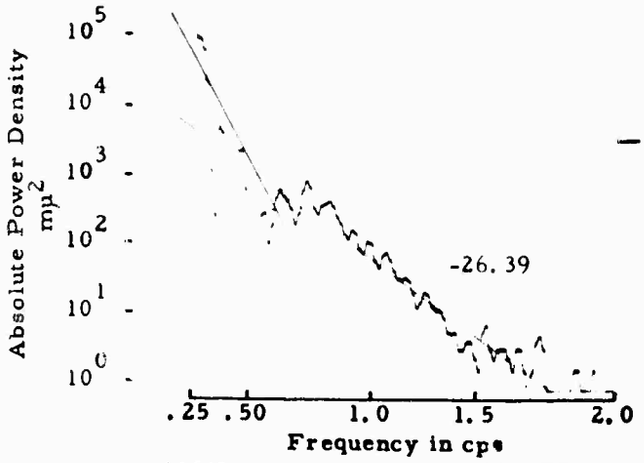

MAN 20 APR.
SPE 12.5 K

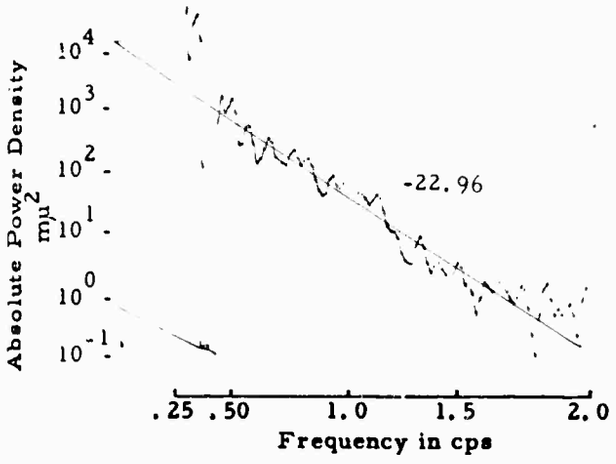

MAN 20 APR.
SPZ 12.5 K

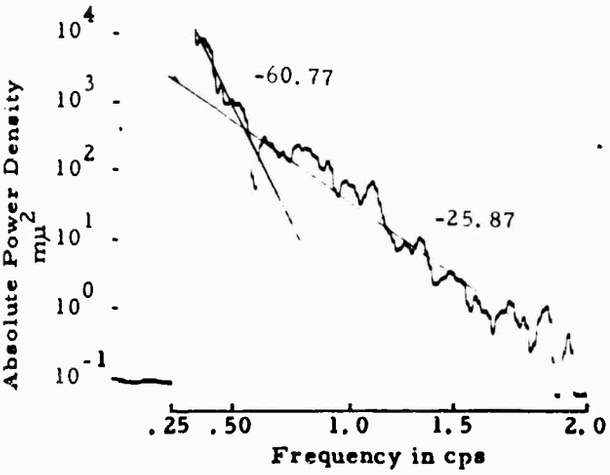

MAN 20 APR.
SPN 12.5 K

Figure A-1c. Absolute Power Density Spectra Obtained From 1963 Data

TABLE A-2d

ABSOLUTE POWER DENSITY SPECTRA LOCATED IN FIGURE A-1d

STATION	DATE	COMPONENT	GAIN(K)
MAN	3 June	SPZ	12.5
MAN	3 June	SPN	12.5
MAN	3 June	SPZ	12.5
MDS	18 January	SPZ	100
MUN	18 January	SPZ	25
MUN	18 January	SPN	25
MUN	18 January	SPE	25
MUN	5 April	SPZ	25
NAI	30 June	SPZ	50
NAI	30 June	SPN	100
NAI	30 June	SPZ	100
NUR	15 January	SPZ	25
NUR	15 January	SPN	25
NUR	15 January	SPE	25
NUR	15 January	SPN	25
NUR	15 January	SPE	25
NUR	19 April	SPZ	25
NUR	19 April	SPN	25
NUR	19 April	SPE	25
PLM	4 January	SPZ	50
PMG	15 January	SPZ	50
PMG	19 April	SPZ	50
PMG	19 April	SPN	50
PMG	19 April	SPE	50
PMG	19 April	SPE	50
PRE	7 January	SPZ	50
PRE	6 April	SPZ	50

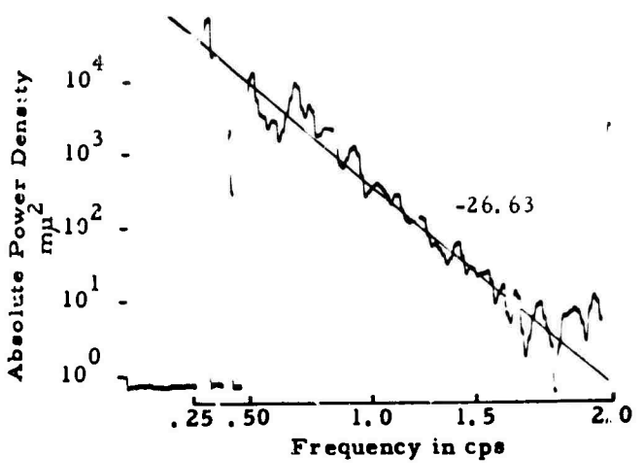

MAN 3 JUNE
SPZ 12.5 K

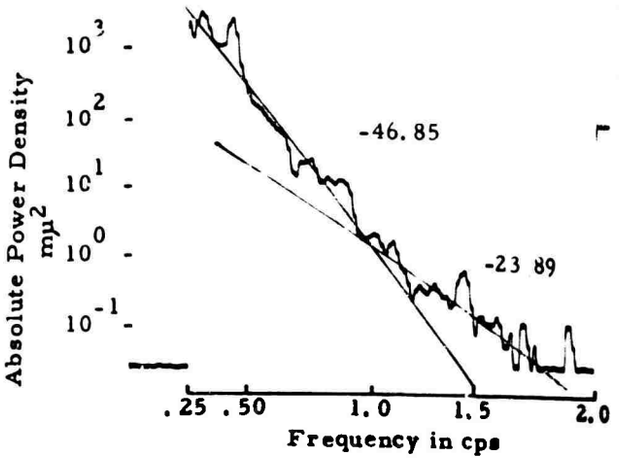

MDS 18 JAN.
SPZ 100 K

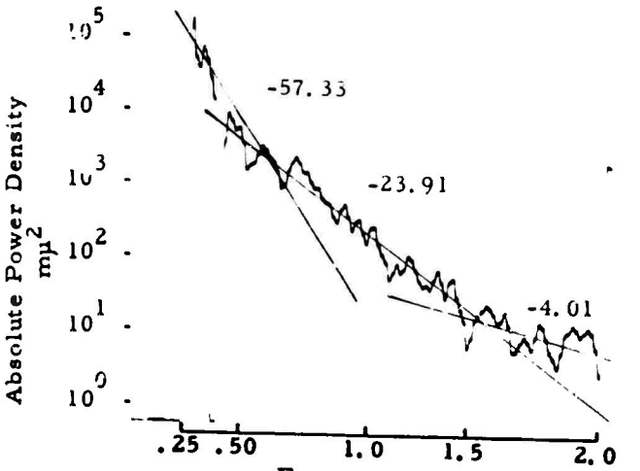

MAN 3 JUNE
SPN 12.5 K

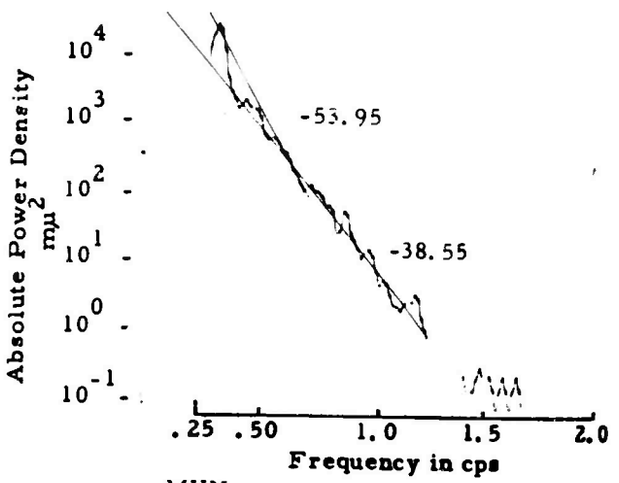

MUN 18 JAN.
SPZ 25 K

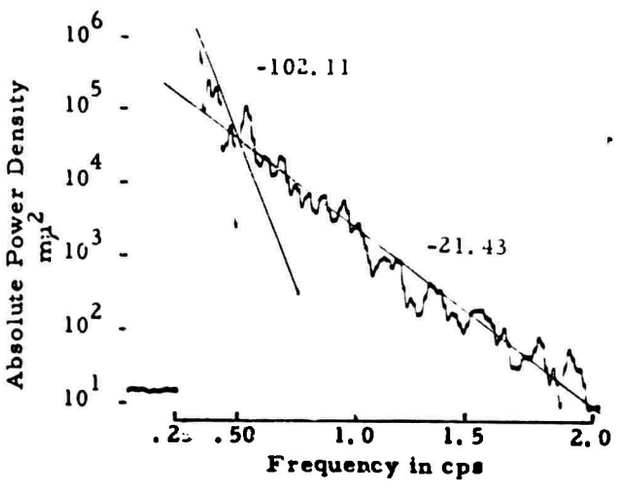

MAN 3 JUNE
SPE 12.5 K

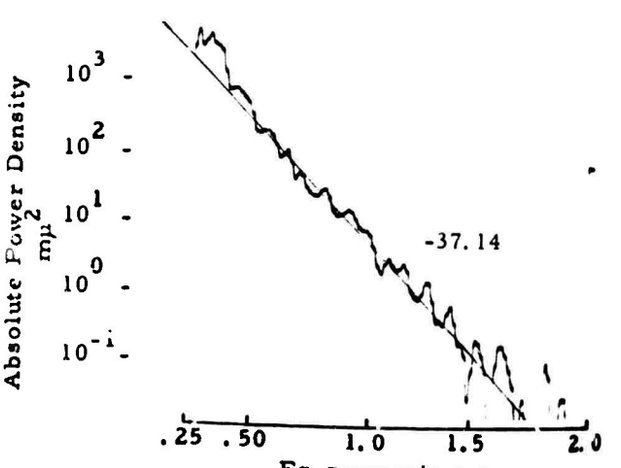

MUN 18 JAN.
SPN 25 K

A

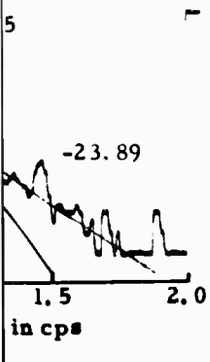

18 JAN.
100 K

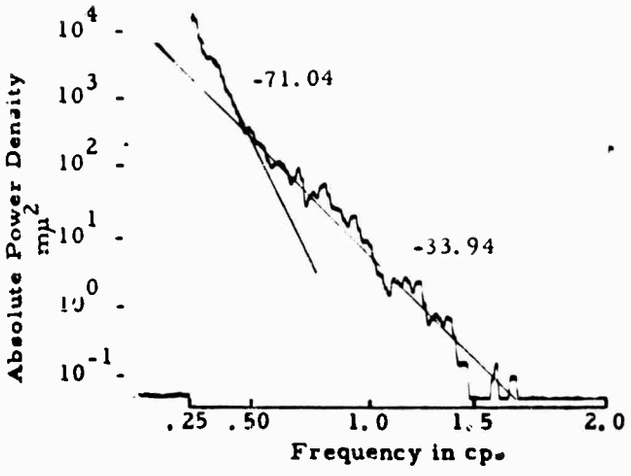

MUN
SPE

18 JAN.
25 K

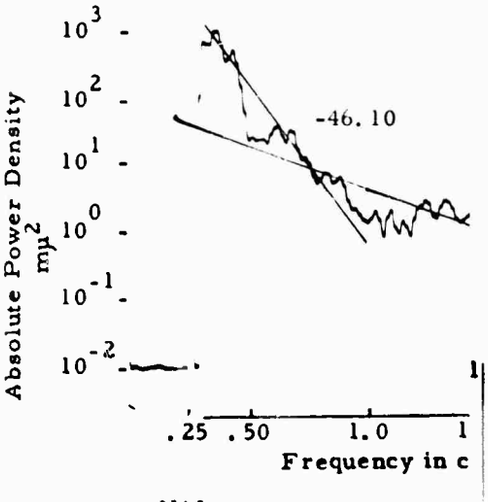

NAI
SPN

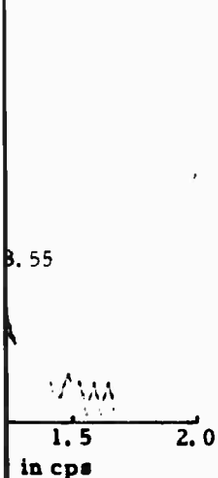

18 JAN.
25 K

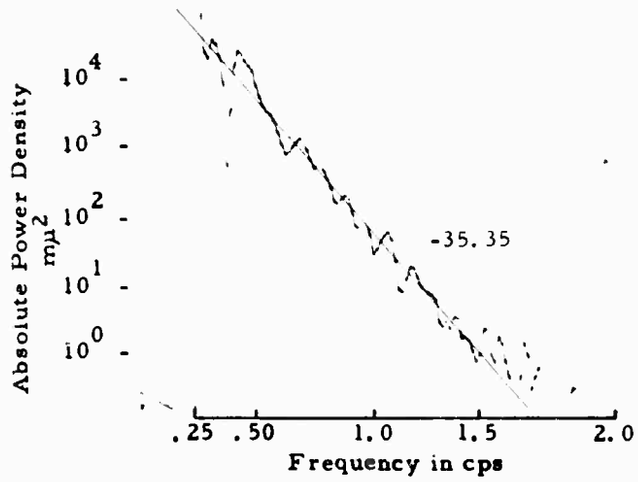

MUN
SPZ

5 APR.
25 K

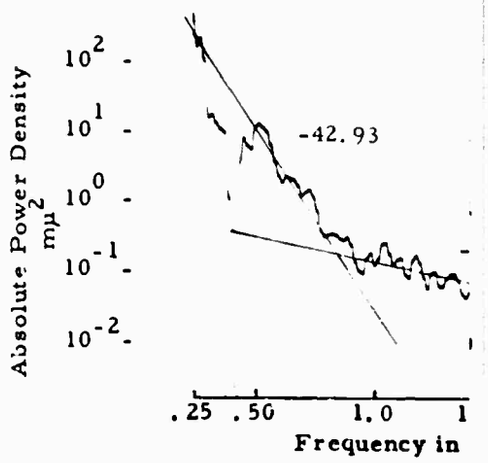

NAI
SPE

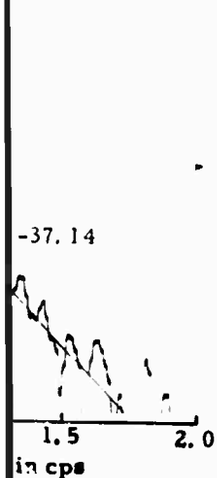

18 JAN.
25 K

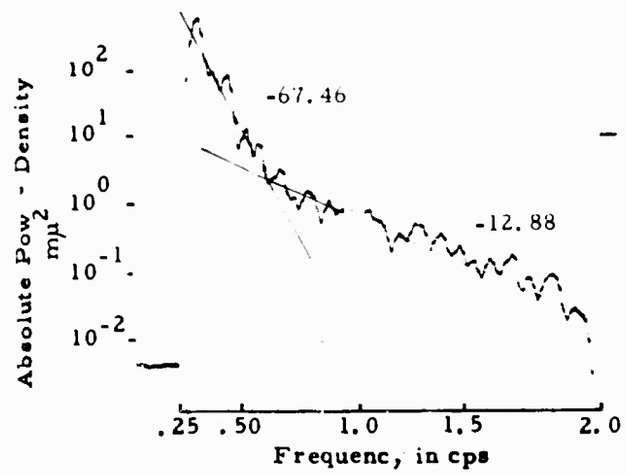

NAI
SPZ

30 JUNE
50 K

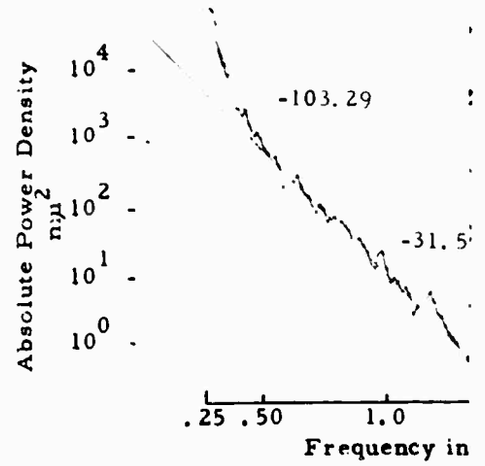

NUR
SPZ

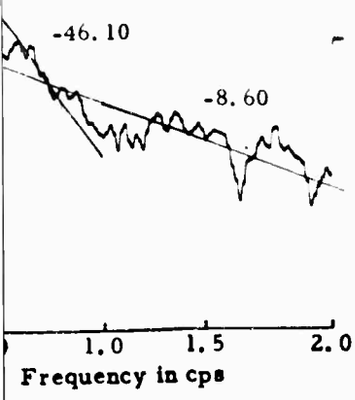

30 JUNE
100 K

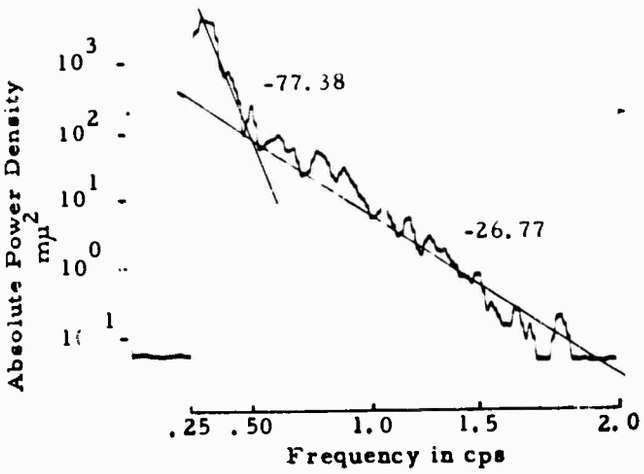

NUR
SPN

15 JAN.
25 K

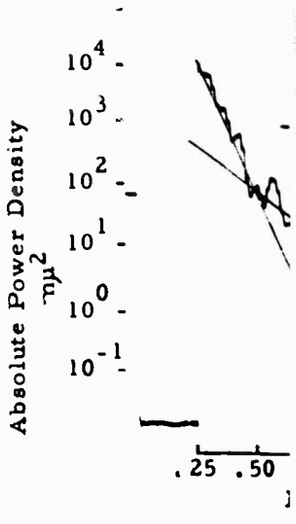

NUR
SPE

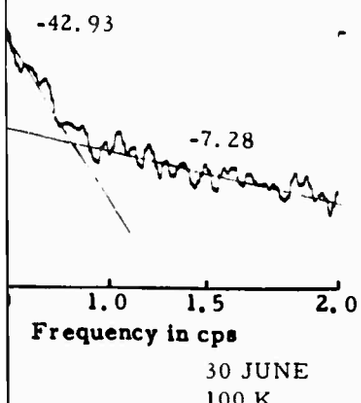

30 JUNE
100 K

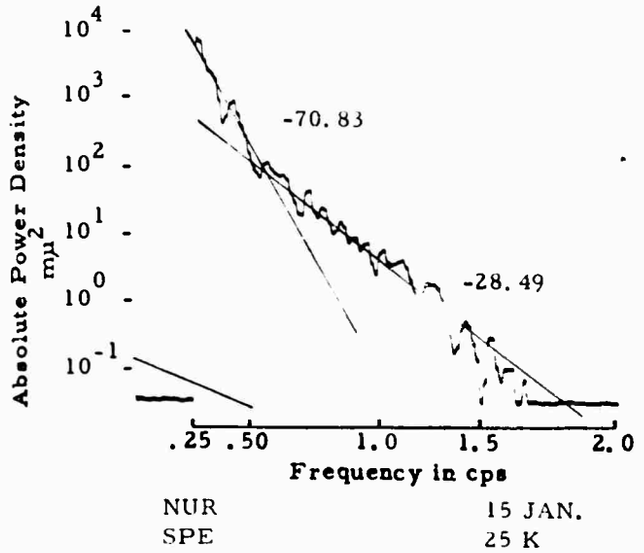

NUR
SPE

15 JAN.
25 K

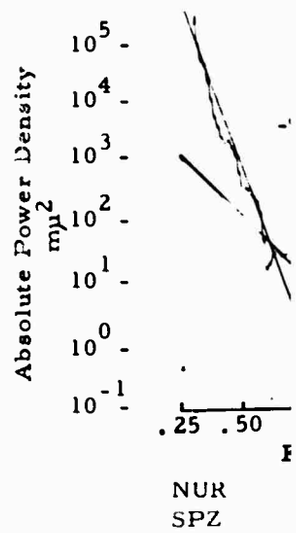

NUR
SPZ

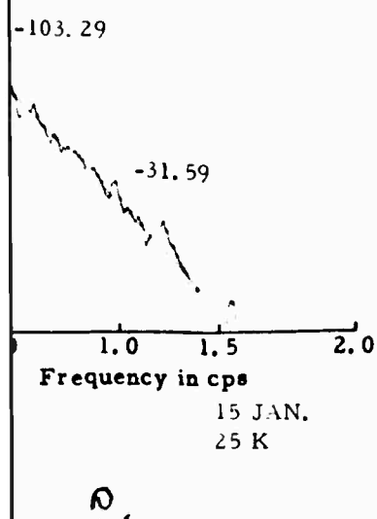

15 JAN.
25 K

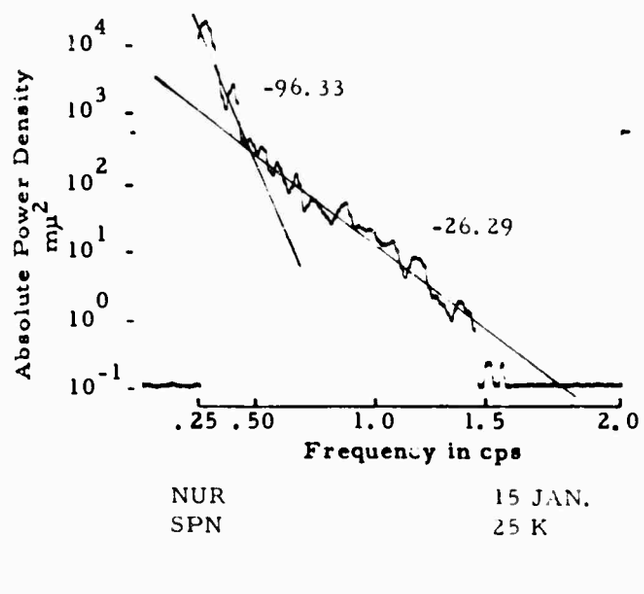

NUR
SPN

15 JAN.
25 K

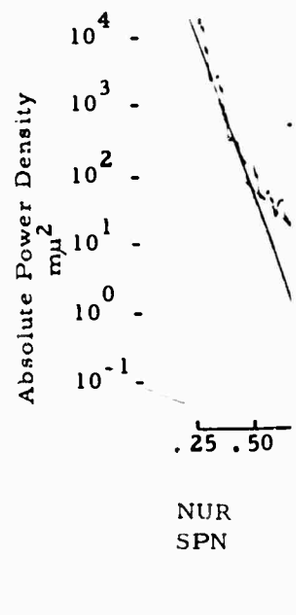

NUR
SPN

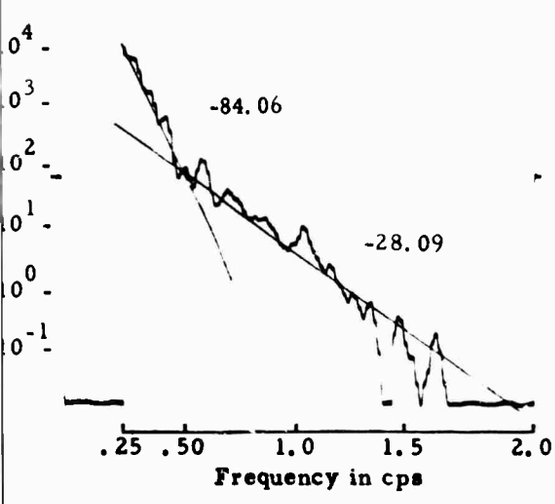

NUR 15 JAN.
SPE 25 K

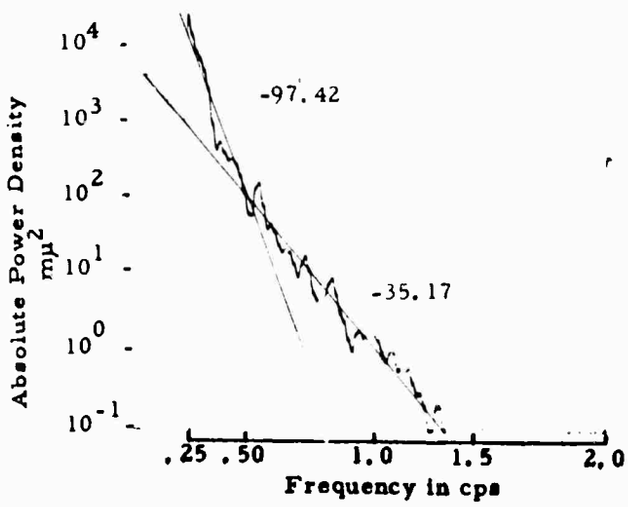

NUR 19 APR.
SPE 25 K

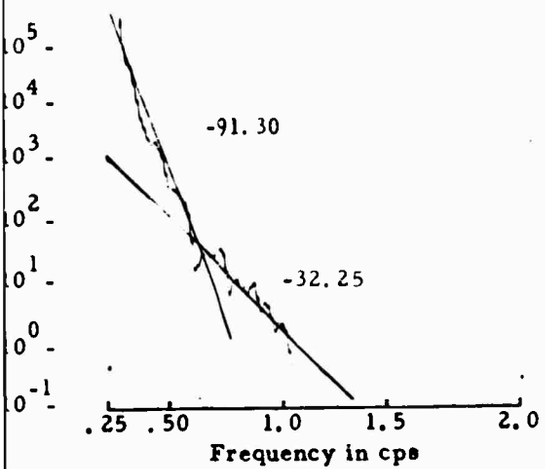

NUR 19 APR.
SPZ 25 K

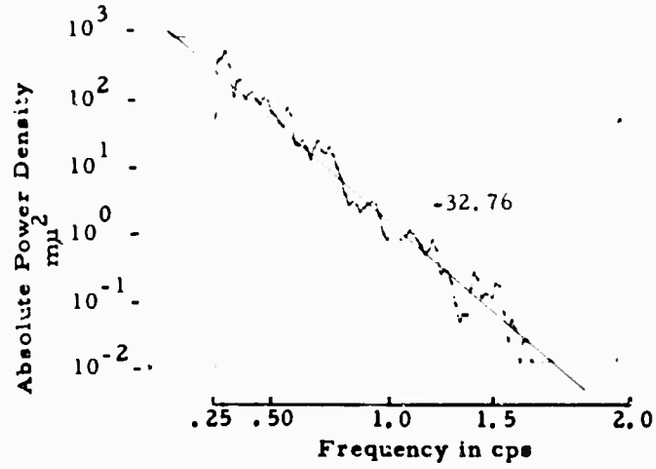

PLM 4 JAN.
SPZ 50 K

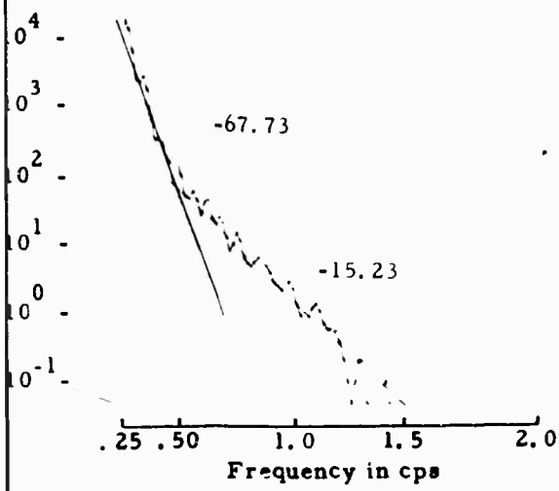

NUR 19 APR.
SPN 25 K

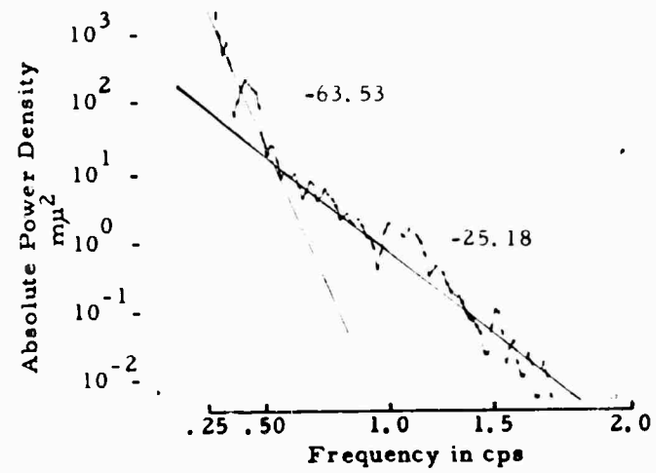

PMG 15 JAN.
SPZ 50 K

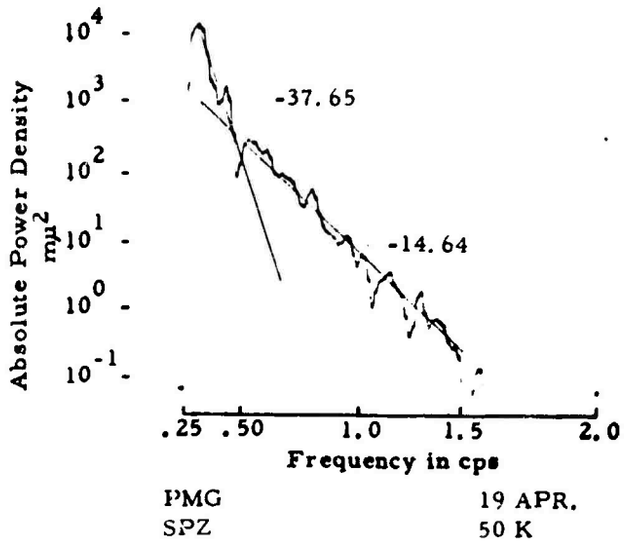

PMG 19 APR.
SPZ 50 K

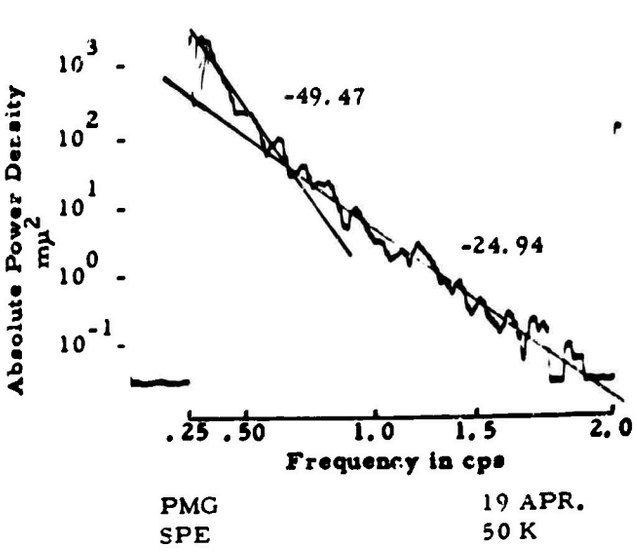

PMG 19 APR.
SPE 50 K

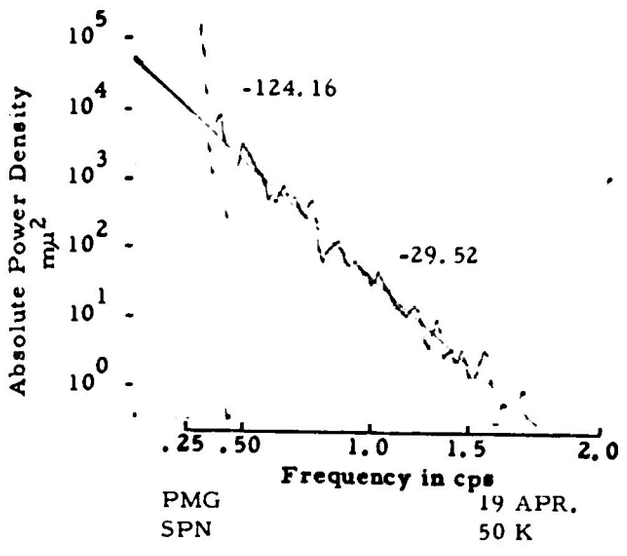

PMG 19 APR.
SPN 50 K

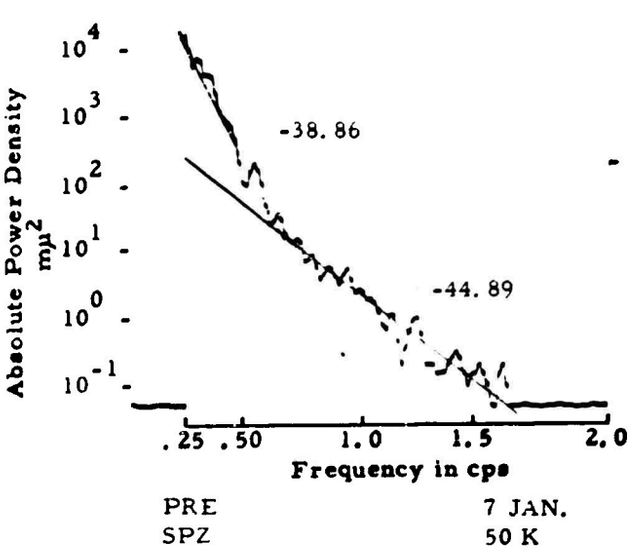

PRE 7 JAN.
SPZ 50 K

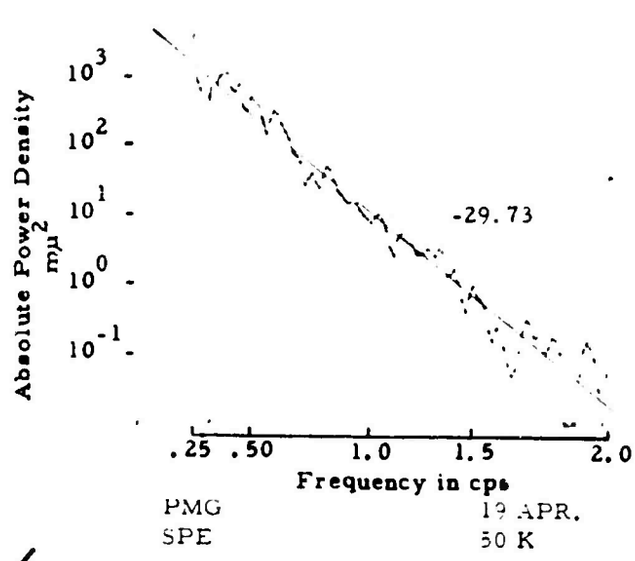

PMG 19 APR.
SPE 50 K

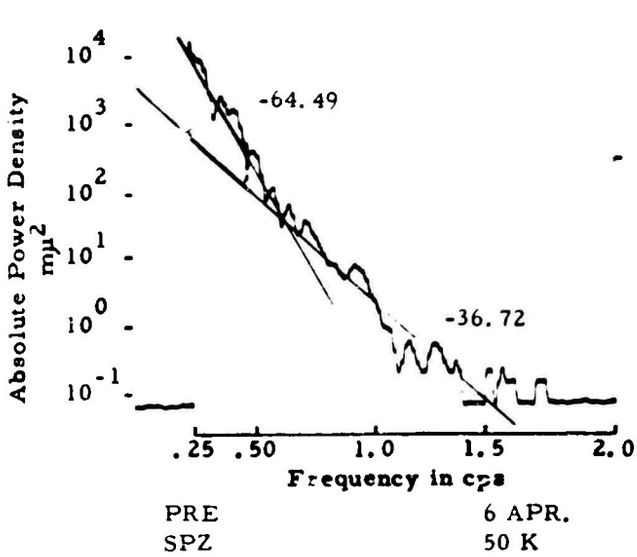

PRE 6 APR.
SPZ 50 K

Figure A-1d. Absolute Power Density Spectra Obtained From 1963 Data

TABLE A-2e

ABSOLUTE POWER DENSITY SPECTRA LOCATED IN FIGURE A-1e

STATION	DATE	COMPONENT	GAIN(K)
PTO	15 April	SPZ	25
QUE	24 January	SPZ	200
QUE	24 January	SPZ	200
SCP	29 April	SPZ	100
SEO	18 March	SPZ	100
SEO	18 March	SPN	100
SEO	18 March	SPE	100
SEO	16 April	SPZ	100
SEO	16 April	SPN	100
SEO	16 April	SPE	100
SEO	6 June	SPZ	100
SEO	6 June	SPN	100
SEO	6 June	SPE	100
SHL	29 April	SPZ	200
SPA	10 January	SPZ	50
SPA	7 April	SPZ	100
SPA	7 June	SPZ	100
SPA	7 June	SPN	100
SPA	7 June	SPE	100
TOL	15 January	SPZ	50
TOL	15 January	SPN	25
TOL	15 January	SPE	25
TOL	2 April	SPZ	25
TOL	2 April	SPN	25
TOL	2 April	SPE	25
WES	5 January	SPZ	50
WIN	4 January	SPZ	100

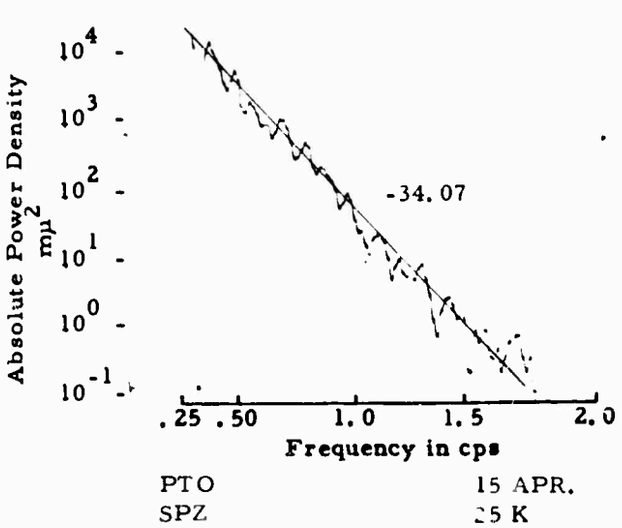

PTO 15 APR.
SPZ 25 K

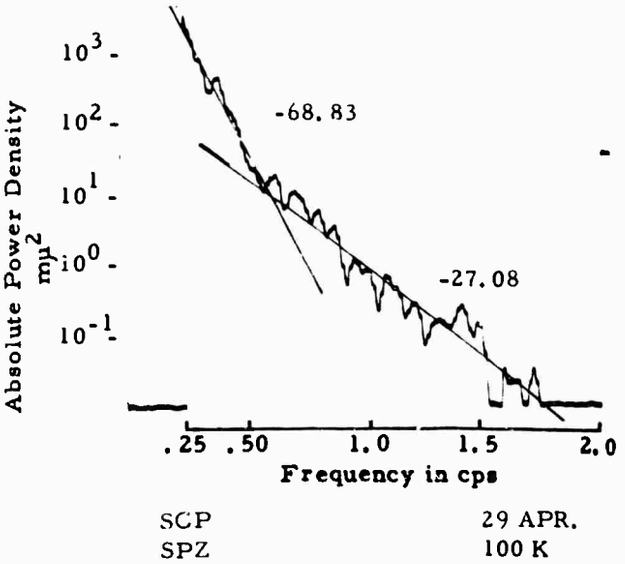

SCP 29 APR.
SPZ 100 K

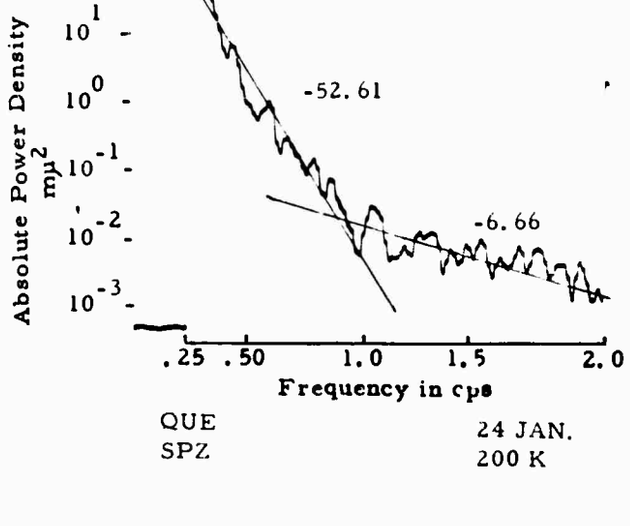

QUE 24 JAN.
SPZ 200 K

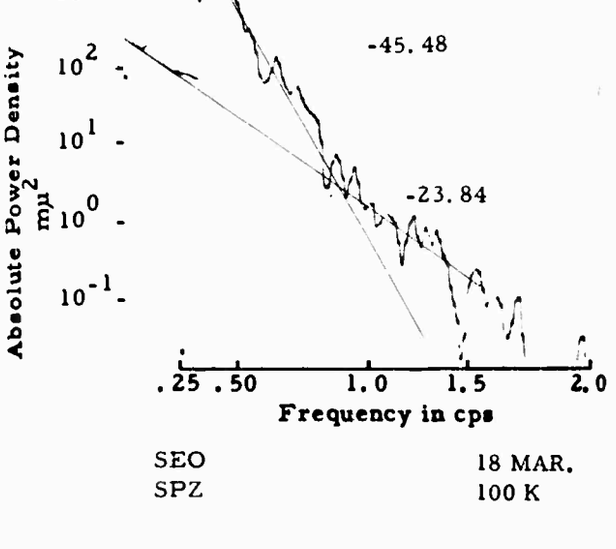

SEO 18 MAR.
SPZ 100 K

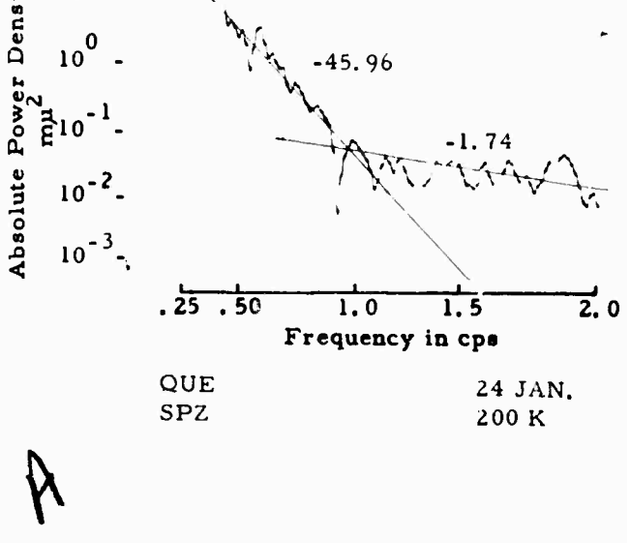

QUE 24 JAN.
SPZ 200 K

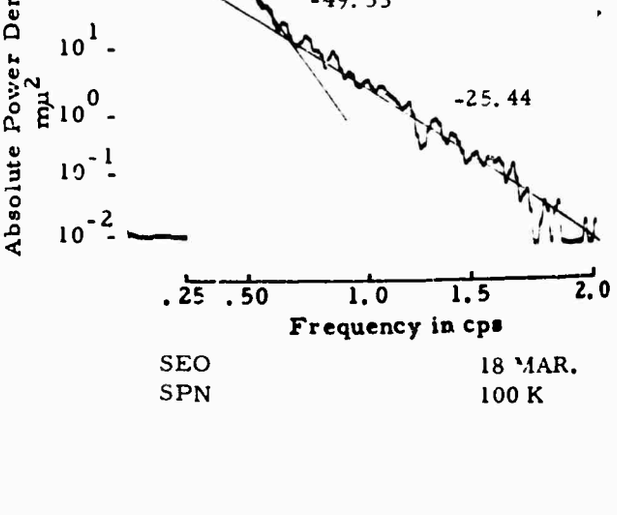

SEO 18 MAR.
SPN 100 K

A

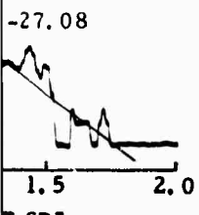

29 APR.
100 K

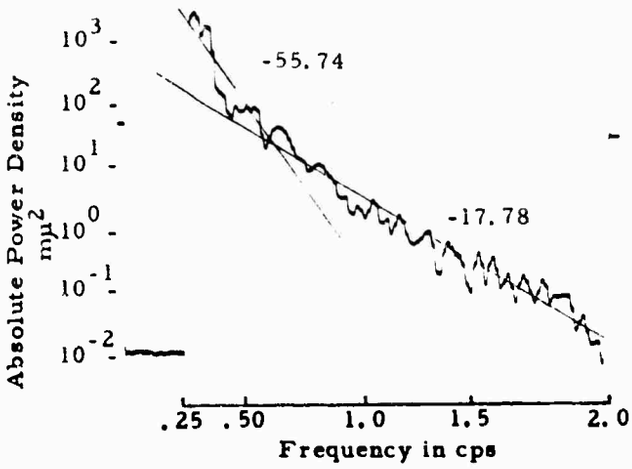

SEO
SPE

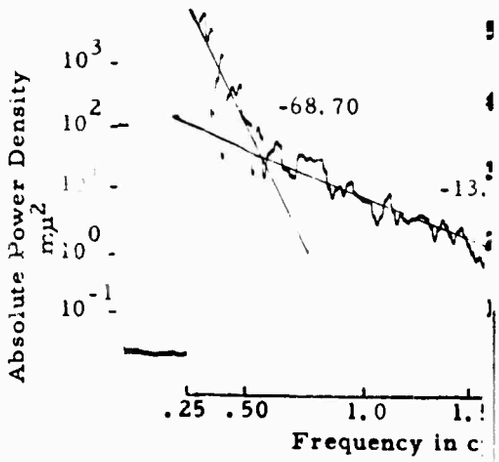

18 MAR.
100 K

SEO
SPE

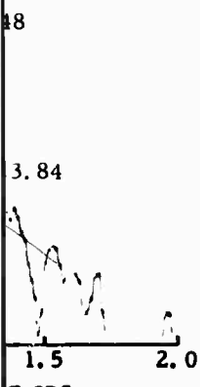

18 MAR.
100 K

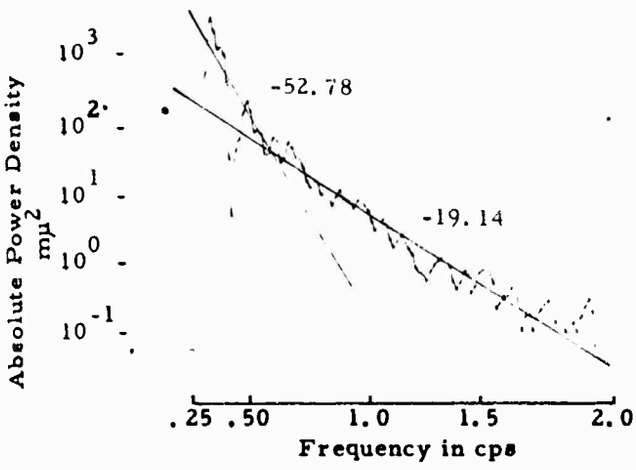

SEO
SPZ

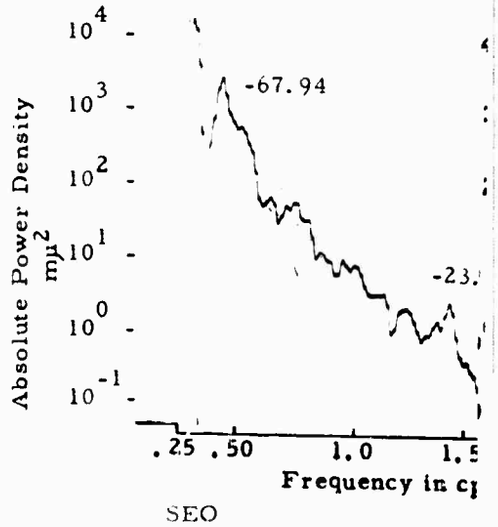

16 APR.
100 K

SEO
SPZ

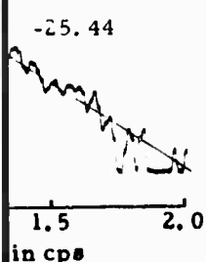

18 MAR.
100 K

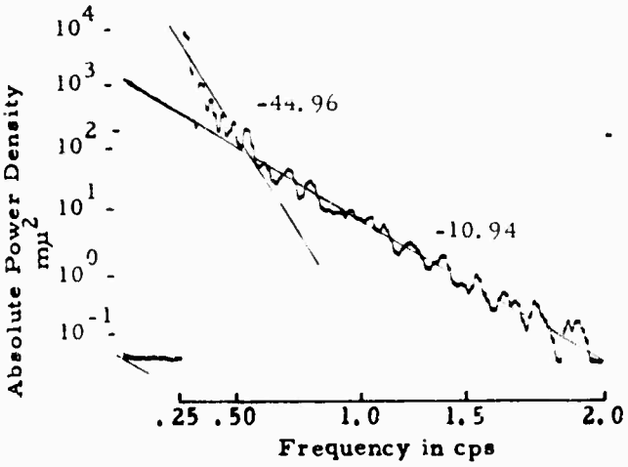

SEO
SPN

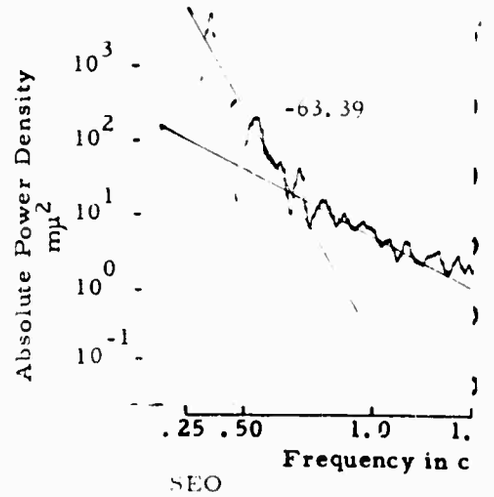

16 APR.
100 K

SEO
SPN

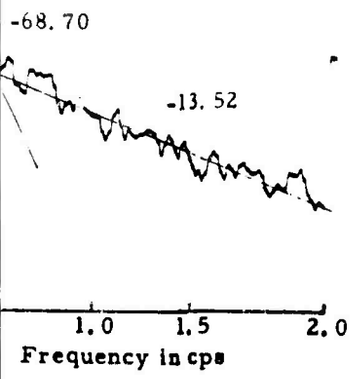

16 APR.
100 K

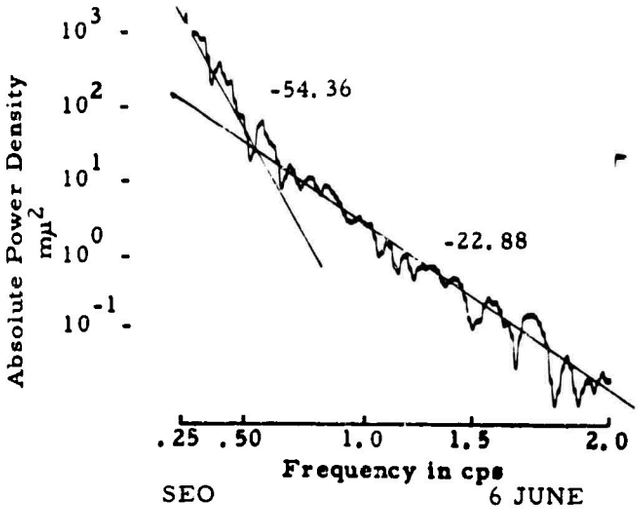

SEO
SPE
6 JUNE
100 K

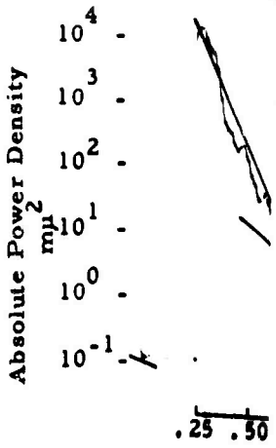

SPA
SPZ

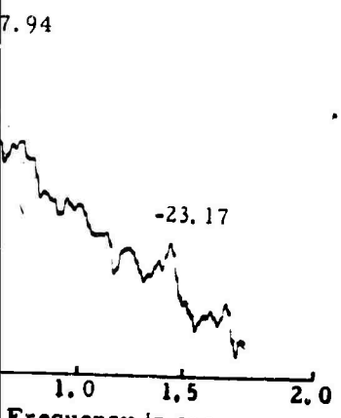

6 JUNE
100 K

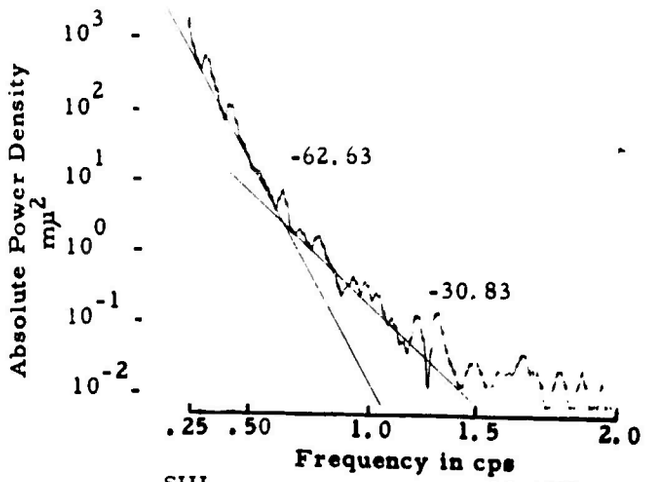

SHL
SPZ
29 APR.
200 K

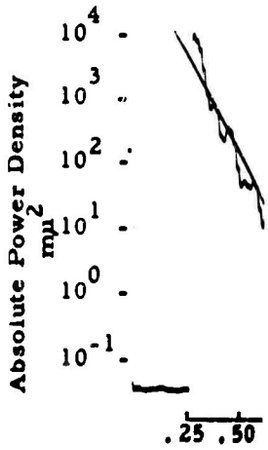

SPA
SPZ

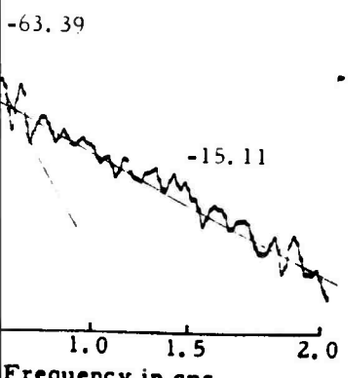

6 JUNE
100 K

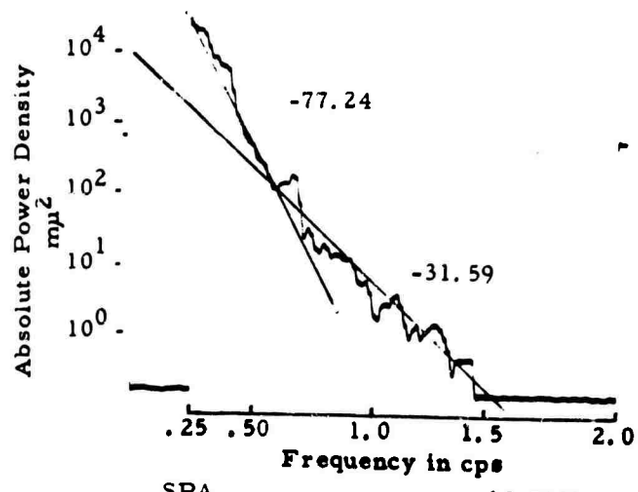

SPA
SPZ
10 JAN.
50 K

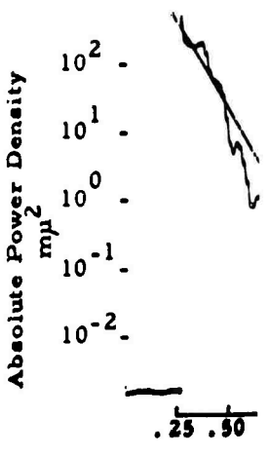

SPA
SPN

e

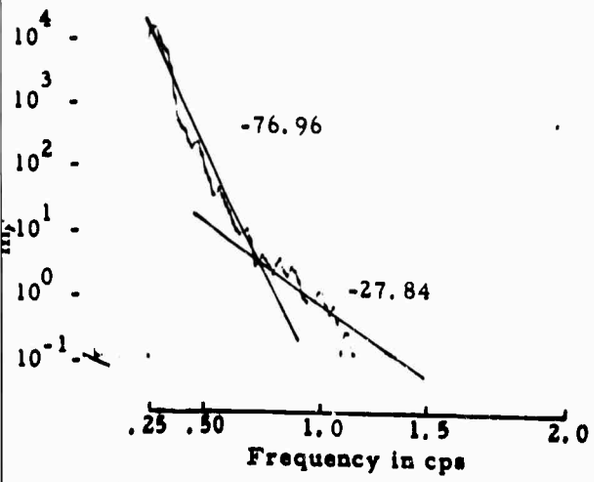

SPA 7 APR.
SPZ 100 K

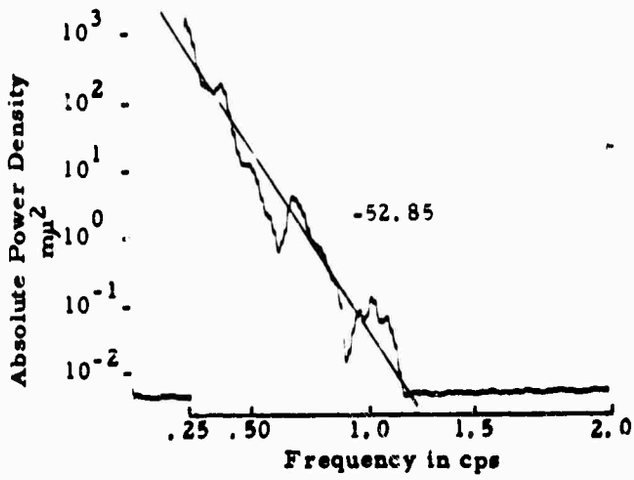

SPA 7 JUNE
SPE 100 K

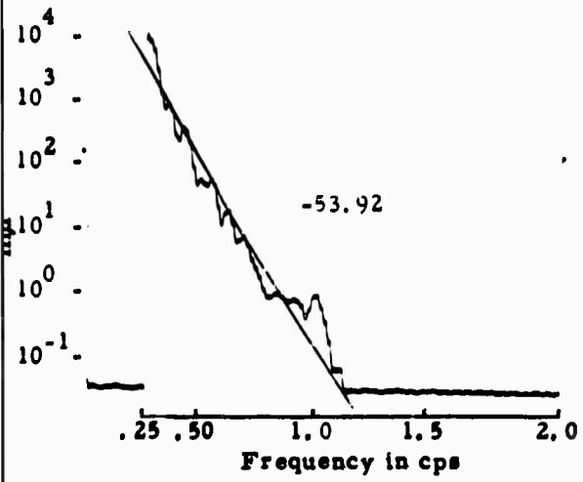

SPA 7 JUNE
SPZ 100 K

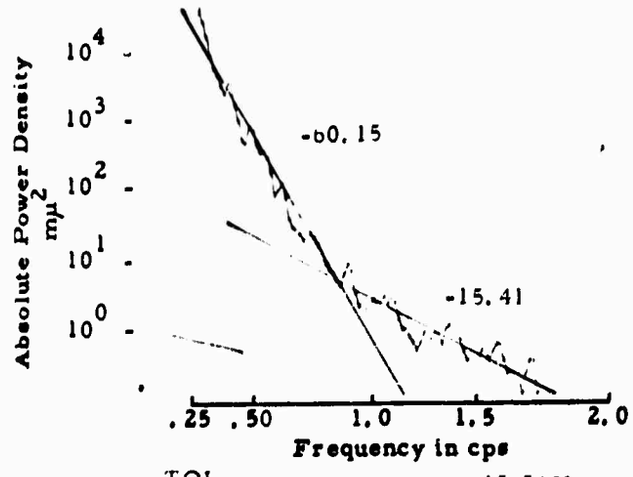

TOL 15 JAN.
SPZ 50 K

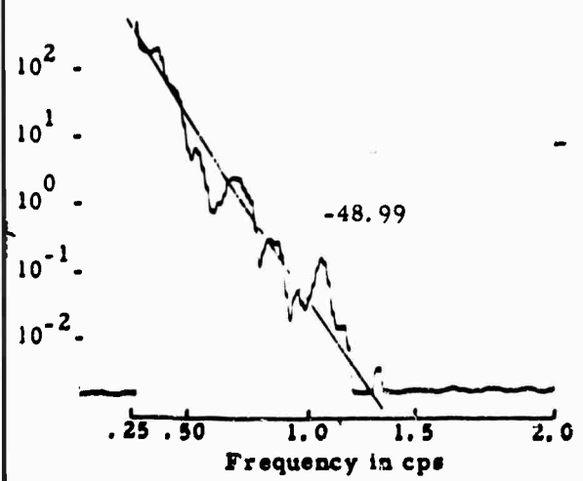

SPA 7 JUNE
SPN 100 K

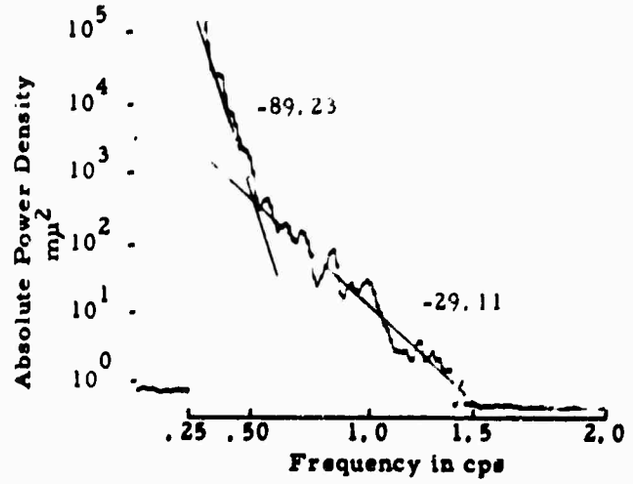

TOL 15 JAN.
SPN 25 K

D

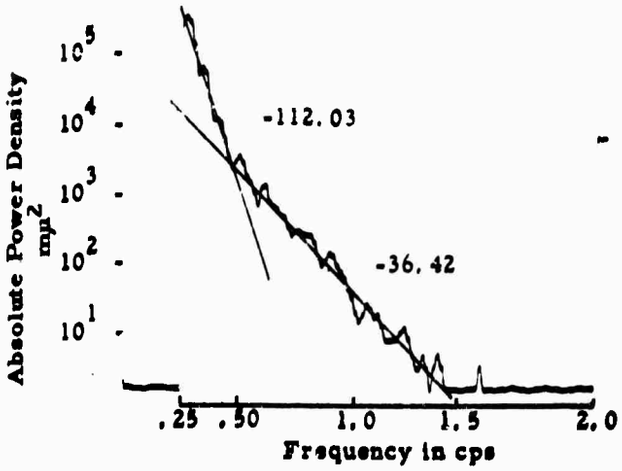

TOL 15 JAN.
SPE 25 K

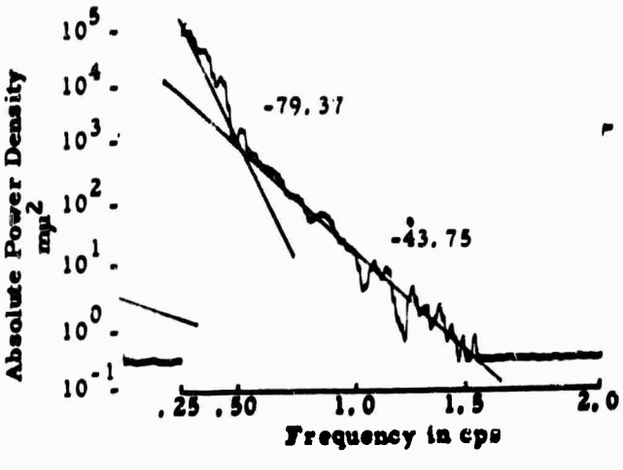

TOL 2 APR.
SPE 25 K

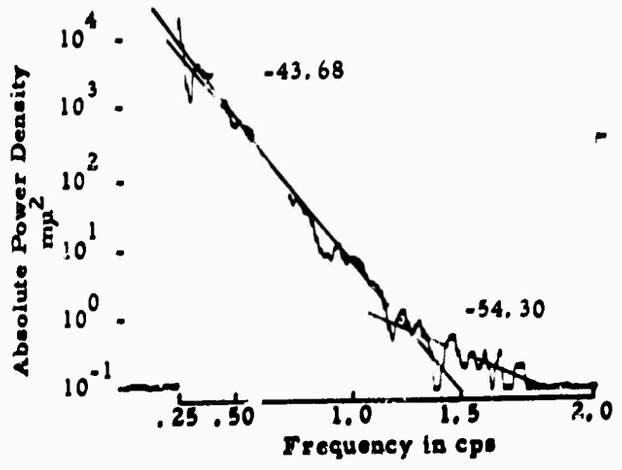

TOL 2 APR.
SPZ 25 K

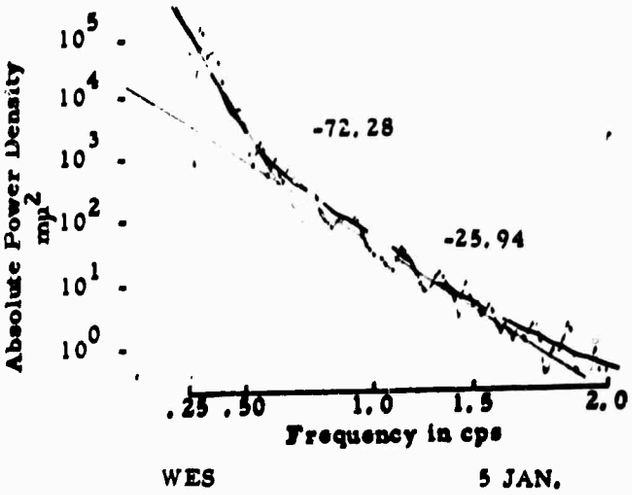

WES 5 JAN.
SPZ 50 K

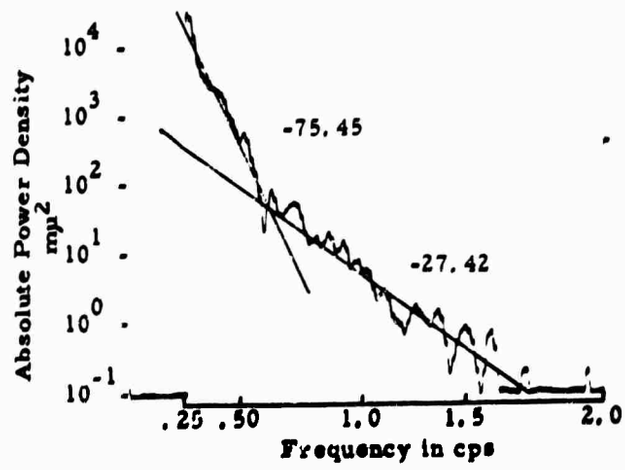

TOL 2 APR.
SPN 25 K

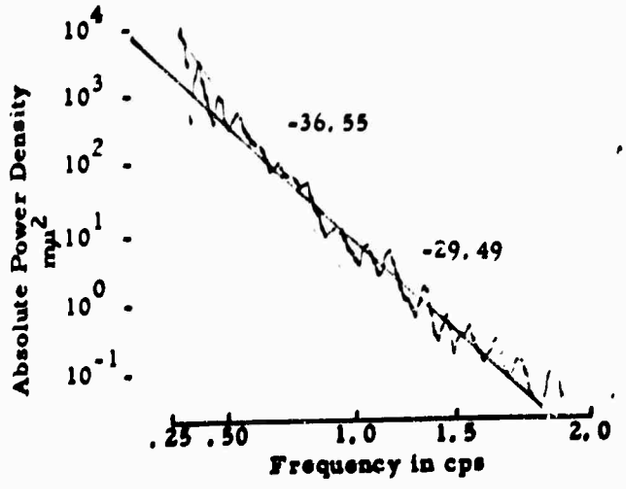

WIN 4 JAN.
SPZ 100 K

Figure A-1e. Absolute Power Density Spectra Obtained From 1963 Data

E

TABLE A-2f

ABSOLUTE POWER DENSITY SPECTRA LOCATED IN FIGURE A-1f

STATION	DATE	COMPONENT	GAIN(K)
VAL	15 January	SPZ	12.5
VAL	15 January	SPN	12.5
VAL	15 January	SPE	12.5
VAL	18 January	SPZ	12.5
VAL	7 February	SPZ	12.5
VAL	7 February	SPN	12.5
VAL	7 February	SPE	12.5
VAL	1 March	SPZ	12.5
VAL	1 March	SPN	12.5
VAL	1 March	SPE	12.5
VAL	2 April	SPZ	12.5
VAL	3 April	SPZ	12.5
VAL	3 April	SPN	12.5
VAL	3 April	SPE	12.5
VAL	19 May	SPZ	12.5
VAL	19 May	SPN	12.5
VAL	19 May	SPE	12.5
VAL	6 June	SPZ	12.5
VAL	6 June	SPN	12.5
VAL	6 June	SPE	12.5

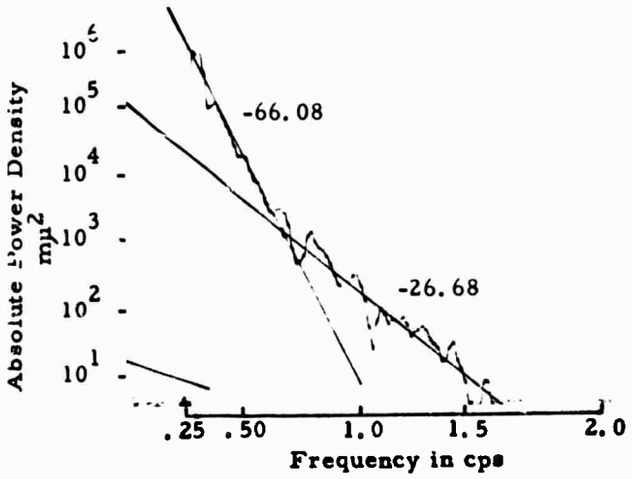

VAL 15 JAN.
SPZ 12.5 K

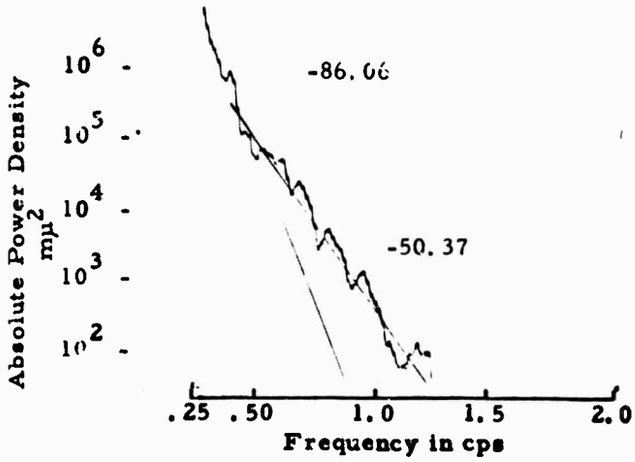

VAL 18 JAN.
SPZ 12.5 K

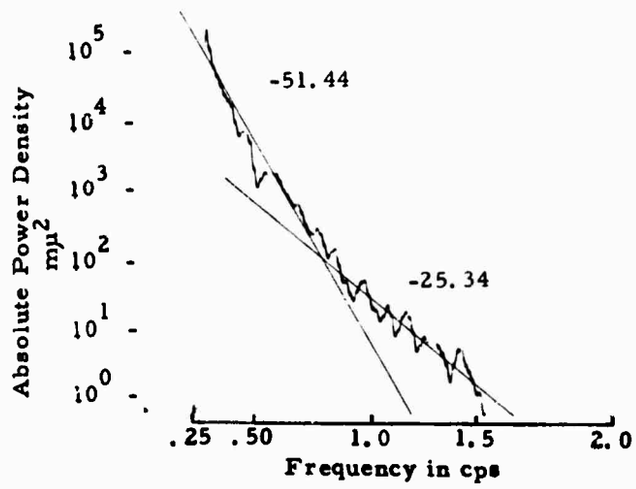

VAL 15 JAN.
SPN 12.5 K

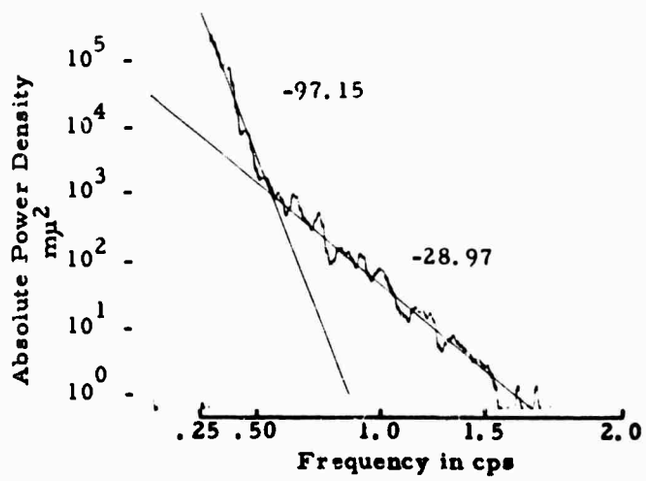

VAL 15 JAN.
SPE 12.5 K

A

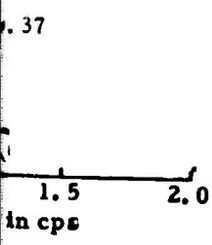

18 JAN.
12.5 K

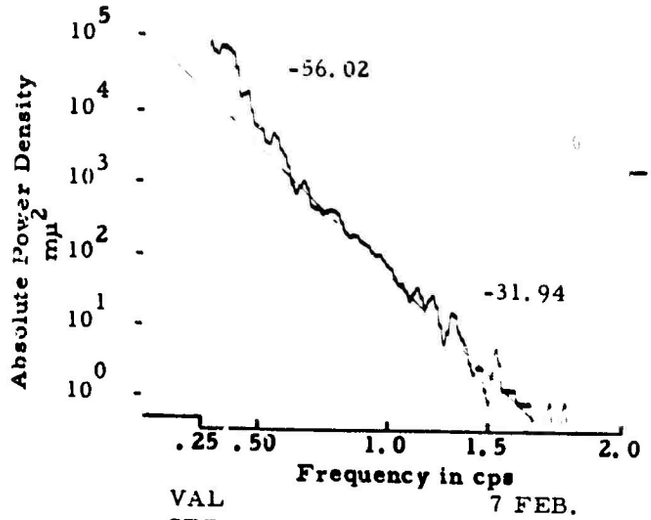

VAL
SPZ

7 FEB.
12.5 K

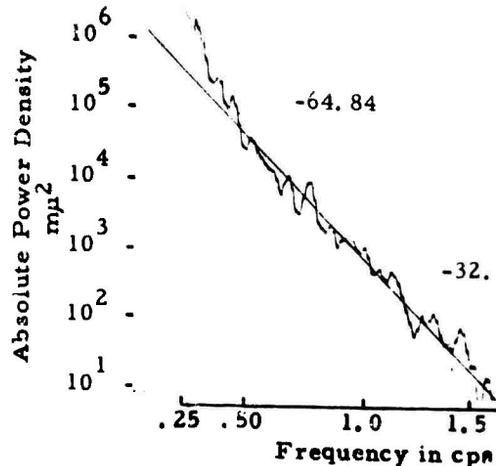

VAL
SPZ

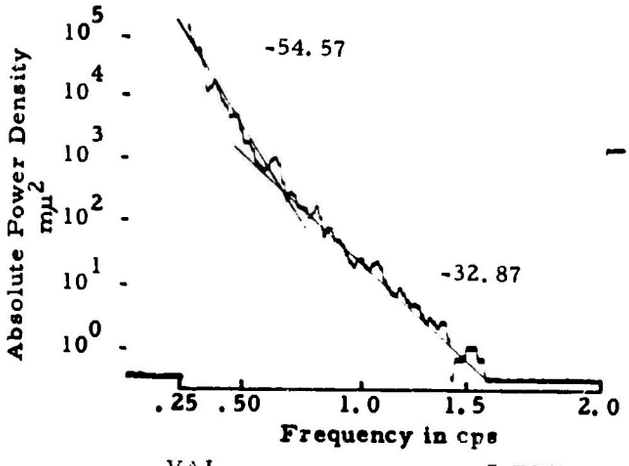

VAL
SPN

7 FEB.
2.5 K

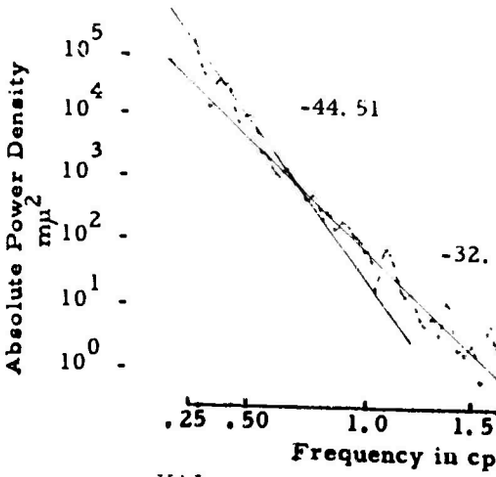

VAL
SPN

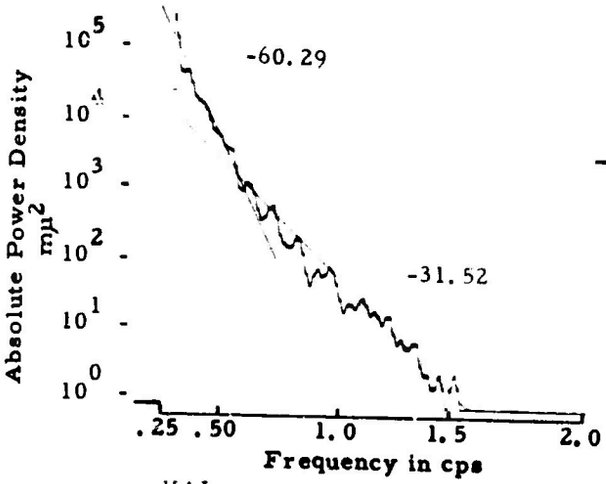

VAL
SPE

7 FEB.
12.5 K

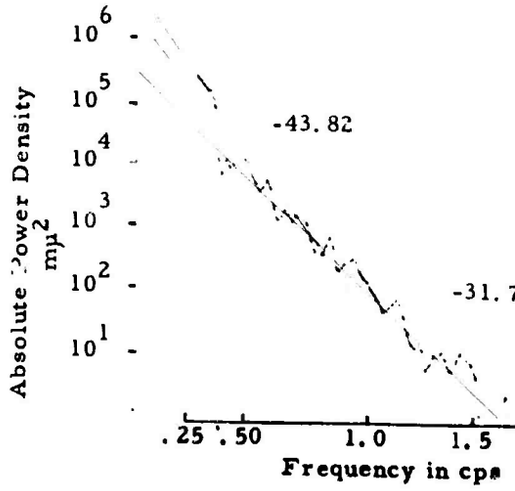

VAL
SPE

B

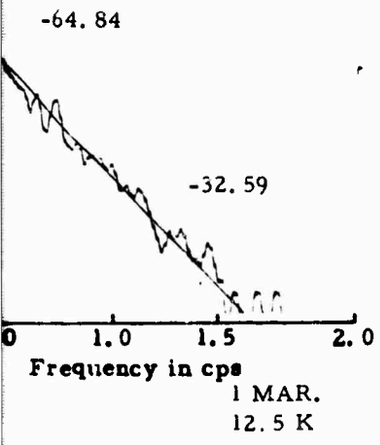

1 MAR.
12.5 K

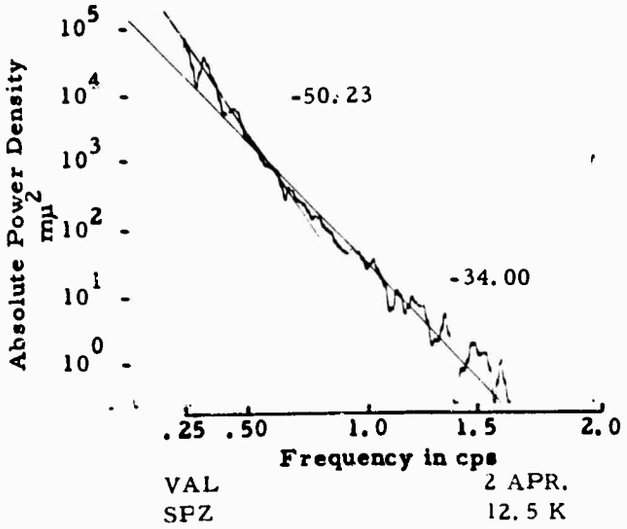

VAL
SPZ

2 APR.
12.5 K

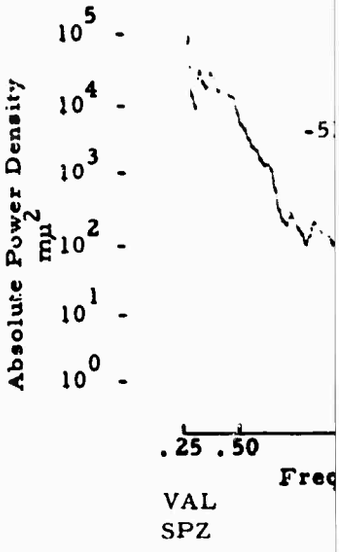

VAL
SPZ

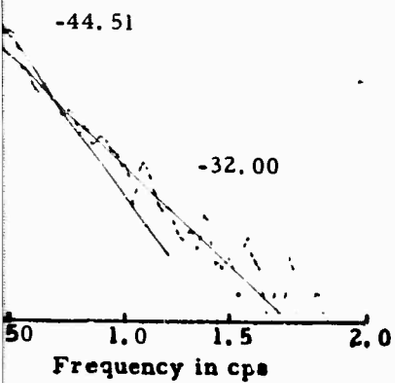

1 MAR.
12.5 K

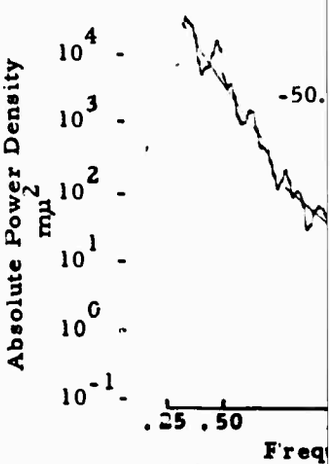

VAL
SPN

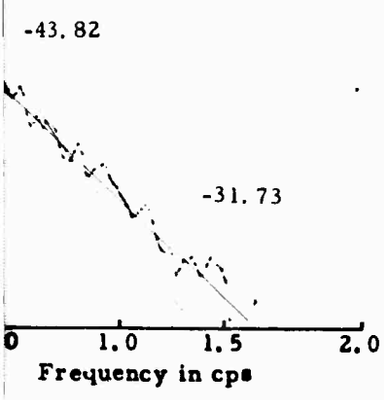

1 MAR.
12.5 K

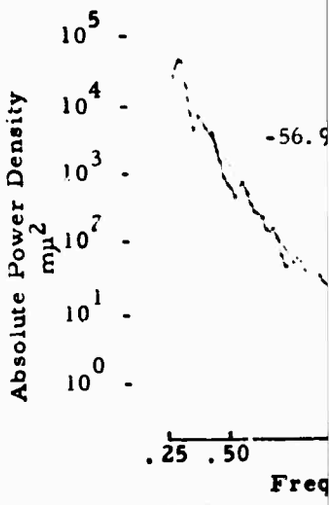

VAL
SPE

C

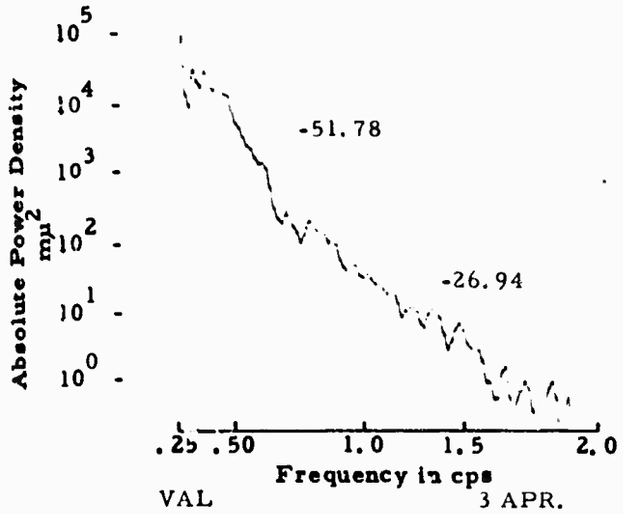

VAL 3 APR.
SPZ 12.5 K

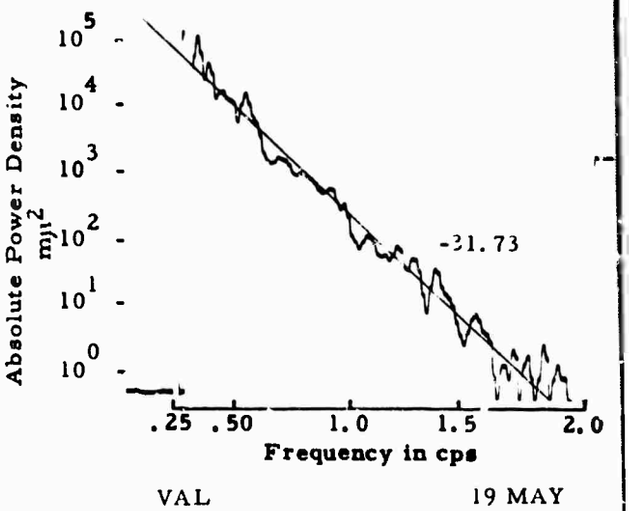

VAL 19 MAY
SPZ 12.5 K

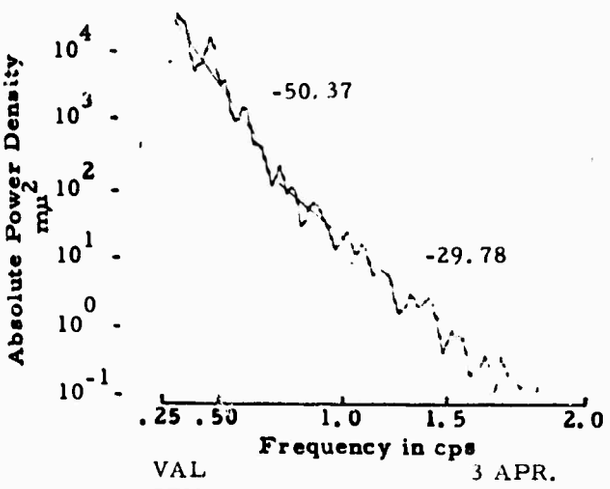

VAL 3 APR.
SPN 12.5 K

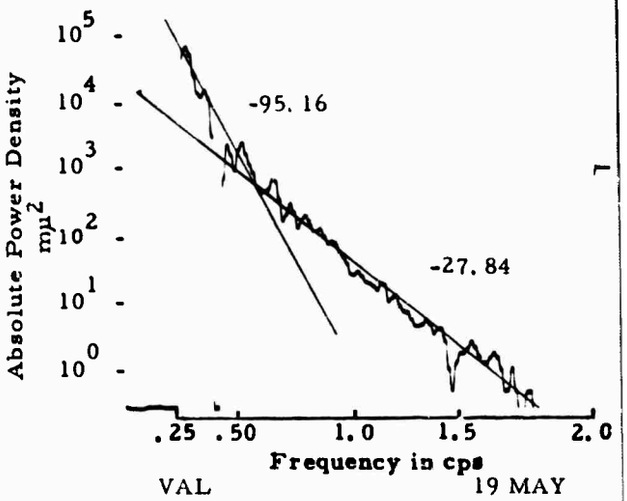

VAL 19 MAY
SPN 12.5 K

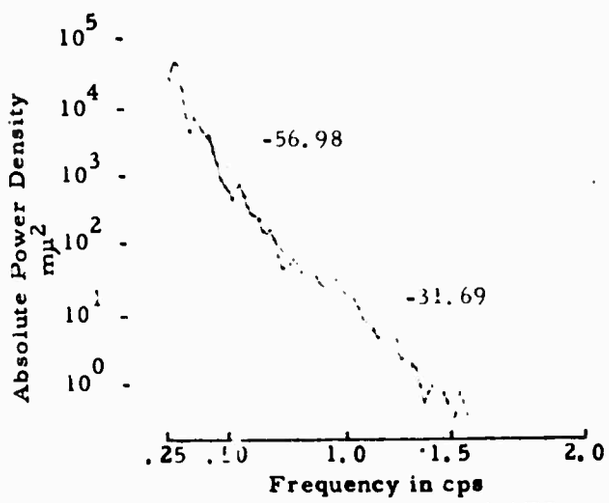

VAL 3 APR.
SPE 12.5 K

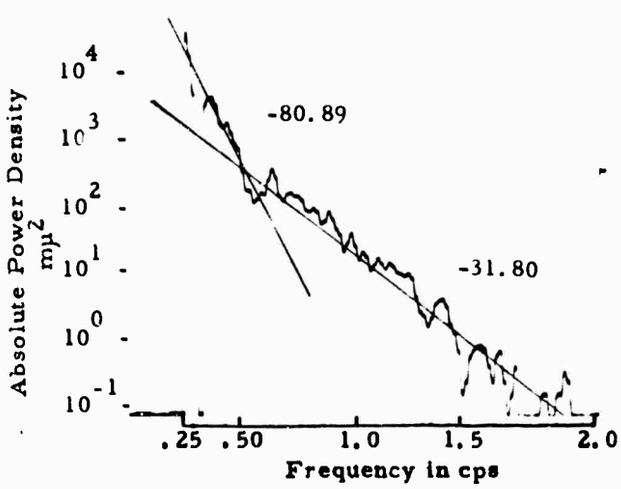

VAL 19 MAY
SPE 12.5 K

Figure A-1f. Absolute Pow

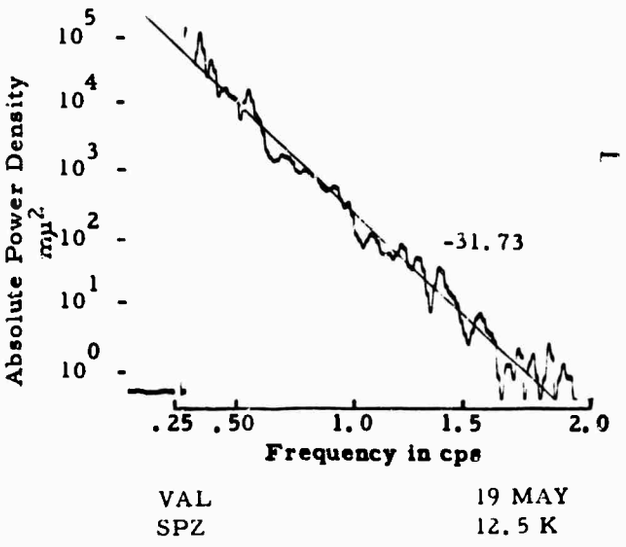

VAL 19 MAY
SPZ 12.5 K

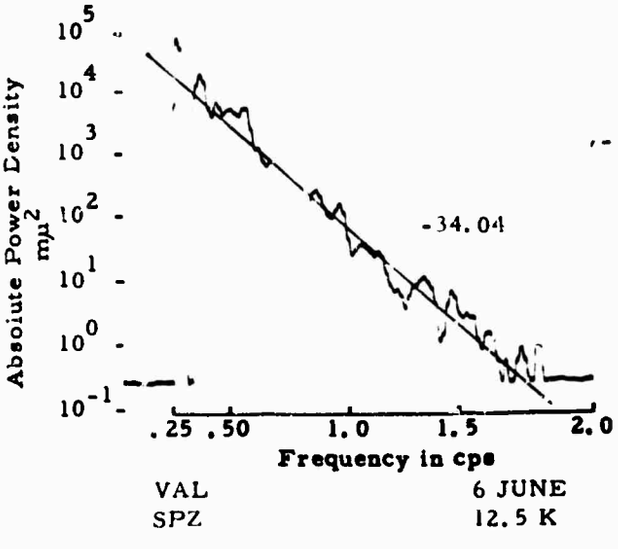

VAL 6 JUNE
SPZ 12.5 K

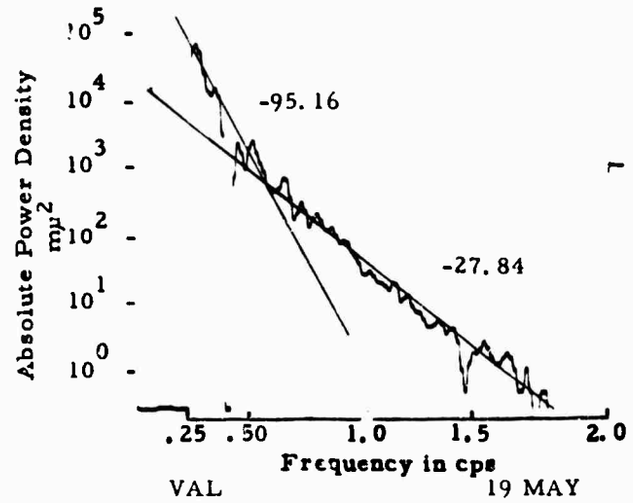

VAL 19 MAY
SPN 12.5 K

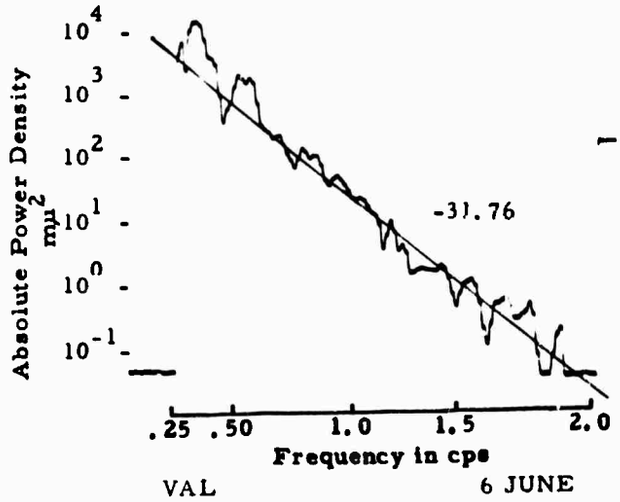

VAL 6 JUNE
SPN 12.5 K

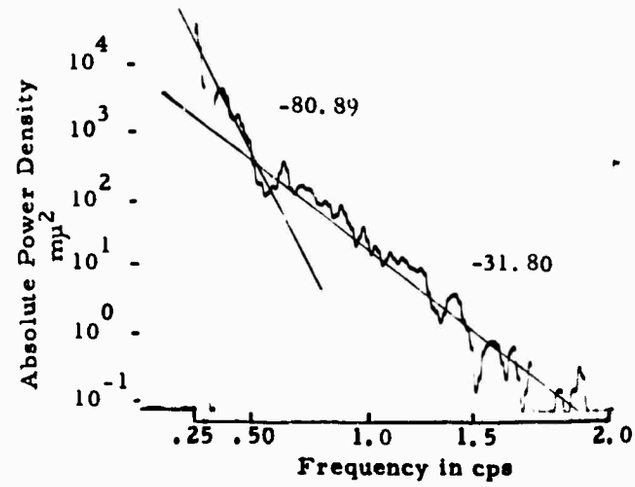

VAL 19 MAY
SPE 12.5 K

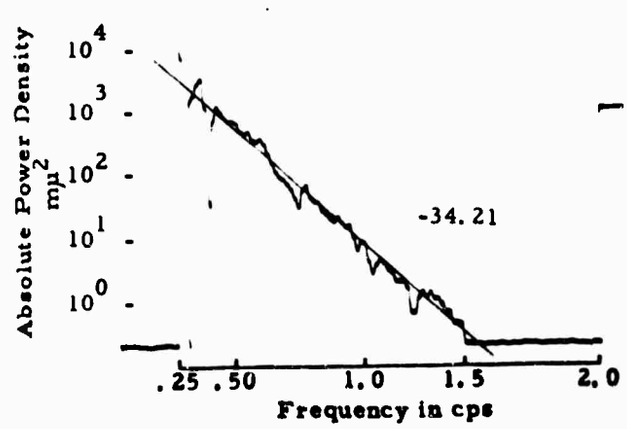

VAL 6 JUNE
SPE 12.5 K

Figure A-1f. Absolute Power Density Spectra Obtained From 1963 Data

APPENDIX B

NOISE MAPS

APPENDIX B

NOISE MAPS

This appendix contains the noise maps for nine months in 1963. The short period maps (0.5 - 2.0 sec) precede the long period maps (3.0 - 8.0 sec) for each month so that comparison may be more easily made. These maps comprise Figures B-1 through B-18.

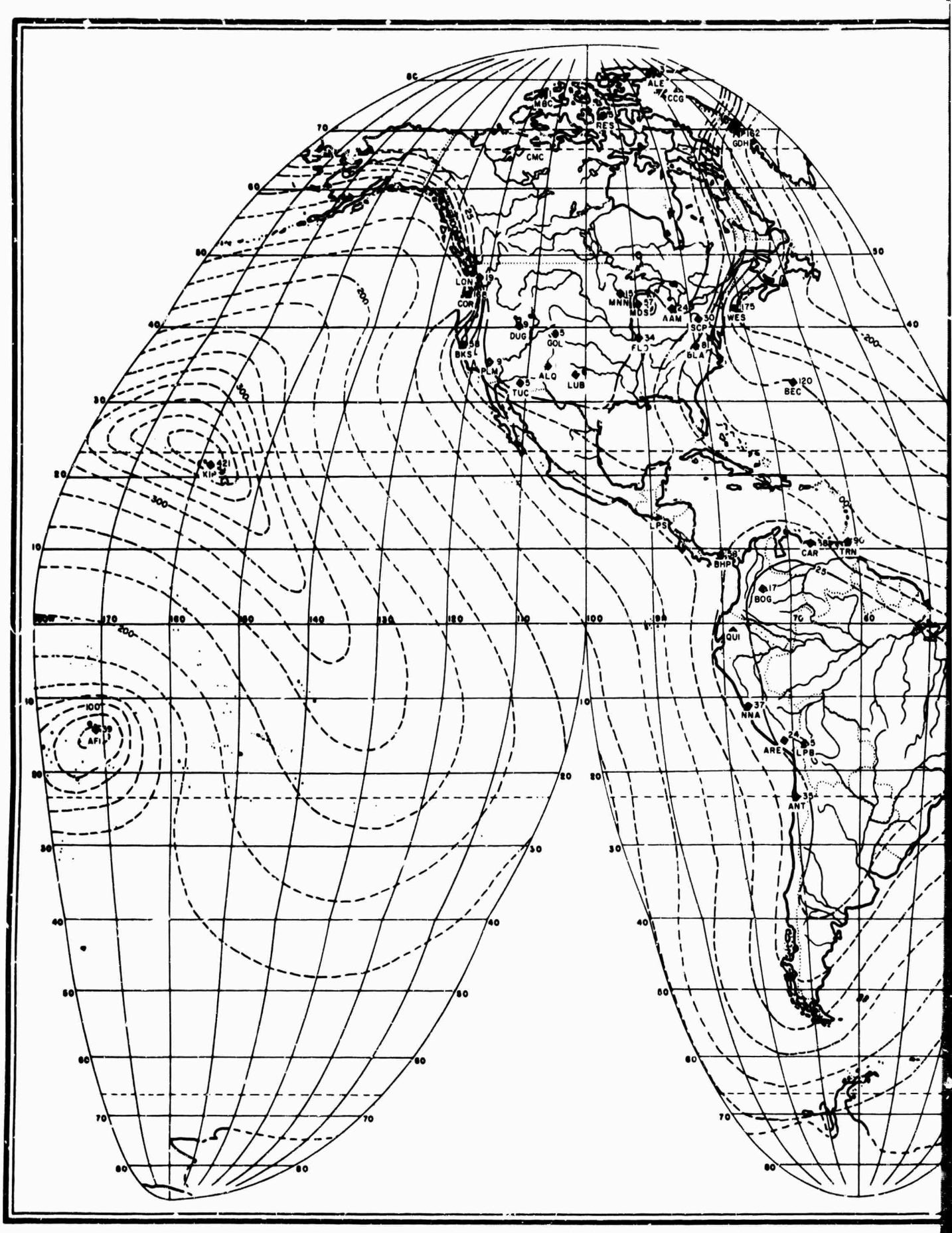
ALE
CCG
RES
WBC
CMC
GDH
LON
COR
DUG
GOL
BKS
PLM
ALQ
LUB
TUC
MNN
MDS
AAM
SCP
FLJ
BLA
WES
BEC
KIP
LPS
BHP
CAR
TRN
BOG
QUI
NNA
ARE
LPB
ANT
AFI
300
200
100

A

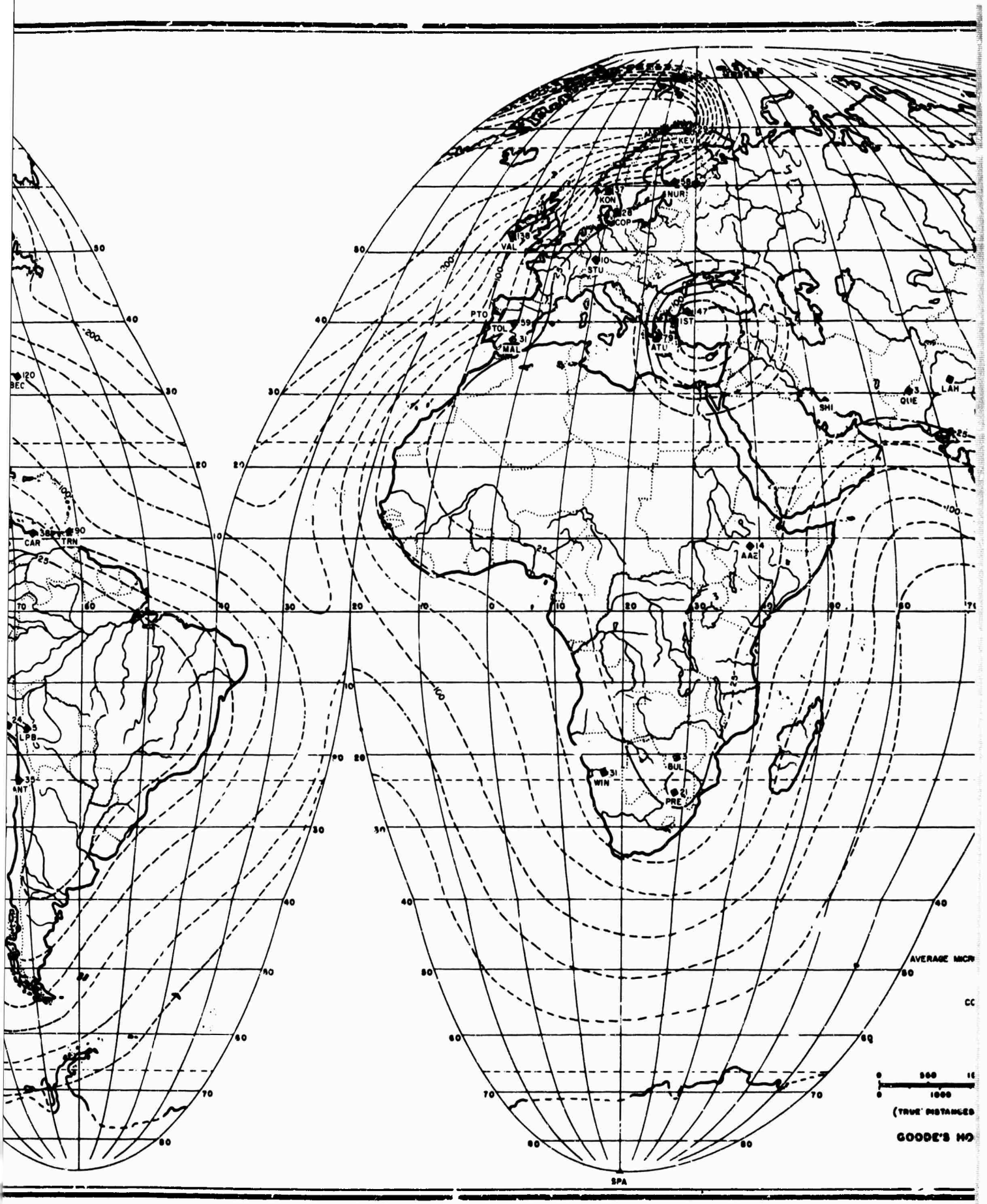
KEV
KON
NUR
COP
VAL
STU
PTO
TOL
MAL
IST
ATU
BEC
SHI
QIE
LAH
CAR
TRN
AAE
LPB
ANT
WIN
BUL
PRE
SPA
AVERAGE MICR
CC
(TRUE DISTANCES
GOODE'S HO

Figu

B

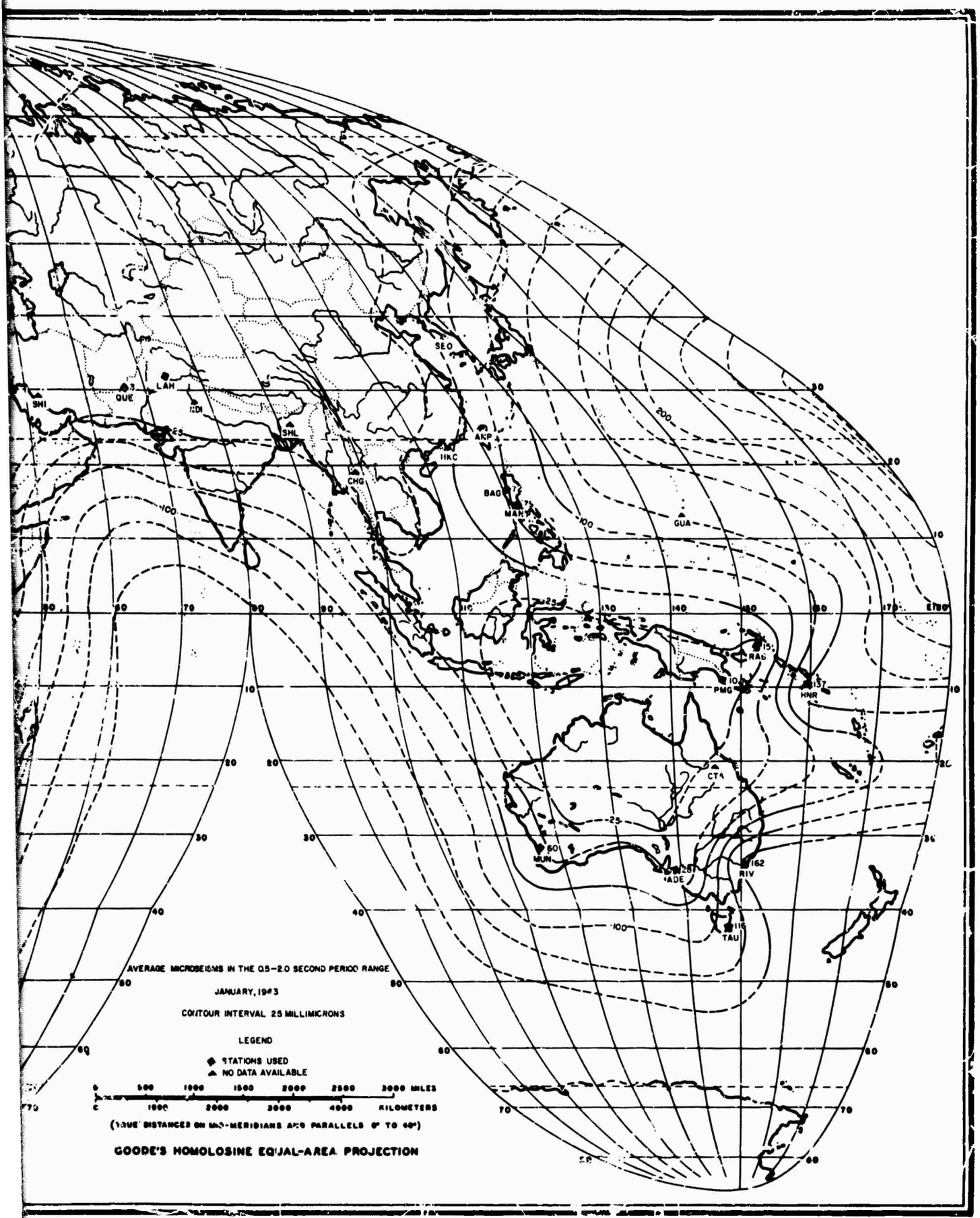

Figure B-1. World Map of 0.5-2.0 Second Microseismic Activity, January, 1963

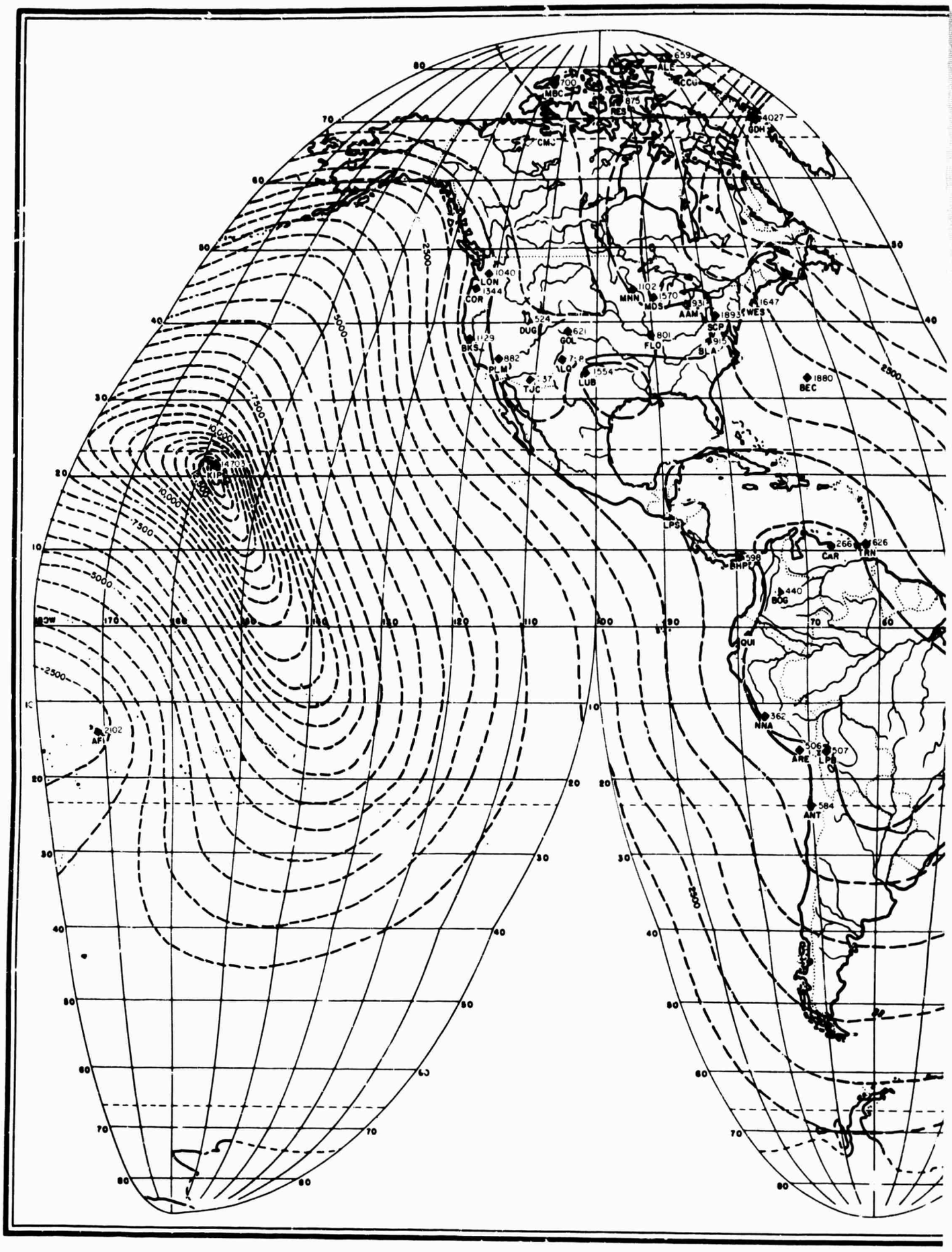
659
ALE
700
MBC
875
RES
4027
GDH
CMJ
1040
LON
1344
COR
1102
MNN
1570
MDS
931
AAM
1647
WES
1893
SCP
915
BLA
524
DUG
621
GOL
1129
BKS
882
PLM
801
FLO
1554
LUB
37
TJC
1880
BEC
14703
KIP
PS
266
CAR
626
TRN
598
BHPL
440
BOG
QUI
362
NNA
306
ARE
507
LPB
584
ANT
2102
AFI
2500
5000
7500
10,000
170
160
150
140
130
120
110
100
90
80
70
60
50
40
30
20
10

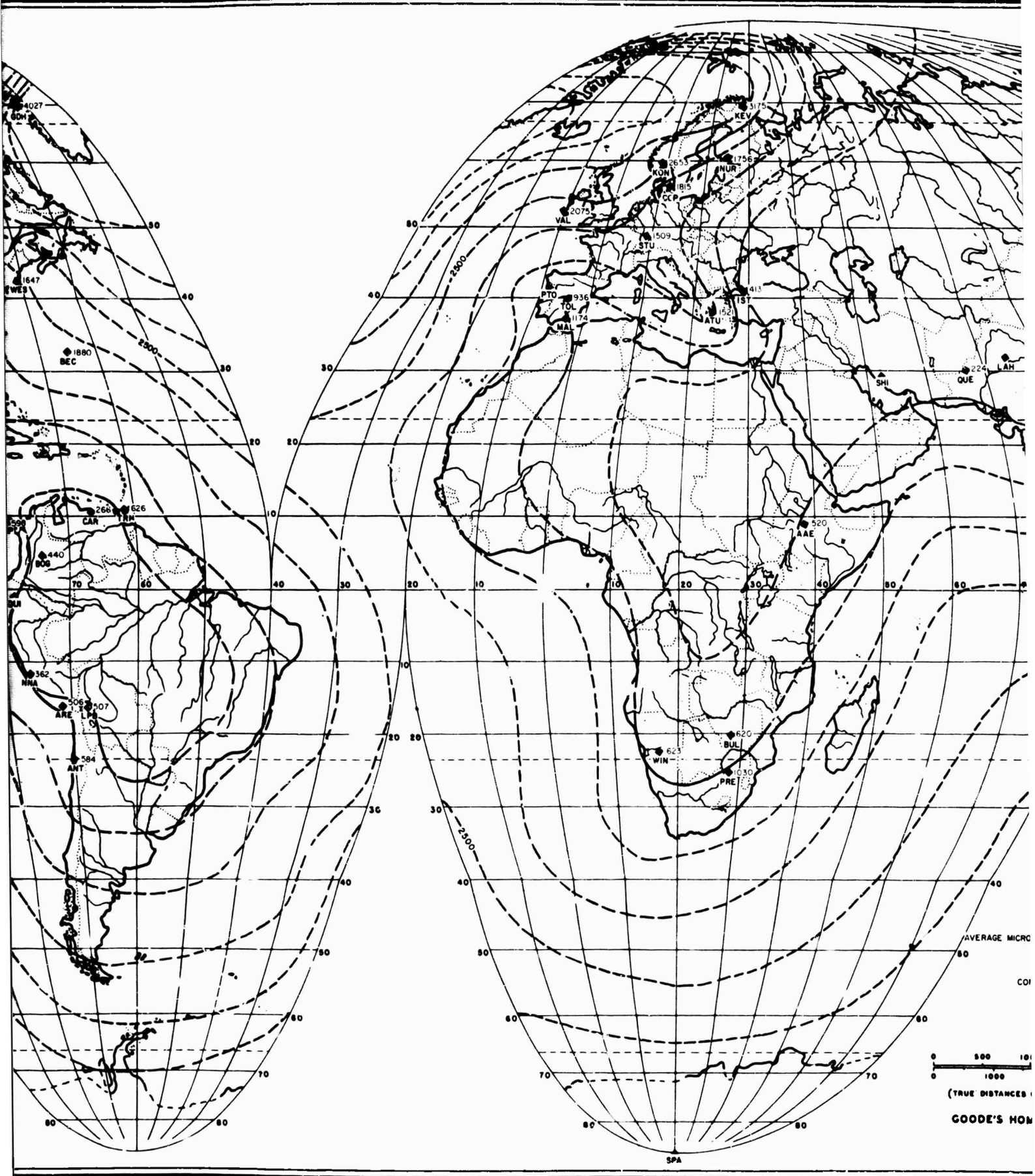
4027
GDH
1647
WES
1880
BEC
268
CAR
626
TRN
440
BUR
362
NNA
506
507
AKE
LPB
584
ANT
2653
KON
1756
NUR
1815
CCP
3175
KEV
2075
VAL
1509
STU
936
PTO
TOL
1174
MAL
1621
ATU
413
IST
SHI
224
QUE
LAH
520
AAE
620
BUL
623
WIN
1030
PRE
2500
SPA
AVERAGE MICRO
COI
(TRUE DISTANCES
GOODE'S HOM

b

Figure

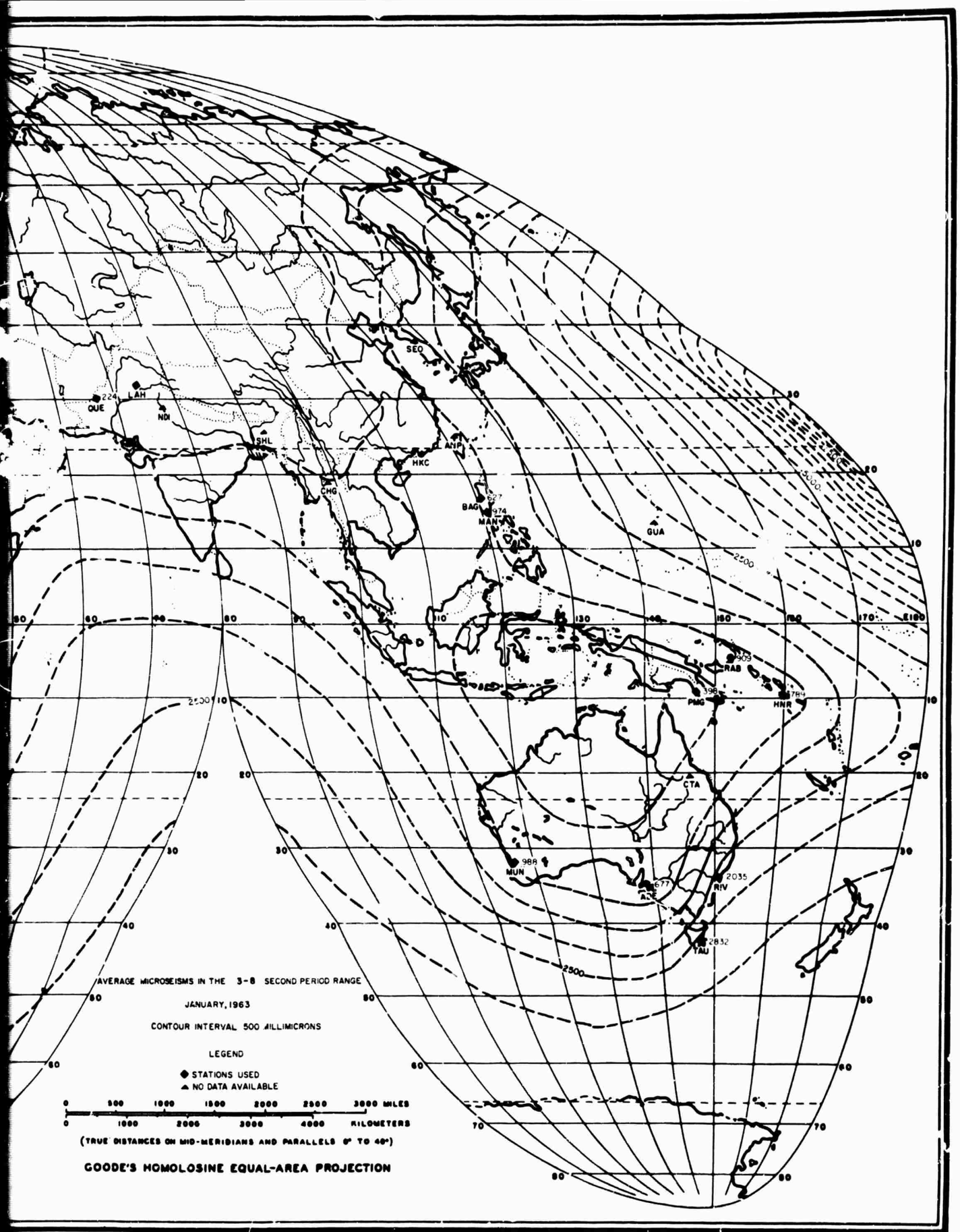

Figure B-2. World Map of 3.0-8.0 Second Microseismic Activity, January, 1963

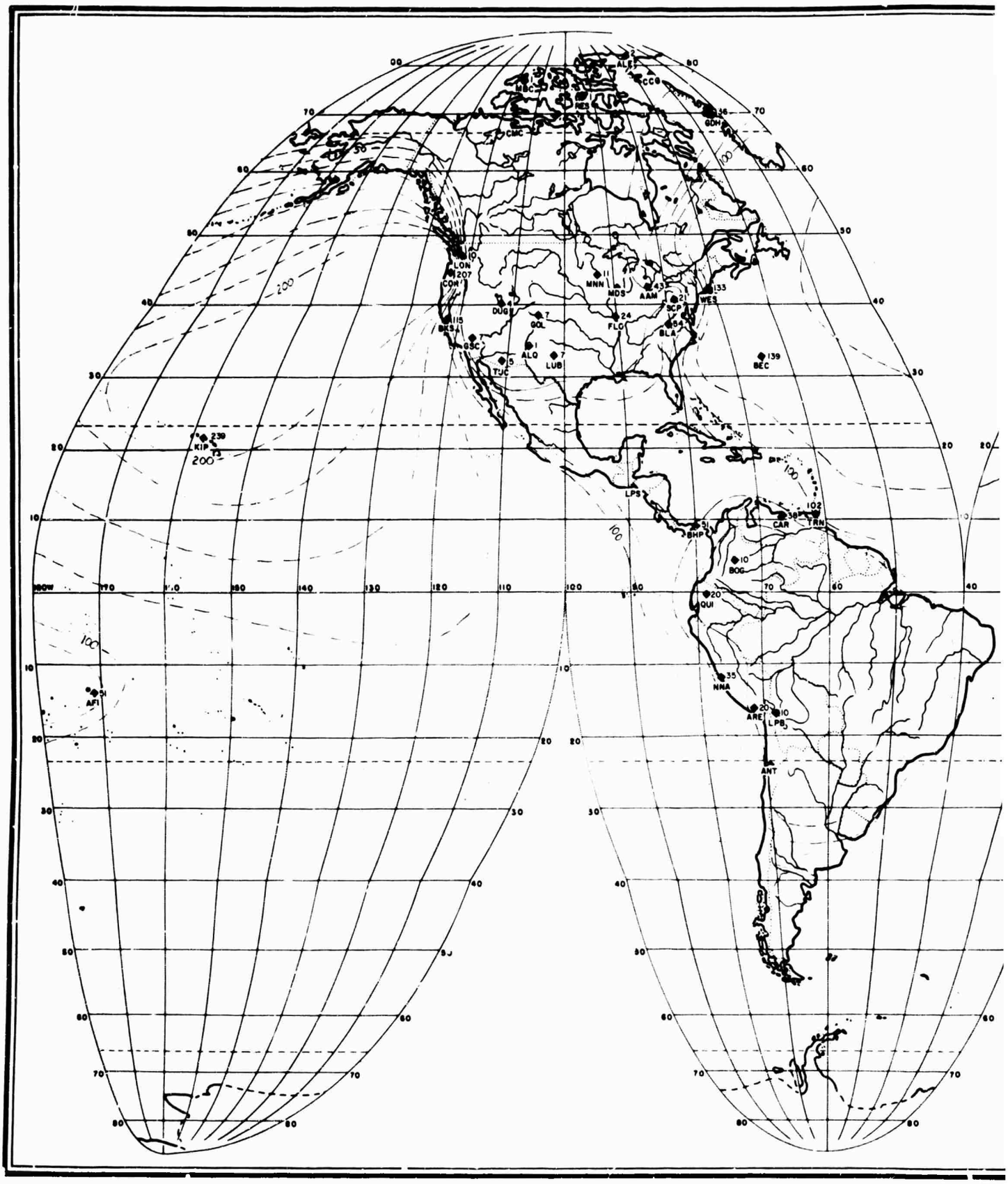
ALE
BRW
CCB
RES
CMC
GDH
LON
COM
DUG
BKS
GSC
TUC
ALQ
LUB
GOL
FLG
MNN
MDS
AAM
SCP
BLA
WES
BEC
KIP
LPS
BHP
CAR
TRN
BOG
QUI
NNA
ARE
LPB
ANT
AFI

A

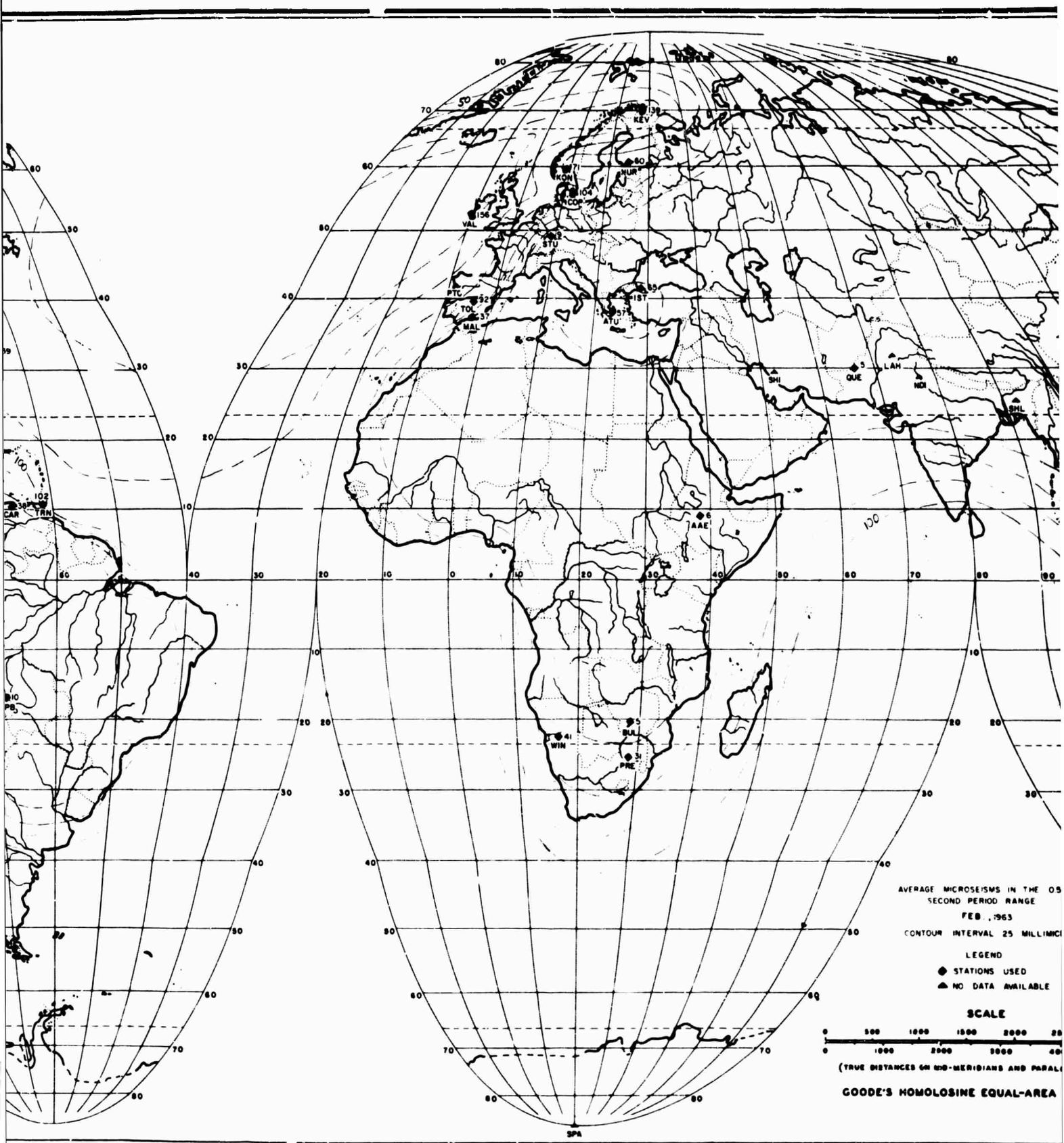

Figure B-3. World Map

B

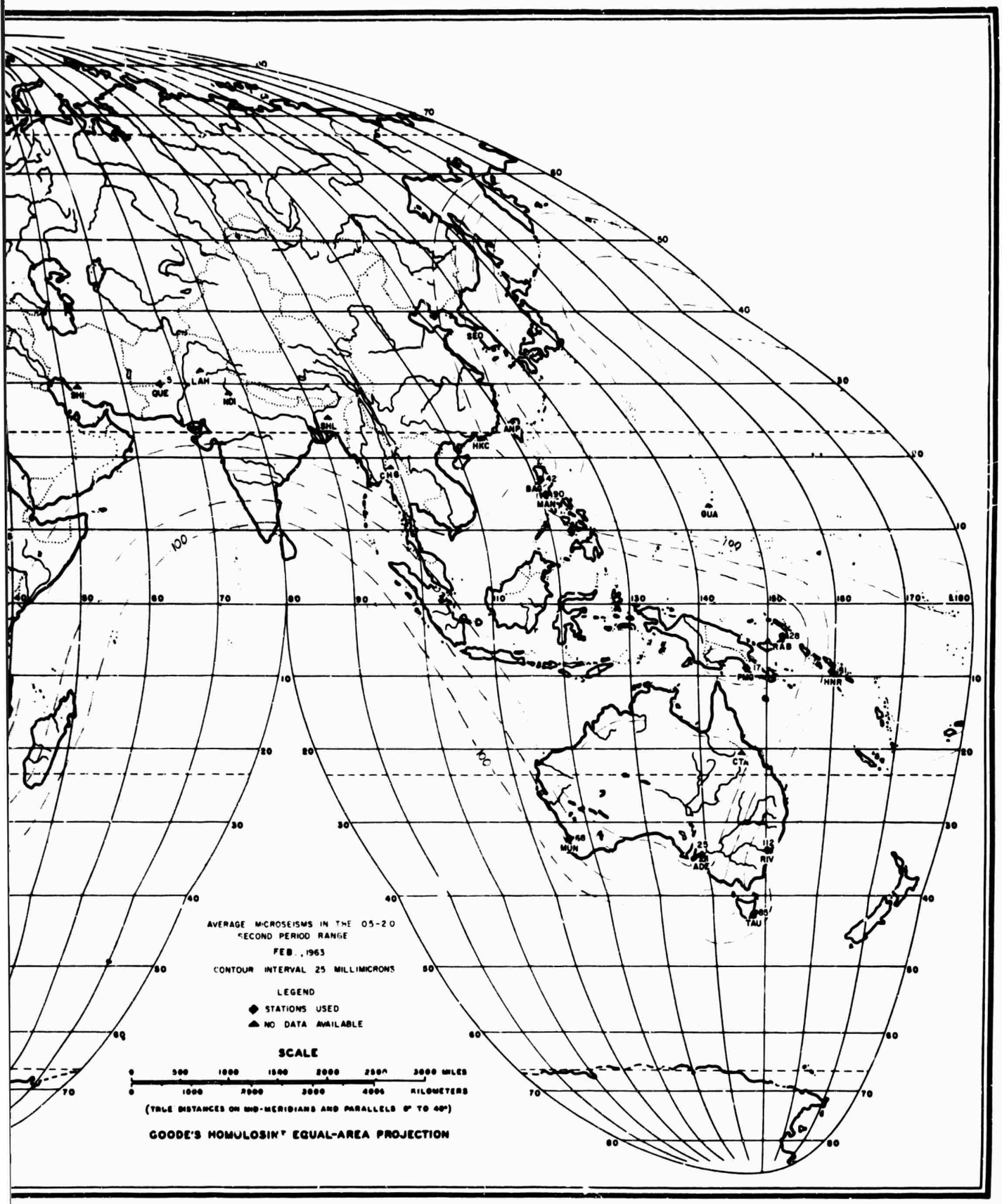

Figure B-3. World Map of 0.5-2.0 Second Microseismic Activity, February, 1963

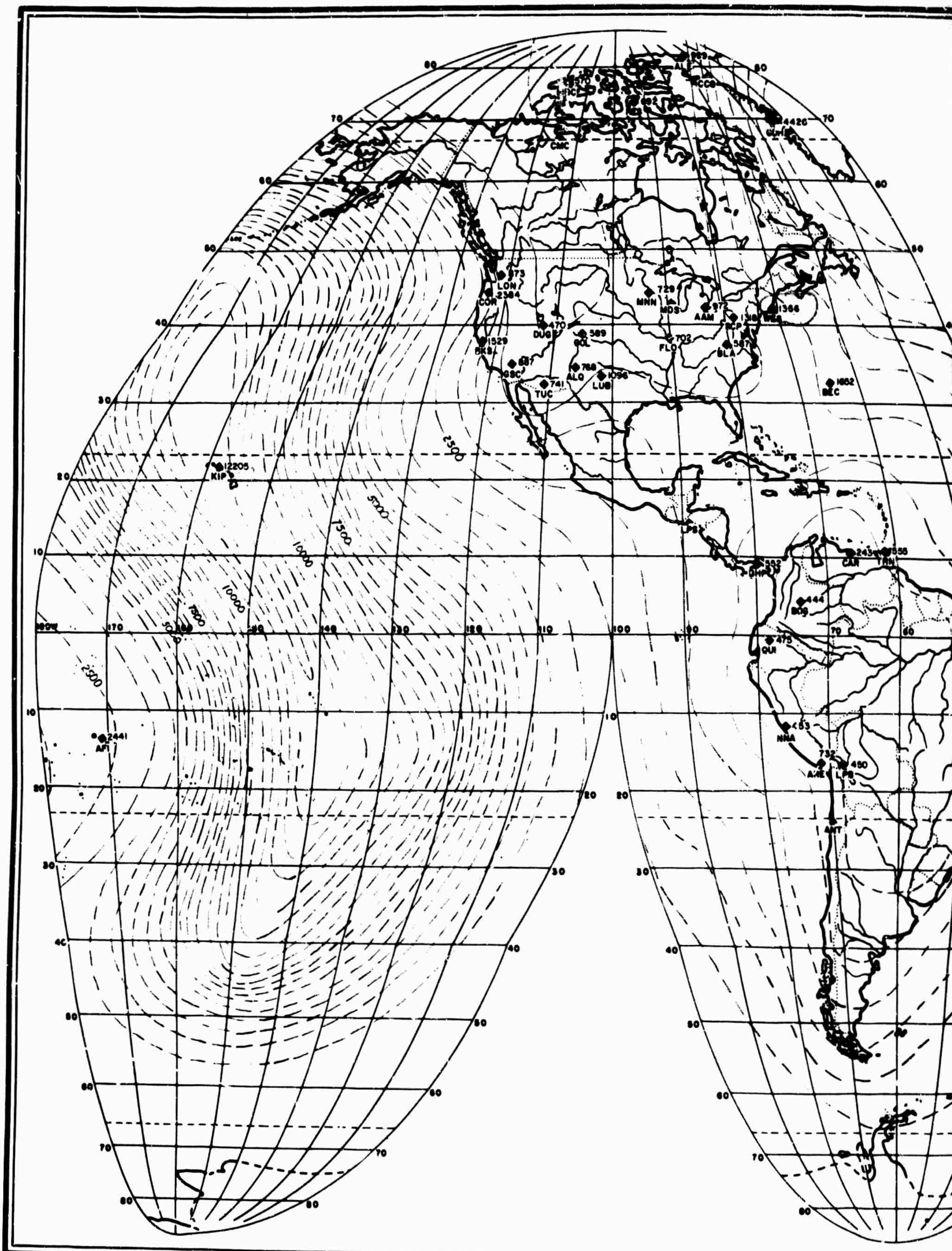

12205
KIP
2441
AFI
2384
COR
1529
BKS
741
TUC
1096
LUB
729
MNN
702
FLO
1662
BEC
CAR
TRN
444
BOG
475
QUI
450
ANT
2500
5000
7500
10000
180W

A

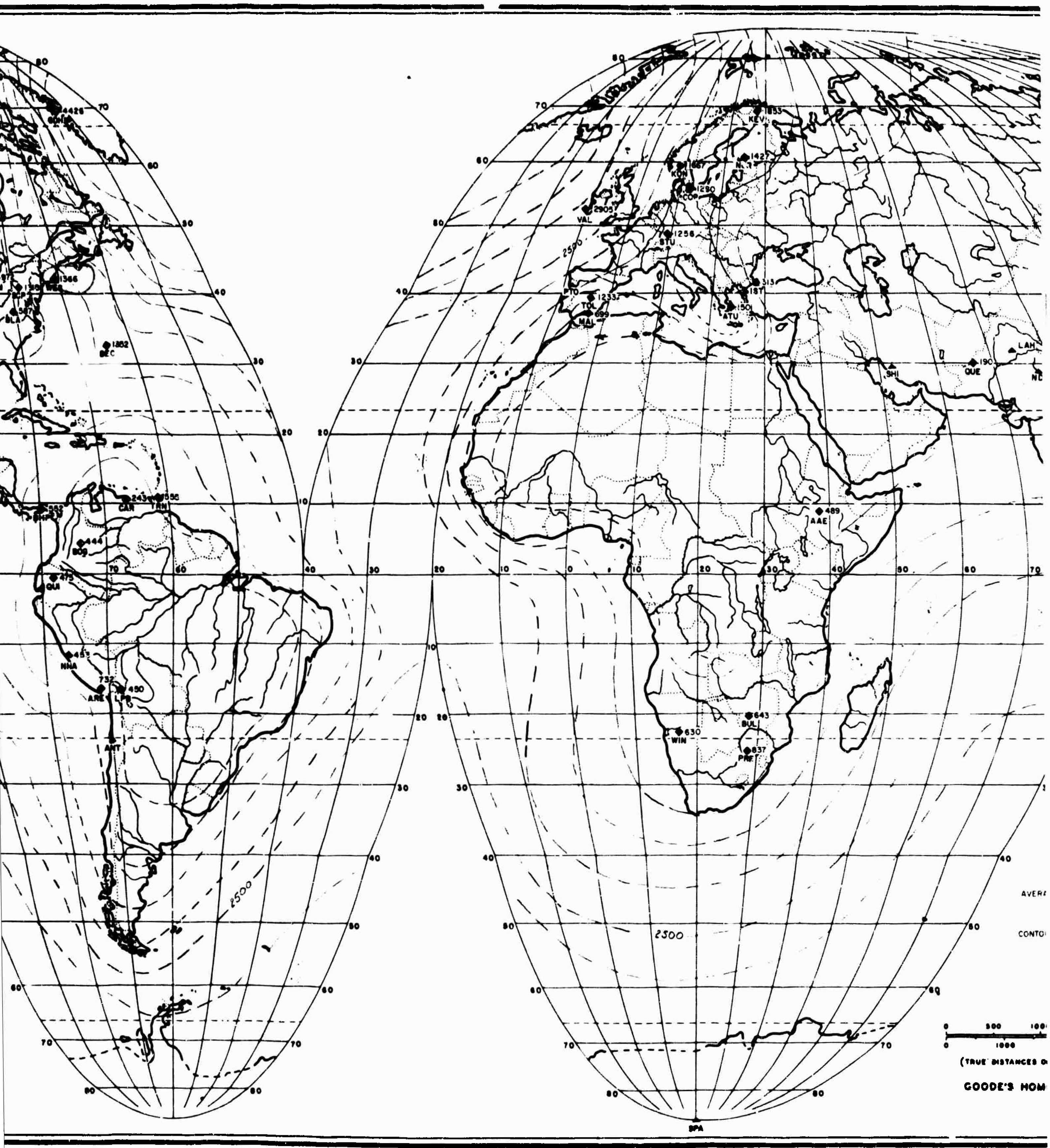
4426
1366
1852
BEC
243
CAN
TAN
444
BOG
473
QUI
453
NNA
732
ARE
450
LPB
ANT
2500
1853
KEV
1427
1290
COP
2905
VAL
1256
STU
313
IST
150
ATU
PTO
1233
TOL
699
MAL
LAH
190
QUE
SHI
489
AAE
630
WIN
643
BUL
837
PRE
SPA
AVER
CONTO
0
500
1000
(TRUE DISTANCES O
GOODE'S HOM

Figure B-4.

b

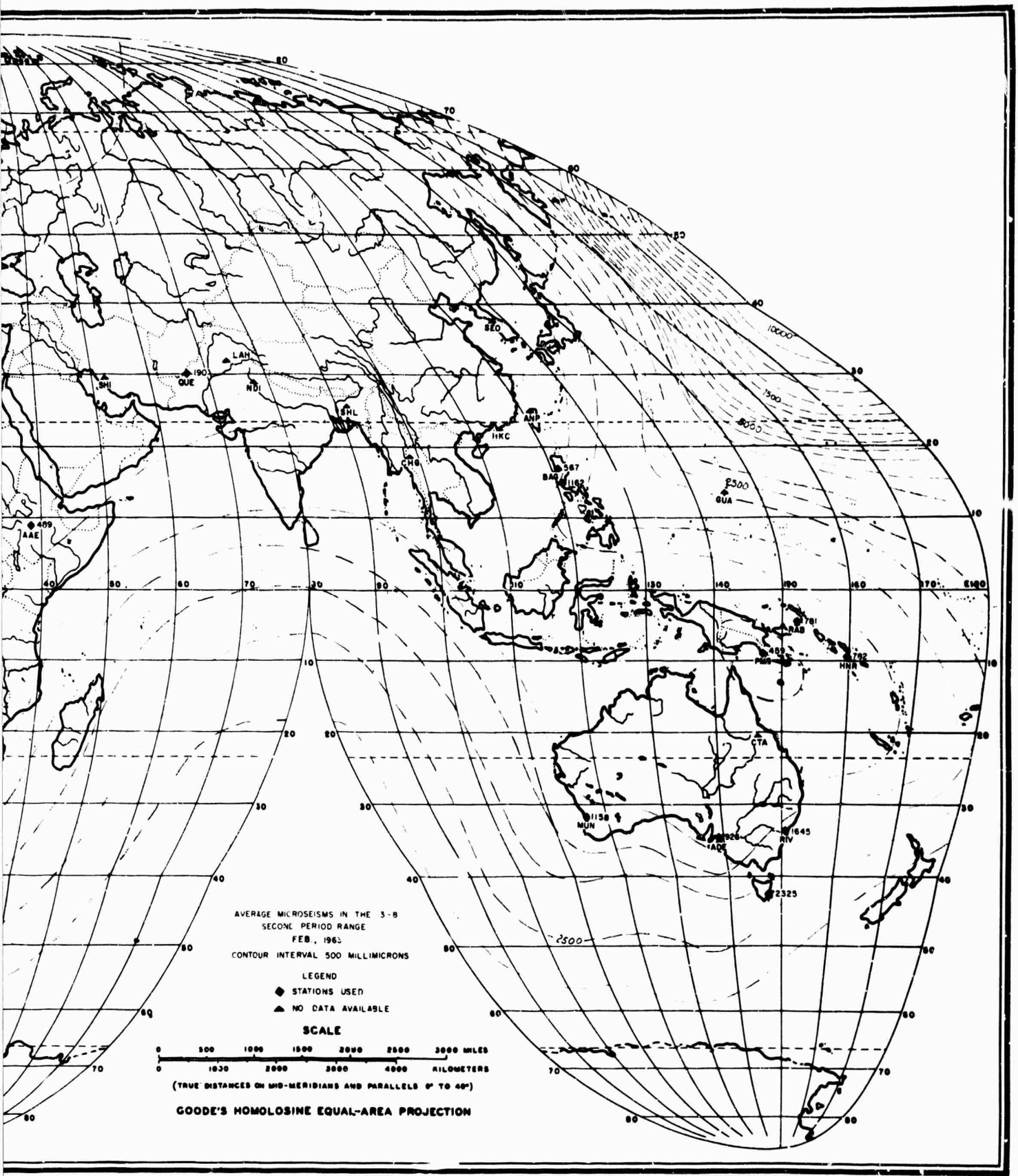

Figure B-4. World Map of 3.0-8.0 Second Microseismic Activity, February, 1963

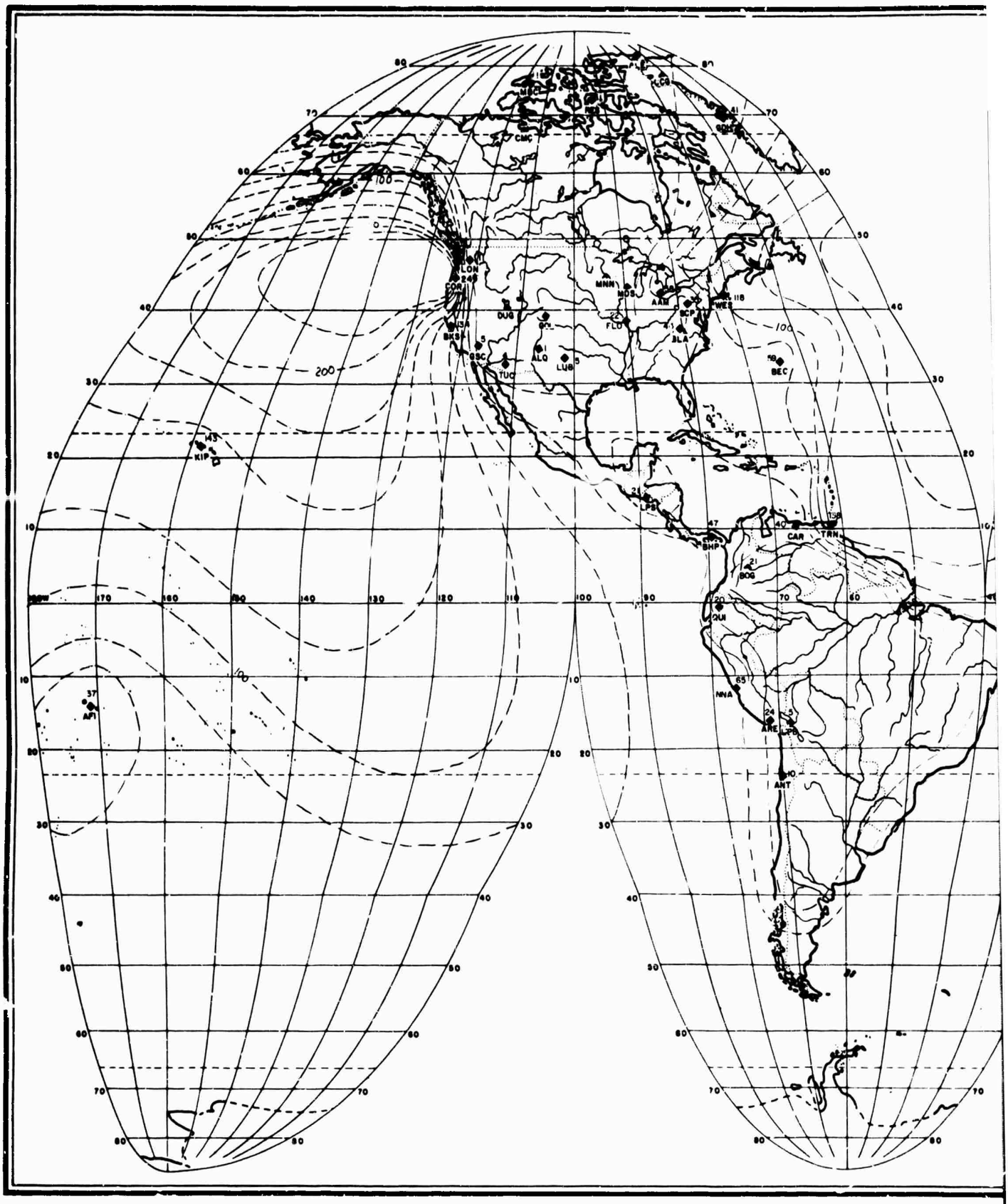
CMC
LON
240
COR
DUG
BKS
GSC
TUC
ALQ
LUB
MNN
MDS
AAM
SCP
FLO
BLA
WES
118
BEC
KIP
143
PSS
BHP
CAR
TRN
BOG
QUI
NNA
ARE
LPB
ANT
API
37
100
200

A

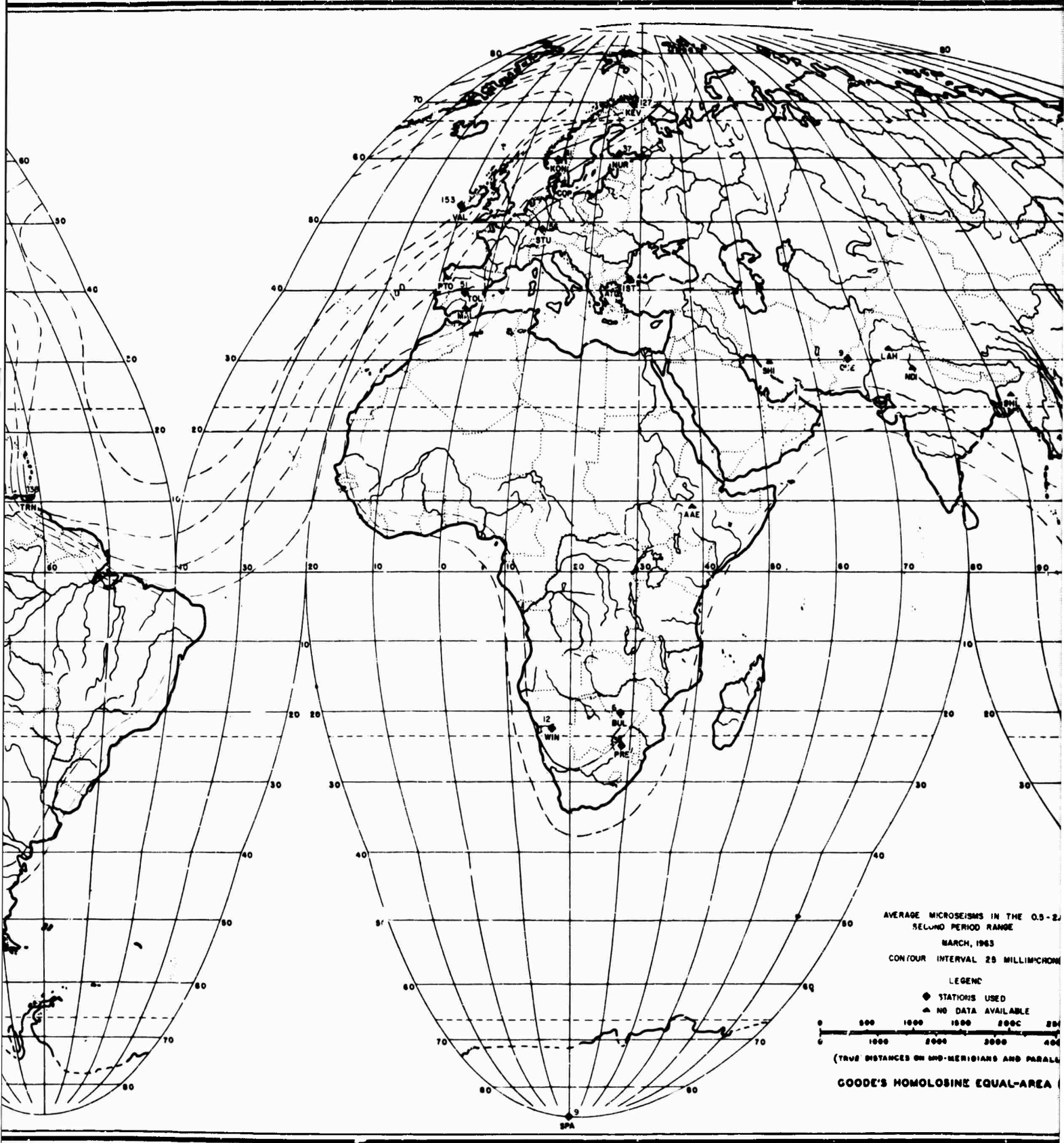

Figure B-5. World Map

B

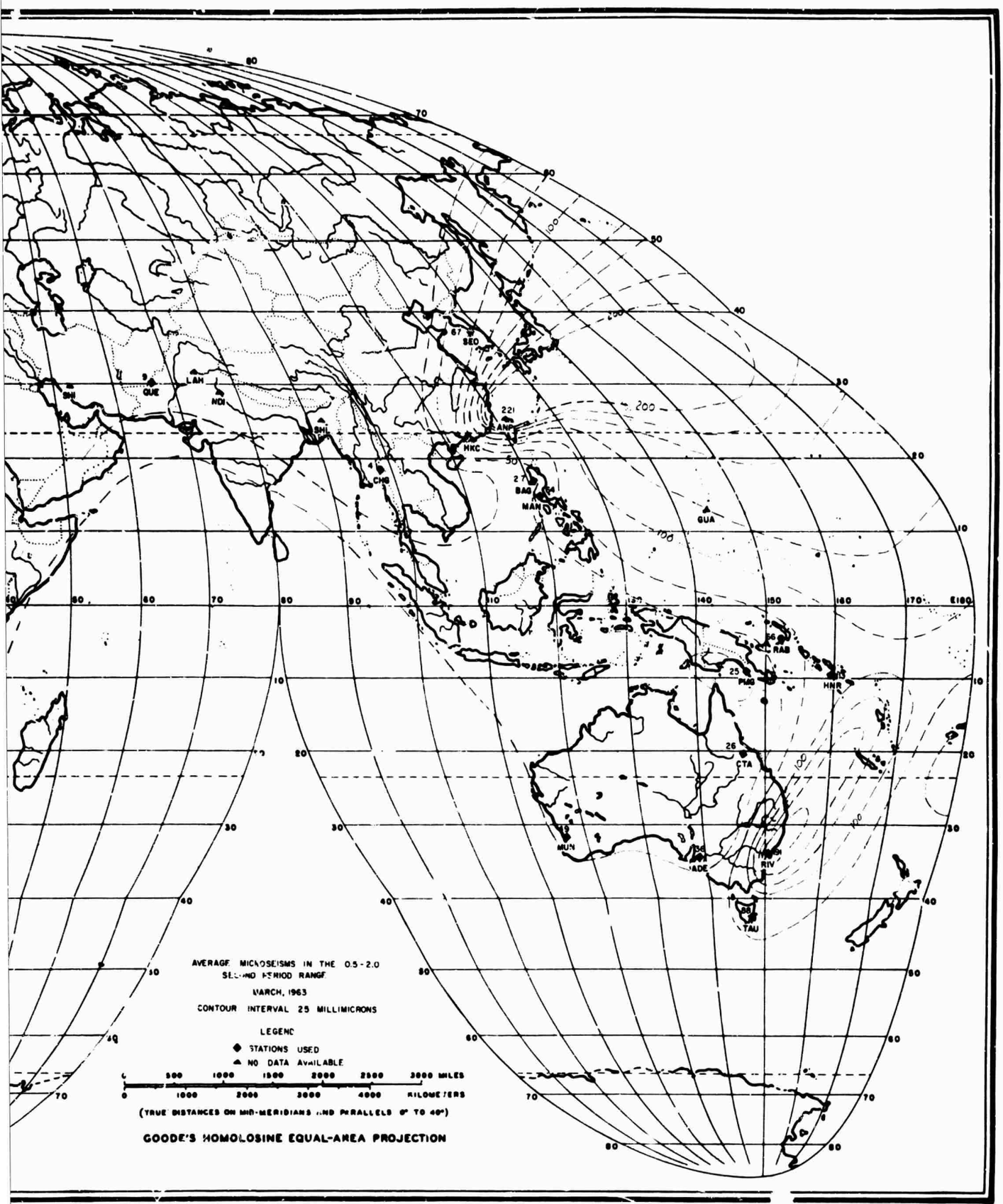

Figure B-5. World Map of 0.5-2.0 Second Microseismic Activity, March, 1963

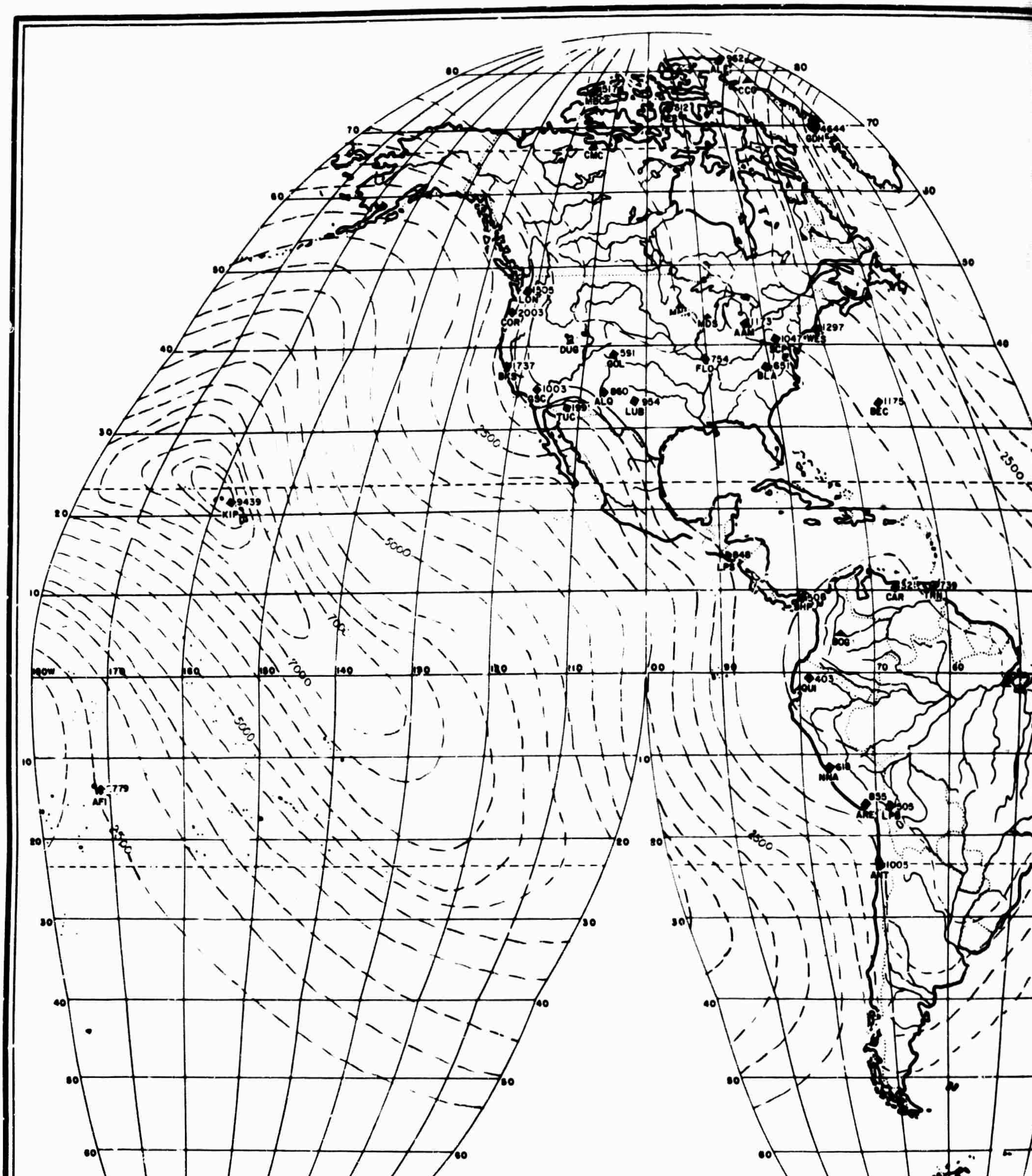

CMC
1305
LON
2003
COR
DUG
591
GOL
1737
BRS
1003
GSC
860
ALQ
954
LUB
TUC
754
FLO
MDS
AAM
1047
1297
651
BLA
1175
BEC
CCO
4644
GDH
9439
KIP
5000
7000
2500
LPS
CAR
BOG
403
QUI
NHA
ARE
1005
ANT
779
AFI

A

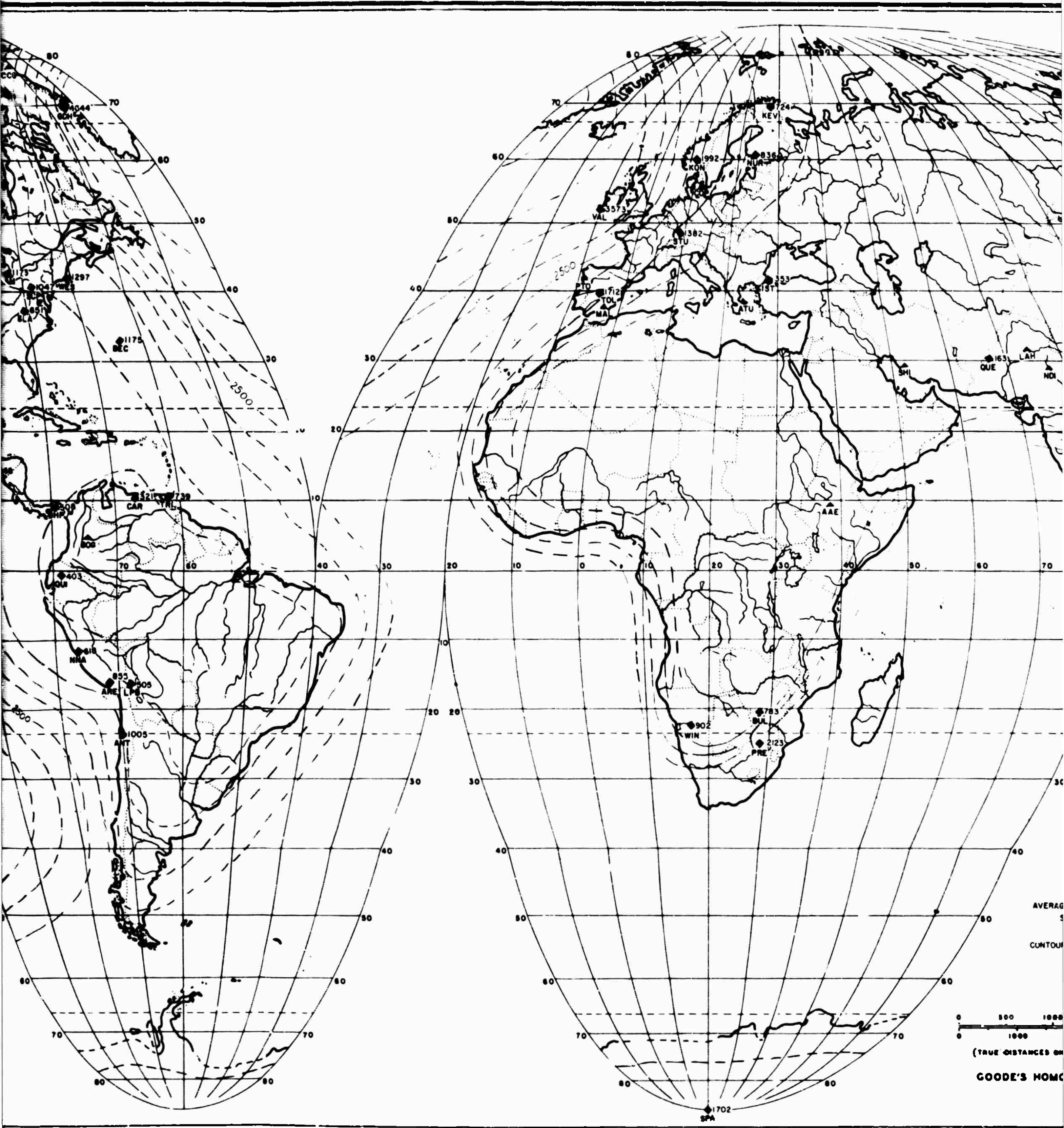
1044 SCH
1297 WES
1047
651 BLA
1175 BEC
1521 CAR
1739 TRI
BOG
403 QUI
NNA
855 ARE
LPB
1005 ANT
1992 KON
836 NUR
724 KEV
3573 VAL
1382 STU
1712 TOL
PTO
MA
IST
ATU
QUE
LAH
NDI
SHI
AAE
902 WIN
783 BUL
2123 PRE
1702 SPA
2500
AVERAG
CONTOU
(TRUE DISTANCES ON
GOODE'S HOMO

Figure B-

B

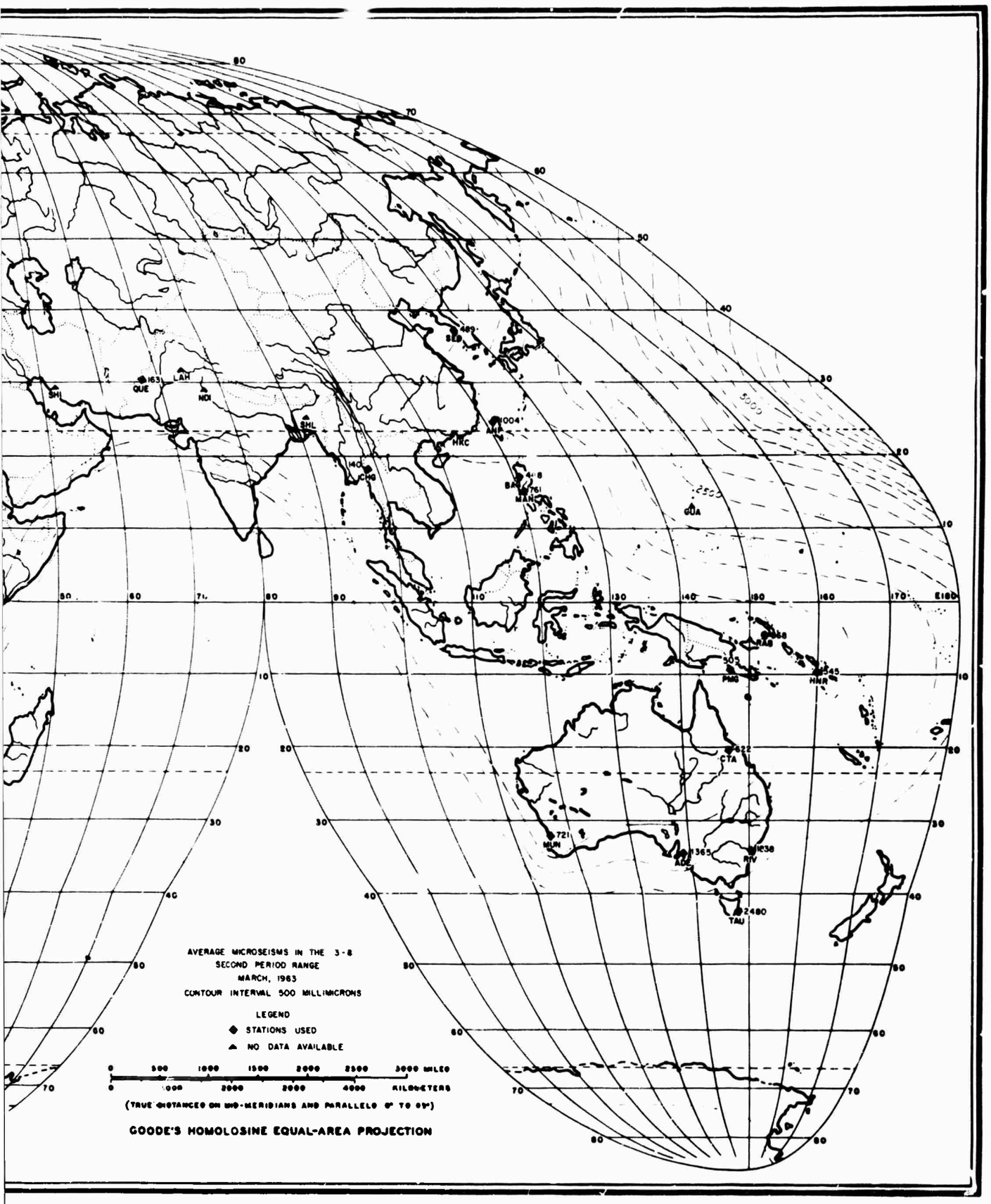

Figure B-6. World Map of 3.0-8.0 Second Microseismic Activity, March, 1963

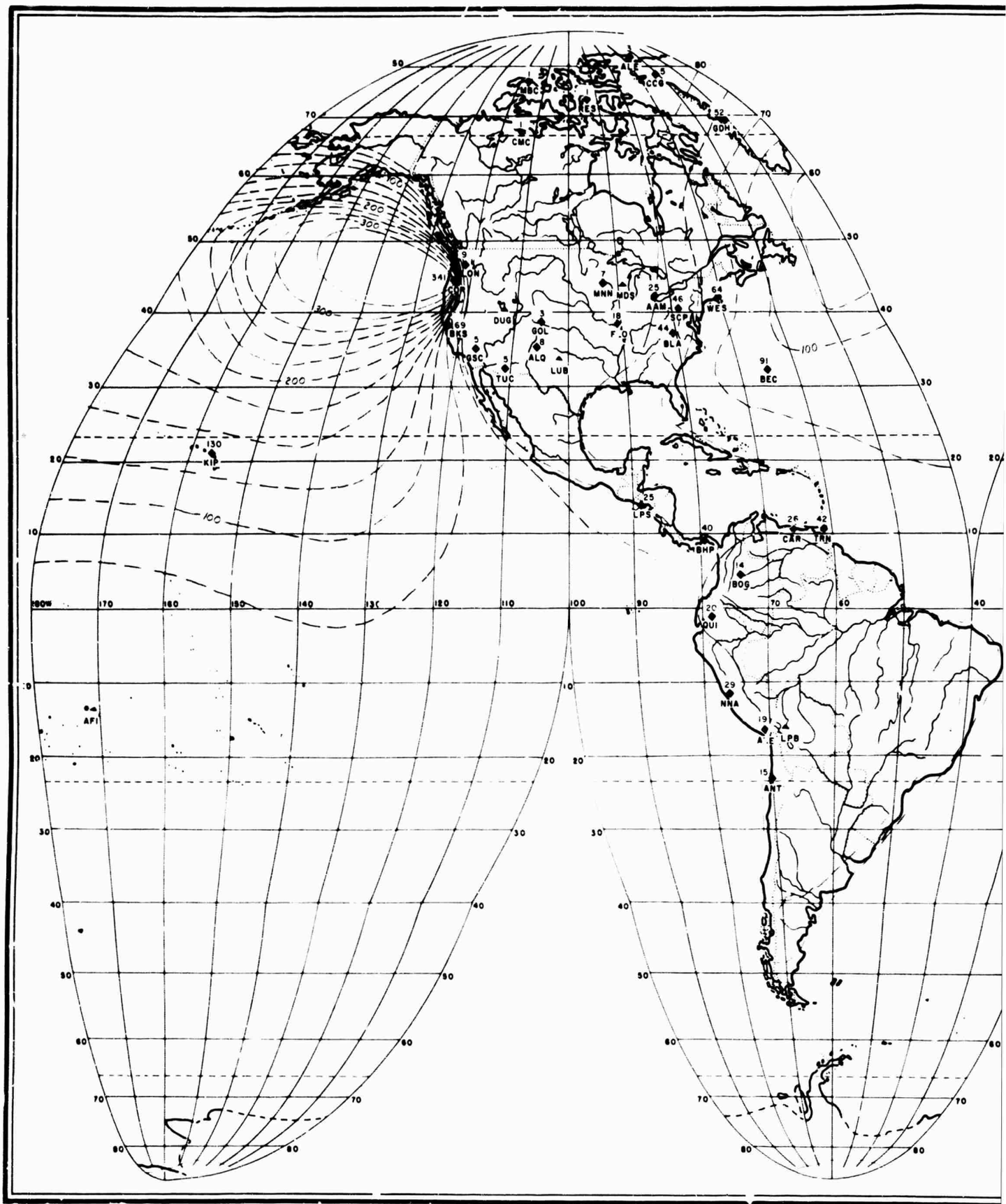
ALE
CCC
RES
MBC
CMC
YDH
MNN
MDS
AAM
SCP
WES
BLA
DUG
GOL
ALQ
LUB
TUC
BKS
PSC
BEC
KIP
LPS
BHP
CAR
TRN
BOG
QUI
NNA
LPB
ANT
AFI
100
200
300

A

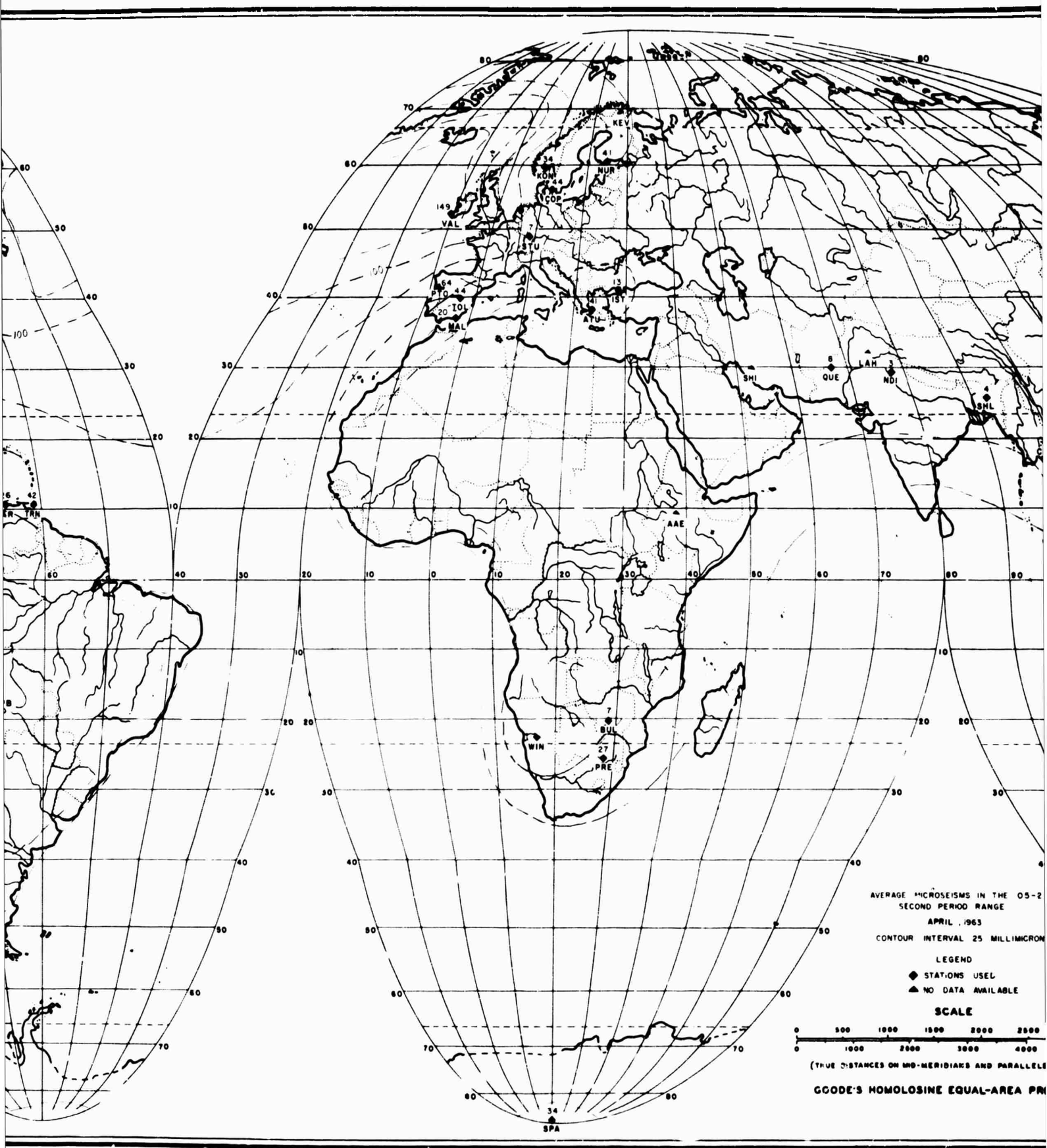

Figure B-7. World Map o

B

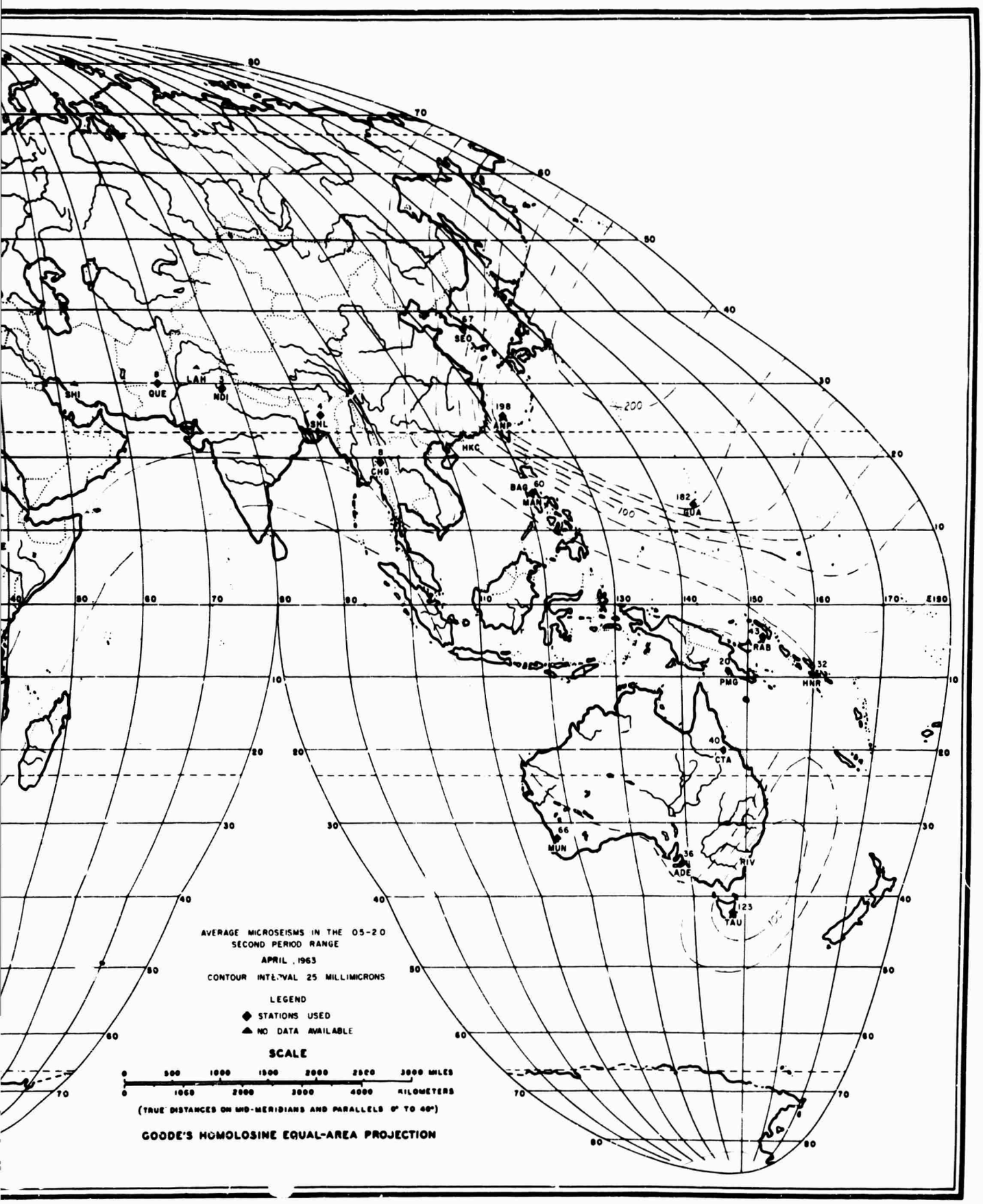

Figure B-7. World Map of 0.5-2.0 Second Microseismic Activity, April, 1963

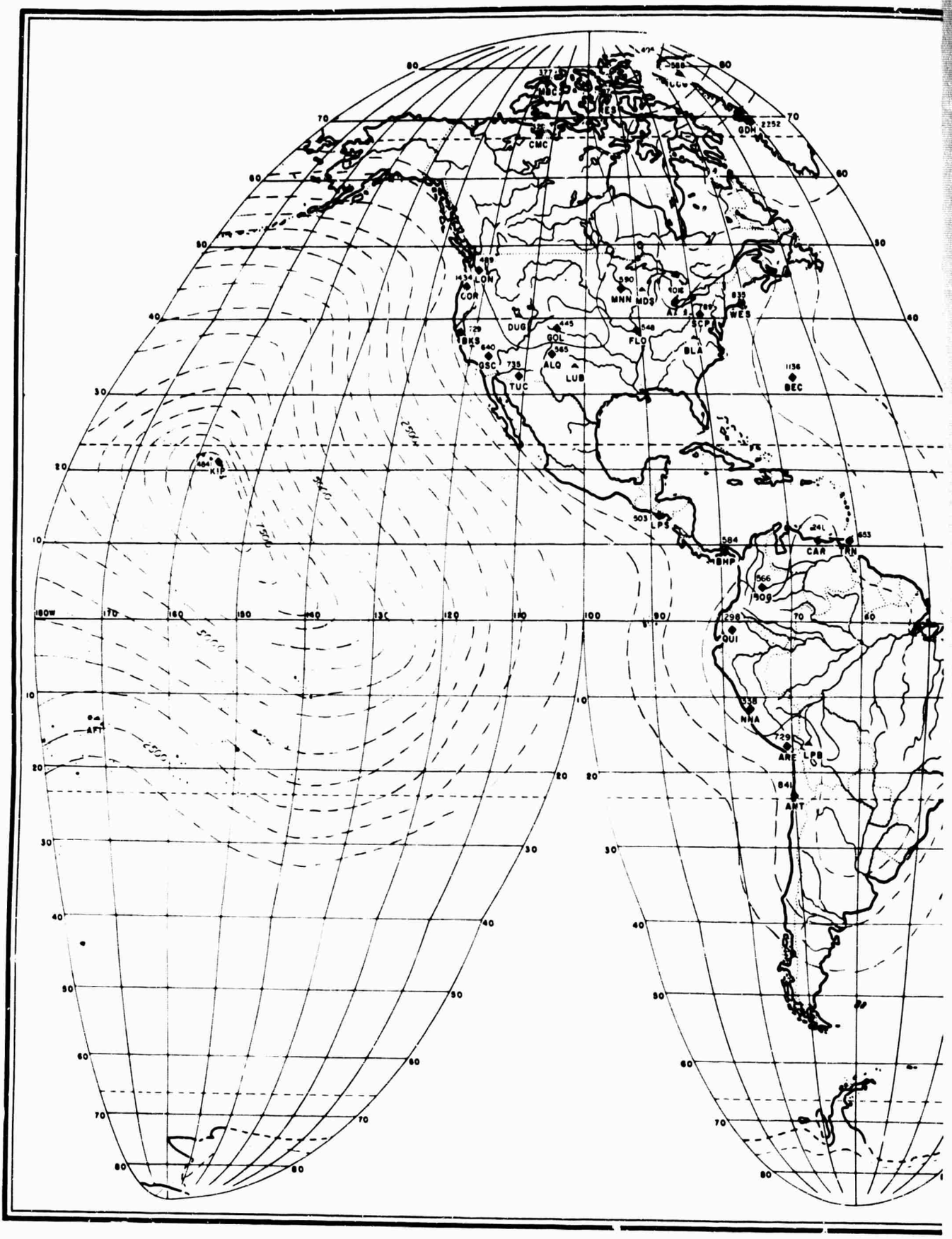
CMC
GDH
LON
COR
MNN
MDS
SCP
WES
DUG
GOL
FLO
BLA
TBS
GSC
ALQ
LUB
TUC
BEC
KIP
LPS
BNP
CAR
TRN
QUI
NHA
ARE
LPB
ANT
APT
180W
170
160
150
140
130
120
110
100
90
80
70
60
50
40
30
20
10

A

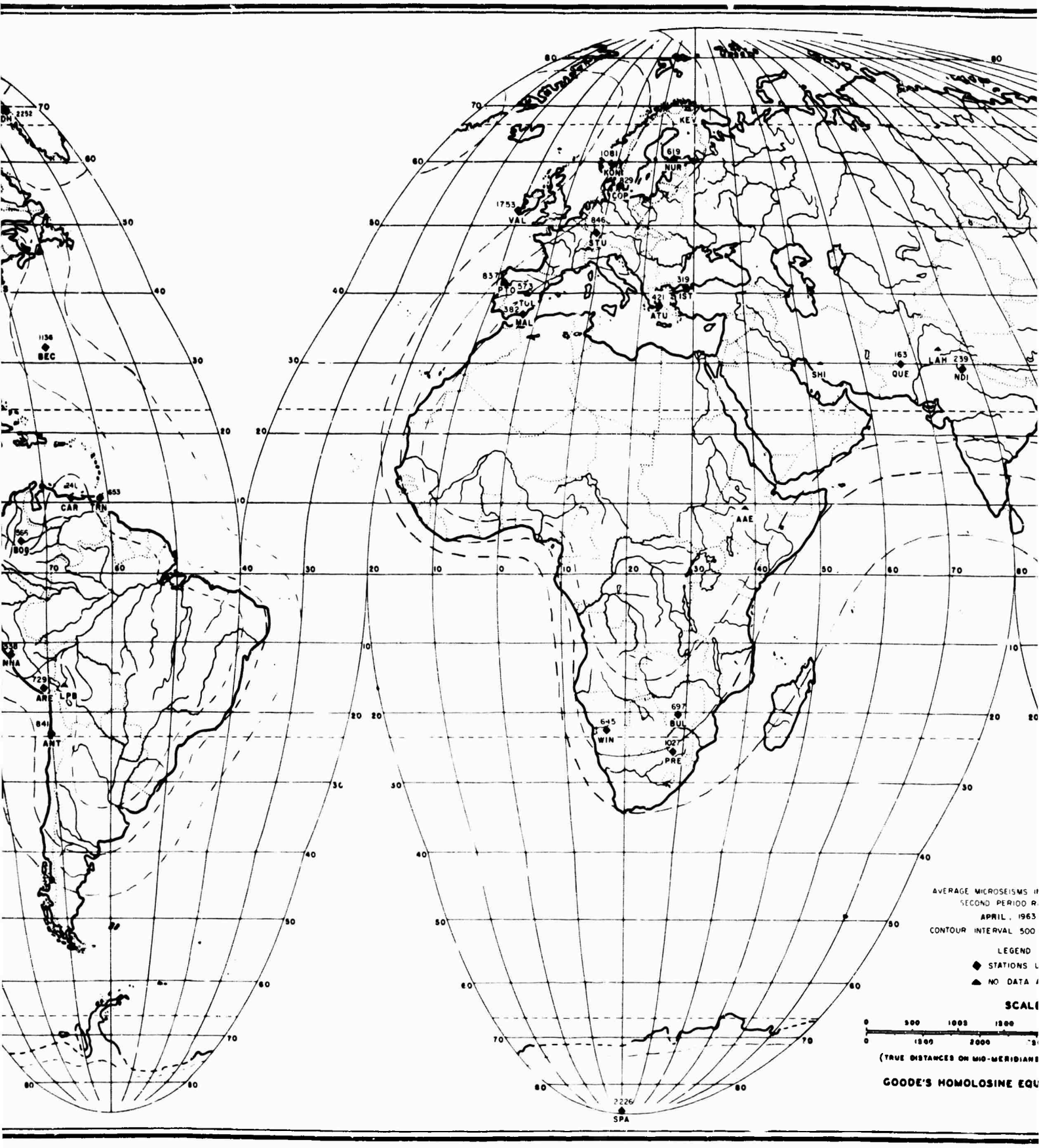

Figure B-8. Wor

b

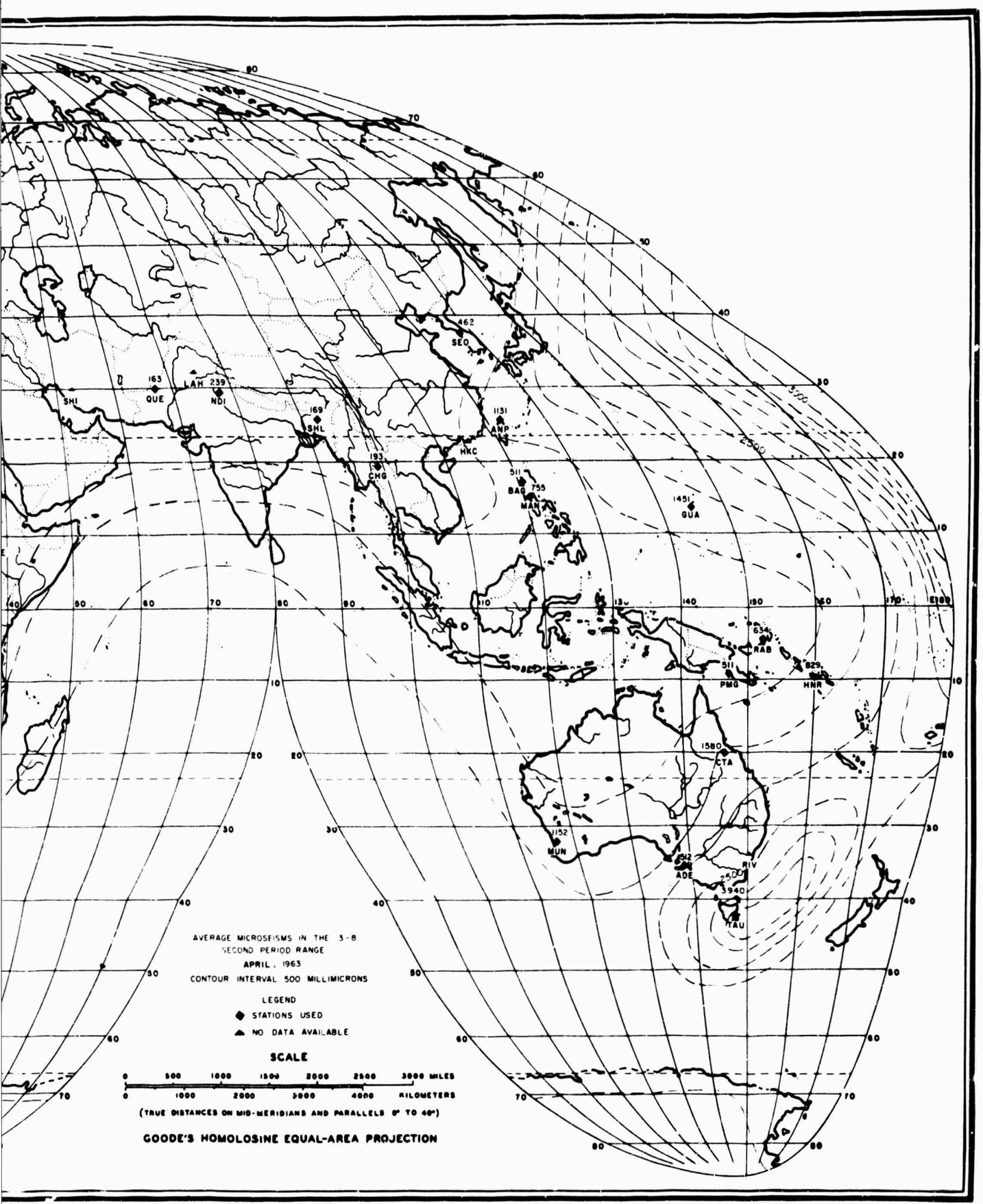

Figure B-8. World Map of 3.0-8.0 Second Microseismic Activitv, April, 1963

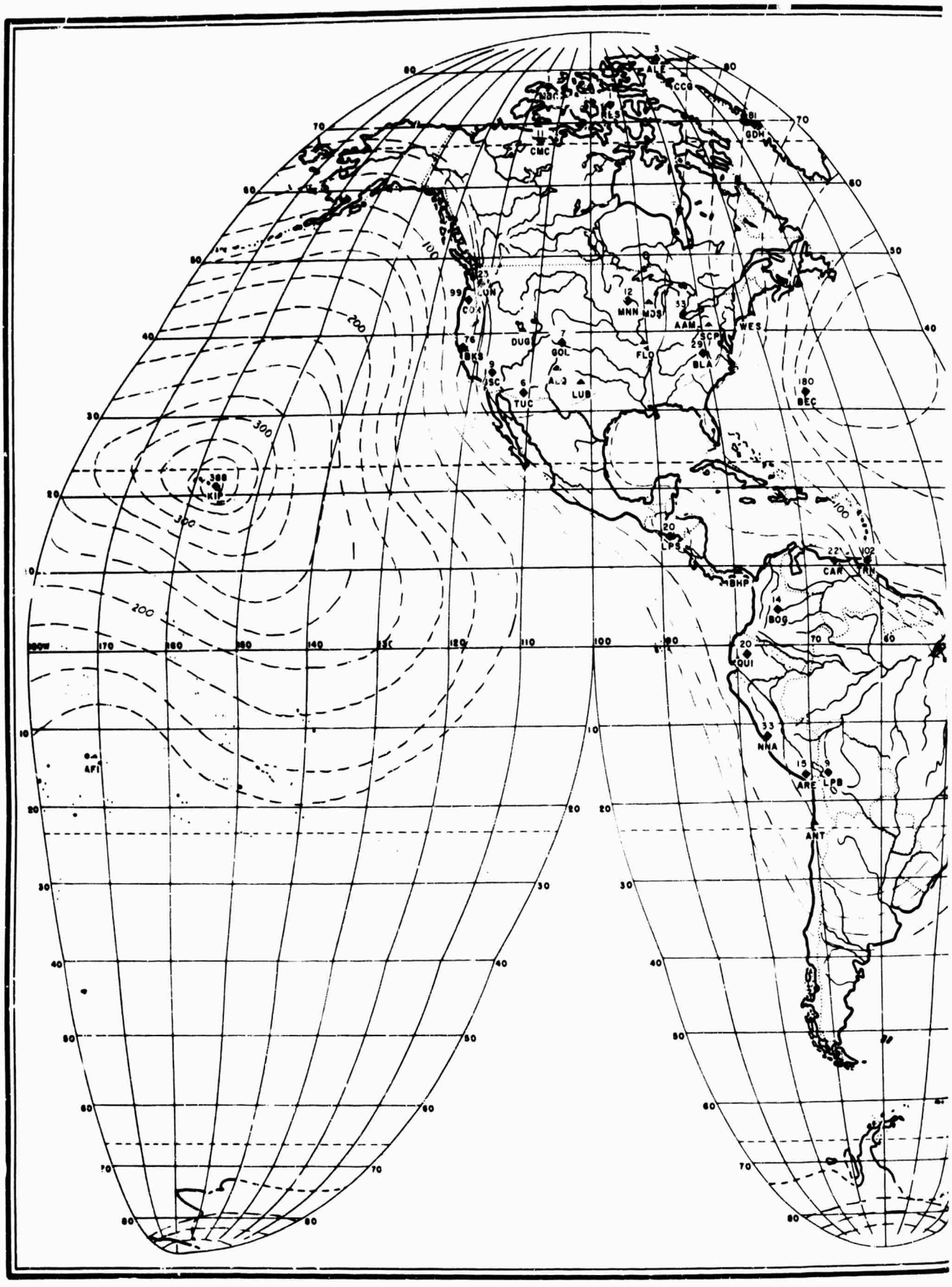
ALE
CCG
YEV
GDH
CMC
MNN
NDB
AAM
WES
SCP
FLO
BLA
DUG
GOL
TUC
LUB
BEC
KIP
LPS
BHP
CAR
VQQ
BOG
QUI
NNA
ARE
LPB
ANT
AFI
100
200
300

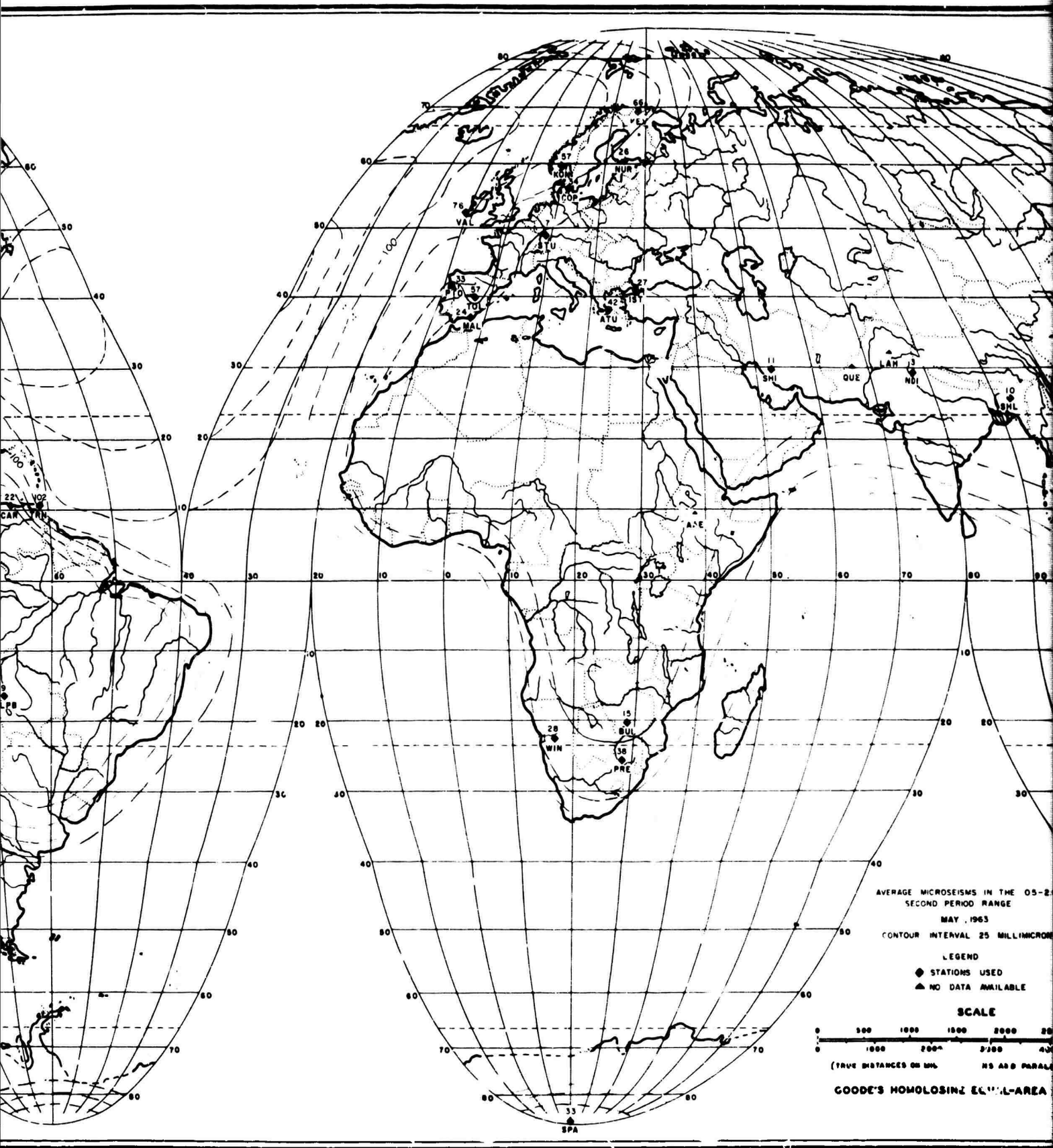

Figure B-9. World Ma

B

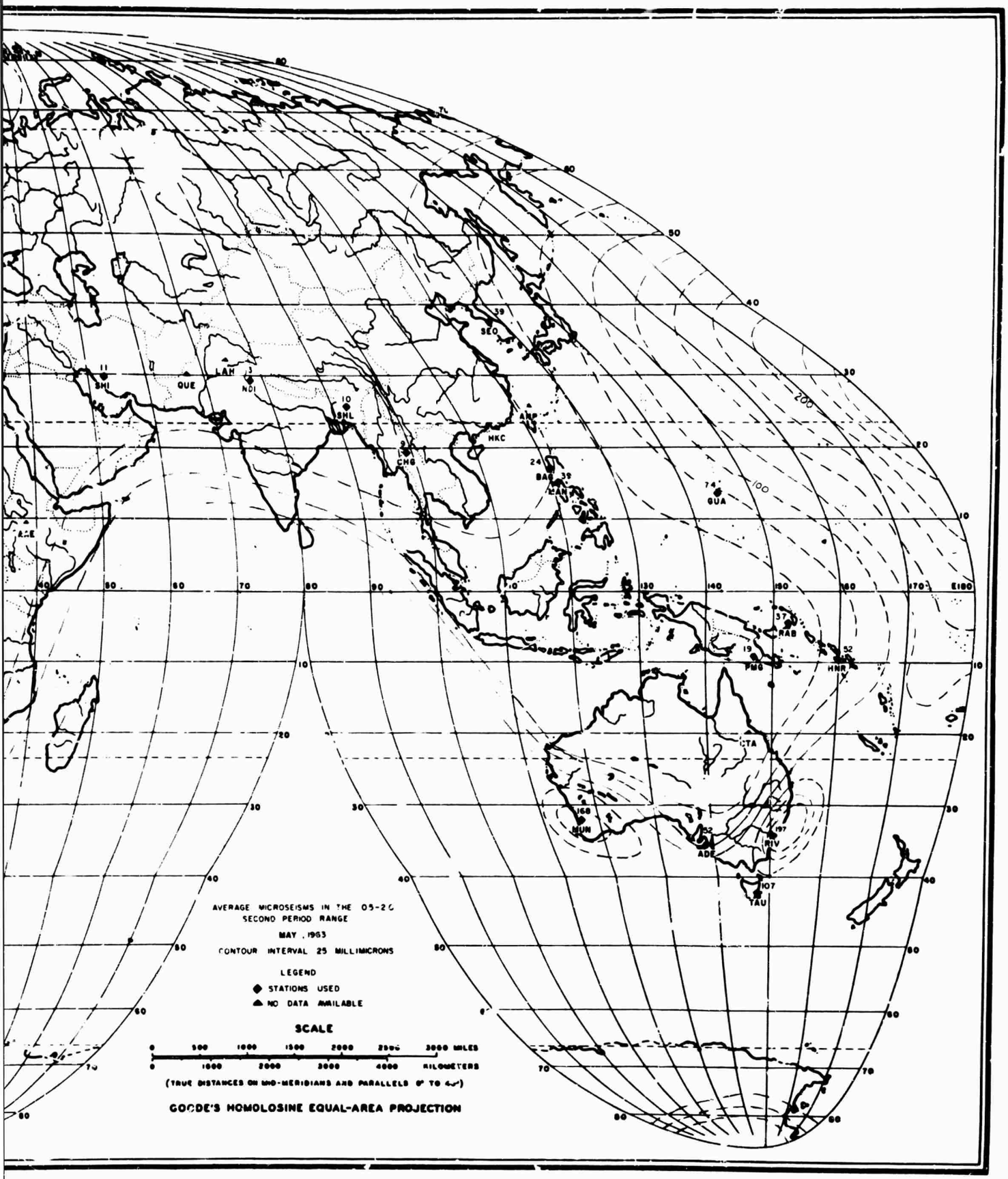

Figure B-9. World Map of 0.5-2.0 Second Microseismic Activity, May, 1963

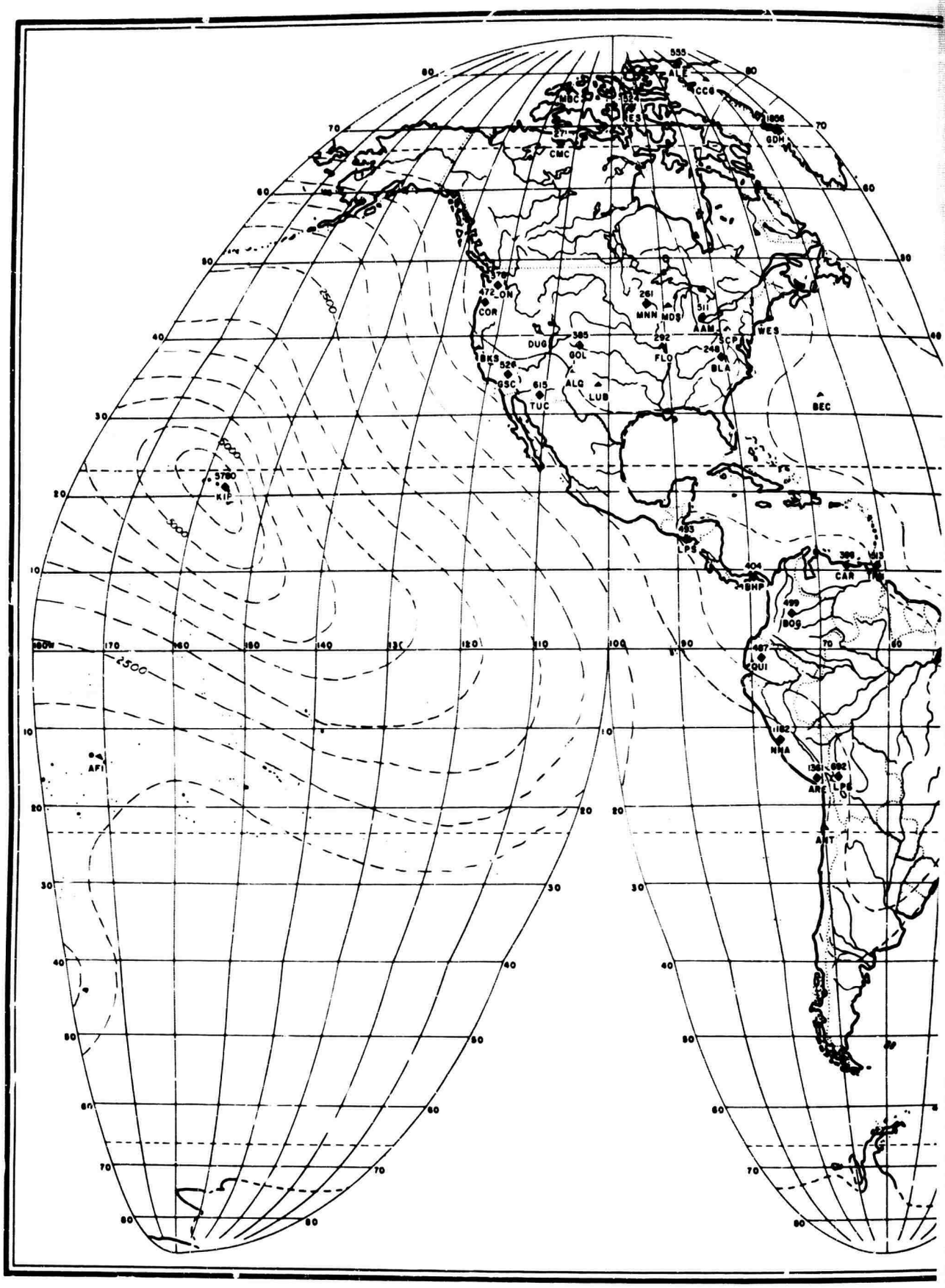
555
ALE
CCB
MBC
FES
1856
GDH
CMC
472
ON
COR
DUG
385
GOL
BKS
524
GSC
615
TUC
ALG
LUB
261
MNN
MDS
511
AAM
292
FLO
SCP
240
BLA
WES
BEC
5700
KIP
LPS
404
BHP
CAR
499
BOG
487
QUI
1182
NNA
1361
692
ARE
LPS
ANT
AFI
180W
170
160
150
140
130
120
110
100
90
80
70
60
2500
5000
7500

A

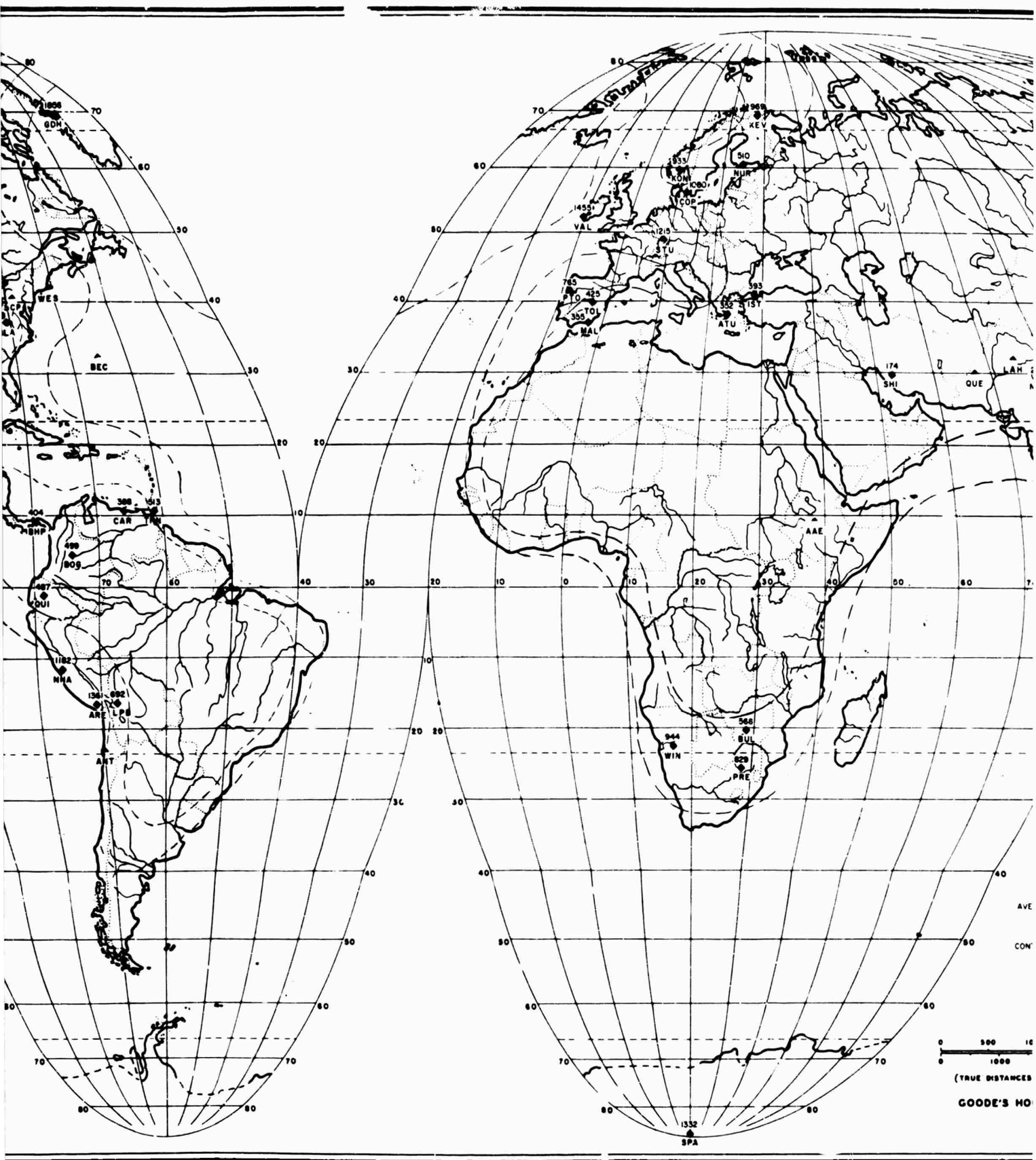
GDH
KEV
KOM
NUR
COP
VAL
STU
PTO
TOL
MAL
ATU
SHI
QUE
BEC
CAR
BHP
BOG
QUI
NNA
ARE
LPB
ANT
WIN
BUL
PRE
AAE
SPA
(TRUE DISTANCES
GOODE'S HO

Figure B-

b

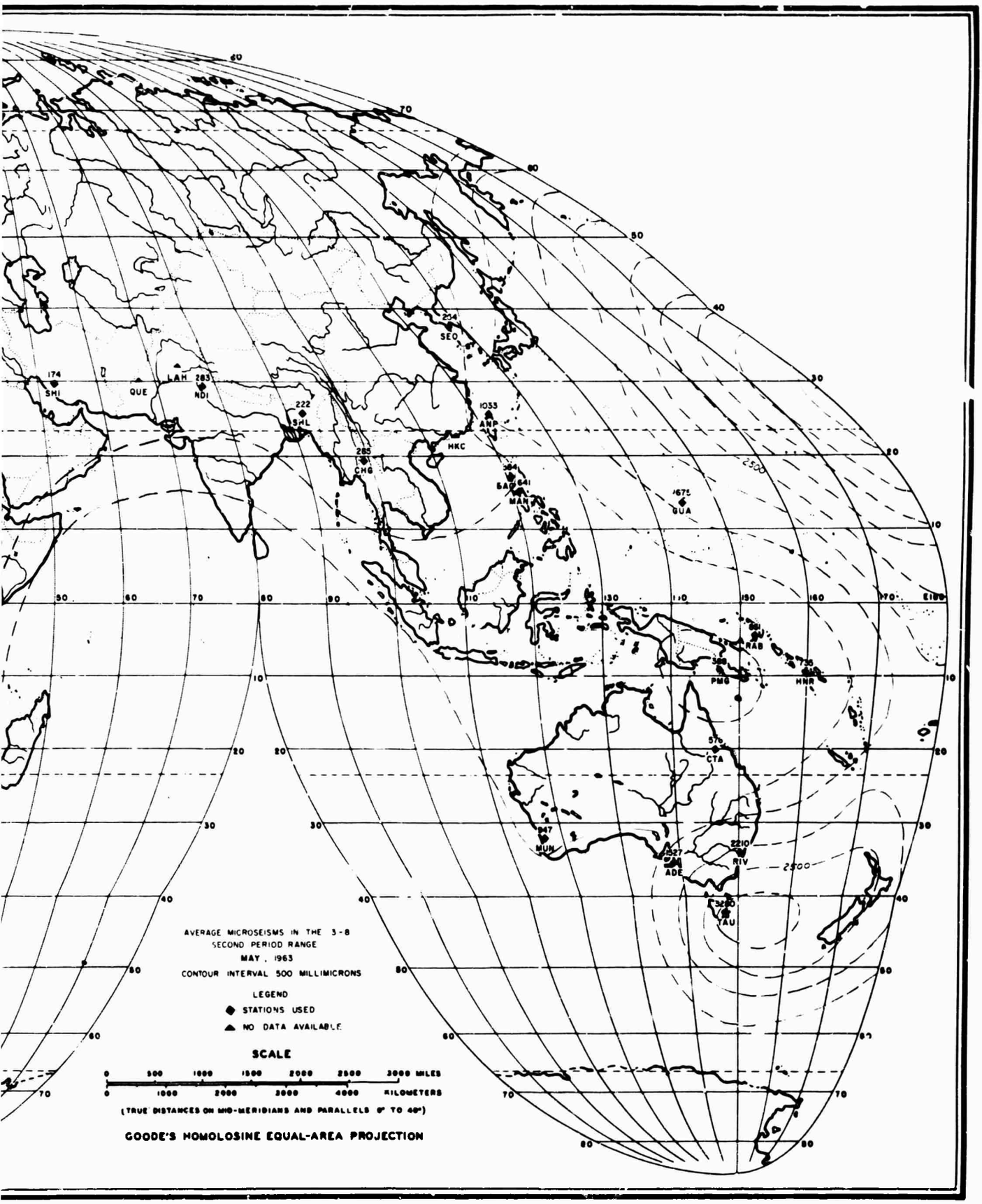

Figure B-10. World Map of 3.0-8.0 Second Microseismic Activity, May, 1963

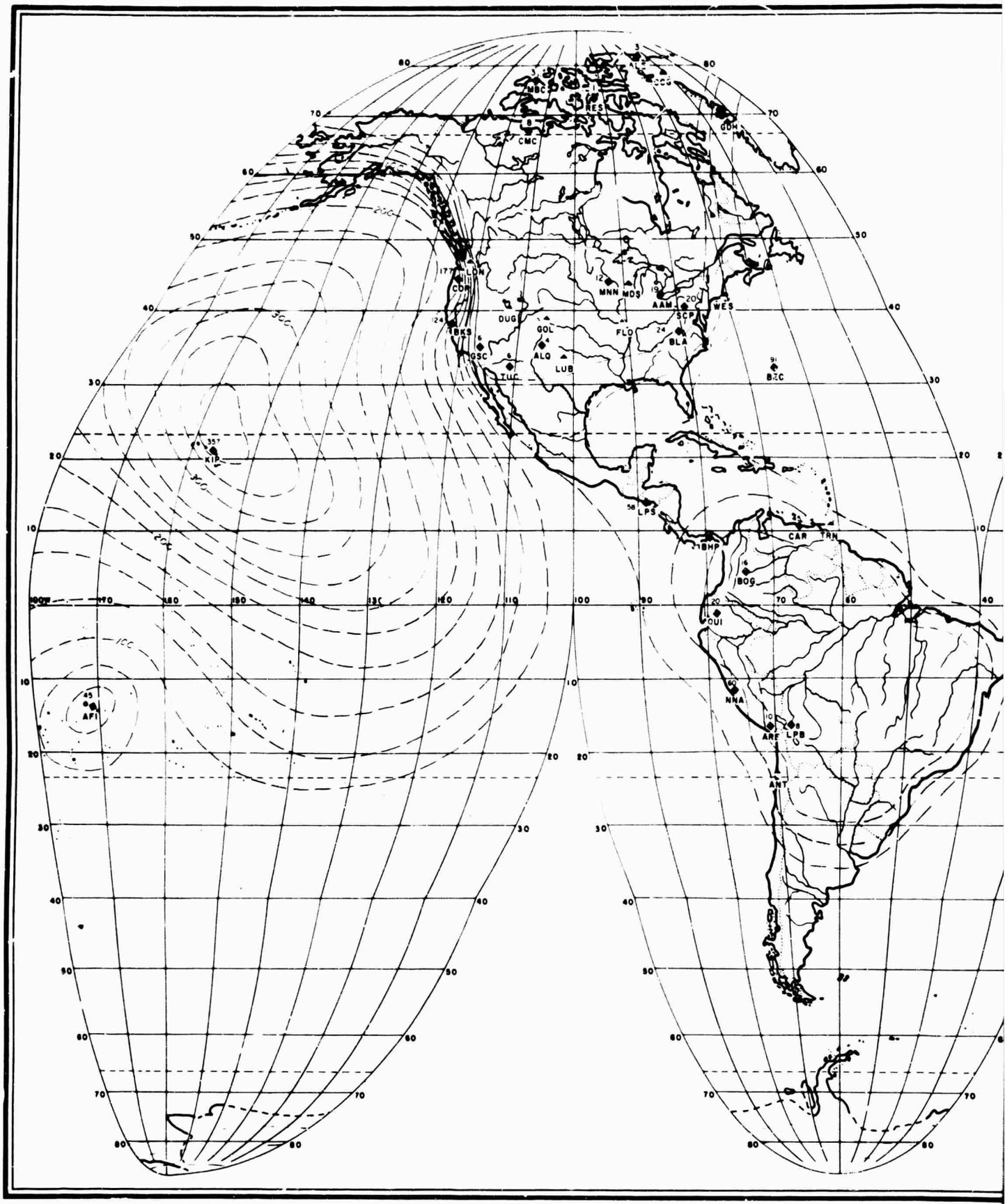
MBC
RES
CMC
GDH
LON
CDR
MNN
MDS
AAM
WES
SCP
DUG
GOL
FLO
BLA
BKS
GSC
ALQ
LUB
TUC
BZC
KIP
LPS
BHP
CAR
TRN
BOG
OUI
NNA
ARE
LPB
ANT
AFI

A

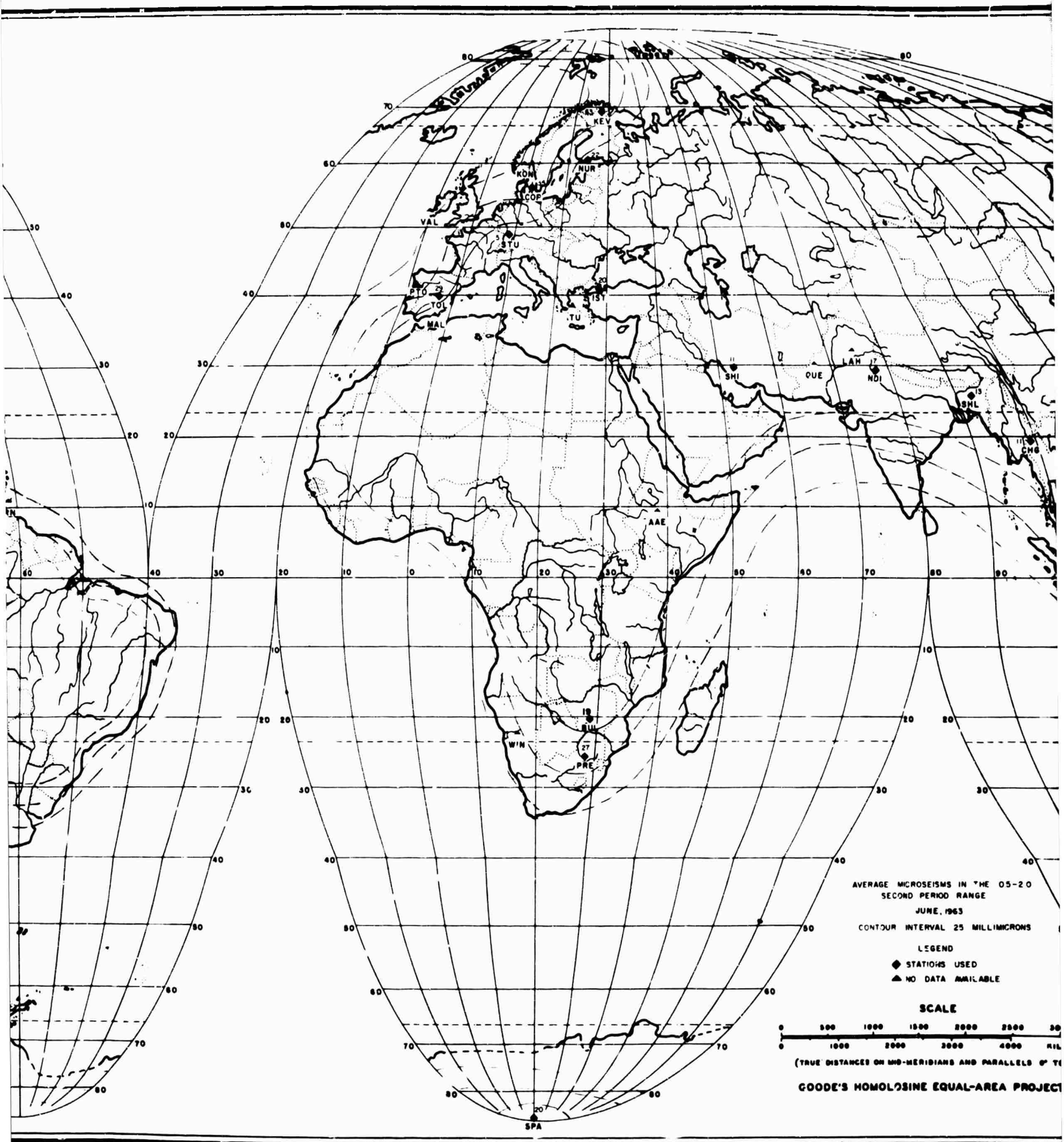

Figure B-11. World Map of (

b

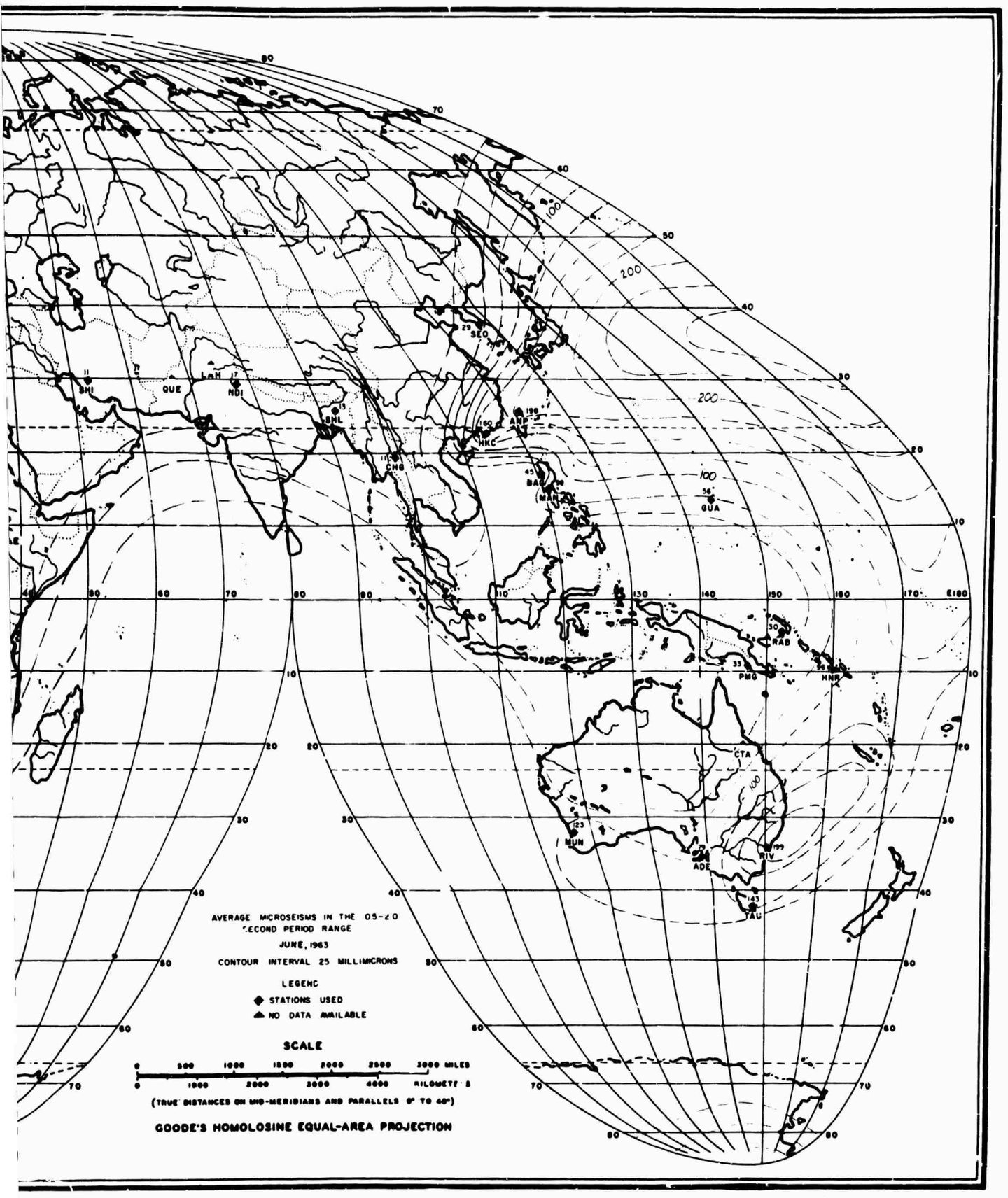

Figure B-11. World Map of 0.5-2.0 Second Microseismic Activity, June, 1963

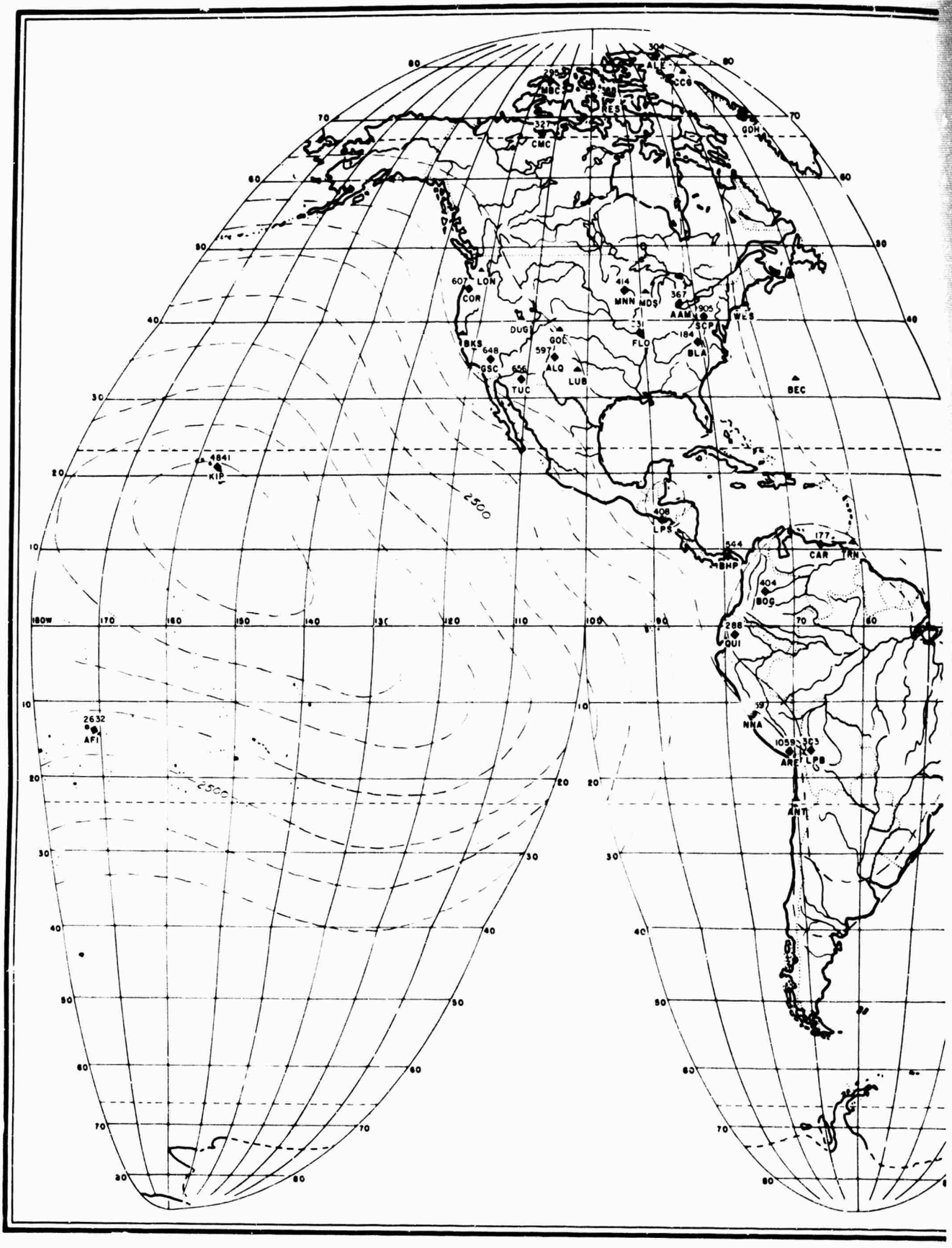
ALE
CCB
QDH
MBC
NES
CMC
LON
COR
MNN
MDS
AAM
SCP
WES
DUG
GOE
FLO
BLA
BKS
GSC
ALQ
LUB
TUC
BEC
KIP
LPS
CAR
TRN
BMP
BOG
QUI
NHA
ARE
LPB
ANT
AFI
2500
2500

A

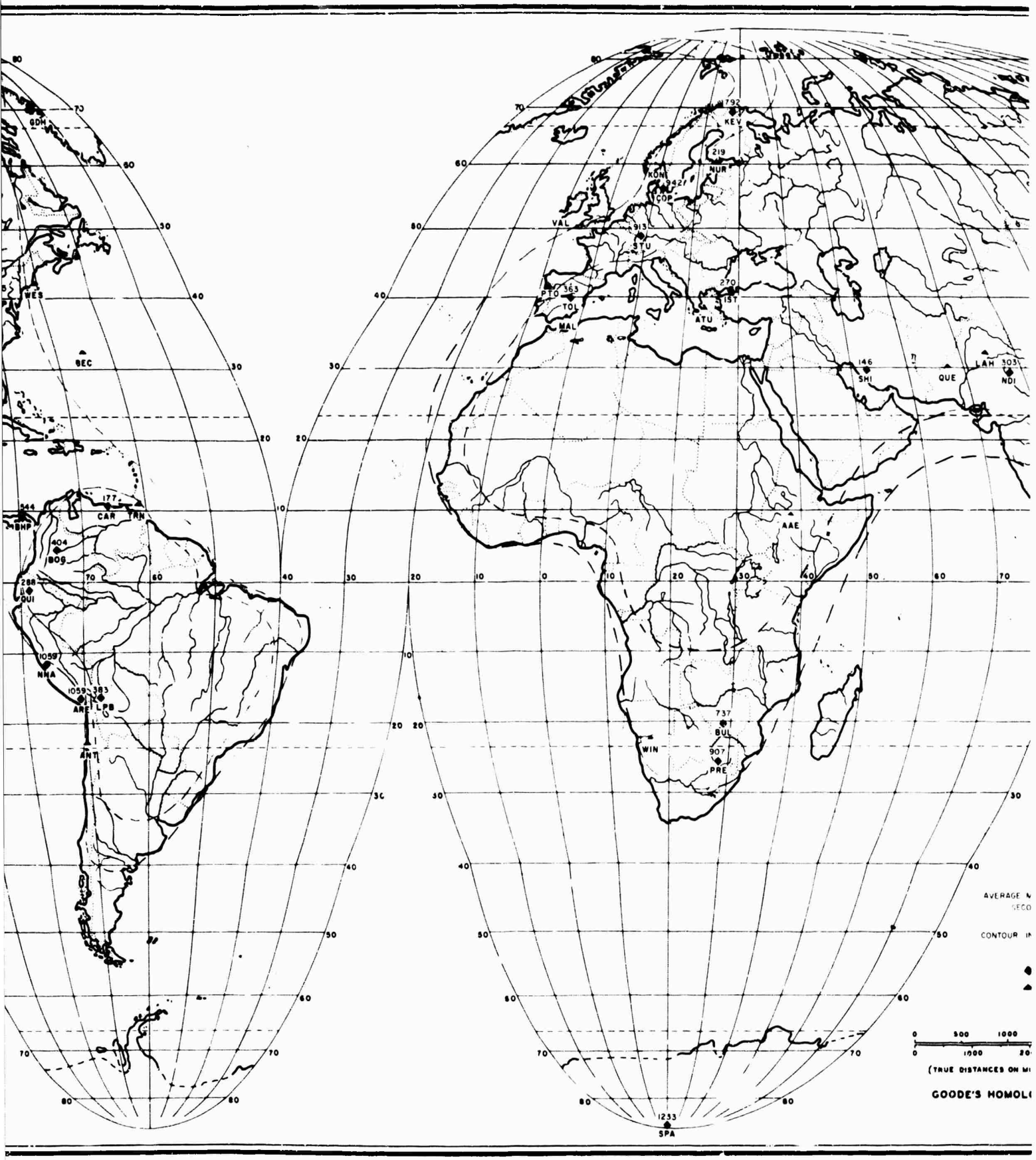
GDH
WES
BEC
BHP
CAR
TRN
BOG
GUI
NNA
ARE
LPB
ANT
792
KEV
219
NUR
KON
GOP
VAL
913
STU
PTO
TOL
MAL
270
ATU
SHI
QUE
LAH
NDI
AAE
737
BUL
WIN
907
PRE
1233
SPA
AVERAGE
CONTOUR
0 500 1000
(TRUE DISTANCES ON
GOODE'S HOMOL

Figure B-12.

B

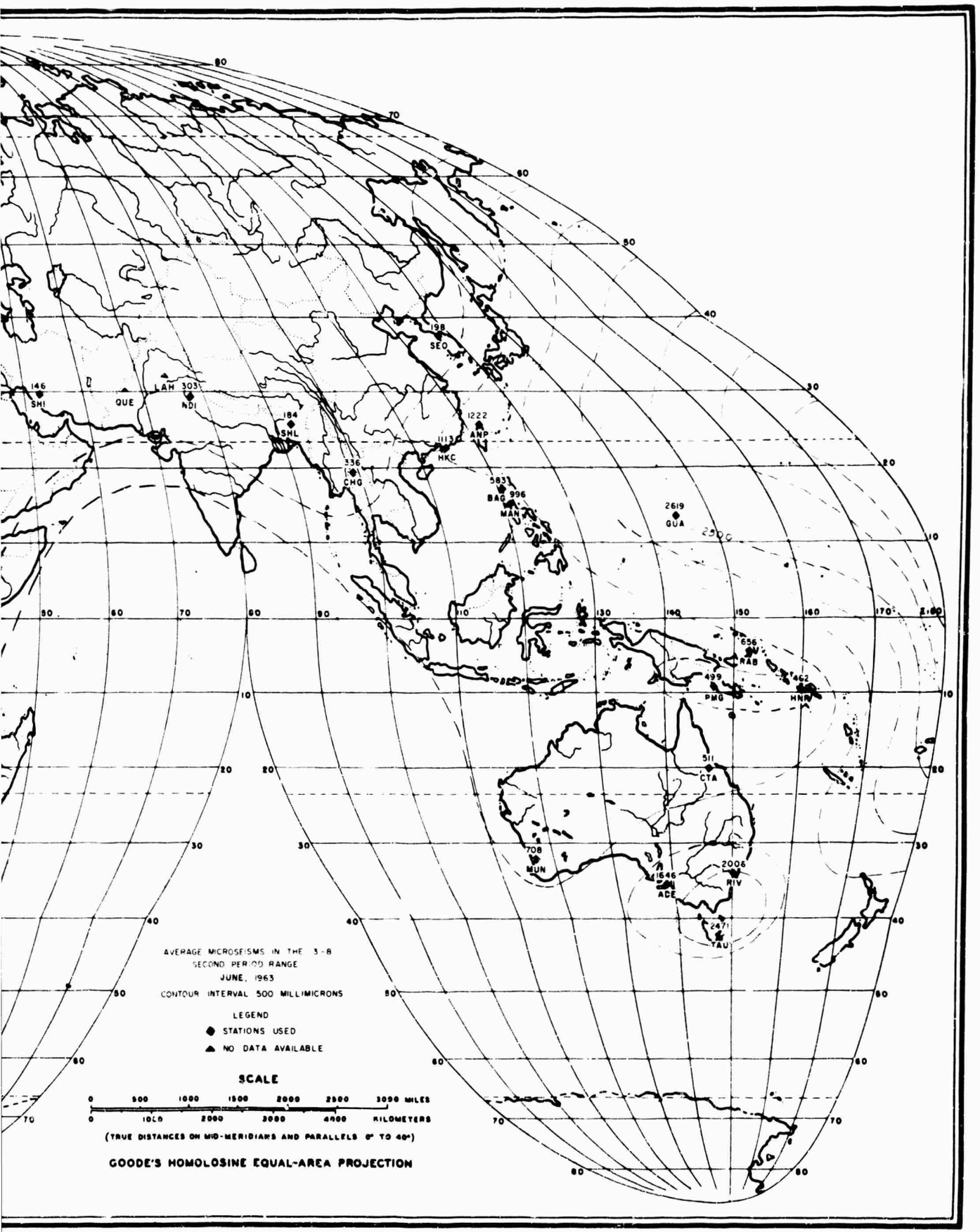

Figure B-12. World Map of 3.0-8.0 Second Microseismic Activity, June, 1963

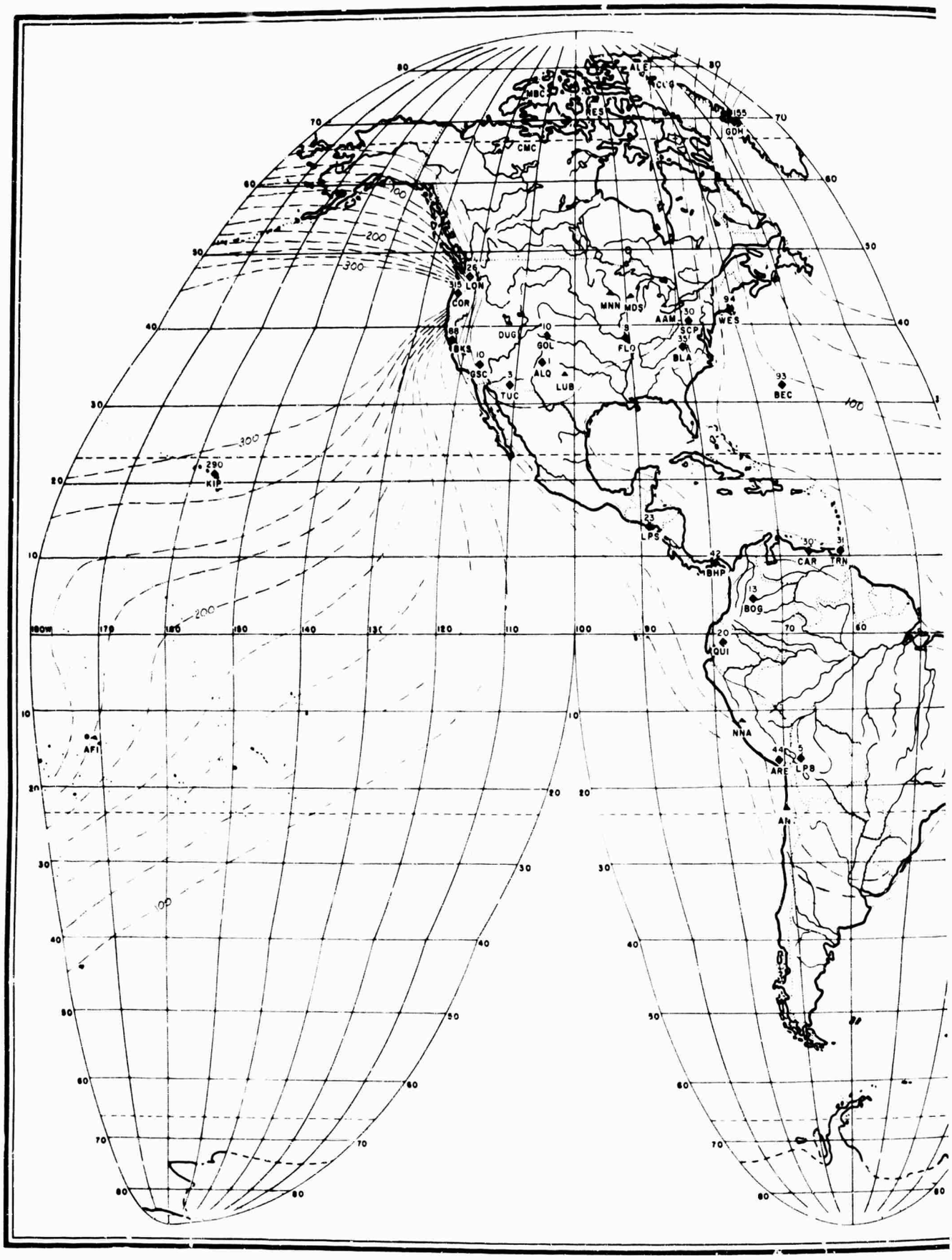
ALE
CLG
MBC
RES
GDH
CMC
LON
COR
MNN
MDS
AAM
SCP
WES
DUG
GOL
FLO
BKS
GSC
ALQ
BLA
TUC
LUB
BEC
KIP
LPS
BHP
CAR
TRN
BOG
QUI
NNA
AFI
ARE
LPB
AN

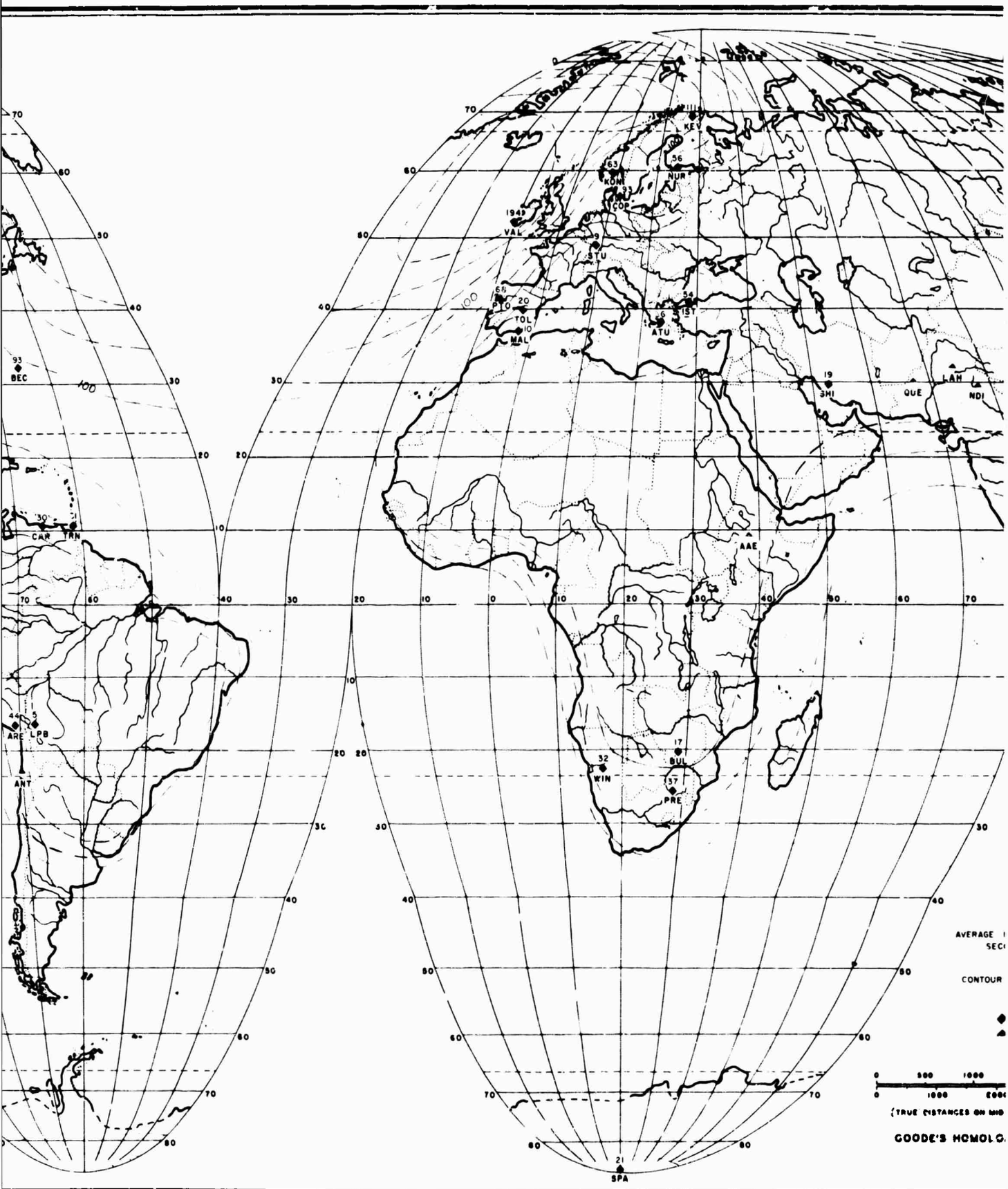
KEV
KON
NUR
COP
VAL
STU
PTO
TOL
MAL
ATU
IST
BEC
SMI
QUE
LAH
NDI
CAR
TRN
AAE
ARE
LPB
ANT
WIN
BUL
PRE
SPA
AVERAGE
CONTOUR
GOODE'S HOMOLO

Figure B-13.

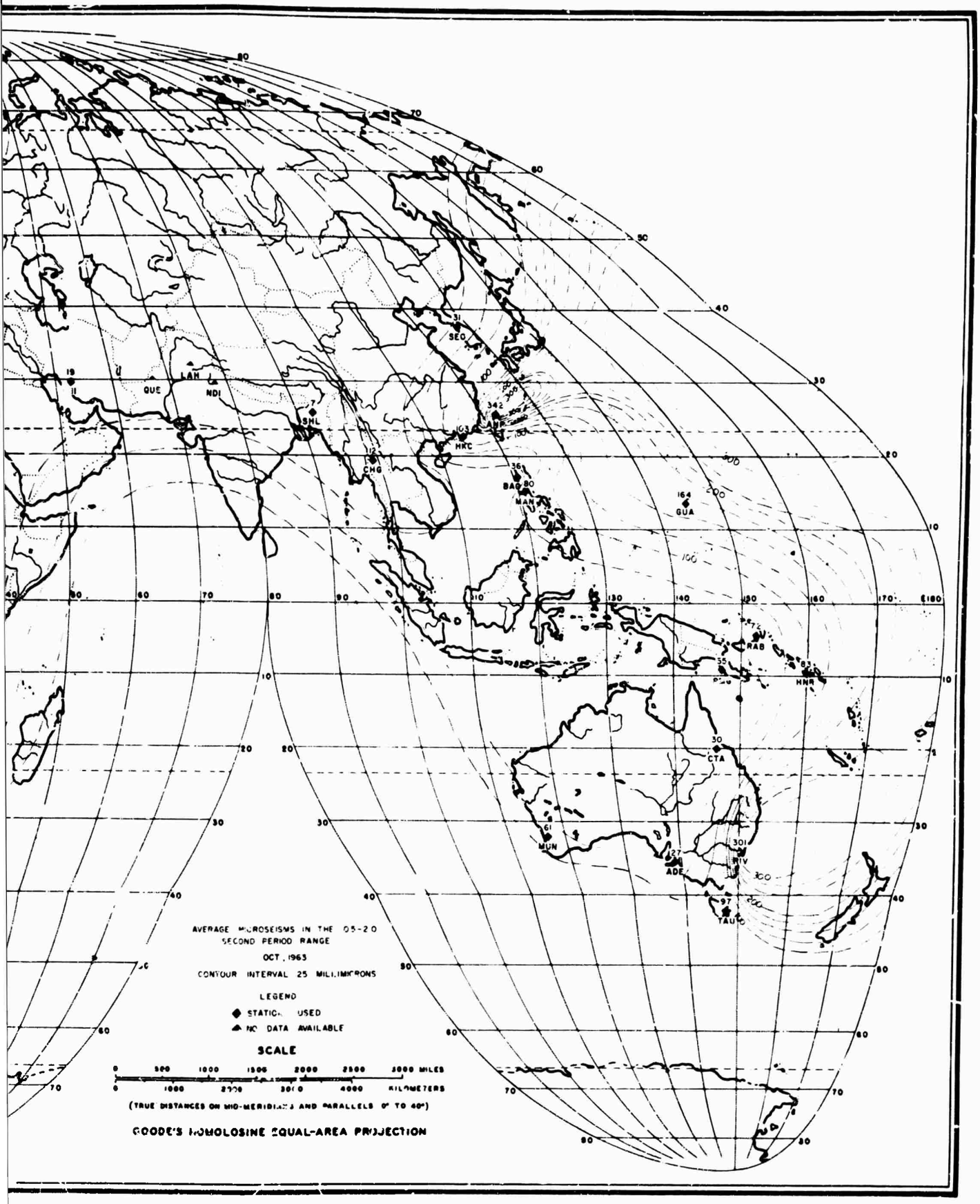

Figure B-13. World Map of 0.5-2.0 Second Microseismic Activity, October, 1963

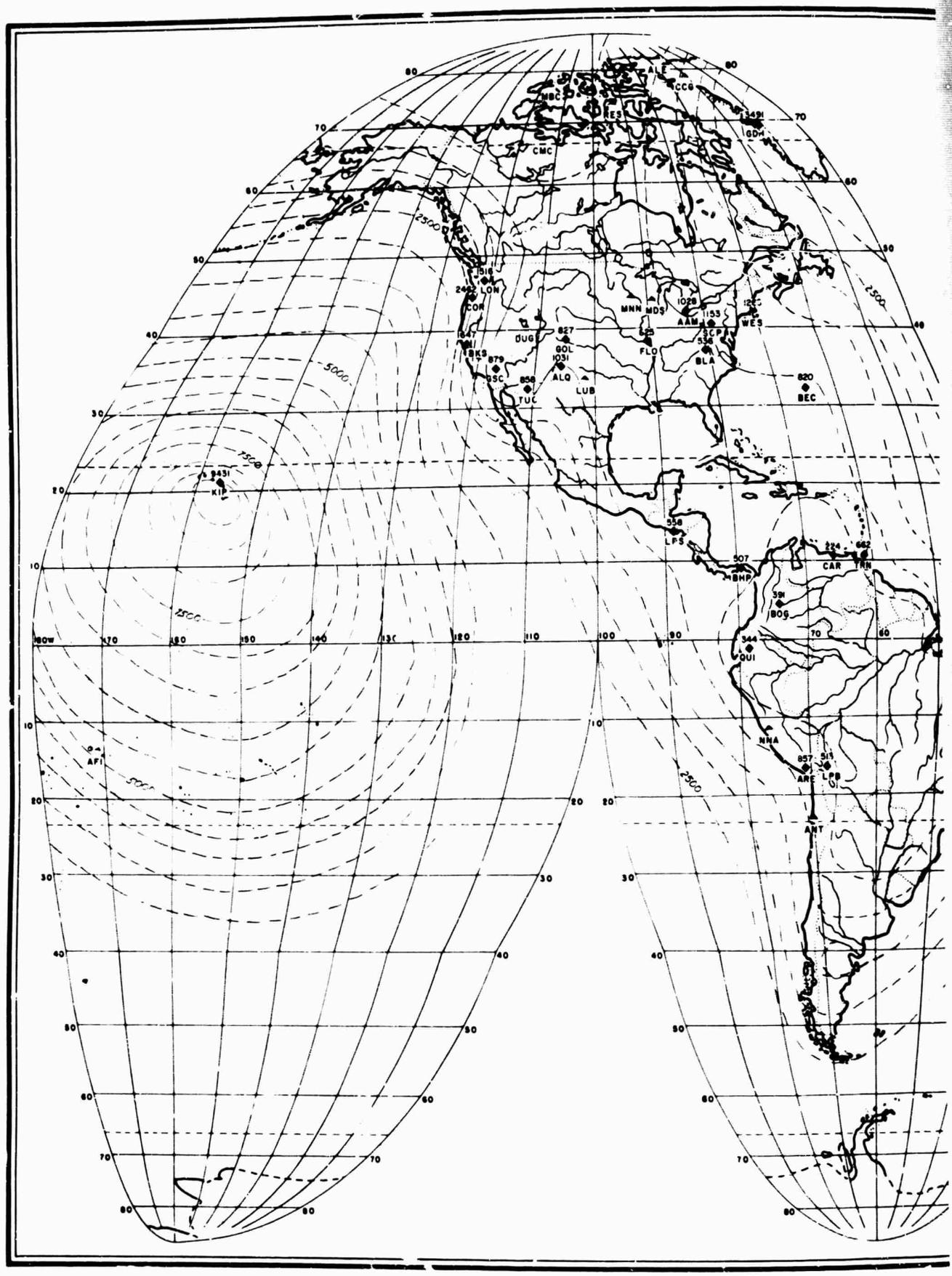
ALE
CCG
RES
MBC
CMC
GDH
LON
COR
DUG
GOL
ALQ
LUB
TUC
FLO
BLA
AAM
WES
MNN
MDS
BEC
LPS
BMP
CAR
TRN
BOG
QUI
NMA
ARE
LPB
ANT
AFI
KIL
2500
5000
7500

A

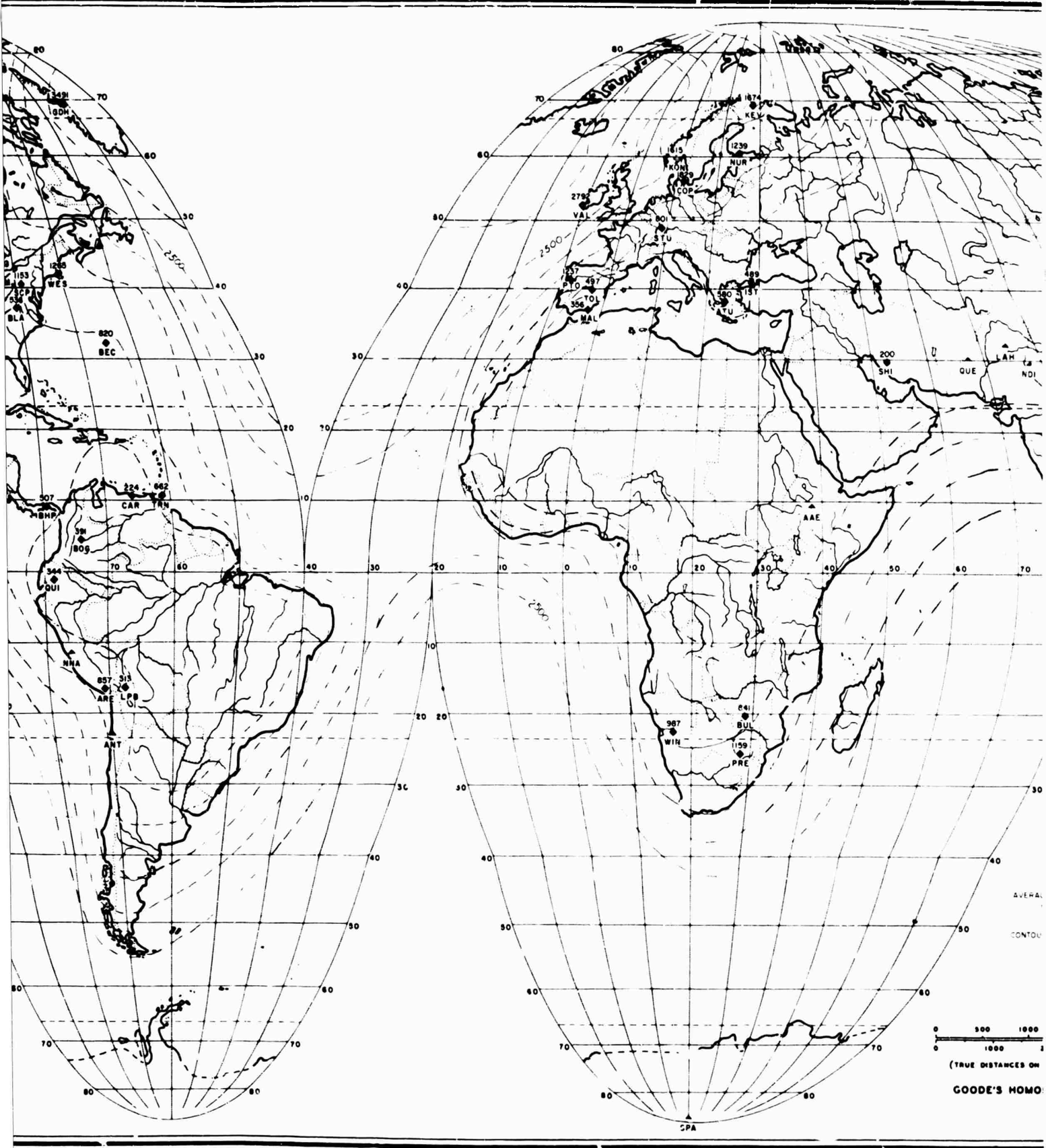
BLA
BEC
WES
BHP
CAR
TRN
GUI
NNA
ARE
LPB
ANT
SPA
KEV
NUR
KON
COP
VAL
STU
PTO
TOL
MAL
IST
ATU
SHI
QUE
AAE
BUL
WIN
PRE
2500
GOODE'S HOMO

Figure B-14

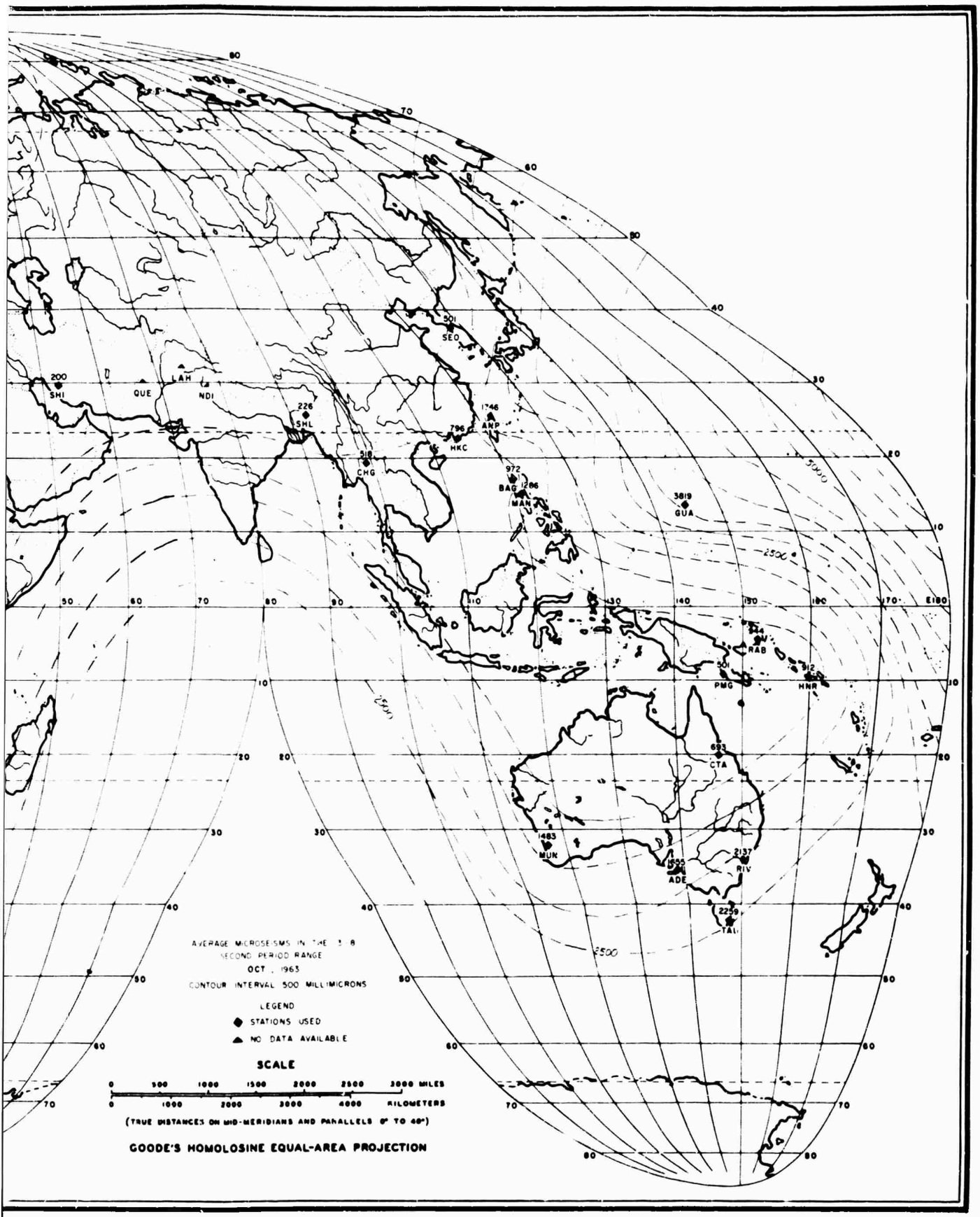

Figure B-14. World Map of 3.0-8.0 Second Microseismic Activity, October, 1963

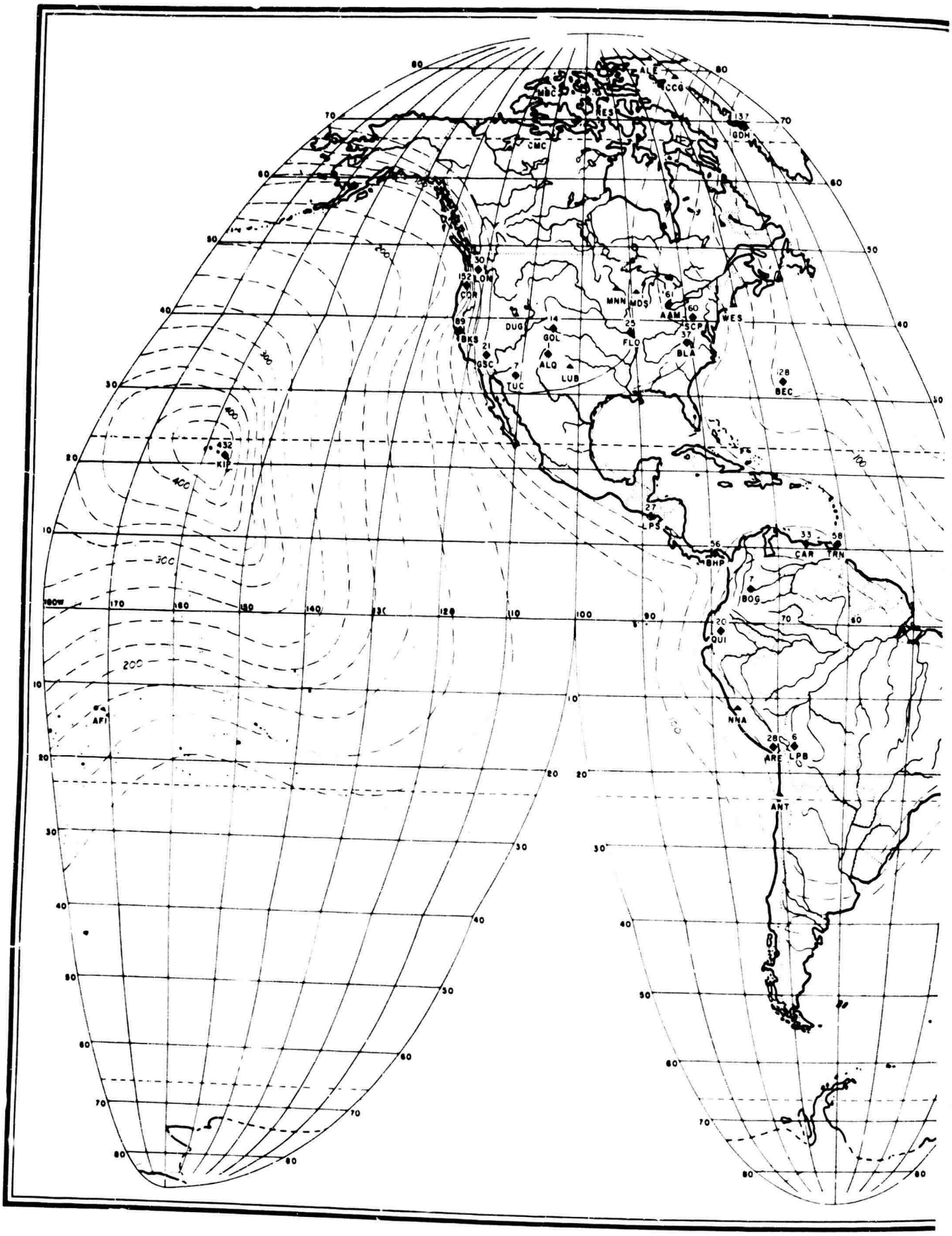
ALE
CCG
YBC
YES
CMC
GDH
LOM
CDR
MNN
MDS
A&M
SCP
WES
DUG
GOL
FLO
BLA
BKS
OSC
ALQ
LUB
TUC
BEC
KIP
LPS
BHP
CAR
TRN
BOG
QUI
NHA
ARE
LPB
ANT
AFI
100W
170
160
150
140
130
120
110
100
90
80
70
60
50
40
30
20
10
100
200
300
400

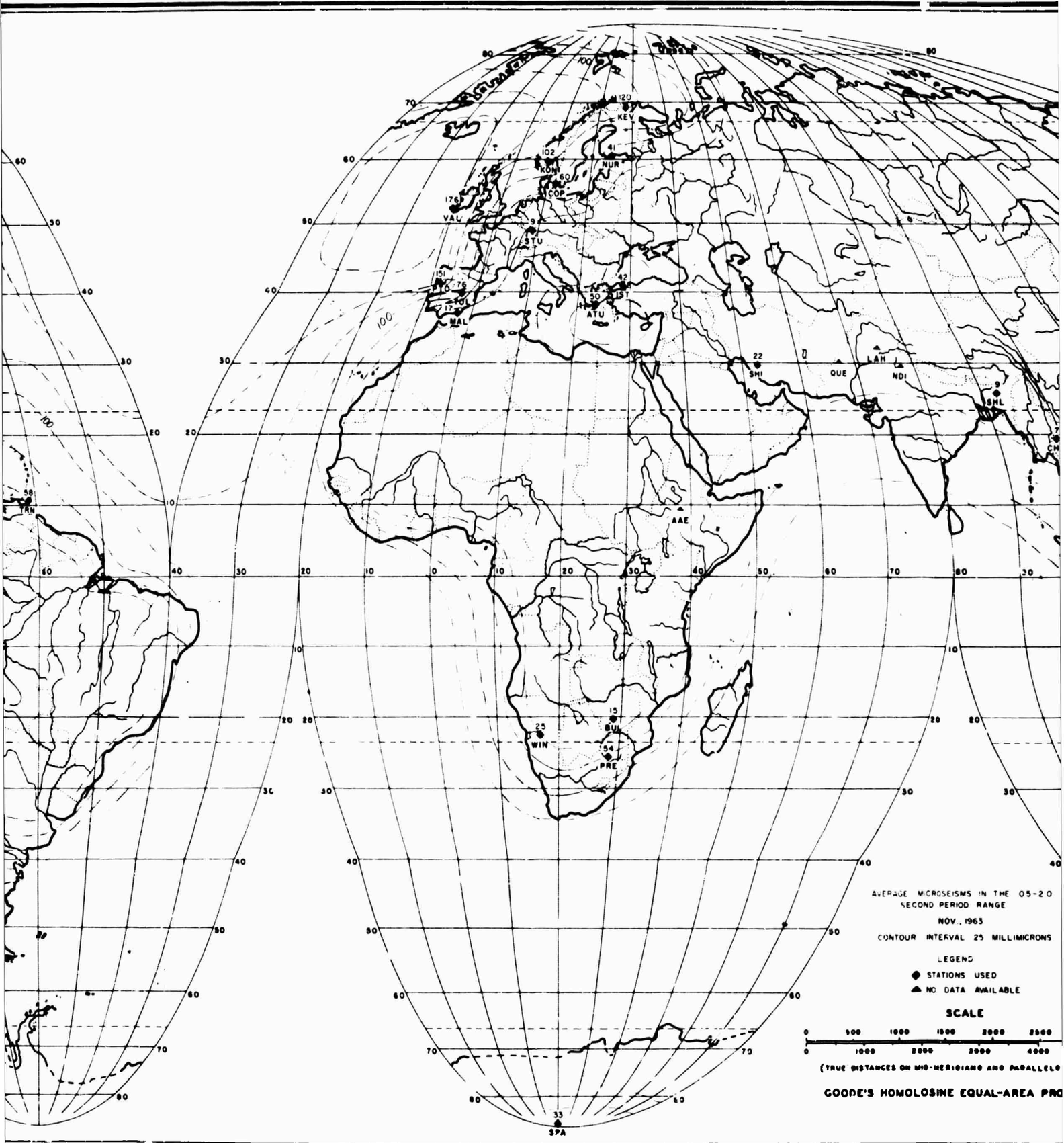

Figure B-15. World Map of C

B

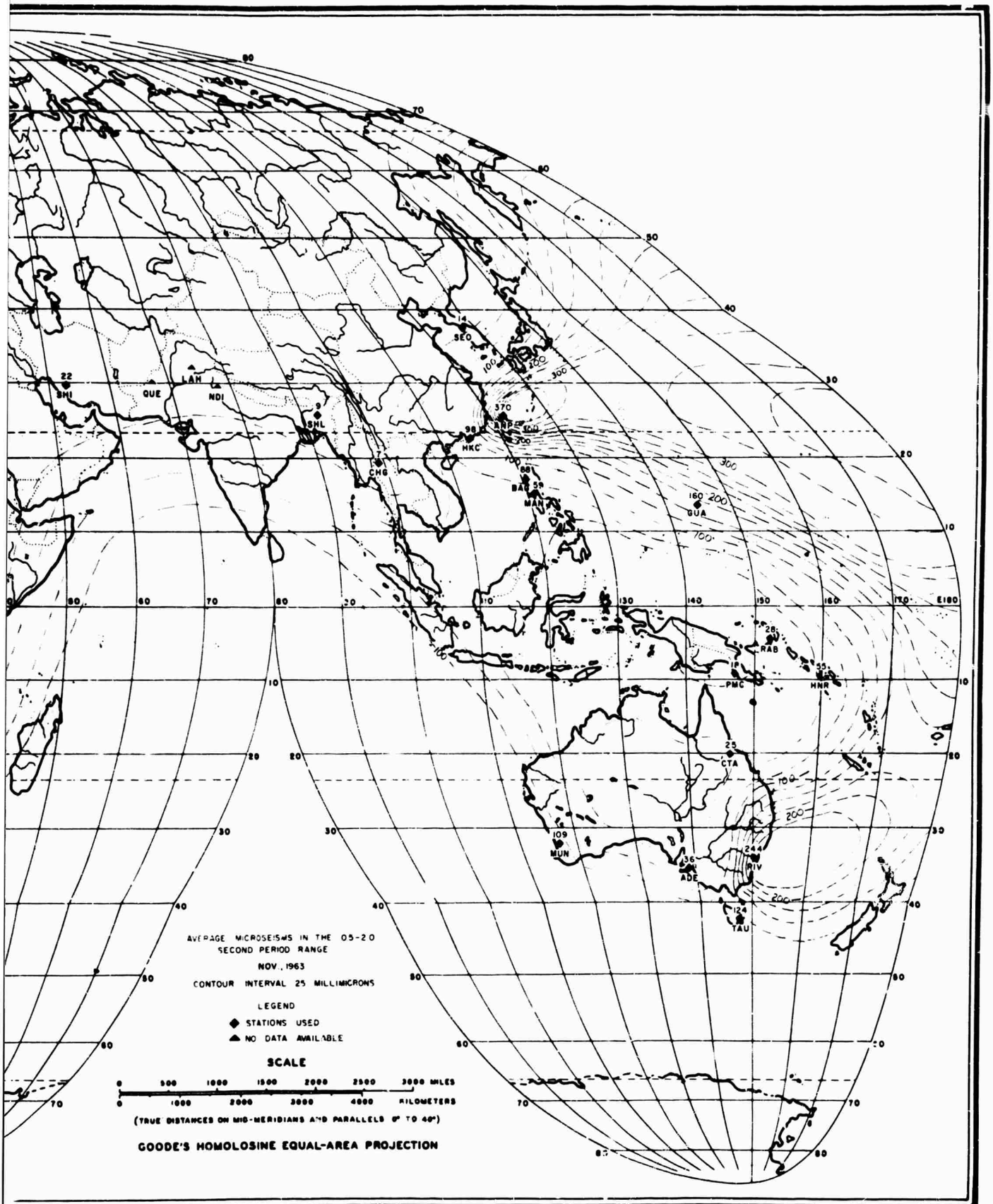

Figure B-15. World Map of 0.5-2.0 Second Microseismic Activity, November, 1963

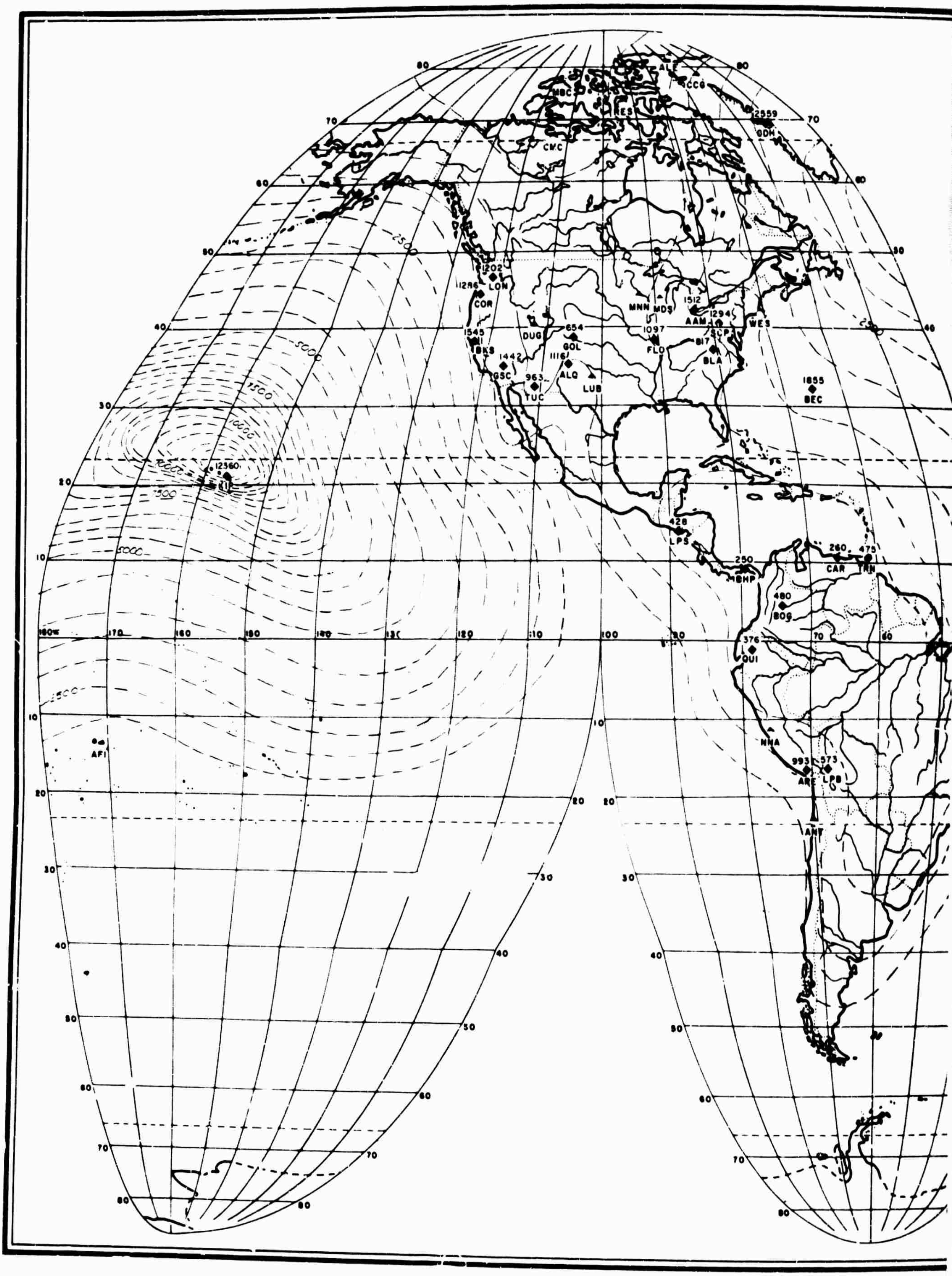

ALE
CCG
MBC
RES
CMC
ODH
2500
1202
LON
1286
COR
1545
BKS
DUG
654
GOL
1116
ALQ
1442
GSC
963
TUC
LUB
MNN
MDS
1512
AAM
1294
SCP
WES
1097
FLO
817
BLA
1855
BEC
5000
7500
10000
12560
428
LPS
250
BHP
260
CAR
475
TRN
480
BOG
376
QUI
NNA
993
ARE
573
LPB
ANF
AFI

A

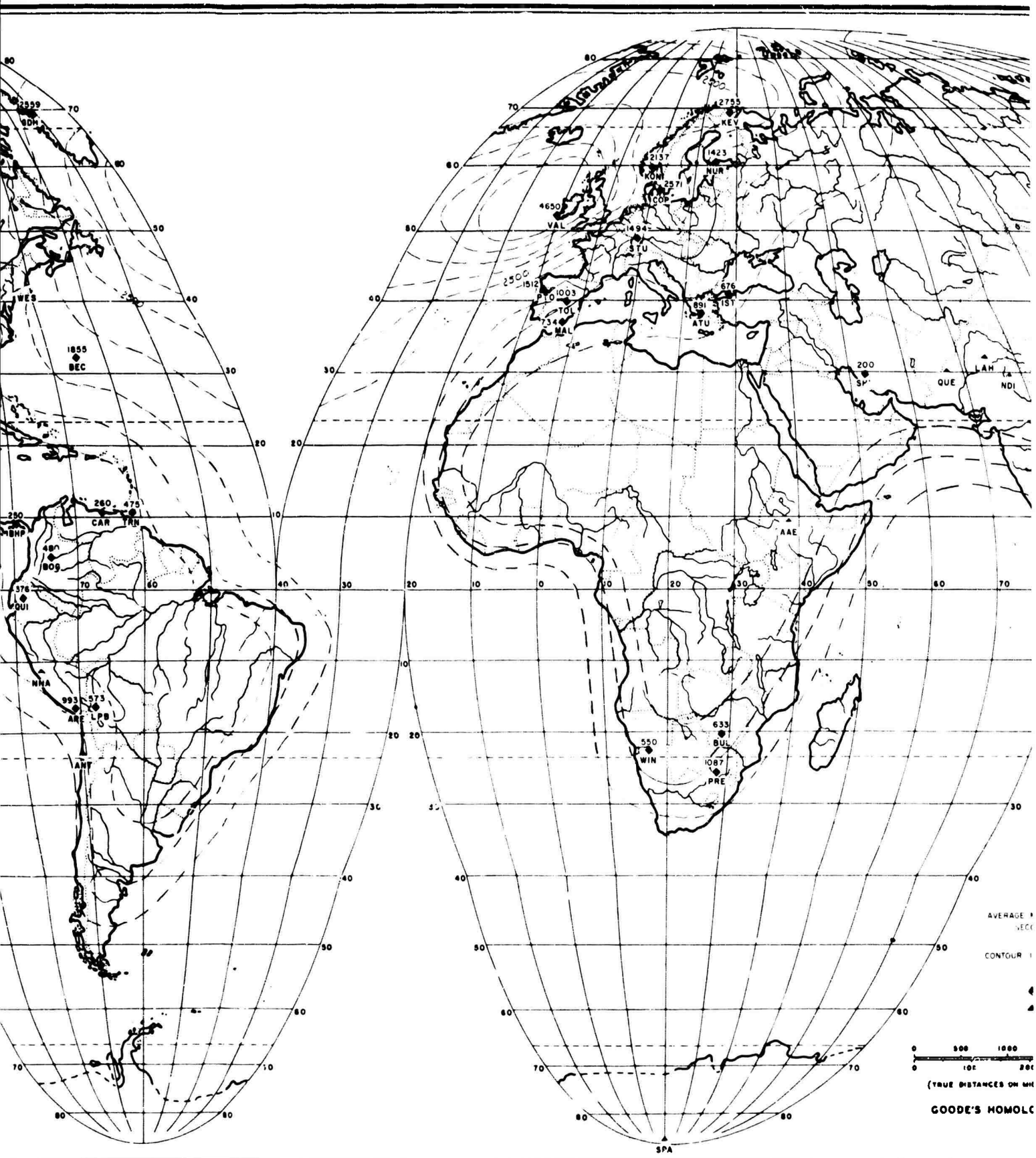

Figure B-16. V

B

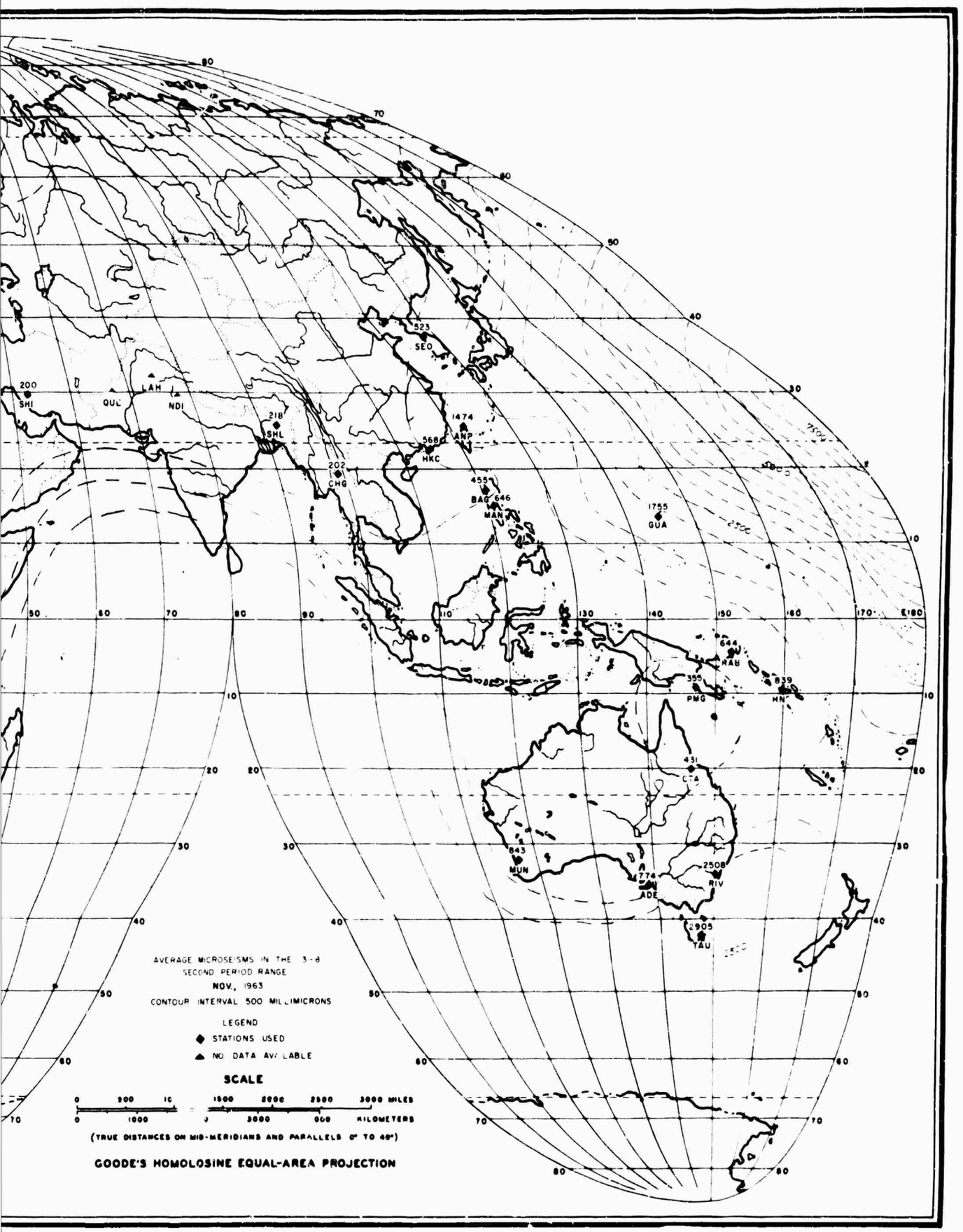

Figure B-16. World Map of 3.0-8.0 Second Microseismic Activity, November, 196

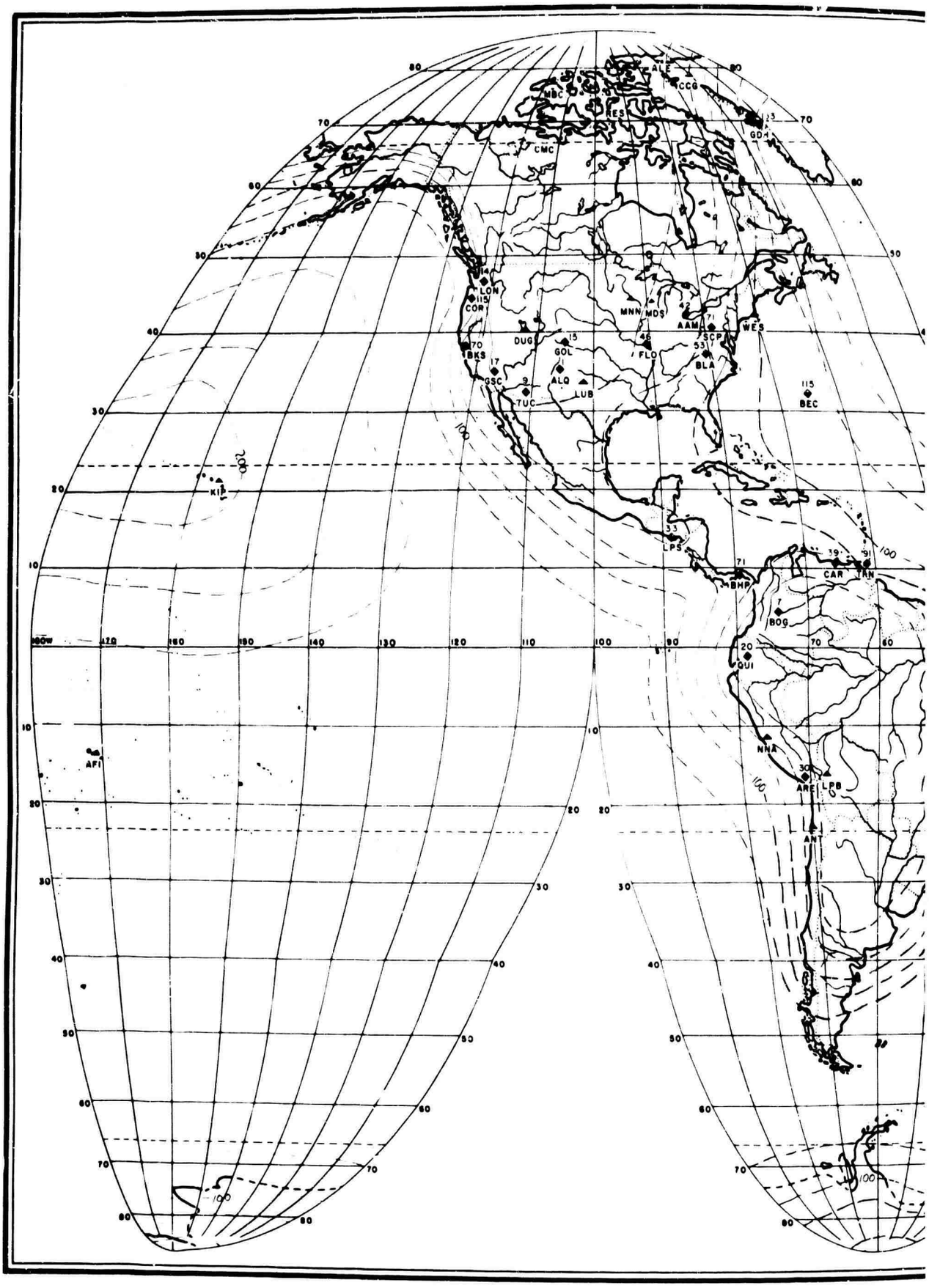
ALE
CCG
WBC
RES
GDA
CMC
LON
115
COR
70
BKS
17
GSC
DUG
15
GOL
9
TUC
ALQ
LUB
MNN
MDS
42
AAM
71
SCP
46
FLO
53
BLA
WES
115
BEC
KIP
33
LPS
71
BHP
19
CAR
91
BOG
20
QUI
NHA
30
ARE
LPB
AFI
100
120
130
140
150
160
180

A

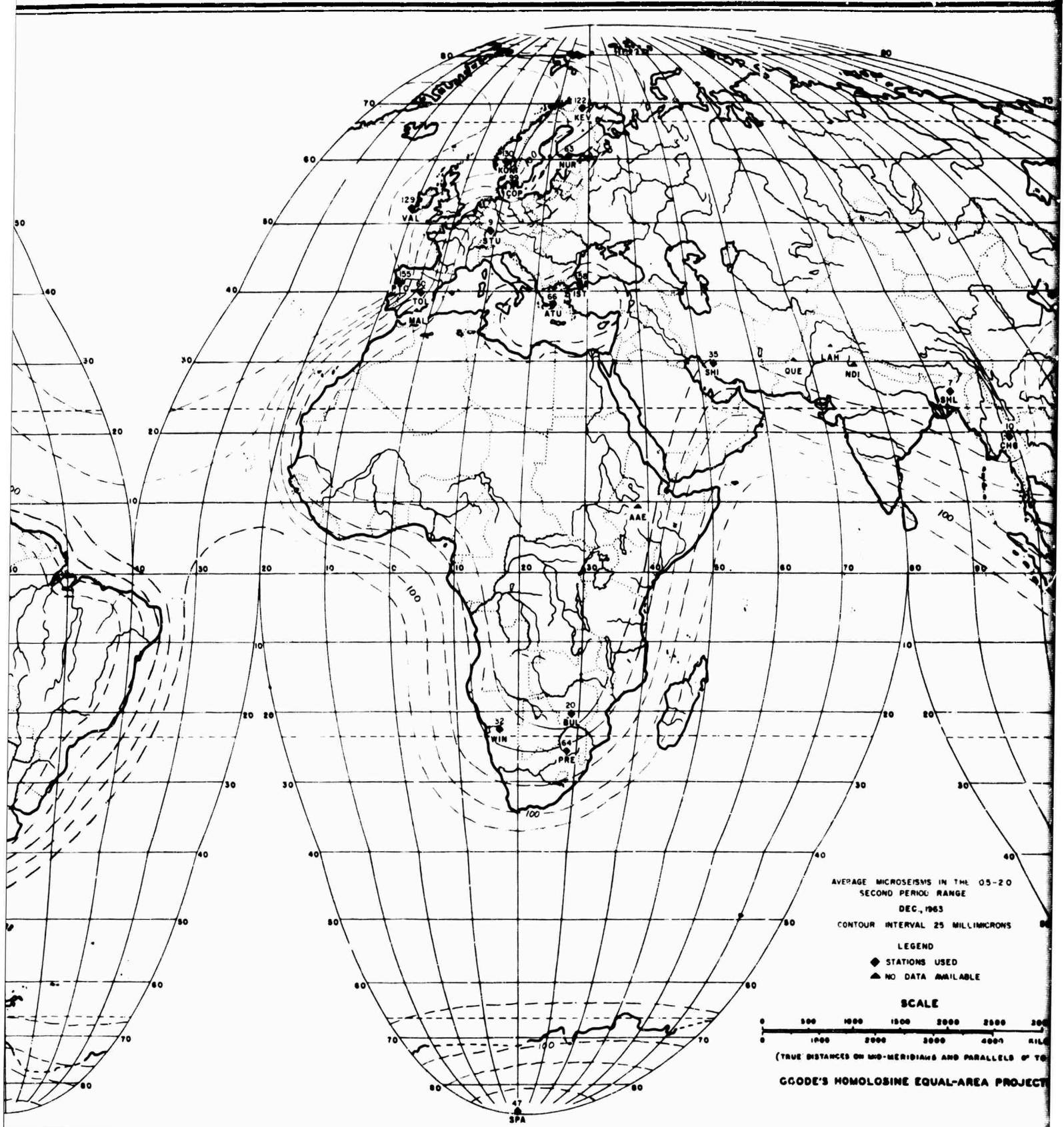

B

Figure B-17. World Map of 0.5

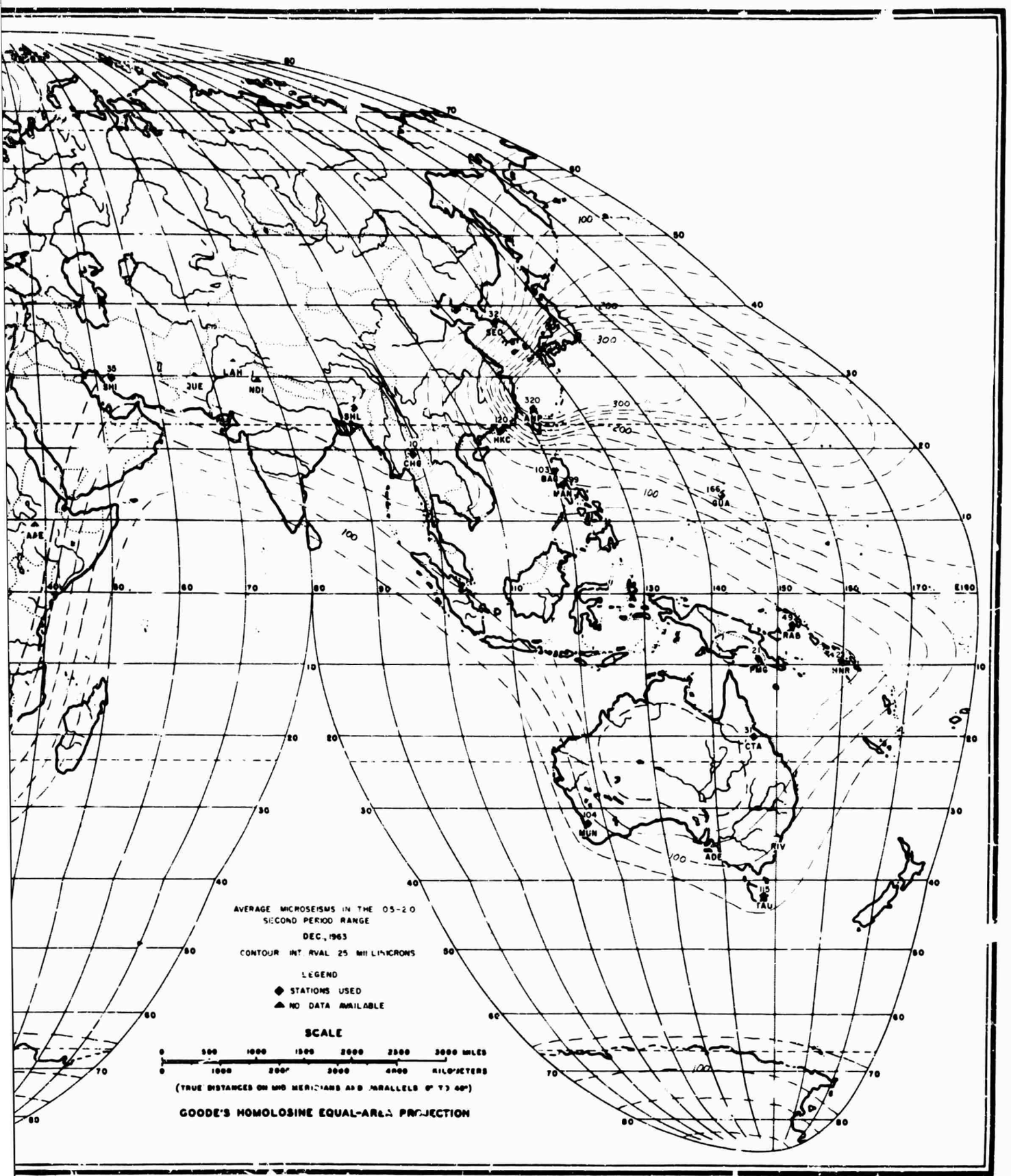

Figure B-17. World Map of 0.5-2.0 Second Microseismic Activity, December, 1963

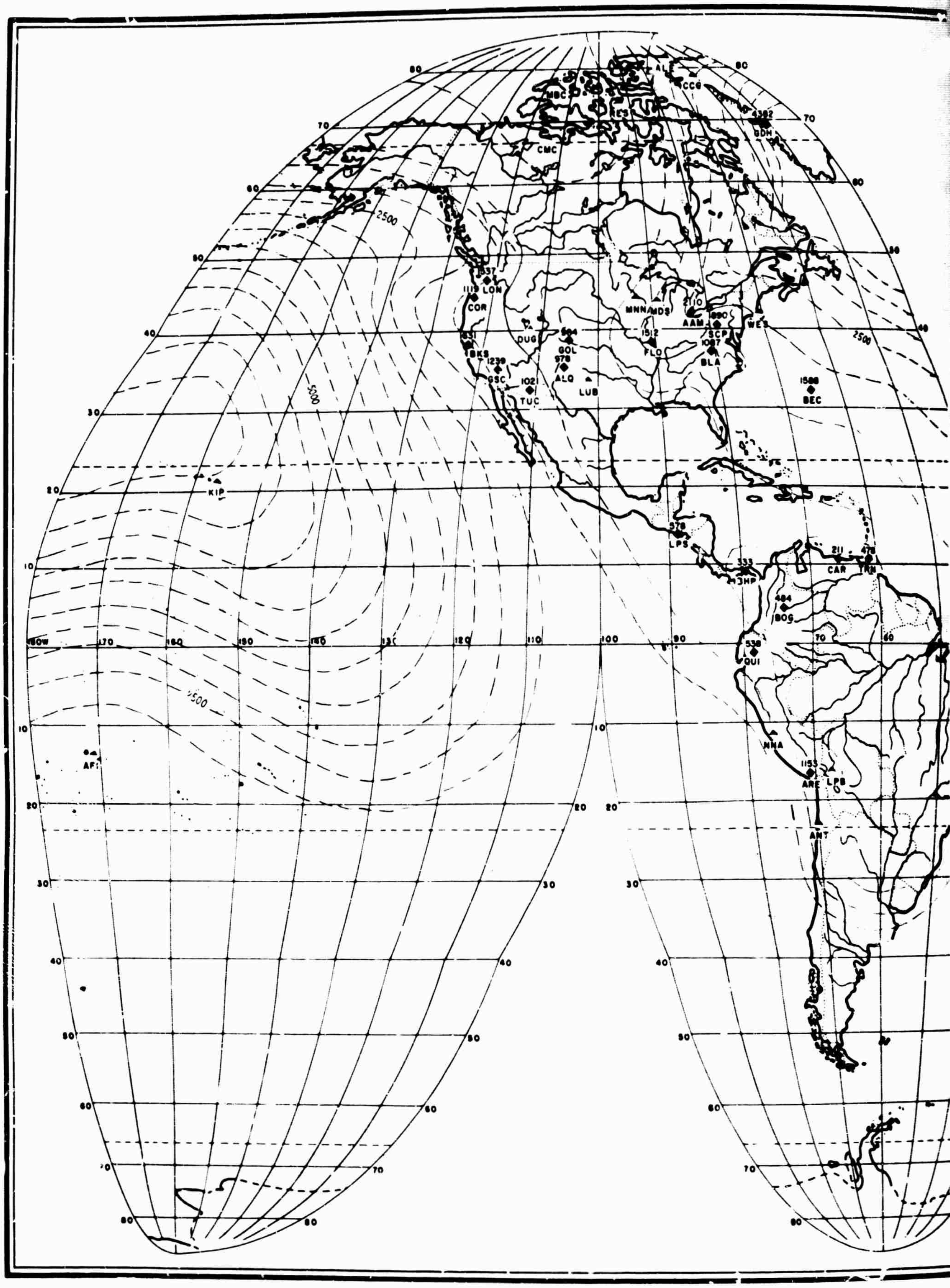

MBC
CCG
4392
GDH
CMC
2500
537
LON
1119
COR
MNN
MDS
2110
AAM
890
SCP
1097
BLA
WES
1512
FLO
DUG
594
GOL
978
ALQ
1239
GSC
BKS
1021
TUC
LUB
1588
BEC
5000
KIP
578
LPS
333
211
CAR
479
TRN
484
BOG
538
QUI
NNA
1153
ARE
LPB
ANT
AF

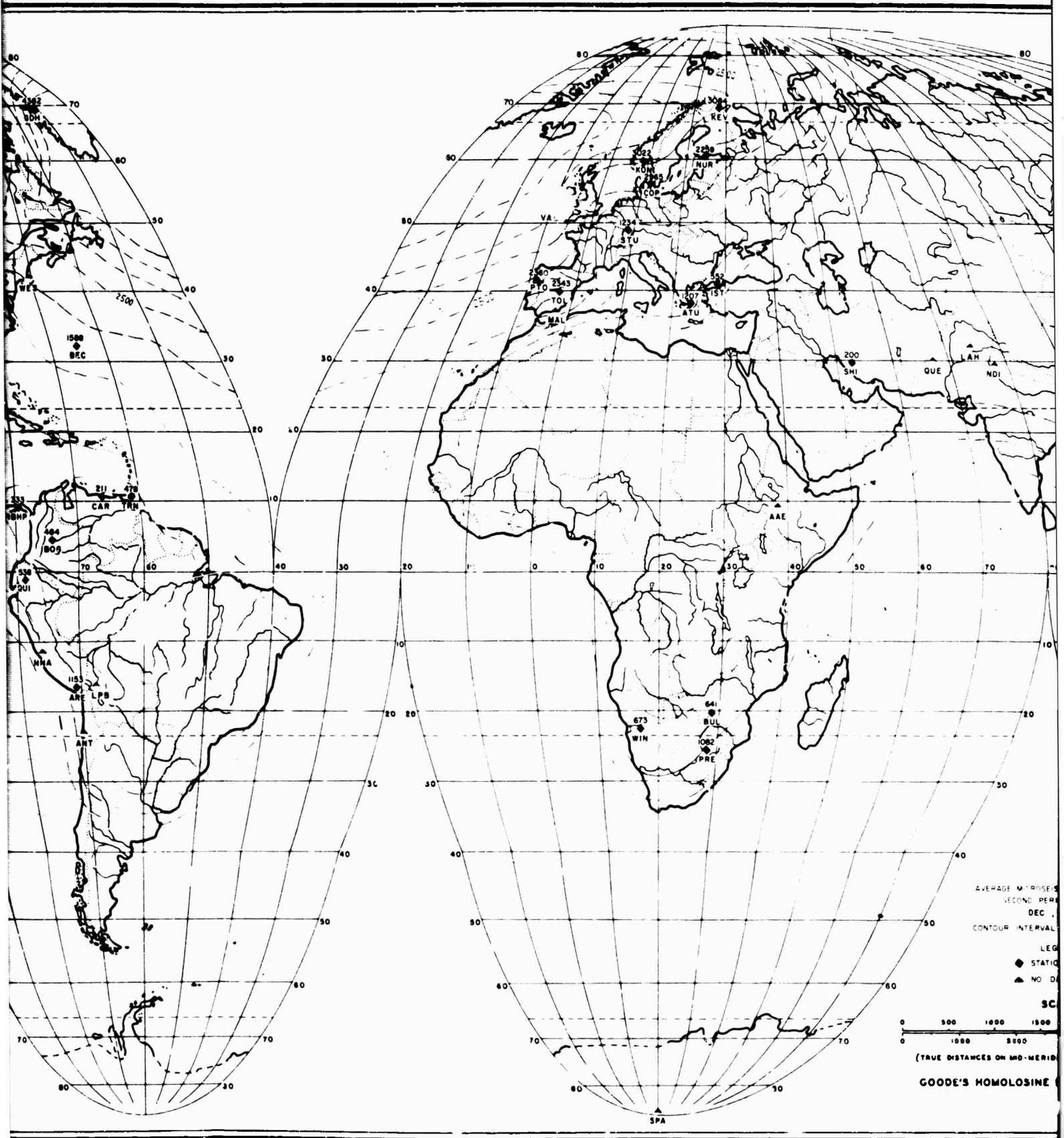

Figure B-18. Wor

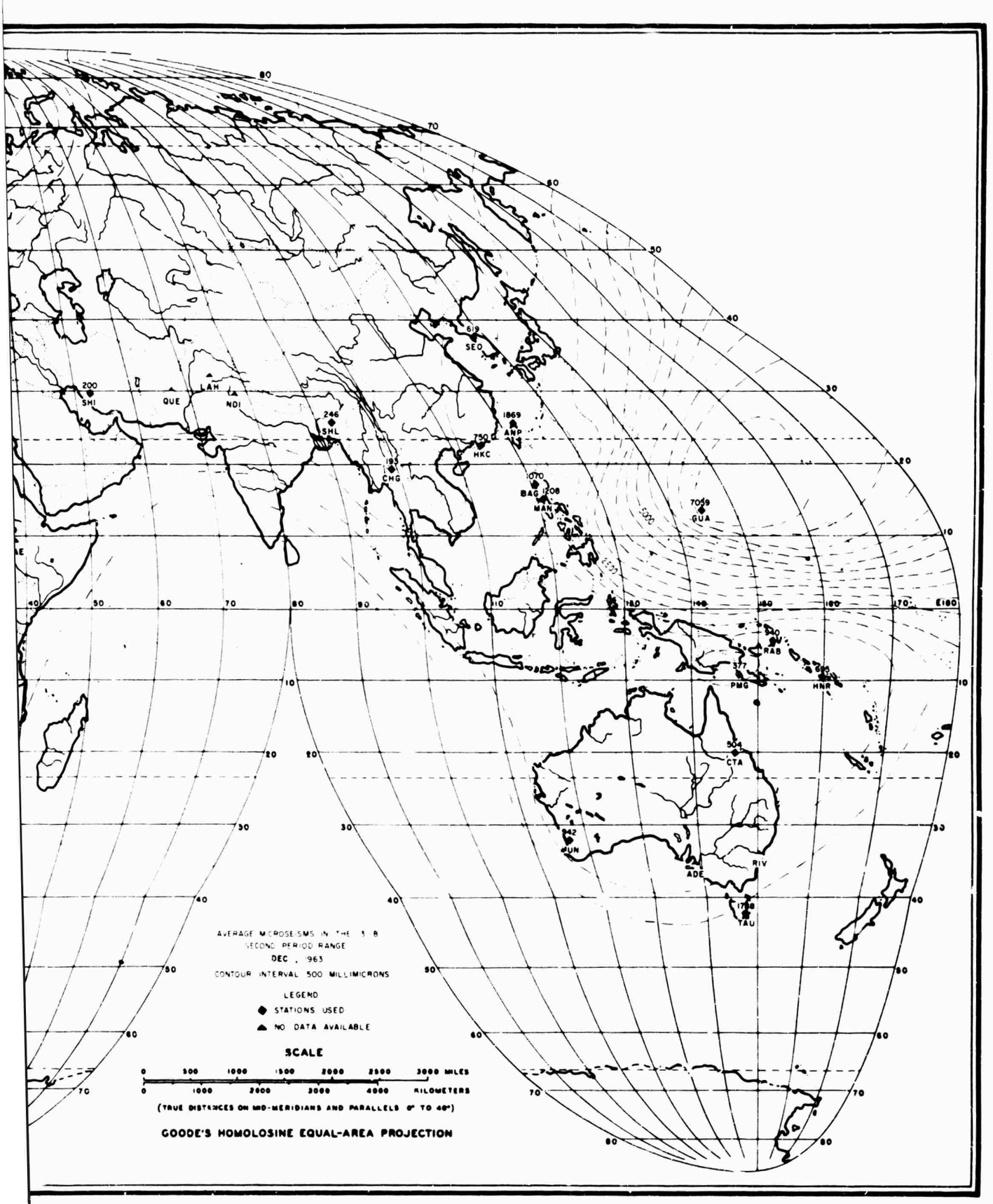

Figure B-18. World Map of 3.0-8.0 Second Microseismic Activity, December, 1963

REFERENCES

Benndorf, H., 1910, Uber die mikroseismischen bewegungen: Sonderabdruck Aus Geologische Rundschau, v. 1, p. 183-186.

Bradford, J. C., Weather seismic noise correlation study: Semiannual Report 1 June 1963 to 30 Nov. 1963, Contract AF 19(628)-230, United Electrodynamics, Inc., Alexandria, Va.

Bradner, Hugh, 1964, Seismic measurements on the ocean bottom: Science, v. 146, 9 Oct.

Caloi, Pietro, 1950, Due caratteristic tipi di microseismi: Annali Di Geofisica, v. 3, p. 303-314.

Carder, Dean S., 1951, The continent and ocean floor as transmitting media of microseisms (ABS): Earthquake Notes, v. 22, n. 3, p. 26.

Ewing, M. and Frank Press, 1952, Propagation of elastic waves in the ocean with reference to microseisms: Pontificiae Acadamiae Scientiarvm Scripta Varia, n. 12, p. 121-127.

Ewing, Maurice and William L. Dunn, 1952, Studies of microseisms from selected areas: Pontificiae Academiae Scientiarvm Scripta Vara, n. 12, p. 351-360.

Gutenberg, B., 1931, Microseisms in North America: Bull. Seis. Soc. Am., v. 21, p. 1-24, 1940.

Iyer, H. M., 1964, The history and science of microseisms: A VESIAC State of the Art Report No. 4410-64-X, Apr.

Iyer, H. M., 1964, Worldwide microseismic study: Nature magazine, v. 194 (June).

Ramirez, J. E., 1940, An experimental investigation of the nature and origin of microseisms at St. Louis, Missouri: Bull. Seis. Soc. Am., v. 30, p. 35-84, 139-178.

Texas Instruments Incorporated, 1962: Semiannual Tech. Rept. No. III, Contract AF 19(604)-8517, 31 Oct.

Vinnik, L. P. and N. M. Pruchkina, 1964, A study of the structure of short period microseisms: Bull. (Izv.) Acad. of Sci., USSR, Geophys. Ser. n. 5. May, p. 412-419.

DOCUMENT CONTROL DATA - R&D

(Security classification of title, body of abstract and indexing annotation must be entered when the overall report is classified)

1. ORIGINATING ACTIVITY *(Corporate author)*

Texas Instruments Incorporated
6000 Lemon Avenue
Dallas, Texas 75222

2a. REPORT SECURITY CLASSIFICATION

Unclassified

2b. GROUP

3. REPORT TITLE

NOISE STUDY

4. DESCRIPTIVE NOTES *(Type of report and inclusive dates)*

Scientific. Interim.

5. AUTHOR(S) *(Last name, first name, initial)*

Hair, George D.; Funk, James H.; and Research Staff

6. REPORT DATE	7a. TOTAL NO. OF PAGES	7b. NO. OF REFS
15 November 1964	51	13

8a. CONTRACT OR GRANT NO. ARPA Order No. 292
AF19(604)-8517

b. PROJECT AND TASK NO.
8652-07

c. DOD ELEMENT
6250601R

d. DOD SUBELEMENT

9a. ORIGINATOR'S REPORT NUMBER(S)

Special Report No. X

9b. OTHER REPORT NO(S) *(Any other numbers that may be assigned this report)*

None

10. AVAILABILITY/LIMITATION NOTICES

1 - Distribution of this document is unlimited. It may be released to the Clearinghouse, Department of Commerce, for sale to the general public.

11. SUPPLEMENTARY NOTES

This research was supported by the Advanced Research Projects Agency

12. SPONSORING MILITARY ACTIVITY

Air Force Cambridge Research Laboratories (CRJ), L.G.Hanscom Field Bedford, Massachusetts 01730

13. ABSTRACT

Worldwide seismic noise levels and characteristics for 1963 are discussed. Data for evaluation includes absolute power density spectra and contour maps of average worldwide microseismic activity.

Relative power density spectra were computed from 1963 data from Worldwide Standard Stations. Slopes of the least-mean-square line through the power density points were computed and a pattern of slope changes appeared at a frequency of 1.0 cps. A uniform worldwide pattern of slopes was observed between 1 cps and 2 cps. This suggests two separate sources generating microseisms above and below 1 cps, respectively, and that the spectra above 1 cps are independent of storms, fronts, etc.

The spectra for frequencies less than 1.0 cps show greater seasonal variations. These were concluded to be mostly meteorological in origin.

Monthly contour maps of average noise show that noise is seasonally variable and that it is attenuated at continental structures.

DD FORM 1 JAN 64 1473

14. KEY WORDS	LINK A		LINK B		LINK C	
	ROLE	WT	ROLE	WT	ROLE	WT
Worldwide seismic noise, 1963 noise levels, power density spectra.						

INSTRUCTIONS

1. ORIGINATING ACTIVITY: Enter the name and address of the contractor, subcontractor, grantee, Department of Defense activity or other organization *(corporate author)* issuing the report.

2*a*. REPORT SECURITY CLASSIFICATION: Enter the overall security classification of the report. Indicate whether "Restricted Data" is included. Marking is to be in accordance with appropriate security regulations.

2*b*. GROUP: Automatic downgrading is specified in DoD Directive 5200.10 and Armed Forces Industrial Manual. Enter the group number. Also, when applicable, show that optional markings have been used for Group 3 and Group 4 as authorized.

3. REPORT TITLE: Enter the complete report title in all capital letters. Titles in all cases should be unclassified. If a meaningful title cannot be selected without classification, show title classification in all capitals in parenthesis immediately following the title.

4. DESCRIPTIVE NOTES: If appropriate, enter the type of report, e.g., interim, progress, summary, annual, or final. Give the inclusive dates when a specific reporting period is covered.

5. AUTHOR(S): Enter the name(s) of author(s) as shown on or in the report. Enter last name, first name, middle initial. If military, show rank and branch of service. The name of the principal author is an absolute minimum requirement.

6. REPORT DATE: Enter the date of the report as day, month, year, or month, year. If more than one date appears on the report, use date of publication.

7*a*. TOTAL NUMBER OF PAGES: The total page count should follow normal pagination procedures, i.e., enter the number of pages containing information.

7*b*. NUMBER OF REFERENCES: Enter the total number of references cited in the report.

8*a*. CONTRACT OR GRANT NUMBER: If appropriate, enter the applicable number of the contract or grant under which the report was written.

8*b*, 8*c*, & 8*d*. PROJECT NUMBER: Enter the appropriate military department identification, such as project number, subproject number, system numbers, task number, etc.

9*a*. ORIGINATOR'S REPORT NUMBER(S): Enter the official report number by which the document will be identified and controlled by the originating activity. This number must be unique to this report.

9*b*. OTHER REPORT NUMBER(S): If the report has been assigned any other report numbers *(either by the originator or by the sponsor)*, also enter this number(s).

10. AVAILABILITY/LIMITATION NOTICES: Enter any limitations on further dissemination of the report, other than those imposed by security classification, using standard statements such as:

(1) "Qualified requesters may obtain copies of this report from DDC."

(2) "Foreign announcement and dissemination of this report by DDC is not authorized."

(3) "U. S. Government agencies may obtain copies of this report directly from DDC. Other qualified DDC users shall request through

_____."

(4) "U. S. military agencies may obtain copies of this report directly from DDC. Other qualified users shall request through

_____."

(5) "All distribution of this report is controlled. Qualified DDC users shall request through

_____."

If the report has been furnished to the Office of Technical Services, Department of Commerce, for sale to the public, indicate this fact and enter the price, if known.

11. SUPPLEMENTARY NOTES: Use for additional explanatory notes.

12. SPONSORING MILITARY ACTIVITY: Enter the name of the departmental project office or laboratory sponsoring *(paying for)* the research and development. Include address.

13. ABSTRACT: Enter an abstract giving a brief and factual summary of the document indicative of the report, even though it may also appear elsewhere in the body of the technical report. If additional space is required, a continuation sheet shall be attached.

It is highly desirable that the abstract of classified reports be unclassified. Each paragraph of the abstract shall end with an indication of the military security classification of the information in the paragraph, represented as *(TS), (S), (C), or (U).*

There is no limitation on the length of the abstract. However, the suggested length is from 150 to 225 words.

14. KEY WORDS: Key words are technically meaningful terms or short phrases that characterize a report and may be used as index entries for cataloging the report. Key words must be selected so that no security classification is required. Identifiers, such as equipment model designation, trade name, military project code name, geographic location, may be used as key words but will be followed by an indication of technical context. The assignment of links, rules, and weights is optional.